Analysis of cyclic thermodynamic

Commisso, Marcello Benito; Carlsen, Henrik; Qvale, Einar Bjørn; Thomsen, Per Grove

Publication date:
1994

Document Version
Publisher's PDF, also known as Version of record

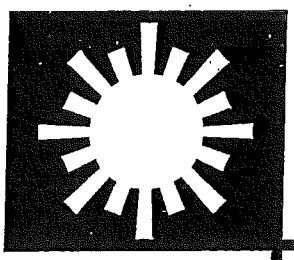

LABORATORY FOR ENERGETICS

RE 94 - 4

ANALYSIS OF CYCLIC THERMODYNAMIC PROCESSES

Marcello Benito Commisso

RE 94 - 4

ANALYSIS OF CYCLIC THERMODYNAMIC PROCESSES

Marcello Benito Commisso

ISBN 87 - 7475 - 160 - 3

Printed 1994

Laboratory for Energetics

The Technical University of Denmark

Building 403

DK-2800 Lyngby

PREFACE

This thesis is part of the requirements for achieving the Ph.D. degree at Technical University of Denmark. The thesis is also documentation for the research carried out at the Laboratory for Energetics (Laboratoriet for Energiteknik, LfE) during the period of March 1991 to February 1994.

Supervisors have been Associated Professor Henrik Carlsen (LfE), Professor Bjørn Qvale (LfE) and Docent Per Grove Thomsen (Institute for Mathematical Modelling). Without their support this project would not have been possible and for this I am very grateful. I hope we may work together again sometime in the future.

I spent nine months at University of California Los Angeles (UCLA), Department of Mathematics, as a guest of Professor Stanley Osher. Special thanks to him, to Professor Björn Engquist from this department, and to Per Christian Hansen at UNI-C, who made my stay at UCLA possible.

Finally, thanks to my fellow Ph.D. stud. Bent Lorentzen (LfE) for many helpful discussions, and for his debugging of this text.

April 1994, Lyngby, Denmark

Marcello Benito Commisso

SUMMARY

Cyclic thermodynamic processes are the subject of this thesis. These processes are typically realized in thermodynamic devices, where the cyclic nature is exploited. In the steady-state operation, conditions inside the device are characterized by the fact that the state variables are periodic in time. The main emphasis has been laid on reciprocating devices, and the Stirling engine has been chosen as the model example.

Physical models of different complexity of a Stirling engine have been created. These models have been translated into mathematical models using conservation laws and constitutive relations. Different approaches and numerical methods are discussed with special reference to obtaining the periodic steady-state solution in a fast and conceivable way.

Classically, such a problem is solved as an initial-value problem integrating forward in time until the periodic steady-state is reached (this approach is named the *Integration-to-Convergence method*). In the thesis, other alternatives, which have turned out to be faster and more reliable, are considered. Foremost, in form of the *Shooting method*, which also solves the problem as an initial-value problem, but accelerates the convergence towards the periodic steady-state, and partly in form of the *Finite-Difference method*, which solves the problem as a boundary value problem.

Semi-implicit Runge-Kutta methods have mainly been used for the time integration for the Integration-to-Convergence method and the Shooting method, while simple divided differences have been used in the Finite-Difference method.

The full implementations for these three approaches (the Integration-to-Convergence method, the Shooting method and the Finite-Difference method) have been carried out in detail. A simulation program in form of computer code has been developed. This program solves the mathematical model of the Stirling engine using each of these approaches. Comparisons of the different approaches regarding numerical properties, such as stability, accuracy and speed, have been made and discussed. The superiority of the Shooting method and the Finite-Difference method has been demonstrated for the numerical solution of the considered Stirling models. The application for other thermodynamic processes has been discussed.

TABLE OF CONTENTS

NOMENCLATURE

Letter

a	: constant	-
b	: constant	-
c	: heat capacity	J/(kg·K)
d	: diameter	m
e	: specific total energy	J/kg
f	: friction factor	-
f	: specific force	N/kg
h	: heat transfer coefficient	$W/(m^2 \cdot K)$
h	: specific enthalpy	J/kg
i	: specific internal energy	J/kg
k	: heat conductivity	W/(m·K)
l	: length	m
p	: pressure	N/m^2
q	: specific heat	J/kg, J/m^3
u	: velocity	m/s
t	: time	s
w	: specific work	J/kg, J/m^3
x	: position	m
y	: differential variable	
z	: algebraic variable	

A	: area	m^2
D	: diameter	m
E	: total energy	J
F	: force	N
G	: momentum	kg·m/s
H	: total specific enthalpy	J/kg
L	: length	m
M	: mass	kg
N	: number	-
Q	: heat	J
R	: gas constant	J/(kg·K)
S	: general surface	
S	: wetted perimeter	m
T	: temperature	K
U	: general variable	
V	: volume	m^3
W	: work	J

Greek letter

α	: temperature gradient	K/m
β	: angle	°
δ	: displacement	
δ	: Kronecker's delta	
η	: efficiency	-
γ	: heat capacity ratio c_p/c_v	-
λ	: general parameter	
φ	: phase angle	°
ρ	: density	kg/m^3
σ	: stress tensor	N/m^2
τ	: shear stress	N/m^2
ω	: angular velocity	rad/s
μ	: dynamic viscosity	$N \cdot s/m^2$
ϱ	: porosity	-
Γ	: general source term	
Φ	: general flux term	
Ω	: general volume	

Subscript

c	: free flow
e	: external
h	: hydraulic
p	: period
p	: constant pressure
v	: constant volume
C	: cold, compression
D	: diffusive
E	: expansion
H	: hot
R	: regenerator
S	: surface
cl	: clearance
cond	: conduction
conv	: convection
fr	: frontal
fric	: friction
ln	: logarithmic
ref	: reference
sw	: swept
tot	: total
w	: wall
Ω	: general volume

Superscript

$\dot{}$	: flux
$\hat{}$	: interpolant, molar
$\sim$	: dimensionless variables

Others

$'$	: derivative
$-$	: vector
$=$	: matrix

Dimensionless numbers

j_H	: Colburn factor
NTU	: Number of Transfer Units
Nu	: Nusselt number
Pr	: Prandtl number
Re	: Reynolds number
St	: Stanton number

Abbreviations

BVP	: Boundary-Value Problem
IVP	: Initial-Value Problem
DAE	: Differential-Algebraic Equation
ODE	: Ordinary Differential Equation
PDE	: Partial Differential Equation
CFD	: Computational Fluid Dynamics
SFVSM	: Simple Five-Volume Stirling Model
EFVSM	: Extended Five-Volume Stirling Model
MVSM	: Multi-Volume Stirling Model
ERK	: Explicit Runge-Kutta
IRK	: Implicit Runge-Kutta
DIRK	: Diagonally Implicit Runge-Kutta
BDF	: Backward Differentiation Formulae
LMM	: Linear Multistep Methods
HEX	: Heat exchanger
REG	: Regenerator
VVC	: Variable Volume with Cyclic heat transfer
MVC	: Manifold Volume with Cyclic heat transfer

1.0 INTRODUCTION

Cyclic thermodynamic processes are very common for energy exchanging devices or systems. Almost all processes used in engines, heat pumps or refrigerators are in some sense cyclic in their steady state operation. Conditions in the thermodynamic process are repeatedly produced after a given time interval, defined as the period of the cycle.

Some practical examples:

- In a conventional steam power plant running in steady state operation, a "flow particle" returns to the same thermodynamic state after passing through the components.

- In a combustion engine running at a steady-state constant speed, the temperature profiles in the manifolds and combustion chamber will be periodic in time, and the whole combustion process is repeated in form of intake, ignition, combustion and exhaust.

- In a Stirling engine, each "flow particle" inside the engine goes through different state changes, but after one time period, the particle returns to the same state for steady-state operation.

The key idea for any cyclic thermodynamic process is being able to use the same cycle, process or equipment over and over.

For some of these processes, numerous real life cycles are required before the periodic steady-state conditions are established. An example would be the Stirling engine where several minutes are required for a "cold" start-up. If the engine runs at a speed of 1500 RPM, it adds up to many cycles.

An accurate physical model and the related mathematical model should, of course, reflect the true dynamics of the engine, but if the main interest is the periodic steady-state solution, fast and efficient ways to obtain the numerical solution for the periodic problem will be attractive. This is the main objective of the thesis or in other words:

> *Finding a fast, accurate and stable numerical solution to the mathematical model of a periodic, thermodynamic problem.*

Describing theoretical cycles is a convenient way of introducing the thermodynamic processes although the real cycles, for the embodiment in a real thermodynamic device (such as an engine or a heat pump), are often significantly different. Numerous real cycles can be considered, and it may be difficult to analyze all cycles in a general way without being too vague and losing most of the practical aspects for the development of a simulation model especially with regard to obtaining a numerical solution through an implementation into computer code. Mainly for this reason, it has been chosen to concentrate on reciprocating devices. Specifically one cycle, namely the Stirling cycle and the real embodiment in form of the Stirling engine.

Different models of a Stirling engine will be considered. A simple model will be developed to test the feasibility of different approaches to obtain the solution, including the choice of a specific numerical method. The experience gained from the simulations of the simple model will be used by means of two more advanced models to produce more realistic simulations and to address more complicated issues.

The structure of the thesis is the following:

Chapter 1 is a basic introduction.

Chapter 2 contains a short description to general thermodynamic cycles. As mentioned, the main emphasis of the thesis will be laid on Stirling engine simulations and for which reason the classic Stirling cycle only will be given as an example.

Chapter 3 is devoted to a description of the real embodiment of a Stirling engine. Problems in Stirling modelling are discussed and classic analysis as well as state-of-the-art in Stirling analysis are considered.

The basic modelling process is addressed in chapter 4.

A simple physical and mathematical model of a Stirling engine is described in detail in chapter 5. This so-called Simple Five-Volume Stirling Model is based on a "lumped parameter" formulation. All the basic assumptions and limitations of the model are discussed and the governing equations in the mathematical model are listed in this chapter.

The resulting system of differential-algebraic equations is put on a general form in chapter 6, which makes the classification and implementation into computer code much easier. Different approaches for obtaining a numerical solution of the mathematical model are considered in the chapter and the actual implementation for the most interesting and attractive of these approaches is also discussed.

The results of the numerical tests of the simulation model for the simple Stirling model is discussed in chapter 7. Here are also included conclusions regarding the properties of the considered approaches and numerical methods.

In chapter 8, two sophisticated Stirling models are discussed. One model (the Extended Five-Volume Stirling Model) is basically an extension of the simple model, where additional physical effects, such as variable convection heat transfer, variable solid temperature and friction, have been included. The other model (Multi-Volume Stirling Model) features a spatial discretization opposed to the "lumped" formulation of the two first models. Results from the simulations of these two models are also discussed in this chapter.

The last chapter contains a discussion of the general results. The most important conclusions are summarized and recommendations are made. Furthermore, the application of the considered approaches and methods for other thermodynamic processes is addressed.

2.0 THERMODYNAMIC CYCLES

2.1 Introduction

Cyclic thermodynamic processes are normally the basis for work and heat transferring thermodynamic machines for the purpose of producing mechanical work and exchanging heat between two reservoirs.

A cyclic process may be described as a process, where the working medium undergoes a number of sub processes until it finally returns to the original state. This is usually realized principally in two different ways:

- Reciprocating devices, where the working medium successively is taken through sub processes which ultimately bring it back to the original state.

- In turbomachinery devices, the working medium continuously flows through a number of components in a closed loop. The medium undergoes sub processes in each of these components in a way that it returns to the original state.

The theoretical cycle is a convenient way of introducing the basic process of the classic thermodynamic cycles, but in reality the idea can often be difficult to carry out. This is usually due to either limitations in the technology (in form of lacking performance of the components involved) or economical concerns.

A Stirling engine is a typical example. The Stirling cycle looks very simple in a temperature-entropy diagram (two isochors and two isotherms), but the embodiment of the process in a real engine is much more complicated and the real cycle is different in many ways. Conditions, such as flow, heat transfer, steady state operation, etc. are not considered by the theoretical cycle.

For a reliable calculation of the performance and operation of a real device, the theoretical cycle is not of much use. An accurate physical and mathematical model must be developed to describe the real conditions inside the machine. This may include phenomena such as turbulence, friction, combustion and heat transfer which are all difficult to model correctly unless the geometry is very simple.

Solving the mathematical model of a real thermodynamic device must always be accomplished numerically because of the complexity of the system of equations involved.

For processes that are periodic in time, the main interest is often the *periodic steady-state*. This is the condition, where all state variables are periodic in time when the process is repeated over and over.

2.2 Basic concepts

In this section, basic definitions for some often used terms will be stated.

Cycles

A *theoretical cycle* is the basic reference cycle, where the working gas undergoes certain changes in form of a number of specified thermodynamic processes. There is no concern whether the process can be realized in a real embodiment. No losses or other irreversibilities are considered.

An *ideal cycle* is defined as a theoretical cycle with the highest possible efficiency (Carnot efficiency). Carnot, Stirling and Ericsson theoretical cycles are all examples of ideal cycles.

A *real cycle* is then the actual cycle in a real, thermodynamic device. The real cycle is the outcome of the given real embodiment of the theoretical cycle.

Closed cycles

A wide range of thermodynamic processes falls into the category of closed thermodynamic cycles. For these cycles, the working medium undergoes a series of changes until it returns to its initial state and the process is repeated.

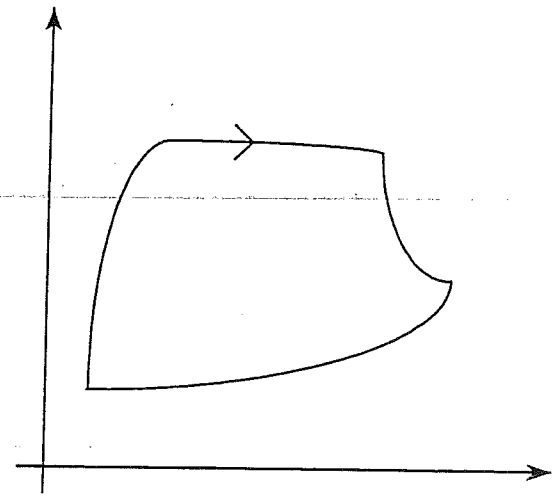

Figure 2.1 Closed thermodynamic cycle.

Classical examples of devices based on closed cycles are:

- Rankine cycle (steam power plants, heat pumps and refrigerators).
- Stirling cycle (engines, heat pumps and refrigerators).
- Vuilleumier cycle (heat pumps).

"Open" cycles

Other thermodynamic devices operate as "open" cycles. Typically, the working medium enters the device, undergoes a series of changes and then leaves the device at a different state. Then the process is repeated.

Internal combustion engines and gas turbines are classical examples. Air and fuel enters, combustion takes place and the exhaust gases leave the devices.

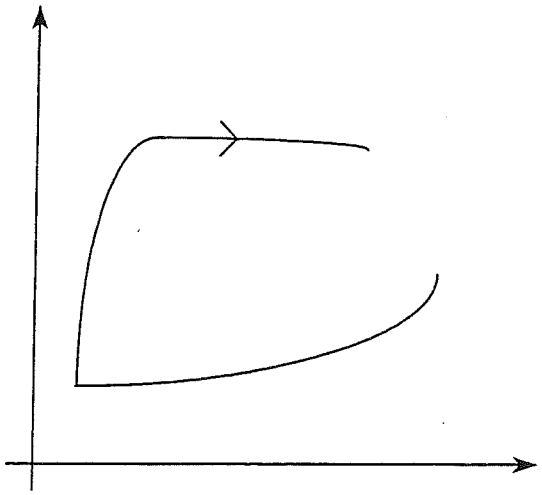

Figure 2.2 Open thermodynamic cycle.

Examples of devices based on open cycles are:

- Otto cycle (combustion engines).
- Diesel cycle (diesel engines).
- Brayton cycle (gas turbines).

For simple analysis purposes open cycles are often "closed" by inserting pseudo-components which bring the working medium back to its original state.

A detailed description of each of these cycles can be found in any standard text book dealing with energy converting devices. It has not been the intention to cover all the particular features of these cycles, so further considerations have been omitted. Instead, the analysis will be concentrated on reciprocating devices and in particularly devices based on the Stirling cycle, which will be described later in this chapter.

Devices

An *engine* is defined as a work producing thermodynamic device. The terms *refrigerator* and *heat pump* will be used for a thermodynamic device removing heat from low temperature level and adding heat to a high temperature level. If the main interest is heat removal, the device will be called a refrigerator and a heat pump in the other case.

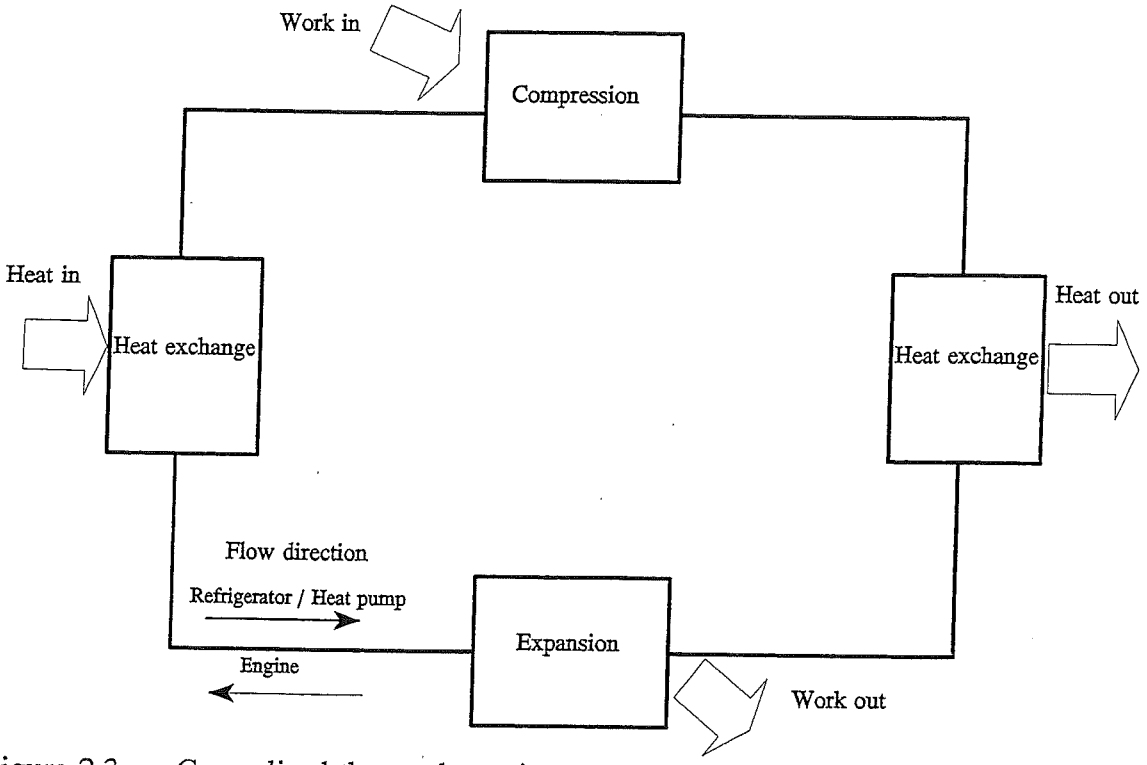

Figure 2.3 Generalized thermodynamic process.

Work and heat transfer

For a given volume or component, work and heat transfer are positive when added to the considered volume, *unless* stated otherwise. Notice, that this means that when subscript "in" or "out" are given, the work and heat transfer are positive accordingly, e.g., W_{out} for an engine is positive.

Efficiency

The efficiency η of an engine is defined as the ratio between work output and heat input, i.e.,

$$\eta = \frac{W_{out}}{Q_{in}} \qquad (2.1)$$

where W_{out} is the total work output from the engine and Q_{in} is the heat transfer to the engine.

2.3 The Stirling cycle

2.3.1 Introductory remarks

The study of periodic general thermodynamic processes is the subject of the thesis, but it has been chosen to look closely at one process only, namely the process of a Stirling engine, which is based on the ideal Stirling cycle.

This choice has been made mainly because it is possible to be more specific looking at one particular cycle instead of all cycles. Hereby problems in the modelling and solving procedure can directly be addressed and analyzed, and the obtained results are easier evaluated. Of course, the developed theory and computer code for simulation programs will then be confined to the chosen cycle or process, but the general results can still be discussed with regard to other related cycles.

The Stirling engine is of particular interest because of the following reasons:

- The engine consists of components, such as heat exchanger, cylinder volumes etc. which are typical for real embodiments of other thermodynamic cycles in reciprocating devices.

- The Stirling cycle has regained new interest, due to the Stirling machines potential of high efficiency, low pollution and low noise. Because of the late development, modern Stirling analysis is not fully developed though there has been a great deal of research. The Stirling research level is not as sophisticated as the level found in more traditional areas, such as internal combustion engine research, where three-dimensional CFD-codes are used for complex calculations, including effects of combustion, turbulence, heat transfer and friction.

- At the Technical University of Denmark, the Laboratory for Energetics (LfE), research has been carried out for a number of years, including design and simulations of Stirling engines. This gives an excellent opportunity to test developed simulation programs and computer codes against other codes and the opportunity to test the programs with experimental data from real Stirling engines.

- Solving the mathematical model of the Stirling engine requires the application of numerical methods. Problems of obtaining a quick and accurate cyclic solution have been observed by several authors. Furthermore, the codes used at LfE have also shown these deficiencies. Calculations of many cycles are required before a cyclic state is reached and many time steps are required to obtain numerically accurate results.

2.3.2 Ideal Stirling cycle

The Stirling cycle is named after Robert Stirling, who proposed this cycle already in 1816. It is reversible and can be used for both engine and refrigerator / heat pump operation, but the Stirling engine cycle only will be described in this chapter.

The theoretical Stirling cycle is composed of two isochors and two isotherms as shown in the pressure-volume and temperature-entropy diagrams just below.

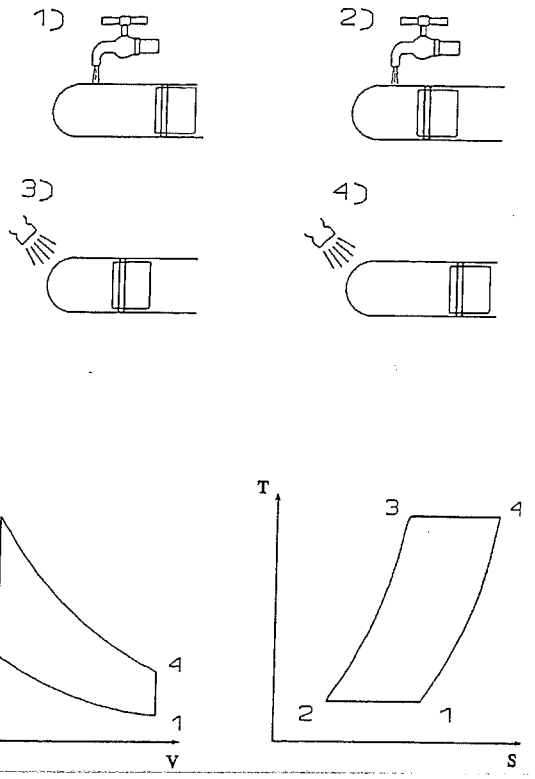

Figure 2.4 Ideal Stirling cycle.

The different stages in the theoretical Stirling cycle can be described as follows:

1→2: Isothermal compression. Heat must be removed during the compression to keep the temperature constant.

2→3: Isochoric heat exchange. Heat is added and the volume is kept constant in order to create a pressure rise.

3→4: Isothermal expansion. Heat must be added during the expansion to keep the temperature constant.

4→1: Isochoric heat exchange. Heat is removed and the volume is kept constant in order to reduce the pressure.

The amount of heat removed from 2 to 3 equals the heat added from 4 to 1,and the ability to store and reuse the heat is an essential part of the Stirling cycle concept. See reference [1] for a detailed description of the ideal cycle.

The efficiency η of the ideal Stirling cycle engine is only dependent of the two temperatures and it is given as

$$\eta = 1 - \frac{T_L}{T_H} \tag{2.2}$$

which is equal to the efficiency of the Carnot cycle working between the two temperature levels T_H (high) and T_L (low).

References

[1] Carlsen, H.
Stirling Motorer vol. II (Stirling Engines vol. II).
Laboratory for Energetics, Technical University of Denmark (1993).

3.0 STIRLING ENGINES AND ANALYSIS

3.1 Introduction

In this chapter, the real embodiment of the cycle in form of a real Stirling engine is considered and Stirling modelling and analysis are discussed. There exists a vast amount of literature dealing with Stirling machines including subjects such as history, thermodynamics, mechanics, construction, simulation and applications. Recent books by Urieli and Berchowitz [1], Walker [2], Organ [3] and Hargreaves [4] are often cited for a general description of Stirling machines. Here, it is not the intention to present a full review of Stirling research. Only a basic introduction and a few references for more comprehensive literature will be given.

The first part of this chapter is devoted to the real embodiment of a Stirling engine, which will be described in such detail that the basic concepts should be clear. The second part addresses Stirling modelling and concerns the physical and mathematical models of the engine in a traditional Stirling analysis as well as "state-of-the-art" in form of simulation programs for the design of real Stirling engines.

3.2 Stirling engine design

3.2.1 Introductory remarks

The ideal Stirling cycle, which has been described in chapter 2, cannot be realized in a real engine.

- It is not possible in practice to have the working gas in just one cylinder volume, heat must be added and removed from physically different parts of the machine.
- Isothermal compression and expansion are impossible to realize.
- It is difficult to obtain sufficient heat transfer without introducing new components in form of heat exchangers.
- Heat must be stored when the gas flows from the hot part of the engine to the cold part and returned when the flow reverses. Otherwise, the performance will become poor. It can be accomplished by introducing another component in form of a regenerator.
- Mechanical considerations and practical design limitations make the piston motion less ideal.
- Dead spaces in internal volumes and connections are impossible to avoid.

All these conditions make the real Stirling cycle far from the ideal cycle. Nevertheless, the principle still works well and it is still a periodic, thermodynamic problem.

3.2.2 Real Stirling design

To separate the cold and hot heat transfer in cylinder volumes, a displacer is often introduced in the real Stirling engine design. The displacer divides the engine into a hot and cold part, where heat can be added and removed continuously. Working gas is moved from one part to the other just by moving the displacer.

This is shown in the figure below, which should be compared with the figure on page 2.6.

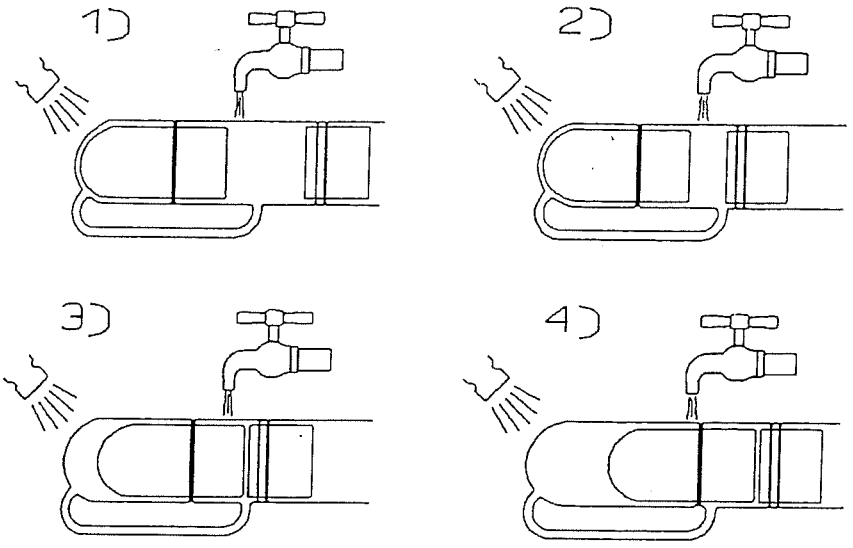

Figure 3.1 Stirling engine with displacer.

In order to recover some of the energy used for the heating of the working gas, a heat storage, in form of a regenerator, is always included in the real design. When the working gas flows from the hot part of the engine to the cold part, it delivers heat to the regenerator and the heat is returned when the flow reverses. The presence of the regenerator is very essential for the performance of the Stirling engine.

In practice, the heat exchange must take place in separate components in form of two heat exchangers to ensure that the heat transfer is sufficient. Heat is added in the hot heat exchanger and heat is removed in the cold heat exchanger.

The different components of the Stirling engine are described in detail later in this chapter.

3.2.3 Mechanical configurations

There exist several different real mechanical embodiments of the Stirling cycle. The configurations are usually divided into three groups, namely Alpha-, Beta- and Gamma-engines (machines) and drive methods are divided into two groups, kinematic drives and free-piston drives.

The three basic configurations are shown in Figure 3.2 (taken from Carlsen [5]).

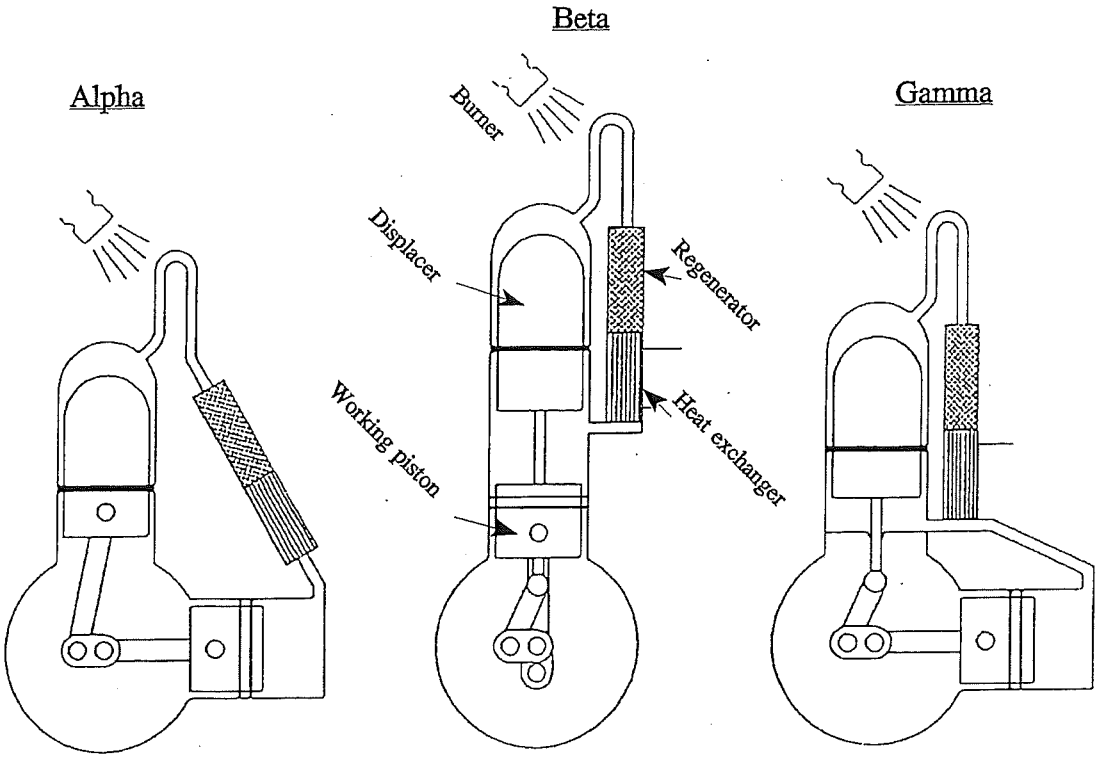

Figure 3.2 Classic Stirling engine configuration.

Alpha-configuration

This configuration has two independent pistons and is very simple mechanically. It is easy to make compact multiple cylinder configuration with high specific power output, which has made this configuration attractive for automotive Stirling engine applications. The main disadvantage is that power has to be transferred from the power producing piston in the expansion volume to the piston in the compression volume (for engine operation).

Beta-configuration

This is the classical Stirling engine configuration. One of the pistons is replaced by a displacer and the piston and displacer are placed in the same cylinder, but there are still two variable volumes.

Gamma-configuration

The Gamma-configuration is basically the same as a Beta-configuration, but the piston and displacer are now placed in two different cylinders. This gives large, unswept (dead) volumes and consequently, a reduction in specific output compared to Alpha- and Beta-engines. Occasionally, the advantage of having two separate cylinders is important and Gamma engines become attractive.

For a further discussion of mechanical configurations, see reference [2].

Kinematic drives

For a kinematic drive, mechanical elements are used to move the pistons in a prescribed manner, implying that volume variations are given and independent of the actual thermodynamic state in the engine. This is the classical way reciprocating engines transfer thermodynamic work to an output shaft. Sinusoidal piston motion is ideal for most of these drive mechanisms, since it gives a quiet engine operation.

For a full description of the geometry and the equations for the motion of the pistons for kinematic drives, see reference [1] or [3].

Free-Piston drives

In a Free-Piston drive, a combination of springs and dampers and the pressure variation of the working gas control the motion of the pistons. Work output is collected using a linear alternator or a hydraulic device. For a description and simple analysis of this drive mechanism, see reference [1].

In the thesis, the main emphasis is laid on the thermodynamics inside the Stirling engine. Further discussion of conditions "outside" the engine, such as the mechanical configuration and drives and the burner system, is therefore omitted.

3.2.4 Components

A practical and very convenient approach to describe a real Stirling engine is to divide it into *components*. These components represent functionally and physically different parts of the engine.

The most simple schematic figure of a Stirling engine is shown in the figure below. This configuration is equivalent of an Alpha-engine, but it can be shown (see the Appendix C) that the two other classical Stirling engine configurations can be reduced to this basic configuration for analysis purposes.

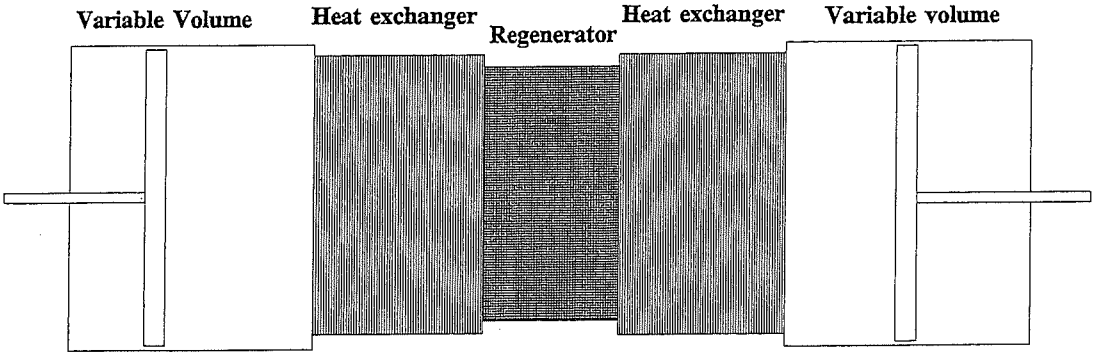

Figure 3.3 The Stirling cycle engine.

The five standard components in any traditional Stirling engine are:

- Two variable cylinder volumes (usually called the compression space and the expansion space) with pistons or displacers for the work transfer.
- Two heat exchangers (the cooler and the heater) for the heat transfer.
- One regenerator for the heat exchange and heat storage.

Dead space between two components is often included as a part of one of these, but for more accurate models, the dead spaces could be treated as separate components in form of so-called manifold volumes.

On the following pages, the Stirling engine components will be described in more detail.

Variable volumes

A variable volume is a cylinder volume, where the total volume varies during the period of the cycle, due to either the movement of pistons or displacers in a prescribed manner for kinematic drives or to working gas pressure variations for free-piston drives. The variable volume has an active swept volume and an inactive clearance volume.

According to the ideal Stirling cycle, a variable volume should be isothermal, but in a real Stirling engine it is closer to adiabatic. In reality, some heat transfer between working gas and the cylinder wall will occur, but the net heat transfer for one cycle will be close to zero. Due to the large heat capacity of the solid wall compared to the working gas and the fast fluctuations in temperature inside the volume, the penetration of temperature changes into the solid wall will be relatively small. This gives rise to the assumption of "cyclic heat transfer" in the variable volumes, which will be explained in detail in a later chapter.

A variable volume in a real engine typically has a relatively large diameter compared to the length (meaning that the bore and stroke are of the same size) and furthermore, a piston or a displacer resides in the volume. All this implies that the flow will be highly irregular and complex inside the component and difficult to model properly.

Heat exchangers

The ideal Stirling cycle has isothermal variable volumes, which is impossible to achieve within the limitations of current technology. Instead, the heat is added and removed from the process through separate components in form of heat exchangers. Integration of heat exchangers in the variable volumes has been used in engines with low specific power, but in modern Stirling engines separate components seem to be the only realistic prospect.

In most Stirling engines, the heat exchangers are made in form of bundles of circular tubes, where the working gas flows inside the tubes. Heat is removed in the cooler by a cooling medium which flows across outside the tubes, while heat is added in the heater, where typically a burner is directly applied on the outside of the heat exchanger tubes.

The heat exchangers can be considered both as a strength and a weakness in the Stirling engine concept. External heat transfer through heat exchangers (opposed to internal combustion heat transfer through chemical reaction) extends the number of usable fuels significantly. In principle, any high temperature heat source may be used for a Stirling engine. Requirements for low pollution can also be achieved in a simple manner compared to internal combustion engines, since the combustion is continuous. On the other hand, the requirements for sufficient heat transfer are critical for the performance of the engine and this can be a problem, especially when air is used as a working gas.

Cold heat exchanger
The cold heat exchanger is placed next to the compression volume, removing heat from the process. Usually water at the ambient temperature is used as cooling medium, which means that the temperature in the cooler typically is in the range of 300-330 K.

Hot heat exchanger
The hot heat exchanger is placed next to the expansion space. Usually heat is added directly using a burner and, due to limitations in the construction materials for the engine, the temperature in the heater is typically restricted to 1000-1100 K.

Regenerator

The regenerator is a very essential part of a Stirling engine and it has primarily two functions:

- Separation of the cold and hot parts of the machine.
- Storage of energy in form of heat when the working gas flows from the hot part to the cold part and returns heat to the gas after flow reversal.

It is critical to the engine performance to obtain very efficient heat transfer from gas to matrix without any significant losses due to friction and heat conduction. Friction losses mean reduction of power output and any heat transport from the hot part to the cold part will also decrease the efficiency of the engine due to the related irreversibilities. The net enthalpy flux carried by the mass flow through the regenerator during one period is (in classic Stirling terminology) usually called the regenerator-loss, and in a well-designed engine this loss should be kept at a minimum.

Most regenerator designs have packs of woven wire screens. The regenerator material is usually stainless steel in form of very thin treads (diameter around 50 μm), but other materials have also been considered. The porosity (defined as the ratio between gas volume and total volume) in the regenerator is 0.65-0.80. All this gives a very large surface area per unit length, which is necessary to obtain the sufficient heat transfer. The friction loss is the limiting factor, and a good compromise (meaning optimum) has to be found for any well-designed Stirling engine.

Manifold volumes and other dead spaces

Dead space between and inside the components in a real engine are inevitable, due to compromises in the practical design. The effect of large dead spaces will be a significant drop in the performance of the engine in form of a lower specific work output, so these volumes should be kept small in a well-designed engine.

3.2.5 Working gas

Since the working gas remains inside the engine, it is possible to use other gases with better properties than atmospheric air.

Air can be used, but the requirements for heat transfer in the heat exchangers and regenerator are critical. Higher molecular weight means higher losses due to friction and lower specific heat capacity means higher requirements for heat transfer. This has been discussed in detail in reference [6] pp.19-28 and it makes air less attractive as a working gas in Stirling engines than for example Hydrogen or Helium.

Hydrogen (H_2) has excellent working gas properties (low molecular weight and high specific heat capacity), but problems are encountered due to constructional and operational considerations. Any leak from an engine using Hydrogen means severe danger for explosion. Furthermore, Hydrogen is more difficult to keep inside the engine because of diffusion.

Helium (He) is used as working gas in many Stirling engines. Helium is a good compromise between obtaining sufficient heat transfer in the heat exchangers and regenerator without losing too much power due to friction losses.

Important properties of matter at different temperatures for these three working gases are shown in the table just below. T is temperature, $\hat{M}$ is molar weight, c_p is specific heat capacity, μ is dynamic viscosity, k is heat conductivity and Pr is the Prandtl number.

	Air			Helium			Hydrogen		
$\hat{M}$ [g/mole]	28.95			4.00			2.02		
T [K]	300	650	1000	300	650	1000	300	650	1000
c_p[kJ/kg·K]	1.007	1.063	1.141	5.193	5.193	5.193	14.31	14.65	14.99
μ [N·s/m^2]	$18.46 \cdot 10^{-6}$	$32.25 \cdot 10^{-6}$	$42.44 \cdot 10^{-6}$	$19.9 \cdot 10^{-6}$	$33.2 \cdot 10^{-6}$	$44.6 \cdot 10^{-6}$	$8.96 \cdot 10^{-6}$		$20.13 \cdot 10^{-6}$
k [W/m·K]	0.0263	0.0497	0.0667	0.152	0.264	0.354	0.183		0.448
Pr	0.707	0.690	0.726	0.680		0.654	0.701		0.673

Table Properties for Air, Hydrogen and Helium (taken from [7]).

3.2.6 Stirling engine operation

In this section a brief summary of typical data for Stirling engine operation is given. Stirling heat pumps and refrigerators could also have been considered, but (as mentioned previously) Stirling engines only will be discussed here.

Typical data:

- Stirling engines run at a speed from 750 to 3000 RPM.
- Helium is mostly used as working gas.
- The temperature of the cold heat exchanger is usually equal to the temperature of the surroundings, i.e., ~ 300 K, while the temperature in the hot heat exchanger is restricted to ~ 1100 K due to limitations of the construction materials.
- Mean pressure is in the range of 1-15 MPa with a relatively small pressure ratio, typically less than two.
- Efficiency of a well-designed Stirling engine is in the range of 0.30-0.40. This could be compared with the Carnot efficiency, which is 0.73 for engine operation between the two temperature levels 300 K and 1100 K.

3.2.7 Applications

Stirling machines have not been widely applied commercially in this century. The only exception has been Stirling refrigerators used for cryogenic applications, where Stirling Cryocoolers have been used successfully for low-temperature generation.

Renewed interest for the Stirling cycle has taken place in many different areas of engineering because of increasing fuel prices during the seventies and recently because of the raising interest in reducing pollution of the environment and reducing noise problems.

Stirling cycle engines have found applications for military use and in the area of Space Power engineering (mainly by NASA). Automotive use of Stirling engines and power production using the sun as heat source have also been considered by some companies.

Small plants and heat pumps for stationary use and requirements of low maintenance, high efficiency and low pollution are applications where the Stirling cycle machines also seem to be very competitive with more traditional technologies.

3.3 Stirling modelling

3.3.1 Introductory remarks

Although the thermodynamics of a Stirling engine is quite complex, it is a standard approach to make a simple physical and mathematical model which may be used for qualitative considerations, such as finding a feasible design or for giving an initial understanding of the basic characteristics of the engine. Only the simplest and most idealized models give closed analytical solutions and therefore computational effort is required to solve the problem for models which in a more realistic way describe the real, thermodynamic conditions.

A computer simulation of the full three-dimensional flow in a real Stirling engine including the effects of friction, heat transfer and turbulence is still not possible even on the supercomputers of today. Furthermore, many of the loss mechanisms in the engine are not fully understood, and others can only be modelled (i.e., approximated) using empirical correlations based on experimental studies. These facts make "engineering" methods, where several simplifications are introduced in the physical model, an obvious alternative. One-dimensional flow is a classical assumption made even in the most sophisticated Stirling models of today. Prediction of real engine performance is often achieved by *calibration*, which basically means adjusting heat transfer coefficients and friction coefficients so that the results from the simulation are consistent with the actual measurements from the real engine.

As mentioned, the complexity of a real Stirling engine makes it necessary to introduce some simplifications into the physical and mathematical model. The variation in detail and accuracy of the different Stirling models can roughly be categorized according to the treatment the following subjects:

- Thermodynamics.
- Gas dynamics.
- Losses.
- Numerical solution method.

3.3.2 Thermodynamics

The thermodynamics of the Stirling engine is usually described by an equation of state for the working gas:

Equation of state
- Ideal gas.
- Van der Waals gas.
- Real gas.

Almost all practical Stirling models employ the ideal gas equation with the additional assumption of constant specific heat capacity.

Process

Alternatively, it is possible to explicitly specify the process. For a very simple model based on the ideal Stirling cycle (see the description in chapter 2), where the working gas is present at one uniform state, isochoric and isothermal changes of state are prescribed. Adiabatic, isentropic or polytropic are other processes which can be more useful in describing the conditions qualitatively in a real Stirling engine.

Properties

- Specific heat capacity (constant pressure) : c_p
- Specific heat capacity (constant volume) : c_v
- Dynamic viscosity : μ
- Heat conductivity : k
- Prandtl number : Pr

The assumption of constant properties is made in most Stirling simulation models, but this is often difficult to justify completely. Variations in Prandtl number and heat capacity as a function of pressure and temperature are relative small. For the considered working gases (Helium, Hydrogen and Air), the variation is less than 10% in the temperature range from 300 to 1000 K. In contrast, the dynamic viscosity and the heat conductivity vary by a factor 2-2.5 for all three gases, and make the assumption of constant properties very dubious (see the table on page 3.8).

3.3.3 Gas dynamics

Continuous / Discontinuous piston motion

In the Stirling models, the flow is generated from continuous or discontinuous piston motion. Only the most simple models based on the ideal Stirling cycle apply the discontinuous piston motion. All other more realistic models use either a mathematical expression for the variation in volume (e.g., sinusoidal variation) or even better, a system of dynamic equations describing the true kinematics of the drive linkage.

Conservation equations

For continuous flows, the equations of mass, momentum and energy are applied to describe the flow through the Stirling engine. The mathematical model must at least include the equations for conservation of mass and energy, while the full momentum equation can be omitted under certain assumptions as discussed next.

Coupled / Decoupled equations.

The momentum equation should also be included into the system of equations to describe the true flow field, but simplifying assumptions, which will be of great advantage for obtaining a quick and stable numerical solution, may be used to eliminate the direct use of this equation.

In a well-designed Stirling engine, the pressure gradient in space is relatively small, such that only small fluctuations around the spatial mean pressure are produced. It can then be argued that the main effect of the pressure gradient is to change the pressure on the pistons reducing work output.

Assuming that the spatial pressure distribution is due to friction only and using a quasi-steady approximation of the momentum equation (meaning that the time dependent term is ignored), *decouple* the momentum equation from the mass and energy equations. This will significantly simplify the numerical solution of the problem, since the small time constants introduced by the true momentum equation are eliminated.

The calculated pressure gradient can then be used to make corrections to the pressure on the pistons for the computation of work. A special simple case is the assumption of a uniform pressure in space meaning that the influence of friction also has been neglected.

Dimensions

Real flow in a Stirling engine is at least two-dimensional in some parts of the engine. Due to the complexity of the problem (geometry, modelling of losses etc.) and the requirements for computational effort, all current Stirling models are still one-dimensional at most.

Employing a one-dimensional mode with the formulation of the equations for conservation of mass, momentum and energy, implies that several important characteristics of the flow have to be modelled empirically. Viscous stresses, convective heat transfer and turbulence are multidimensional phenomena implying that friction and heat convection between gas and solid walls must be modelled using empirical correlations, or other simplifications must be introduced to account for these effects. For a differential formulation of the conservation equations, the solution to the governing system of partial differential equations will give a variation of the state variables in both time and space, while for a simplified "lumped" formulation the spatial variation within each volume will be lost.

3.3.4 Losses

Modelling of losses is an important feature of any simulation model of a Stirling engine. Losses can be defined as conditions, which degrades the performance of the real engine compared to the ideal theoretical Stirling cycle. Any irreversibility, such as friction, finite heat transfer or heat conduction, will reduce the efficiency of the engine from the Carnot efficiency of the ideal Stirling cycle. The losses can roughly be put into two categories, external and internal losses.

External losses

External losses, such as mechanical friction associated with the drive mechanisms and burner losses, are very specific for the given design and are not directly related to the thermodynamic process. These losses will not be considered in further detail here. Most Stirling simulation models deal separately with the external and internal losses. The actual simulation includes the internal losses and the results are then given in form of indicated work and efficiency. These results must be adjusted using corrections for the external losses (in form of mechanical efficiency, burner efficiency etc.) in order to be related to the experimental brake output.

Internal losses

The internal thermodynamic losses can be accounted for in a full rigorous three-dimensional model, but for a realistic one-dimensional model, empirical correlations will have to be used for the modelling of convection heat transfer and friction losses. For Stirling engines recent research subjects have included:

Heat transfer
- Oscillating flow heat transfer (heat transfer coefficients and correlations).
- Effects of turbulence (transition).
- Heat transfer in variable volumes (convection and conduction).
- Effects of acoustics phenomena (enhanced heat transfer).

Friction
- Oscillating flow friction (friction factors and correlations).
- Effects due to the geometry (entrance/exit friction losses).
- Effects of turbulence (transition).
- Effect of acoustic phenomena.

Many experimental studies of friction and heat transfer in oscillating flows have been carried out during recent years (see reference [8] and [9] for a review). Though providing insight in the complicated processes, the research has not given any clear conclusions and in particular no general expression for neither friction factors nor heat transfer coefficients.

As a consequence (i.e., in the lack of any better alternatives), the use of steady flow correlations (often called quasi-steady approximation) for convection heat transfer and friction coefficients has become standard approach in Stirling modelling and simulation. This observation is also true for recently developed Stirling codes, although some of these experimental studies have showed that for example steady flow correlations for friction in regenerators can both underpredict and overpredict the actual values in oscillating flows.

Heat transfer in the variable volumes is another complicated problem. The flow conditions, including inflow/outflow, turbulence, large diameter-to-length ratio, oscillating flow, expansion cooling and compression heating, are some of the major concerns for the modelling. Gedeon [10] introduces an enhanced conduction to include the effect of turbulence.

Acoustic phenomena (pressure information propagation) and the influence on heat transfer and friction has been discussed by Rix [11] and Organ [3] pp.196-208.

Other more specific losses include (see [1] pp.125-151 for a detailed discussion):

- Conduction losses.
- Gas spring hysteresis losses.
- Seal leakage.
- Appendix gap losses.
- Displacer conduction losses.

Characteristically, these so-called parasitic losses are very specific for the given Stirling engine design and often difficult to model properly (due to complexity of geometry, flow and heat transfer conditions). Parasitic losses are typically small (less than 5-10% of the work output, see [1] pp.126), but still not insignificant for the overall performance of the engine, and a simulation program used for design of real Stirling machines must take these losses into account.

It has not been the intention to give a full and comprehensive review of problems in modelling of losses in Stirling machines, but only to illustrate some of the difficulties that are to be encountered when trying to make a general and rigorous Stirling model. Most simulation programs for Stirling engines neglect the parasitic losses and use some kind of calibration (i.e., calibrating factors introduced in the equations to correct losses) to predict the performance of a given engine. Other models do not account for losses during the actual simulation, but settle with correcting work output and heat transfer afterwards. This makes it possible to study the significance of each of these losses, but the influence on the thermodynamic behavior is lost.

If all of the losses are directly included in the model, it can be difficult to single out one specific loss mechanism. To deal with this problem, sophisticated Stirling simulation models incorporate calculation of the entropy production (using the second law of thermodynamics) to identify the thermodynamic losses in the engine. This makes it possible to evaluate and compare the losses, and at the same time retain the influence on the thermodynamic behavior.

3.3.5 Numerical methods

Only the most simple Stirling models give closed form analytical solutions, but for all other cases an approximate numerical solution must be found. Depending on the formulation of the physical and mathematical model, obtaining a numerical solution usually involves a discretization in space and time, a choice of a numerical method and the implementation into computer code. Validation and verification of the obtained results should also be carried out.

"Lumped" formulation

For a so-called "lumped" formulation (or lumped parameter formulation), each component in the Stirling engine is treated as one single control volume (this corresponds to a Finite-Volume type formulation on a very coarse grid). The spatial variation of the state variables inside the components will be lost, and the obtained values for the variables from the numerical solution can only be considered as average values in space.

The equations for conservation of mass, momentum and energy will be given in form of a system of ordinary differential equations (ODEs), and these will be coupled with algebraic equations from the equations of state. A numerical method for the time integration is required for solving the resulting system of differential-algebraic equations (DAEs).

Classical methods for solving initial-value problems (IVPs) include:
- Multistep methods.
- Runge-Kutta methods.

Continuous formulation

More sophisticated Stirling models take the spatial variation into account and the equations of conservation of mass, momentum and energy are now given as a system of partial differential equations (PDEs).

Classical methods for solving systems of PDEs include

- Finite-Difference.
- Finite Volume.
- Finite-Element.
- Spectral methods.
- Method of Characteristics.
- Method of Lines.

Finite-Difference methods and *Finite-Volume* methods [12] are classical methods used in Stirling analysis. For a one-dimensional model, the discretized equations for these two methods are almost identical when the equations are kept on a recommended conservation form (such that the numerical solution also satisfies the conservation equations).

Finite Element methods have not been much used in Stirling analysis. This is probably because the advantageous features of these methods disappear for simple geometries, one-dimensional flow and simple boundary conditions. A Finite-Element method has been used by Olsen and Andersen [13] in a simulation model for a regenerator in a Stirling heat pump.

Spectral methods have been used in simple forms. Since the steady-state solution is periodic in time, all the variables can very naturally be resolved in periodic functions. Qvale and Smith [14] seem to be some of the first to suggest this idea for Stirling engine analysis.

The *Method of Characteristics* is strongly advocated by Organ [3] and Taylor has also used this method in his code [15]. It should be noted that the method only can be used for hyperbolic systems (i.e., for systems that show wavelike behavior and no dissipation).

The *Method of Lines* uses a spatial discretization to generate a system of ordinary differential equations, which then is solved using a classical numerical method for ODEs at each discretized point.

The different methods have different characteristic numerical properties, but so far no single approach (model and method) has turned out to be significantly better. Every Stirling researcher has his own code, and only very few comparisons have been made.

Almost all Stirling codes solve the problem of finding the periodic solution as an initial-value problem. This means that the periodic solution is found by integrating forward in time until the cyclic conditions are reached. It could take hundreds of cycles or maybe thousands if an assumption of finite heat capacity of the regenerator is included in the model.

3.3.6 Classic Stirling analysis

Some confusion also exists when it comes to classification of the different Stirling models. Unfortunately, many Stirling people classify the degree of sophistication of a model in terms of *order*, e.g., a first order model or a third order analysis. Definitely, this must not be confused with the order of accuracy of the applied numerical method. The results obtained from a "higher" order analysis are not necessarily closer to the real conditions than the results obtained from a "lower" order analysis and the term will not be used further here in connection with the classification of the Stirling models.

Next, some traditional Stirling models are very briefly reviewed.

Ideal isothermal analysis

The assumption of isothermal volumes is made only in the most trivial Stirling models. The most simple of these is the model of the ideal Stirling cycle (see chapter 2), which is described in detail in all standard Stirling text books.

The efficiency is identical to that of the Carnot cycle, and the model overpredicts both the capacity and the efficiency of a real engine. Though of little value in predicting the performance of a real Stirling engine, the model of the ideal cycle can be useful for establishing a standard reference, since it gives the optimal performance of a Stirling engine.

Schmidt analysis

For a long period (from the last century to the modern age of computers) Stirling analysis was more or less restricted to the model developed by Schmidt in 1871. In the Schmidt analysis, the classical five Stirling components can be recognized. The assumption of isothermal volumes is kept, but regenerator and heat exchangers now have internal volumes, there is a linear temperature gradient in the regenerator and the pistons move in a sinusoidal pattern.

The Schmidt analysis gives closed form analytical solutions (see Appendix B). There are no irreversibilities and the efficiency of the Schmidt analysis is still identical to the ideal cycle, but the presence of dead volumes makes the prediction of the specific output lower and closer to the real engine. Schmidt analysis is still applied for basic analysis of feasible Stirling engine operation.

Adiabatic analysis

Closed form analytical solutions cannot be found when the assumptions of isothermal volumes are deserted, and a numerical solution must be found instead. Some of the first models without the assumption of isothermal variable volumes were developed in the early 1960's by Finkelstein. Conditions in the expansion and compression volume could be specified anywhere from adiabatic to isothermal, but the assumptions of perfect regeneration and isothermal heat exchangers are maintained from the Schmidt analysis.

Real analysis

Departing from the simple approach and introducing real effects such as

- finite heat transfer in the regenerator
- finite heat capacity of the regenerator matrix
- finite heat transfer in the heat exchangers
- heat transfer in cylinder volumes
- flow losses (friction)

in the physical model implies that the solution to the corresponding mathematical model must be found numerically.

The next and most sophisticated level in current Stirling analysis involves a discretization in space (in Stirling literature often called nodal analysis) so that the spatial variation of the variables can be found. Such a model has potential of high accuracy compared to a model based on a lumped formulation. For a discretization with a sufficiently high number of volumes (cells, nodes or grid points) and time steps, this can yield a very accurate solution, provided that the expressions used for modelling of heat transfer, friction and other losses are appropriate. The immediate problem is, of course, the increasing CPU-time required (so far only one-dimensional models have been considered) and the problem of modelling losses, which has been addressed previously in this chapter.

In practice, all Stirling models use the quasi-steady approximation, where the heat transfer coefficients and friction factors are calculated using correlations for stationary flow, but with the instantaneous value of the Reynolds number. Corrections (calibration) can then be made to adjust the calculated values against measured experimental values. All new Stirling codes are of this type, but their success in predicting real engine performance has not been overwhelming compared to the much simpler analysis based on a lumped formulation. This is primarily accredited to the inability of properly modelling the losses.

A sophisticated Stirling model should include some of the following physical effects:

- Turbulence (non-adiabatic, compression/expansion, oscillatory flow).
- Heat transfer in heat exchanger (oscillatory flow, compression/expansion).
- Heat transfer in regenerator (oscillatory flow).
- Heat transfer in variable volumes from gas to the solid walls.
- Heat transfer from gas to piston or displacer.
- Leak flow.
- Pressure losses in heat exchanger and regenerator.
- Complex inlet/outlet conditions of components (turbulence, pressure loss).
- Heat conduction in regenerator matrix and gas.
- Real gas.
- Non-constant properties of matter (dependency on temperature).
- Parasitic losses.

Some of these are of course more crucial for predicting the performance, but if most are neglected the obtained results will be useless in real Stirling engine simulation and design.

3.3.7 State-of-the-art in Stirling analysis

There exist many simulation models and codes for Stirling analysis. Almost every Stirling researcher has his own code, which has its specific features. Simple codes are available from universities or as public domain, but all the sophisticated codes are either expensive, commercial codes or even unavailable.

State-of-the-art simulation programs in Stirling analysis which have been described in the literature include the following codes: MS*2, HFAST and GLIMPS. These three codes are all commercial codes used for the design and analysis of real Stirling engines, and they cover the most common approaches very well.

MS*2

The MS*2 code is developed by Mitchell/Stirling Machines/Systems Inc. and described by Bauwens and Mitchell in several papers (see [16], [17] and [18]).

The code solves a one-dimensional model of an initial-boundary value problem. Partial differential equations for conservation of mass, momentum and energy are formulated in conservation form for the working gas and coupled with the equation of state for an ideal gas to give the necessary equations. Empirical coefficients for convection and friction determined from steady flow experiments are used with the local, instantaneous Reynolds number.

MS*2 is closer to traditional codes (for solving the Euler equations) from the area of Computational Fluid Dynamics than any of the other codes. The code uses a fixed grid and 1.order, monotone, explicit finite-difference scheme of Godunov type, which means that the scheme is first order accurate in both time and space, and it can handle discontinuities (relevant for flow reversals and abrupt changes in flow areas). It requires many time steps to obtain an accurate solution because of numerical diffusion introduced by the low order discretization in space. The cyclic solution is found by dealing with the problem as an initial-value problem, and solving it by marching forward in time until the solution becomes periodic.

HFAST

HFAST is developed at Mechanical Technology Inc. (MTI) as a further development of HSCAC-code described by Rausch [19] in 1980. This code is used by NASA and its contractors.

The model is also one-dimensional and uses a control volume formulation of the problem. All variables which are periodic functions of time are represented by their Fourier series and the variables are approximated by the second order harmonics. The equations are resolved using a Discrete Fourier Transform (DFT). The model enforces the conservation laws for mass, momentum and energy up to the first of the harmonics. A Fast Fourier Transform (FFT) is applied for the numerical solution and the periodic conditions are found in a few iterations. For a further discussion of the HFAST code, see [20].

GLIMPS

GLIMPS (GLobally-IMPlicit Stirling cycle simulation) is developed by Gedeon [21]. The first version of this code occurred in 1986 and in 1992 version 4.0 [22] has been released for commercial use. This code is also used by NASA and its contractors [23].

The model is spatially one-dimensional. Up to seven components can be defined, the number of computational cells (sub volumes) in each component can be specified by the user, and the number of time steps pr. cycle is also set by the user. The governing equations (conservation of mass, momentum and energy for the working gas and conservation of energy for the solid walls) are discretized in both time and space, and the resulting system of discretized equations are solved using a Newton type method. In this way, the full cyclic solution is obtained directly. In an early version of the code the NTU-number and friction factors were calculated from a simplified analysis in a separate routine.

Stirling Machine Simulation Program (SMSP) version 2.3

This is the simulation model and code, developed and used by Carlsen at the Laboratory for Energetics. The code [24] has been used in the design of several Stirling engines and heat pumps.

This simulation program uses a lumped parameter formulation. Steady flow correlations are applied for the calculation of heat transfer and friction. Corrections for friction (reducing work output), shuttle conduction, pumping loss, mechanical loss and piston ring losses are made after the actual calculation of the periodic thermodynamic state variables.

Time integration of the resulting system of ordinary differential equations is performed using a fourth order explicit Runge-Kutta method with variable step length (error estimates based on Richardson extrapolation). The periodic solution is found from integration of the initial value problem forward in time, until the periodic steady state is reached. This is combined with a secant type iteration on parameters, which must be adjusted to fulfill certain conditions from the periodic steady-state operation.

Remarks

- The limitations in the physical and mathematical models, which the different codes have been based on, can be very difficult to uncover.
- Most codes require some kind of calibration before they are capable of giving reliable predictions for the performance of a specific type of engine.
- It is difficult to find comparisons of the different models with regard to their numerical properties, such as accuracy and speed. Not many benchmark tests can be found in the literature.

3.3.8 Selecting a Stirling model

When selecting or developing a simulation model for a Stirling engine, it is important to know whether the simulation model should be used just for finding a feasible design or it should be used for design optimization and prediction of real engine performance.

Feasible design

In order to a feasible design, exploring basic properties of the Stirling cycle or establishing a general frame of reference for Stirling engine performance, a simple model is very helpful. Using only a few basic parameters (such as swept volume, temperature in hot heat exchanger, temperature in cold heat exchanger, etc.) it is much easier to keep the general overview and the significant results will not disappear due to small unimportant details or large amount of output data. Furthermore, the effort required to obtain a solution will be small compared to more sophisticated models.

Optimal design

For optimal design or real engine performance simulation, a more sophisticated Stirling model is required. The model should include a large number of very specific parameters describing the giving configuration including geometry, drive mechanism and component characteristics. Empiricism should be included in the simulation model as little as possible.

Numerical results from the simulation have to be accurate and consistent, especially when used as input for an optimization routine.

3.4 Concluding Remarks

Due to the complexity of the problem, a compromise between the accuracy of the physical model and the required computational effort must be made. It is important not to underestimate the fast development of new and faster computers. Calculation tasks which seemed almost impossible just a few years ago, is now possible even on a small 486-based PC. This fact has made it possible to make more complex and accurate models without being too uneconomical in computing time or money. Since the hardware improvements seem to continue, it is tempting to try to develop new and even more sophisticated Stirling codes.

Still, making a two-dimensional model, closer to the true fluid dynamics of the problem, seem to be problematic, especially as long as the problem of modelling losses is not fully resolved.

References

[1] Urieli, I. and Berchowitz, D.M.
Stirling Cycle Engine Analysis.
Adam Hilger Ltd, Bristol (1984).

[2] Walker, G.
Stirling Engines.
Oxford University Press, Clarendon, Oxford (1980).

[3] Organ, A.J.
Thermodynamics and Gas Dynamics of the Stirling Cycle Machine.
Cambridge University Press (1992).

[4] Hargreaves, C.M.
The Phillips Stirling Engine.
Elsevier (1991).

[5] Carlsen, H.
Stirling motorer vol II. (Stirling Engines vol. II.)
Laboratory for Energetics, The Technical University of Denmark (1993).

[6] Andersen, N.E. and Qvale, B.
Mathematical Models in Energetics Vol. VI: Heat Exchangers.
Laboratory for Energetics, the Technical University of Denmark (1986).

[7] Incropera, F.P. and De Witt, D.P.
Fundamentals of Heat and Mass Transfer.
John Wiley and Sons (1985).

[8] Tew, R.C.
Status of Several Stirling Loss Characterization Efforts and their Significance for Stirling Space Power Development.
23rd IECEC proceedings, pp.113-119 (1988).

[9] Tew, R.C., Thieme, L.G. and Dudenhoefer, J.E.
Recent Stirling Engine Loss-Understanding Results.
25th IECEC proceedings, pp. 377-382 (1990).

[10] Gedeon, D.
GLIMPS version 3.0 User's Manual.
Gedeon Associates (1990).

[11] Rix, D.H.
Some observations of the behavior of a High Performance Stirling Machine.
19th IECEC proceedings (1984).

[12] Hirsch, C.
Numerical Computation of Internal and External flows, vol I and II.
Wiley (1991).

[13] Olsen, N.K. and Andersen, N.E.
Simuleringsmodel for Stirling varmepumpe. (Simulation Model for Stirling Heat Pump)
Laboratory for Energetics, the Technical University of Denmark (1986).

[14] Qvale, E.B. and Smith, J.L.
A Mathematical Model for Steady Operation of Stirling Type Engines.
Trans. ASME Journal Engineering for Power Jan. 1968, pp.45-50.

[15] Taylor, D.R.
The Method of Characteristics Applied to Stirling Engines.
19th IECEC proceedings, pp. 2037-2042 (1984).

[16] Bauwens, L.
Stirling Engine Modeling: The MS*2 Code.
ISEC 6th International Stirling Engine Conference pp. 371-376 (1993).

[17] Bauwens, L.
Consistency, Stability, Convergence of Stirling Engine Models.
25th IECEC proceedings, vol. 5 pp.352-358 (1990).

[18] Mitchell, M.P and Bauwens, L.
Validation of Numerical Models: Empiricism vs. The Laws of Physics.
25th IECEC proceedings, pp.424-429 (1990).

[19] Rauch, J.S.
Harmonic Analysis of Stirling Engine Thermodynamics.
15th IECEC proceedings, pp.1696-1700 (1980).

[20] Huang, S.C.
HFAST - A Harmonic Analysis Program for Stirling Cycles.
27th IECEC proceedings, pp. 5.47-5.52 (1992).

[21] Gedeon, D.
A Globally-Implicit Stirling Cycle Simulation.
21st IECEC proceedings, vol.1, pp. 550-554 (1986).

[22] Gedeon, D.
GLIMPS version 4.0 User's manual.
Gedeon Assiciates (1993).

[23] Geng, S.M. and Tew, R.S.
Comparison of GLIMPS and HFAST Stirling Engine Code Predictions with Experimental Data.
27th IECEC proceedings, pp.5.53-5.58 (1992).

[24] Carlsen, H.
10 KW Stirling Engine for Stationary Applications.
ISEC 6th International Stirling Engine Conference (1993).

4.0 MODELLING

4.1 Introduction

The modelling process involves several stages. First a physical model must be developed. The physical model has to be translated into a mathematical model and then a numerical solution must be implemented. Finally, an evaluation of the model and of the results obtained should be considered.

It is important to try to make a distinction between the different stages, when making a simulation model for a thermodynamic device. The advantage of this approach is that it will be easier to see the significance of each approximation and to identify the problems.

The modelling process includes an important element of feedback. It is natural to start with the formulation of a physical model, but changes can and will be made during the later stages. The final simulation model will be a compromise of the approximations and considerations made in each stage.

4.2 Physical model

The development of a satisfactory physical model of the given problem is probably the most important part of modelling.

Making a physical model involves an accurate and detailed description of the problem including:

- Formulation of the problem.
- Description of the system.
- Classification.
- Identification of variables and parameters.
- List of assumptions.
- Evaluation of assumptions.

It is impossible to take everything into account, but a reliable physical model should include all significant features of the problem.

In reality, for all complex problems a compromise between accuracy of the model and accuracy of the numerical solution has to be made.

A very sophisticated physical model of a thermodynamic device, which is close to the real conditions, can include three-dimensional, viscous, compressible flow with effects from turbulence, complex geometry, chemical reaction etc. This cannot be solved numerically when translated into a mathematical model. It is still too expensive computationally even for the super computers of today.

On the other hand, a simple physical and mathematical model may be solved using sophisticated and accurate numerical methods, but the results will not be closer to the real conditions, than the design of the model permits.

The Stirling engine could be an example. The real flow is three-dimensional, compressible and turbulent, and is affected by expansion and compression. Heat transfer conditions are very complex, and flow friction in regenerator and heat exchangers are not negligible. As a consequence of this complexity, there exists no operational simulation programs based on true two or three-dimensional models for flow in Stirling engines.

4.3 Mathematical model

General classes of equations can be identified when translating the physical model of the problem into a mathematical model. Of course, the specific choice of equations depends on the actual problem, but in the area of fluid mechanics and thermodynamics the following types of equations are common:

General conservation laws:
- Conservation of mass.
- Conservation of momentum.
- Conservation of energy.

Constitutive equations:
- Equation of state.
- Stress.
- Heat conduction.

Empirical correlations:
- Turbulence.
- Convection heat transfer.
- Friction.

The motion of a continuous medium is governed by the general Navier-Stoke's equations which express conservation of mass, momentum and energy. Combined with an equation of state for the medium, the flow is fully described for laminar flow. For turbulent flow additional information is required, usually in the form of a k-ε model for the Reynold's stresses.

For an incompressible fluid the flow field is known if the velocity field and one static property (pressure) are known. For a compressible fluid an additional static property (usually density or temperature) must also be known.

In the following, an overview of the types of equations, which are used for modelling of a thermodynamic device, will be given.

First conservation laws are discussed, and the equations for three-dimensional, one-dimensional and "lumped" formulation are given. Then examples of constitutive relations are given, and finally modelling of friction and heat transfer is discussed.

The principal formulation of the equations may be done in two different ways, an Eulerian or a Lagrangian formulation.

In an Eulerian approach the characteristic properties of the fluid are considered as a function of space and time, e.g., $U=U(t,x_1,x_2,x_3)$. This is different from a Lagrangian approach, where the properties of each material flow particle are the dependent variables. A flow particle is described by its position, velocity, temperature etc. For some problems (moving boundaries or interfaces) a Lagrangian or a combined Eulerian-Lagrangian approach could simplify the problem, but generally an Eulerian approach is used in fluid dynamics.

For other problems (turbomachinery in particular) a rotating frame of reference could be advantageous, but otherwise a fixed (absolute) frame of reference is natural.

A fixed frame of reference and an Eulerian formulation is only considered here.

4.3.1 Conservation laws

General form of a conservation law

Consider a finite volume Ω with a surface S

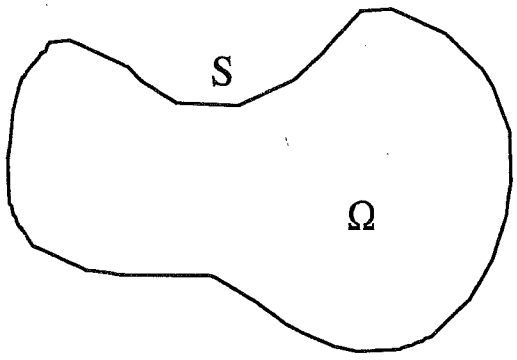

Figure 4.1 Control volume Ω with surface S

For a scalar quantity U, a general conservation equation in *integral form* can be written as

$$\frac{d}{dt}\int_{\Omega} U\cdot d\Omega + \int_{S} \underline{\Phi}\cdot d\underline{S} = \int_{\Omega} \Gamma_{\Omega}\cdot d\Omega + \int_{S} \underline{\Gamma}_{S}\cdot d\underline{S} \qquad (4.1)$$

where $\underline{\Phi}$ is the flux through the surface S, Γ_{Ω} and $\underline{\Gamma}_{S}$ are the volume and surface sources respectively.

For a vector quantity $\underline{U}$ the equation has the following form

$$\frac{d}{dt}\int_{\Omega} \underline{U}\cdot d\Omega + \int_{S} \underline{\underline{\Phi}}\cdot d\underline{S} = \int_{\Omega} \underline{\Gamma}_{\Omega}\cdot d\Omega + \int_{S} \underline{\underline{\Gamma}}_{S}\cdot d\underline{S} \qquad (4.2)$$

Now the flux $\underline{\underline{\Phi}}$ is a tensor, the volume source $\underline{\Gamma}_{\Omega}$ is a vector, and the surface source $\underline{\underline{\Gamma}}_{S}$ may be written as a tensor.

The integral form of the conservation laws is the most general, and remains valid even when flow discontinuities are present.

However, if the properties of the medium and the flow are continuous and sufficiently differentiable then, using Gauss' theorem, the two equations can be transformed into the following:

Scalar case:

$$\frac{\partial U}{\partial t} + \underline{\nabla}\cdot\underline{\Phi} = \Gamma_{\Omega} + \underline{\nabla}\cdot\underline{\Gamma}_{S} \qquad (4.3)$$

Vectorial case:

$$\frac{\partial \underline{U}}{\partial t} + \underline{\nabla}\cdot\underline{\underline{\Phi}} = \underline{\Gamma}_{\Omega} + \underline{\nabla}\cdot\underline{\underline{\Gamma}}_{S} \qquad (4.4)$$

where $\underline{\nabla}$ denotes the gradient operator.

These last two equations are the general conservation equations in *differential form.*

Conservation equations in a three-dimensional formulation

The classical conservation equations for mass, momentum and total energy in a three-dimensional formulation can be found in standard text books, e.g., [1]. The equations will be given here with the main purpose of introducing the equations and variables used in the mathematical models developed later.

Conservation of mass

$$\frac{d}{dt}\int_{\Omega}\rho\cdot d\Omega + \int_{S}\rho\underline{u}\cdot d\underline{S} = 0 \tag{4.5}$$

where ρ is the density and $\underline{u}$ is velocity vector.

Given the necessary assumptions and using Gauss' theorem, the equation can be transformed into differential form

$$\frac{\partial\rho}{\partial t} + \underline{\nabla}\cdot\rho\cdot\underline{u} = 0 \tag{4.6}$$

or written out in full

$$\frac{\partial\rho}{\partial t} + \frac{\partial(\rho\cdot u_1)}{\partial x_1} + \frac{\partial(\rho\cdot u_2)}{\partial x_2} + \frac{\partial(\rho\cdot u_3)}{\partial x_3} = 0 \tag{4.7}$$

Conservation of Momentum

$$\frac{d}{dt}\int_{\Omega}\rho\cdot\underline{u}\cdot d\Omega + \int_{S}\rho\cdot\underline{u}\cdot(\underline{u}\cdot d\underline{S}) = \int_{\Omega}\rho\cdot\underline{f}_e\cdot d\Omega + \int_{S}\underline{\underline{\sigma}}\cdot d\underline{S} \tag{4.8}$$

where $\underline{f}_e$ is the external force and $\underline{\underline{\sigma}}$ is the stress tensor.

For an isotropic and homogeneous fluid the stress tensor $\underline{\underline{\sigma}} = \sigma_{ij}$ (i,j = 1,2,3) can be written as

$$\sigma_{ij} = \tau_{ij} - p\cdot\delta_{ij} \tag{4.9}$$

where τ_{ij} is the deviatoric stress, p is the pressure of a fluid, which is defined as

$$p = -\frac{1}{3}\cdot\sigma_{kk} = -\frac{1}{3}\cdot(\sigma_{11} + \sigma_{22} + \sigma_{33}) \tag{4.10}$$

and δ_{ij} is Kronecker's delta.

For a fluid at rest and free of shear the deviatoric stress is zero and the state of stress is isotropic. The (hydrostatic) pressure is identical to the thermodynamic pressure of equilibrium. For a fluid in motion the pressure of the fluid can only be identified as the thermodynamic pressure under the assumption of local equilibrium (this will always be assumed in the following considerations).

For a Newtonian fluid the constitutive relationship for the stress tensor can be given in form of the shear stress tensor τ_{ij} as

$$\tau_{ij} = \mu \cdot \left(\left(\frac{\partial u_i}{\partial x_j} + \frac{\partial u_j}{\partial x_i} \right) - \frac{2}{3} \frac{\partial u_k}{\partial x_k} \cdot \delta_{ij} \right) \tag{4.11}$$

where μ is the dynamic viscosity.

The stress tensor will here just be written in form

$$\underline{\underline{\sigma}} = -p \cdot \underline{\underline{I}} + \underline{\underline{\tau}} \tag{4.12}$$

where p is the isotropic pressure, $\underline{\underline{I}}$ is the unit tensor and $\underline{\underline{\tau}}$ is the shear stress tensor.

Inserting this and rearranging some terms gives

$$\frac{d}{dt} \int_{\Omega} \rho \cdot \underline{u} \cdot d\Omega + \int_{S} \left(\rho \cdot \underline{u} \cdot \underline{u} + p \cdot \underline{\underline{I}} - \underline{\underline{\tau}} \right) \cdot d\underline{S} = \int_{\Omega} \rho \cdot \underline{f}_e \cdot d\Omega \tag{4.13}$$

Applying Gauss' theorem to this equation leads to the differential form of the equation of motion

$$\frac{\partial}{\partial t} \left(\rho \cdot \underline{u} \right) + \underline{\nabla} \cdot \left(\rho \cdot \underline{u} \otimes \underline{u} + p \cdot \underline{\underline{I}} - \underline{\underline{\tau}} \right) = \rho \cdot \underline{f}_e \tag{4.14}$$

where $\otimes$ denotes the vector product.

Conservation of Energy

The specific total energy e is defined as

$$e = i + \frac{1}{2}\cdot\underline{u}^2 \tag{4.15}$$

where i is the specific internal energy and the last term is the kinetic energy, while the term for the potential energy has been omitted.

The energy equation is

$$\frac{d}{dt}\int_{\Omega}\rho\cdot e\cdot d\Omega + \int_{S}\rho\cdot e\cdot\underline{u}\cdot d\underline{S} = \int_{\Omega}\dot{w}_e\cdot d\Omega + \int_{S}\underline{\dot{w}}_S\cdot d\underline{S} + \int_{S}\underline{\dot{q}}_D\cdot d\underline{S} + \int_{\Omega}\dot{q}_v\cdot d\Omega + \int_{S}\underline{\dot{q}}_s\cdot d\underline{S} \tag{4.16}$$

$\dot{w}_e$ is the work done by external forces, i.e.,

$$\dot{w}_e = \rho\cdot\underline{f}_e\cdot\underline{u} \tag{4.17}$$

$\underline{\dot{w}}_s$ is the work done on the fluid by internal shear forces acting on the surface, i.e.,

$$\underline{\dot{w}}_s = \underline{\underline{\sigma}}\cdot\underline{u} = -p\cdot\underline{u} + \underline{\underline{\tau}}\cdot\underline{u} \tag{4.18}$$

$\underline{\dot{q}}_D$ is the diffusive heat flux, which is usually written in form of Fourier's law of heat conduction

$$\underline{\dot{q}}_D = -k\cdot\underline{\nabla}T \tag{4.19}$$

where k is the thermal conductivity and T is the temperature.

$\dot{q}_v$ represents volume heat sources (e.g., radiation, chemical reaction).

$\underline{\dot{q}}_s$ represents the surface heat sources (e.g., convection heat transfer).

Inserting this in the expression above gives

$$\frac{d}{dt}\int_{\Omega}\rho\cdot e\cdot d\Omega + \int_{S}\left((\rho\cdot e + p - \underline{\underline{\tau}})\cdot\underline{u} + k\cdot\underline{\nabla}T - \underline{\dot{q}}_s\right)\cdot d\underline{S} = \int_{\Omega}(\rho\cdot\underline{f}_e\cdot\underline{u} + \dot{q}_v)\cdot d\Omega \tag{4.20}$$

or

$$\frac{d}{dt}\int_{\Omega}\rho\cdot e\cdot d\Omega + \int_{S}\left((\rho\cdot H - \underline{\underline{\tau}})\cdot\underline{u} + k\cdot\underline{\nabla}T - \underline{\dot{q}}_s\right)\cdot d\underline{S} = \int_{\Omega}(\rho\cdot\underline{f}_e\cdot\underline{u} + \dot{q}_v)\cdot d\Omega \tag{4.21}$$

where the total enthalpy (or stagnation enthalpy) H has been defined as

$$H = i + \frac{p}{\rho} + \frac{1}{2}\cdot\underline{u}^2 = e + \frac{p}{\rho} \tag{4.22}$$

The differential form of the conservation of energy equation is then given as

$$\frac{\partial}{\partial t}(\rho\cdot e) + \underline{\nabla}\cdot\left((\rho\cdot e + p - \underline{\underline{\tau}})\cdot\underline{u} + k\cdot\underline{\nabla}T - \underline{\dot{q}}_s\right) = \rho\cdot\underline{f}_e\cdot\underline{u} + \dot{q}_v \tag{4.23}$$

The Navier-Stoke's equations can now be written in the form

$$\frac{\partial\underline{U}}{\partial t} + \underline{\nabla}\cdot\underline{\underline{\Phi}} = \underline{\Gamma} \tag{4.24}$$

where

$$\underline{U} = \begin{bmatrix} \rho \\ \rho\cdot u_1 \\ \rho\cdot u_2 \\ \rho\cdot u_3 \\ \rho\cdot e \end{bmatrix} \qquad \underline{\Gamma} = \begin{bmatrix} 0 \\ \rho\cdot f_{e1} \\ \rho\cdot f_{e2} \\ \rho\cdot f_{e3} \\ \dot{w}_e + \dot{q}_v \end{bmatrix} \tag{4.25}$$

and

$$\underline{\underline{\Phi}} = \begin{bmatrix} \rho\cdot u_1 & \rho\cdot u_2 & \rho\cdot u_3 \\ \rho\cdot u_1^2 + p - \tau_{11} & \rho\cdot u_1\cdot u_2 - \tau_{12} & \rho\cdot u_1\cdot u_3 - \tau_{13} \\ \rho\cdot u_1\cdot u_2 - \tau_{21} & \rho\cdot u_2^2 + p - \tau_{22} & \rho\cdot u_2\cdot u_3 - \tau_{23} \\ \rho\cdot u_1\cdot u_3 - \tau_{31} & \rho\cdot u_2\cdot u_3 - \tau_{32} & \rho\cdot u_3^2 + p - \tau_{33} \\ \rho\cdot H\cdot u_1 - \tau_{1i}\cdot u_i + k\cdot\dfrac{\partial T}{\partial x_1} & \rho\cdot H\cdot u_2 - \tau_{2i}\cdot u_i + k\cdot\dfrac{\partial T}{\partial x_2} & \rho\cdot H\cdot u_3 - \tau_{3i}\cdot u_i + k\cdot\dfrac{\partial T}{\partial x_3} \end{bmatrix} \tag{4.26}$$

$\underline{U}$ is a 5x1 vector with the conserved quantities, $\underline{\underline{\Phi}}$ is a 5x3 tensor with fluxes and other surface terms and $\underline{\Gamma}$ is a 5x1 vector with source terms including work done by external forces and heat sources in the energy equation.

For inviscid flow without heat transfer the expression above is reduced to

$$\underline{U} = \begin{bmatrix} \rho \\ \rho \cdot u_1 \\ \rho \cdot u_2 \\ \rho \cdot u_3 \\ \rho \cdot e \end{bmatrix} \qquad \underline{\underline{\Phi}} = \begin{bmatrix} \rho \cdot u_1 & \rho \cdot u_2 & \rho \cdot u_3 \\ \rho \cdot u_1^2 + p & \rho \cdot u_1 \cdot u_2 & \rho \cdot u_1 \cdot u_3 \\ \rho \cdot u_1 u_2 & \rho \cdot u_2^2 + p & \rho \cdot u_2 \cdot u_3 \\ \rho \cdot u_1 \cdot u_3 & \rho \cdot u_1 \cdot u_3 & \rho \cdot u_3^2 + p \\ \rho \cdot H \cdot u_1 & \rho \cdot H \cdot u_2 & \rho \cdot H \cdot u_3 \end{bmatrix} \qquad \underline{\Gamma} = \begin{bmatrix} 0 \\ \rho \cdot f_{e1} \\ \rho \cdot f_{e2} \\ \rho \cdot f_{e3} \\ \dot{w}_e \end{bmatrix} \tag{4.27}$$

These are the *Euler equations*. The system of partial differential equations is first order only (no second order dissipation terms) and the solution changes physical characteristics, so that discontinuities in the flow may occur (i.e., shocks). It should be noted that a different approach in the mathematical formulation and numerical solution must be used when dealing with the Euler equations.

Solving the full three-dimensional system of equations is a formidable task except for very simple geometries and flow conditions. Often some simplifications can be made to reduce complexity of the equations.

Examples of simplifications are:

- Stationary flow.
- Laminar flow.
- Incompressible flow.
- Isothermal flow.
- Inviscid flow.
- One-dimensional flow.

Other approximations in fluid mechanics, such as the "Boundary Layer approximation" or the "Thin Shear Layer approximation", are more specific, but it is beyond the scope of this text to discuss these further.

The problems considered here are so complex regarding geometries and flow conditions that there is no hope of modelling the true flow field in a computer simulation. Instead, a simplified one-dimensional model of the problem will be formulated, and then hopefully this will be sufficient to give a realistic calculation of the average mean flow and overall performance.

Next, the conservation equations for a one-dimensional formulation and a "lumped" formulation will be stated.

Conservation equations in a one-dimensional formulation

Consider a general volume of length L and constant free flow area A_c

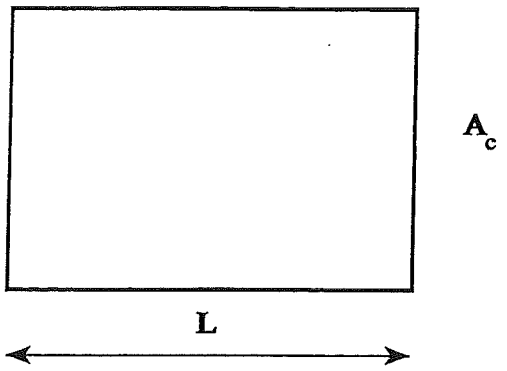

Figure 4.2 One-dimensional control volume.

Conservation of Mass

$$\frac{d}{dt}\int_{x=0}^{L} \rho \cdot A_c \cdot dx + [\rho \cdot A_c \cdot u]_{in}^{out} = 0 \tag{4.28}$$

or in differential form (assuming constant A_c)

$$\frac{\partial \rho}{\partial t} + \frac{\partial(\rho \cdot u)}{\partial x} = 0 \tag{4.29}$$

Conservation of Momentum

$$\frac{d}{dt}\int_{x=0}^{L} \rho \cdot u \cdot A_c \cdot dx + [\rho \cdot A_c \cdot u^2 + p \cdot A_c]_{in}^{out} = \int_{x=0}^{L} \tau_w \cdot S \cdot dx + \int_{x=0}^{L} \rho \cdot f_e \cdot A_c \cdot dx \tag{4.30}$$

or in differential form

$$\frac{\partial}{\partial t}(\rho \cdot u) + \frac{\partial}{\partial x}(\rho \cdot u^2 + p) = \tau_w \cdot \frac{S}{A_c} + \rho \cdot f_e \tag{4.31}$$

where the wetted perimeter S is defined from length L and heat transfer area A as

$$S = \frac{A}{L} \tag{4.32}$$

Friction cannot be described in a one-dimensional formulation, and an empirical expression must be used for the wall friction τ_w. This will be discussed later in this chapter.

Conservation of Energy

$$\frac{d}{dt}\int_{x=0}^{L} \rho \cdot e \cdot A_c \cdot dx + \left[\rho \cdot A_c \cdot u \cdot \left(e + \frac{p}{\rho}\right) + k \cdot \frac{\partial T}{\partial x}\right]_{in}^{out} = \int_{x=0}^{L} \tau_w \cdot S \cdot u \cdot dx + \int_{x=0}^{L} \rho \cdot A_c \cdot u \cdot f_e \cdot dx + \int_{x=0}^{L} h \cdot S \cdot (T_s - T) \cdot dx \tag{4.33}$$

or in differential form

$$\frac{\partial}{\partial t}(\rho \cdot e) + \frac{\partial}{\partial x}\left(\rho \cdot u \cdot \left(e + \frac{p}{\rho}\right)\right) = \tau_w \cdot \frac{S}{A_c} \cdot u + \rho \cdot f_e \cdot u - k \cdot \frac{\partial^2 T}{\partial x^2} + h \cdot \frac{S}{A_c} \cdot (T_s - T) \tag{4.34}$$

where the last two terms are conduction heat transfer and convection heat transfer, h is a heat transfer coefficient, and all volume sources have been omitted.

The integral formulation leads directly to the "lumped" formulation.

Conservation equations in a "lumped" formulation

Conservation of mass

$$\frac{dM}{dt} + \dot{m}_{out} - \dot{m}_{in} = 0 \tag{4.35}$$

where the mass flow is given as

$$\dot{m} = \rho \cdot A_c \cdot u \tag{4.36}$$

Conservation of momentum

$$\frac{dG}{dt} + (\dot{m} \cdot u)_{out} - (\dot{m} \cdot u)_{in} = F_v + F_S \tag{4.37}$$

where total momentum G is

$$G = M \cdot u \tag{4.38}$$

and F_v and F_s denote volume forces and surface forces.

Conservation of energy

$$\frac{dE}{dt} + (\dot{m} \cdot H)_{out} - (\dot{m} \cdot H)_{in} = \dot{Q} + \dot{W} \tag{4.39}$$

where the total energy E is defined as

$$E = M \cdot e \tag{4.40}$$

and $\dot{Q}$ is the total heat transfer and $\dot{W}$ denote the work.

The derived equations will have to be supplemented with constitutive relations for state, stress, pressure and heat flux. These relations describe the intrinsic behaviour of a specific medium.

4.3.2 Equation of state

The equation of state describes the local behaviour of the medium in terms of the state variables and thermodynamic properties under the assumption of local thermodynamic equilibrium. An equation of state may be expressed as an algebraic equation, a differential equation or in form of tables or graphs.

In the following, the main emphasis is laid on compressible fluids (gases) since these are most relevant for the specific problems discussed here.

Compressible fluids (gases)

For a compressible fluid, all of its thermodynamic properties can be deduced from a single equation connecting the state variables (e.g., pressure, density, temperature, internal energy). The equation of state can be given in the form

$$i = i(p,T) \qquad or \qquad h = h(p,T) \tag{4.41}$$

where i is the specific internal energy, and h is the specific enthalpy. Notice that h, in this section 4.3.2 only, is used for specific enthalpy, while elsewhere it will be used for the convection heat transfer coefficient.

Of particular interest is the equation of state for an ideal gas, which is valid for gases at low density and moderate temperatures.

Ideal gas

An ideal gas satisfies the equation

$$p = \rho \cdot R \cdot T \tag{4.42}$$

R is the gas constant and $\hat{R}=\hat{M}\cdot R$, where $\hat{R}$ is the universal gas constant and $\hat{M}$ is the molar weight.

It can be shown that for an ideal gas, the specific internal energy and the specific enthalpy are only functions of the absolute temperature, i.e.,

$$i = i(T) \qquad h = h(T) \tag{4.43}$$

The specific heat capacities at constant volume and pressure, c_v and c_p respectively, are defined as

$$c_v = \left(\frac{\partial i}{\partial T}\right)_v \qquad c_p = \left(\frac{\partial h}{\partial T}\right)_p \tag{4.44}$$

This implies that

$$c_v = c_v(T) \qquad c_p = c_p(T) \tag{4.45}$$

and

$$c_p - c_v = R \tag{4.46}$$

A simplification is to assume that c_v and c_p are constant. This assumption is frequently made, but it is only valid for processes with small temperature differences.

For constant c_v and c_p the following equations are valid

$$i = c_v \cdot T \qquad h = c_p \cdot T \tag{4.47}$$

and

$$p = (\gamma - 1) \cdot \rho \cdot i \tag{4.48}$$

where γ is the specific heat capacity ratio, i.e.

$$\gamma = \frac{c_p}{c_v} \tag{4.49}$$

Real Gas

The equation of state for an ideal gas cannot be used for dense gases. Deflections are dependent primarily on density.

A so-called virial expansion of the equation of state for an ideal gas gives

$$p = \rho \cdot R \cdot T \cdot \left(1 + B_2(T) \cdot \rho + B_3(T) \cdot \rho^2 + \ldots\right) \tag{4.50}$$

where B_i (i=2,3,...) can be calculated from the theory of statistical thermodynamics.

A real gas equation is often written in the form

$$p = Z \cdot \rho \cdot R \cdot T \tag{4.51}$$

where Z is the compressibility factor.

Several different algebraic equations of state for non-ideal gases have been proposed, including Van der Waal, Beattie-Bridgeman and Redlich-Kwong. These are all well- known and can be found in standard text books. One of these is given as an example:

Van der Waal Gas

A frequently used equation of state for non-ideal gases is Van der Waals' equation

$$(p + a\cdot\rho^2)\cdot(1 - \rho\cdot b) = \rho\cdot R\cdot T \tag{4.52}$$

where a and b are positive constants.

An assumption of real gas behaviour is necessary for some Stirling applications, e.g., heat pumps.

Solids

For solids, the internal energy only depends of the temperature and again

$$c(T) = \frac{di}{dT} \tag{4.53}$$

and for constant specific heat capacity c

$$i = c\cdot T \tag{4.54}$$

4.3.3 Thermodynamic properties

The thermodynamic properties such as specific heat capacity, viscosity and thermal conductivity are not constant, but a function of the local thermodynamic state expressed in form of the state variables. It is mainly a dependence of the temperature (and in lesser extent the pressure), which is significant, i.e.,

$$c_p = c_p(T) \qquad \mu = \mu(T) \qquad k = k(T) \tag{4.55}$$

Tables and empirical expression can be found in the literature.

Example: Sutherland's formula for the viscosity of air

$$\mu = \frac{1.45\cdot T^{\frac{2}{3}}}{T + 110}\cdot 10^{-6} \tag{4.56}$$

For gases the viscosity and the thermal conductivity increase with increasing temperature.

For Helium, which is widely used as a working gas in a Stirling engine, the dynamic viscosity and the thermal conductivity increase by a factor two, when the temperature increases from 350 K to 1000 K, while the specific heat capacity at constant pressure remains almost constant (see the table in chapter 3).

4.4 Modelling of heat transfer and friction

4.4.1 Introductory remarks

Empirical or semi-empirical expression based on experimental data are required for the modelling of heat transfer and friction for a one-dimensional or "lumped" formulation. In this section the general form of these expressions will be given, while the actual equations for the Stirling components will be given later.

4.4.2 Dimensionless numbers

Heat transfer and friction are usually expressed in form of dimensionless numbers.

Let D and u denote characteristic length and velocity respectively, then the following dimensionless numbers will be used:

Reynolds number

$$Re_D = \frac{\rho \cdot u \cdot D}{\mu} \tag{4.57}$$

Prandtl number

$$Pr = \frac{c_p \cdot \mu}{k} \tag{4.58}$$

Nusselt number

$$Nu_D = \frac{h \cdot D}{k} \tag{4.59}$$

Stanton number

$$St = \frac{h}{\rho \cdot u \cdot c_p} = \frac{Nu_D}{Re_D \cdot Pr} \tag{4.60}$$

Colburn j factor

$$j_H = St \cdot Pr^{\frac{2}{3}} \tag{4.61}$$

Number of transfer units

$$NTU = \frac{h \cdot A}{\dot{m} \cdot c_p} \tag{4.62}$$

All variables have been defined previously in this chapter.

4.4.3 Geometry

The following notation is used

Minimum free-flow area	: A_c
Frontal area	: A_{fr}
Heat transfer area	: A
Diameter	: D or d
Length	: L or l
Wetted perimeter	: S
Hydraulic diameter	: D_h

The hydraulic diameter D_h is defined from the expression

$$\frac{D_h}{4 \cdot L} = \frac{A_c}{A} \tag{4.63}$$

Total volume V_{total} and gas volume V is given as

$$\begin{aligned} V_{total} &= A_{fr} \cdot L \\ V &= A_c \cdot L \end{aligned} \tag{4.64}$$

For a regenerator matrix the following useful definitions can be made:

Porosity ϱ

$$\varrho = \frac{V}{V_{total}} = \frac{A_c}{A_{fr}} \tag{4.65}$$

Ratio of heat transfer area to total volume α

$$\alpha = \frac{A}{V_{total}} = \frac{4 \cdot \varrho}{D_h} \tag{4.66}$$

4.4.4 Heat transfer

Heat transfer is an important part of any thermodynamic device. Heat can be added or removed from a thermodynamic process in numerous ways.

In a Stirling engine the heat transfer between the working gas and the solid surface (in form of heat exchanger tubes, regenerator matrix etc.) is due to convection. Heat conduction occurs in the regenerator matrix, through the cylinder walls, in the heat exchanger tubes and in the working gas.

In an internal combustion engine, the most important heat transfer process is the chemical reaction taking place in the combustion chamber.

Convection heat transfer

Convection heat transfer is the most important form of heat transfer in a Stirling engine, and it will be given the main attention here.

Convection can be defined as heat transfer taking place at a solid-fluid interface. The heat transfer is given according to Newton's law of cooling as

$$\dot{q}_{conv} = h \cdot (T_s - T) \tag{4.67}$$

or for a given heat transfer area A

$$\dot{Q}_{conv} = h \cdot A \cdot (T_s - T) \tag{4.68}$$

where $\dot{Q}_{conv}$ is the heat transfer from solid to gas, h is the (local) heat transfer coefficient, and T_s and T are the temperatures of solid walls and gas.

The problem is how to determine the heat transfer coefficient h.

Many correlations for heat transfer coefficients for internal flows are found in the literature. Most of these correlations cannot be directly used for the applications considered here. Even in a one-dimensional model, flow in both directions with pressure, temperature and mass flow variations makes it very difficult to obtain general results. The usual assumptions, such as constant wall temperature, constant heat flux, constant inlet temperature and fully developed flow, are not satisfied.

For laminar flow, and under the assumptions of constant wall temperature or constant heat flux, it is possible to derive analytical expressions for the heat transfer coefficients both locally and globally (average) in simple geometries.

For turbulent flow it is necessary to use empirical or semi-empirical correlations. Typically, dimensional analysis is used to determine the relevant (dimensionless) parameters, and then physical experiments are used to determine constants and exponents for the correlations.

There exist several studies of heat transfer with variable mass flow and temperature, but results are usually only available for a specific design. More general studies give no distinct answers, and there are no general empirical or semi-empirical expressions for heat transfer coefficients for such flows.

A simplified approach using empirical expressions for heat transfer coefficients in heat exchangers, regenerators and tubes is very often used in the lack of better alternatives. These expressions are derived for incompressible, steady-state flows, but are nevertheless used here. The expressions will be given as a heat transfer coefficient h or a NTU-number (Number of Transfer Units) as a function of Reynolds number.

The NTU-number is defined as

$$NTU = \frac{h \cdot A}{|\dot{m}| \cdot c_p} \tag{4.69}$$

This kind of quasi-steady analysis is standard approach for even advanced simulation models of Stirling engines and other related types of machines.

General expression for convection heat transfer

The correlations used for the heat transfer in the Stirling engine are widely based on experimental data given in [2], where the Colburn factor $j_H = St \cdot Pr^{2/3}$ is plotted as a function of the Reynolds number.

Taking the hydraulic diameter D_h as a characteristic length and the velocity u_c at the minimum free-flow area as the characteristic velocity imply

$$Re = \frac{\dot{m} \cdot D_h}{A_c \cdot \mu} \tag{4.70}$$

since the mass flow m is given as

$$\dot{m} = \rho \cdot u_c \cdot A_c \tag{4.71}$$

The heat transfer coefficient h may then be expressed as a function of $St \cdot Pr^{2/3}$ in the following way

$$h = St \cdot \rho \cdot U \cdot c_p = \frac{\dot{m} \cdot c_p}{A_c} \cdot Pr^{-2/3} \cdot St \cdot Pr^{2/3} = \frac{\mu \cdot c_p}{D_h} \cdot Pr^{-2/3} \cdot St \cdot Pr^{2/3} \cdot Re \tag{4.72}$$

or alternatively using the definition of NTU-number

$$NTU = \frac{4 \cdot L}{D_h} \cdot Pr^{-2/3} \cdot St \cdot Pr^{2/3} = \frac{A}{A_c} \cdot Pr^{-2/3} \cdot St \cdot Pr^{2/3} \tag{4.73}$$

The convection heat transfer is then given as

$$\dot{Q}_{conv} = |\dot{m}| \cdot c_p \cdot NTU \cdot (T_s - T) = |\dot{m}| \cdot c_p \cdot \frac{A}{A_c} \cdot Pr^{-2/3} \cdot St \cdot Pr^{2/3} \cdot (T_s - T) \qquad (4.74)$$

The heat transfer area A, the free flow area A_c and the hydraulic diameter D_h are given from the geometry.

The Prandtl number Pr is almost constant in a wide temperature range for most gases. The interesting part of the expression above is $St \cdot Pr^{2/3}$ for which experimental data must be used. For computational purposes it is practical to have an empirical correlation (analytical expression), which is typically derived from the graph where the experimental results are plotted.

If the $St \cdot Pr^{2/3}$ is given as a function of the Reynolds number Re as in [2], it should be noted that the viscosity in the Reynolds number is a strong function of temperature. The standard approach of assuming constant viscosity will not be a good approximation except from processes with small temperature differences. A better way is to make temperature corrections, but of course the correct approach is to have the viscosity directly as a function of temperature (and pressure).

It should be mentioned that there is an advantage of using the NTU-number instead of the heat transfer coefficient h. The NTU-number is only a weak function of Reynolds number (mass flow), at least for turbulent flows, and for simple models it is better to assume constant NTU-number than constant heat transfer coefficient.

Conduction heat transfer

The constitutive relation for conduction heat transfer is given from Fourier's law of conduction.

$$\underline{\dot{q}}_{cond} = -k \cdot \underline{\nabla} T \qquad (4.75)$$

where k is the heat conductivity.

In one dimension and for a cross sectional area A_{cond}

$$\dot{Q}_{cond} = -k \cdot A_{cond} \cdot \frac{dT}{dx} \qquad (4.76)$$

Heat conduction can be of interest in a Stirling engine, but usually the effect is so small compared to the uncertainty of other assumptions that it is neglected.

Radiation heat transfer

Radiation heat transfer is of little interest for Stirling engines, and will not be considered further here.

Internal heat transfer

In a combustion engine the heat transfer takes place inside the volume due to chemical reaction. This is not relevant for Stirling engines, so further discussion will be omitted.

4.4.5 Friction

For a one-dimensional or a "lumped" formulation, friction cannot be represented correctly due to the second order derivatives of the velocities in the Navier-Stoke's equations.

For one-dimensional internal flows, a simplification will be to assume that the effect of the shear stresses is equivalent to a distributed friction force. A reliable estimate of loss mechanisms and loss distribution is then required, and this may be achieved in form of empirical or semi-empirical correlations based on experimental data.

The basic idea is to replace the shear stresses by an equivalent friction force which is an empirical function of certain flow parameters (such as geometry and velocity) and not of the second derivatives of the velocities.

The equivalent friction force F_{fric} over a length L can be defined as

$$F_{fric} = \tau_w \cdot A = \Delta p \cdot A_c \tag{4.77}$$

where τ_w is the equivalent (wall) shear stress and A is the wetted surface.

A friction factor f (Fanning) can be defined for one-dimensional compressible flow

$$f \equiv \frac{\tau_w}{\frac{1}{2}\cdot\rho\cdot u^2} \tag{4.78}$$

which means that the friction force F_{fric} can be written as

$$F_{fric} = f\cdot\frac{1}{2}\cdot\rho\cdot u^2\cdot A \tag{4.79}$$

Instead of a flux term, friction can then be treated as an external force in the equations.

The friction factor f is given from empirical or semi-empirical expressions based on experimental data, and will typically be a function of Reynolds number and geometry, see reference [2].

Pressure difference Δp over the length L is then given as

$$\Delta p = f\cdot\frac{4\cdot L}{D_h}\cdot\frac{1}{2}\cdot\rho\cdot u^2 = f\cdot\frac{A}{A_c}\cdot\frac{1}{2}\cdot\rho\cdot u^2 \tag{4.80}$$

The work done by friction force on the fluid is dissipated into internal energy

$$\dot{E}_{diss} = \Delta p\cdot A_c\cdot u = f\cdot A\cdot\frac{1}{2}\cdot\rho\cdot|u|^3 \tag{4.81}$$

For a Stirling engine, where the physical model consists of a connected system of components (e.g., regenerator, heat exchanger), it will be a practical way to include the effect of friction. A friction loss may be assigned to a specific component and the importance may then be studied.

At this level of approximation, the possibility of studying the detailed structure of the flow inside the component (e.g., velocity gradients and shear stresses) is obviously lost, but it is assumed that the main effects of the averaged flow are adequately described, including the overall performance and behaviour of the component.

Friction is an important factor in the design of a Stirling engine (and of almost any thermodynamic device), and it must be taken into consideration in any accurate and reliable analysis.

References

[1] Arpaci, V.S. and Larsen, P.S.
Convection Heat Transfer.
Prentice-Hall (1984).

[2] Kays, W.M. and London, A.L.
Compact Heat Exchangers.
McGraw Hill (1980).

5.0 SIMPLE FIVE-VOLUME STIRLING MODEL (SFVSM)

5.1 Introduction

As explained in a previous chapter, the Stirling engine has been chosen as the model example. In this chapter a simple model of the classical Stirling configuration will be developed. The Stirling engine considered consists of five components in form of two variable cylinder volumes, two heat exchangers and one regenerator.

In this simple Stirling model each component will be just one volume, and from now on the model will be called the Simple Five-Volume Stirling Model or just SFVSM.

The "lumped" formulation of the governing equations derived in the previous chapter is used and this implies that the spatial variation of the state variables within a component will be entirely lost. Furthermore, the possibility of modelling different loss mechanisms will be rather limited.

In return, the mathematical model will be uncomplicated, and it will be relatively easy to implement a numerical solution of the problem.

The simple model will therefore be ideal for testing different solution approaches including different numerical methods. Of course, there is no guarantee that a method which works well for the simple problem also will work for a related, more complex problem. However, it is very unlikely, that the opposite will be the case (a method that cannot solve the simple problem will probably not be suitable to solve the complex problem).

In this chapter the physical and mathematical model will be discussed, including all the necessary assumptions, equations and boundary conditions. In the next chapters different approaches and numerical methods will be discussed, and the most important results and conclusions will be presented.

Later, more sophisticated models will be developed and a solution approach will be chosen based on the results and conclusions from the simple model.

5.2 Physical model of the SFVSM

A five component Stirling engine is shown in Figure 5.1. This is equivalent to the standard α-engine configuration, which has been described in chapter 3.

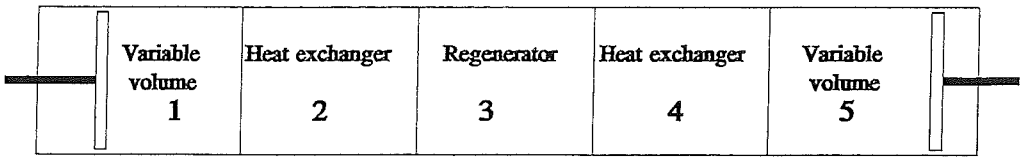

Figure 5.1 Five component Stirling engine.

Volume 1 and 5 are the variable cylinder volumes, volume 2 and 4 are the heat exchangers and volume 3 is the regenerator.

5.2.1 Assumptions

The following assumptions are made:

- Uniform pressure.
  No spatial variation in pressure. This implies that the necessary equations only include conservation of mass and energy and an equation of state.

- Ideal gas.
  The working gas is assumed to be an ideal gas, i.e., the constitutive equation is the equation of state for an ideal gas.

- Constant properties of matters.
  No temperature dependency for the specific heat capacity.

- Kinetic energy is neglected.
  This is usually a very good approximation for almost all Stirling engines. It can be shown that even with the maximum velocities in the heat exchangers the kinetic energy is insignificant compared to the internal energy of the gas.

- Sinusoidal piston motion.
  The pistons are assumed to move so that a sinusoidal variation of volume is achieved in each of the variable volumes. The speed is assumed to be constant and specified.

- No leak flow.
  The total mass in the engine is assumed to be constant.

- Constant NTU-number.

  The heat transfer, in form of a heat transfer coefficient or a NTU-number, is mainly dependent on the mass flow (velocity), but as a first approximation the NTU-number is assumed to be constant.

- Infinite heat capacity of regenerator matrix.

  The heat capacity of the regenerator matrix is very large compared to the heat capacity of the working gas. Therefore, the heat capacity of solid matrix is assumed to be infinite, and this implies that the regenerator matrix temperature is constant in time.

- Linear temperature gradient of gas and matrix in the regenerator matrix.

  Assuming a linear temperature profile in the regenerator is close to the conditions in a real regenerator, except from the entry zone of the working gas.

- Uniform conditions in heat exchangers and variable volumes.

  All state variables are considered as average values for the whole component, i.e., each volume has one pressure, temperature etc. This is also a consequence of the limitations in the "lumped" formulation.

- No heat conduction.

  The heat conduction is neglected. This includes conduction in the flow direction in the regenerator and in the working gas. The solid temperature in a heat exchanger and variable cylinder volume is given as the temperature on the inside of the tube or wall.

- "Cyclic heat transfer" in the variable volumes.

  The heat transfer in the variable volumes is assumed to be cyclic, i.e., the net heat transfer to the solid surface inside a variable cylinder volume during one cycle is assumed to be zero. This means that the solid surface temperature should be adjusted to fulfill this condition.

- No heat transfer to surroundings.

  No heat transfer to surroundings from the regenerator, which means that net heat transfer from gas to matrix over one cycle is zero for cyclic operation of the engine, i.e., equivalent of "cyclic heat transfer" in this component.

- No friction.

  All friction losses will be neglected.

A further discussion of basic Stirling engine modelling and assumptions can be found in [1].

5.3 Mathematical model of the SFVSM

5.3.1 Introductory remarks

In this section the physical model for the Simple Five-Volume Stirling Model is translated into a mathematical model. The equations are based on the theory given in the previous chapter, combined with the simplifying assumptions introduced for the SFVSM-problem.

First, the governing equations for a general volume (component) are given, and then the specific components are discussed. Finally, the full system of equations is derived for two different formulations of the problem.

5.3.2 Equations and boundary conditions

Consider the general *i*th volume:

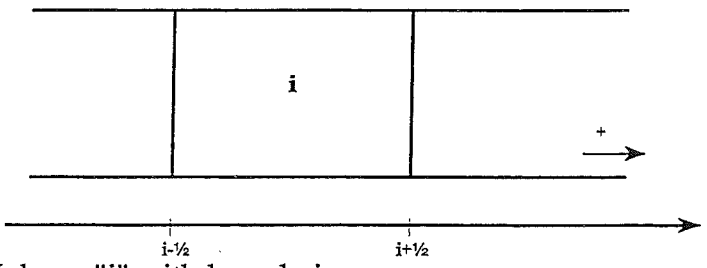

Figure 5.2 Volume "i" with boundaries.

The conservation equations in a "lumped parameter" formulation have been given previously in section 4.3.1 and the general form is the following:

Conservation of mass:

$$\frac{dM_i}{dt} = \dot{m}_{i-1/2} - \dot{m}_{i+1/2} \tag{5.1}$$

Conservation of energy:

$$\frac{dE_i}{dt} = \left(\dot{m}\cdot c_p\cdot T\right)_{i-1/2} - \left(\dot{m}\cdot c_p\cdot T\right)_{i+1/2} + \dot{W}_i + \dot{Q}_{conv,i} \tag{5.2}$$

Equation of state:

$$p\cdot V_i = M_i\cdot R\cdot T_i \tag{5.3}$$

The assumption of uniform pressure means that the pressure in all volumes is the same (no subscript of p in the equations).

There will be some modifications according to the specific volume considered.

Variable volumes

The pistons are assumed to move in a sinusoidal pattern and the period t_p is given as

$$t_p = \frac{60}{RPM} = \frac{2\cdot\pi}{\omega} \tag{5.4}$$

The volumes can then be written as

$$V_i = V_{cl,i} + V_{sw,i}\cdot\frac{1 + \cos(\omega\cdot t + \varphi_{0i})}{2} \tag{5.5}$$

where V_{cl} and V_{sw} are clearance volume (dead volume) and swept volume, respectively and φ_0 is the phase angle at t=0. From this expression, an analytical expression for the derivative can easily be obtained.

The work term is given as

$$\dot{W}_i = -p\cdot\frac{dV_i}{dt} \tag{5.6}$$

and the convection heat transfer term as (see also section 4.4.4)

$$\dot{Q}_{conv,i} = |\dot{m}_i|\cdot c_p\cdot NTU_i\cdot(T_{s,i} - T_i) \tag{5.7}$$

where NTU_i is assumed to be constant and $T_{s,i}$ is the surface temperature in the *i*th volume.

Heat exchangers

Constant volume, which means that the work term is identical to zero, i.e.,

$$\dot{W}_i = 0 \tag{5.8}$$

The convection heat transfer is identical to the expression above

$$\dot{Q}_{conv,i} = |\dot{m}_i|\cdot c_p\cdot NTU_i\cdot(T_{s,i} - T_i) \tag{5.9}$$

Regenerator

Constant volume here too, so

$$\dot{W}_i = 0 \tag{5.10}$$

A linear temperature gradient through the working gas in the regenerator, implies that the equation of state should be replaced with the following expression

$$p \cdot V_i = M_i \cdot R \cdot T_{\ln,i} \tag{5.11}$$

where $T_{\ln,i}$ is given as

$$T_{\ln,i} = \frac{T_{i+1/2} - T_{i-1/2}}{\ln\left(\frac{T_{i+1/2}}{T_{i-1/2}}\right)} \tag{5.12}$$

This is a result from the calculation of the total mass in a volume with uniform pressure and a linear temperature gradient (see Appendix A). The change in total internal energy in the energy equation is not affected by the assumption of a linear temperature gradient, when the temperature is replaced with the mean logarithmic temperature $T_{\ln}$, i.e.,

$$E_i = M_i \cdot c_v \cdot T_{\ln,i} \tag{5.13}$$

This result is also given in Appendix A.

The temperature profiles in the regenerator are shown in Figure 5.3.

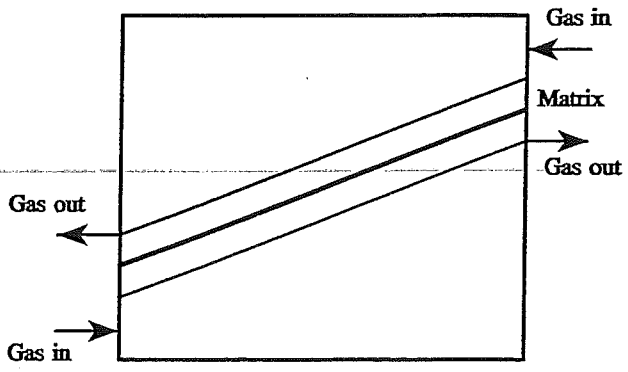

Figure 5.3 Temperature profile in solid matrix and gas in the regenerator.

Now define α as the temperature gradient in the solid matrix (which is assumed to be equal to the gradient in the gas), i.e.,

$$\alpha \equiv \frac{dT_{s,i}}{dx} = \frac{dT_i}{dx} \tag{5.14}$$

where T_i is the gas temperature in the middle of the regenerator.

Let L be the length of the regenerator such that

$$\begin{aligned} T_{i+1/2} &= T_i + \alpha \cdot \frac{L}{2} \\ T_{i-1/2} &= T_i - \alpha \cdot \frac{L}{2} \end{aligned} \tag{5.15}$$

$T_{ln,i}$ can then be expressed as

$$T_{ln,i} = \frac{\alpha \cdot L}{\ln\left(\dfrac{T_i + \alpha \cdot \frac{L}{2}}{T_i - \alpha \cdot \frac{L}{2}}\right)} \tag{5.16}$$

The heat transfer is identical to the expressions above, i.e.,

$$\dot{Q}_{conv,i} = |\dot{m}_i| \cdot c_p \cdot NTU_i \cdot (T_{s,i} - T_i) \tag{5.17}$$

Notice that the heat transfer is determined by the temperature of gas and matrix in the middle of the regenerator and not by the logarithmic mean temperature $T_{ln,i}$. This is most natural under the given assumptions, since this is the temperature difference between gas and matrix everywhere in the regenerator.

For cyclic steady-state conditions and no heat transfer to the surroundings, the net heat transfer from gas to matrix for one cycle is zero, i.e.,

$$Q_{conv,i} = \int_{t=0}^{t_p} |\dot{m}_i| \cdot c_p \cdot NTU_i \cdot (T_{s,i} - T_i) \cdot dt = 0 \tag{5.18}$$

Mass flow

The mass flow $|\dot{m}_i|$ can be evaluated as

$$|\dot{m}_i| = \frac{1}{2} \cdot (|\dot{m}_{i-1/2}| + |\dot{m}_{i+1/2}|) \tag{5.19}$$

It may be discussed, how the two variable volumes should be treated regarding heat transfer. A variable volume has flow only at one boundary, while there is no mass flow through the moving boundary given by the piston, i.e.,

$$\dot{m}_{1/2} = \dot{m}_{5+1/2} = 0 \tag{5.20}$$

It has been chosen to use the expression (5.19) for the variable volumes as well, although it could be argued that the full mass flow should be used. Anyway, since the real heat transfer conditions are complex due to flow conditions and variable heat transfer area, this is not so significant for the results.

Values at volume boundaries

Mass flows are evaluated at the control volume boundaries (i±½), while the other variables (pressure p and temperatures T_i) are evaluated in the middle of the volume. This is a kind of staggered grid formulation of the problem, where some variables are solved at the center of the volume and other variables are solved at the boundaries. It is the most obvious approach for a coarse discretization like the "lumped" control volume formulation used here for the SFVSM.

Since the pressure is assumed to be uniform in space, the evaluation of p at the boundaries is trivial. The temperatures must also be evaluated at the boundaries because of the flux terms. The following upwind type evaluation is used

$$T_{i+1/2} = \begin{cases} T_i & \dot{m}_{i+1/2} > 0 \\ T_{i+1} & \dot{m}_{i+1/2} < 0 \end{cases} \qquad (5.21)$$

and similar for $T_{i-½}$.

For volumes with a linear temperature distribution or adjacent volumes, the above expression has to be modified, so that (under the given assumptions about the temperature distribution) the correct inlet and outlet temperatures are used.

Regenerator matrix-temperature and -gradient

The temperature and gradient in the regenerator matrix determine the net heat transfer from gas to matrix (which should be zero for stationary periodic conditions) and the net enthalpy flux through the matrix during one cycle. The flux represents a transport of heat from the hot end to the cold end of the machine, and can be considered as a loss, which should be kept at a minimum level. This so-called regenerator loss is inevitable in a non-ideal regenerator.

Conceivable ways to set up the two necessary equations to determine the unknown matrix temperature and matrix gradient could be:.

(1) The net enthalpy flux at the boundaries should be equal, and the net heat transfer from gas to matrix should be identical to zero, i.e.,

$$\int_{t=0}^{t_p} \dot{m}_{i-1/2} \cdot c_p \cdot T_{i-1/2} \cdot dt = \int_{t=0}^{t_p} \dot{m}_{i+1/2} \cdot c_p \cdot T_{i+1/2} \cdot dt \qquad (5.22)$$

and

$$\int_{t=0}^{t_p} |\dot{m}_i| \cdot c_p \cdot NTU_i \cdot (T_{s,i} - T_i) \cdot dt = 0 \qquad (5.23)$$

(2) The net enthalpy flux at three different positions (at the boundaries and in the middle of the regenerator) should be identical, i.e.,

$$\int_{t=0}^{t_p} \dot{m}_{i-1/2} \cdot c_p \cdot T_{i-1/2} \cdot dt = \int_{t=0}^{t_p} \dot{m}_i \cdot c_p \cdot T_i \cdot dt = \int_{t=0}^{t_p} \dot{m}_{i+1/2} \cdot c_p \cdot T_{i+1/2} \cdot dt \qquad (5.24)$$

where the mass flow in the middle of the regenerator can be evaluated as the mean value, i.e.,

$$\dot{m}_i = \frac{1}{2} \cdot \left(\dot{m}_{i-1/2} + \dot{m}_{i+1/2} \right) \qquad (5.25)$$

The first of these two approaches cannot be used, since it can be shown that the two integral equations are not independent for periodic steady state conditions. This is not the case for the latter approach, and it has been used in the following.

Heat transfer in the variable cylinder volumes

Adiabatic conditions in the variable volumes is the most simple assumption that can be made about the heat transfer in the variable volumes, when the trivial case of isothermal volumes is excluded.

Adiabatic heat transfer may be expressed as:

$$NTU_i = 0$$

In reality there will be heat transfer in the variable volumes, and it turns out that an assumption of "cyclic heat transfer" is far better for describing the physical conditions in a real Stirling engine.

"Cyclic heat transfer" may be expressed as:

$$\int_{t=0}^{t_p} |\dot{m}_i| \cdot c_p \cdot NTU_i \cdot (T_{s,i} - T_i) \cdot dt = 0 \qquad (5.27)$$

This integral equation can be solved for the unknown temperature $T_{s,i}$ of the solid surface, which is assumed to be constant.

This concludes the description of the mathematical model. All the equations required to solve the problem have been set up, and now follows a complete list of the equations used for the numerical solution of the mathematical model.

It is possible to formulate the full system of equations in two ways, which will have different properties with regard to the later implementation and choice of a numerical method. Both formulations will be given, since both have been used in the developed simulation programs.

5.3.3 Basic formulation of the full system of equations

The general form of the governing equations for the "lumped parameter" formulation has been given previously. The mathematical models developed in this and the next section are all based on these equations.

The total energy E is equal to the internal energy, when the kinetic and gravitational terms are neglected, i.e.,

$$E = M \cdot c_v \cdot T \tag{5.28}$$

E is used as an unknown variable, and the temperature is expressed as a function of internal energy and mass.

The ratio between the (constant) specific heat capacities for the gas is denoted γ

$$\gamma = \frac{c_p}{c_v} \tag{5.29}$$

Volume 1 (variable volume, compression)

$$\begin{aligned}
\frac{dM_1}{dt} &= -\dot{m}_{3/2} \\
\frac{dE_1}{dt} &= -\gamma \cdot \left(\dot{m} \cdot \frac{E}{M}\right)_{3/2} + \frac{1}{2} \cdot |\dot{m}_{3/2}| \cdot c_p \cdot NTU_1 \cdot \left(T_{s,1} - \frac{E_1}{M_1 \cdot c_v}\right) - p \cdot \frac{dV_1}{dt} \\
p \cdot V_1(t) &= (\gamma - 1) \cdot E_1
\end{aligned} \tag{5.30}$$

Volume 2 (heat exchanger, compression)

$$\begin{aligned}
\frac{dM_2}{dt} &= \dot{m}_{3/2} - \dot{m}_{5/2} \\
\frac{dE_2}{dt} &= \gamma \cdot \left(\dot{m} \cdot \frac{E}{M}\right)_{3/2} - \gamma \cdot \left(\dot{m} \cdot \frac{E}{M}\right)_{5/2} + \frac{1}{2} \cdot \left(|\dot{m}_{3/2}| + |\dot{m}_{5/2}|\right) \cdot c_p \cdot NTU_2 \cdot \left(T_{s,2} - \frac{E_2}{M_2 \cdot c_v}\right) \\
p \cdot V_2 &= (\gamma - 1) \cdot E_2
\end{aligned} \tag{5.31}$$

Volume 3 (regenerator)

$$\frac{dM_3}{dt} = \dot{m}_{5/2} - \dot{m}_{7/2}$$

$$\frac{dE_3}{dt} = \gamma \cdot \left(\dot{m} \cdot \frac{E}{M}\right)_{5/2} - \gamma \cdot \left(\dot{m} \cdot \frac{E}{M}\right)_{7/2} + \frac{1}{2} \cdot \left(|\dot{m}_{5/2}| + |\dot{m}_{7/2}|\right) \cdot c_p \cdot NTU_3 \cdot (T_{s,3} - T_3) \qquad (5.32)$$

$$p \cdot V_3 = (\gamma - 1) \cdot E_3$$

Volume 4 (heat exchanger, expansion)

$$\frac{dM_4}{dt} = \dot{m}_{7/2} - \dot{m}_{9/2}$$

$$\frac{dE_4}{dt} = \gamma \cdot \left(\dot{m} \cdot \frac{E}{M}\right)_{7/2} - \gamma \cdot \left(\dot{m} \cdot \frac{E}{M}\right)_{9/2} + \frac{1}{2} \cdot \left(|\dot{m}_{7/2}| + |\dot{m}_{9/2}|\right) \cdot c_p \cdot NTU_4 \cdot \left(T_{s,4} - \frac{E_4}{M_4 \cdot c_v}\right) \qquad (5.33)$$

$$p \cdot V_4 = (\gamma - 1) \cdot E_4$$

Volume 5 (variable volume, expansion)

$$\frac{dM_5}{dt} = \dot{m}_{9/2}$$

$$\frac{dE_5}{dt} = \gamma \cdot \left(\dot{m} \cdot \frac{E}{M}\right)_{9/2} + \frac{1}{2} \cdot |\dot{m}_{9/2}| \cdot c_p \cdot NTU_5 \cdot \left(T_{s,5} - \frac{E_5}{M_5 \cdot c_v}\right) - p \cdot \frac{dV_5}{dt} \qquad (5.34)$$

$$p \cdot V_5(t) = (\gamma - 1) \cdot E_5$$

The values on the control volume boundaries are given as

$$\left(\frac{E}{M}\right)_{3/2} = \begin{cases} \dfrac{E_1}{M_1} & \dot{m}_{3/2} > 0 \\ \dfrac{E_2}{M_2} & \dot{m}_{3/2} < 0 \end{cases} \qquad (5.35)$$

$$\left(\frac{E}{M}\right)_{5/2} = \begin{cases} \dfrac{E_2}{M_2} & \dot{m}_{5/2} > 0 \\ c_v \cdot T_3 - \dfrac{\alpha \cdot L_3}{2} & \dot{m}_{5/2} < 0 \end{cases} \qquad (5.36)$$

$$\left(\frac{E}{M}\right)_{7/2} = \begin{cases} c_v \cdot T_3 + \dfrac{\alpha \cdot L_3}{2} & \dot{m}_{7/2} > 0 \\ \dfrac{E_4}{M_4} & \dot{m}_{7/2} < 0 \end{cases} \tag{5.37}$$

$$\left(\frac{E}{M}\right)_{9/2} = \begin{cases} \dfrac{E_4}{M_4} & \dot{m}_{9/2} > 0 \\ \dfrac{E_5}{M_5} & \dot{m}_{9/2} < 0 \end{cases} \tag{5.38}$$

and T_3 can be expressed in terms of the mean logarithmic temperature as

$$T_3 = \frac{\alpha \cdot L_3}{2} \cdot \frac{\exp\left(\dfrac{\alpha \cdot L_3}{T_{ln,3}}\right) + 1}{\exp\left(\dfrac{\alpha \cdot L_3}{T_{ln,3}}\right) - 1} \tag{5.39}$$

Integral conditions:

Mean pressure

$$\frac{1}{t_p} \cdot \int_{t=0}^{t_p} p \cdot dt = p_{mean} \tag{5.40}$$

Regenerator fluxes

$$\begin{aligned} \int_{t=0}^{t_p} \dot{m}_{5/2} \cdot c_p \cdot T_{5/2} \cdot dt - \int_{t=0}^{t_p} \frac{1}{2} \cdot (\dot{m}_{5/2} + \dot{m}_{7/2}) \cdot c_p \cdot T_3 \cdot dt &= 0 \\ \int_{t=0}^{t_p} \dot{m}_{7/2} \cdot c_p \cdot T_{7/2} \cdot dt - \int_{t=0}^{t_p} \frac{1}{2} \cdot (\dot{m}_{5/2} + \dot{m}_{7/2}) \cdot c_p \cdot T_3 \cdot dt &= 0 \end{aligned} \tag{5.41}$$

Cyclic heat transfer in the variable volumes

$$\begin{aligned} \int_{t=0}^{t_p} \frac{1}{2} \cdot |\dot{m}_{3/2}| \cdot c_p \cdot NTU_1 \cdot \left(T_{s,1} - \frac{E_1}{M_1 \cdot c_v}\right) \cdot dt &= 0 \\ \int_{t=0}^{t_p} \frac{1}{2} \cdot |\dot{m}_{9/2}| \cdot c_p \cdot NTU_5 \cdot \left(T_{s,5} - \frac{E_5}{M_5 \cdot c_v}\right) \cdot dt &= 0 \end{aligned} \tag{5.42}$$

This completes the basic formulation of the system of equations.

5.3.4 Alternative formulation of the full system of equations

It is possible to rewrite the energy equation using the equation of state to get a simplified expression. The first term (the rate of change in internal energy) can be written as

$$\frac{d}{dt}\left(M \cdot c_v \cdot T\right)_i = \frac{c_v}{R} \cdot \frac{d}{dt}\left(p \cdot V_i\right) = \frac{1}{\gamma - 1} \cdot \left(p \cdot \frac{dV_i}{dt} + V_i \cdot \frac{dp}{dt} \right) \tag{5.43}$$

The first term equals zero for constant volumes (heat exchangers and regenerator), while it can be combined with the work term for the variable volumes.

This gives the following system of equations for the alternative formulation:

Volume 1 (variable volume, compression)

$$\begin{aligned} \frac{dM_1}{dt} &= -\dot{m}_{3/2} \\ \frac{V_1(t)}{\gamma - 1} \cdot \frac{dp}{dt} &= -\dot{m}_{3/2} \cdot c_p \cdot T_{3/2} + \frac{1}{2} \cdot \left|\dot{m}_{3/2}\right| \cdot c_p \cdot NTU_1 \cdot \left(T_{s,1} - T_1\right) - \frac{\gamma}{\gamma - 1} \cdot p \cdot \frac{dV_1}{dt} \\ p \cdot V_1(t) &= M_1 \cdot R \cdot T_1 \end{aligned} \tag{5.44}$$

Volume 2 (heat exchanger, compression)

$$\begin{aligned} \frac{dM_2}{dt} &= \dot{m}_{3/2} - \dot{m}_{5/2} \\ \frac{V_2}{\gamma - 1} \cdot \frac{dp}{dt} &= \dot{m}_{3/2} \cdot c_p \cdot T_{3/2} - \dot{m}_{5/2} \cdot c_p \cdot T_{5/2} + \frac{1}{2} \cdot \left(\left|\dot{m}_{3/2}\right| + \left|\dot{m}_{5/2}\right| \right) \cdot c_p \cdot NTU_2 \cdot \left(T_{s,2} - T_2\right) \\ p \cdot V_2 &= M_2 \cdot R \cdot T_2 \end{aligned} \tag{5.45}$$

Volume 3 (regenerator)

$$\begin{aligned} \frac{dM_3}{dt} &= \dot{m}_{5/2} - \dot{m}_{7/2} \\ \frac{V_3}{\gamma - 1} \cdot \frac{dp}{dt} &= \dot{m}_{5/2} \cdot c_p \cdot T_{5/2} - \dot{m}_{7/2} \cdot c_p \cdot T_{7/2} + \frac{1}{2} \cdot \left(\left|\dot{m}_{5/2}\right| + \left|\dot{m}_{7/2}\right| \right) \cdot c_p \cdot NTU_3 \cdot \left(T_{s,3} - T_3\right) \\ p \cdot V_3 &= M_3 \cdot R \cdot T_{\ln,3} \end{aligned} \tag{5.46}$$

Volume 4 (heat exchanger, expansion)

$$\frac{dM_4}{dt} = \dot{m}_{7/2} - \dot{m}_{9/2}$$

$$\frac{V_4}{\gamma - 1}\cdot\frac{dp}{dt} = \dot{m}_{7/2}\cdot c_p\cdot T_{7/2} - \dot{m}_{9/2}\cdot c_p\cdot T_{9/2} + \frac{1}{2}\cdot\left(|\dot{m}_{7/2}| + |\dot{m}_{9/2}|\right)\cdot c_p\cdot NTU_4\cdot(T_{s,4} - T_4) \tag{5.47}$$

$$p\cdot V_4 = M_4\cdot R\cdot T_4$$

Volume 5 (variable volume, expansion)

$$\frac{dM_5}{dt} = \dot{m}_{9/2}$$

$$\frac{V_5(t)}{\gamma - 1}\cdot\frac{dp}{dt} = \dot{m}_{9/2}\cdot c_p\cdot T_{9/2} + \frac{1}{2}\cdot|\dot{m}_{9/2}|\cdot c_p\cdot NTU_5\cdot(T_{s,5} - T_5) - \frac{\gamma}{\gamma - 1}\cdot p\cdot\frac{dV_5}{dt} \tag{5.48}$$

$$p\cdot V_5(t) = M_5\cdot R\cdot T_5$$

The temperatures on the control volume boundaries are given as

$$T_{3/2} = \begin{cases} T_1 & \dot{m}_{3/2} > 0 \\ T_2 & \dot{m}_{3/2} < 0 \end{cases} \tag{5.49}$$

$$T_{5/2} = \begin{cases} T_2 & \dot{m}_{5/2} > 0 \\ T_3 - \dfrac{\alpha\cdot L_3}{2} & \dot{m}_{5/2} < 0 \end{cases} \tag{5.50}$$

$$T_{7/2} = \begin{cases} T_3 + \dfrac{\alpha\cdot L_3}{2} & \dot{m}_{7/2} > 0 \\ T_4 & \dot{m}_{7/2} < 0 \end{cases} \tag{5.51}$$

$$T_{9/2} = \begin{cases} T_4 & \dot{m}_{9/2} > 0 \\ T_5 & \dot{m}_{9/2} < 0 \end{cases} \tag{5.52}$$

The expressions for the cyclic integral conditions for the alternative formulation are basically identical with the ones for the basic formulation, i.e.,

Mean pressure

$$\frac{1}{t_p}\cdot\int_{t=0}^{t_p} p\cdot dt \;=\; p_{mean} \tag{5.53}$$

Regenerator fluxes

$$\begin{aligned}
&\int_{t=0}^{t_p} \dot{m}_{5/2}\cdot c_p\cdot T_{5/2}\cdot dt \;-\; \int_{t=0}^{t_p} \frac{1}{2}\cdot(\dot{m}_{5/2}+\dot{m}_{7/2})\cdot c_p\cdot T_3\cdot dt \;=\; 0 \\
&\int_{t=0}^{t_p} \dot{m}_{7/2}\cdot c_p\cdot T_{7/2}\cdot dt \;-\; \int_{t=0}^{t_p} \frac{1}{2}\cdot(\dot{m}_{5/2}+\dot{m}_{7/2})\cdot c_p\cdot T_3\cdot dt \;=\; 0
\end{aligned} \tag{5.54}$$

Cyclic heat transfer in variable volumes

$$\begin{aligned}
&\int_{t=0}^{t_p} \frac{1}{2}\cdot|\dot{m}_{3/2}|\cdot c_p\cdot NTU_1\cdot(T_{s,1}-T_1)\cdot dt \;=\; 0 \\
&\int_{t=0}^{t_p} \frac{1}{2}\cdot|\dot{m}_{9/2}|\cdot c_p\cdot NTU_5\cdot(T_{s,5}-T_5)\cdot dt \;=\; 0
\end{aligned} \tag{5.55}$$

This completes the alternative formulation of the equations.

For both formulations the following properties are assumed to be known and constant.

- specific heat capacity (constant volume) c_v
- specific heat capacity (constant pressure) c_p
- gas constant R

Furthermore, the temperatures of the walls in the heat exchangers are assumed to be known and constant ($T_{s,2}$ and $T_{s,4}$) and all the NTU-numbers are also assumed to be known and constant for this Simple Five-Volume Stirling Model.

The mechanical dynamics of the engine has not been analyzed, and the volume variation is assumed to be given explicitly as a function of time.

For the variable volumes the following expressions have been used for the total volumes

$$V_1(t) = V_{cl,1} + V_{sw,1}\cdot\frac{1+\cos(\omega\cdot t+\varphi_{0,1})}{2}$$
$$V_5(t) = V_{cl,5} + V_{sw,5}\cdot\frac{1+\cos(\omega\cdot t+\varphi_{0,5})}{2} \qquad (5.56)$$

The derivatives can easily be calculated as

$$V_1'(t) = \frac{dV_1}{dt} = -\frac{\omega}{2}\cdot V_{sw,1}\cdot\sin(\omega\cdot t+\varphi_{0,1})$$
$$V_5'(t) = \frac{dV_5}{dt} = -\frac{\omega}{2}\cdot V_{sw,5}\cdot\sin(\omega\cdot t+\varphi_{0,5}) \qquad (5.57)$$

notice that the phase angle (difference) $\Delta\varphi$ with this notation is given as

$$\Delta\varphi = \varphi_{0,5} - \varphi_{0,1} \qquad (5.58)$$

This concludes the description of the mathematical model for the SFVSM.

5.4 Classification of the SFVSM

The system of equations includes both ordinary differential equations (ODEs) and algebraic equations. There exists a comprehensive theory for such systems of differential-algebraic equations (DAEs), but the more theoretical aspects will not be discussed in great detail in this thesis. References will be given, when results from this theory are used in the forthcoming chapters.

The basic formulation and the alternative formulation are both systems of DAEs, but the number of differential and algebraic variables is different.

Now let N_{vol} denote number of volumes (components) such that N_{vol}= 5.

Basic formulation

Number of differential equations:	$n_f = 2\cdot N_{vol}$	= 10
Number of algebraic equations:	$n_g = N_{vol}$	= 5
Number of differential (dynamic) variables:	$n_y = 2\cdot N_{vol}$	= 10
Number of algebraic (static) variables:	$n_z = N_{vol}$	= 5

Mass M_i and internal energy E_i for ($i=1,2,...,N_{vol}$) are the differential variables, while the mass flows $\dot{m}_{i+1/2}$ ($i=1,2,...,N_{vol}-1$) and the pressure p are the algebraic variables.

Alternative formulation

Number of differential equations:	$n_f = 2 \cdot N_{vol}$	$= 10$
Number of algebraic equations:	$n_g = N_{vol}$	$= 5$
Number of differential (dynamic) variables:	$n_y = N_{vol} + 1$	$= 6$
Number of algebraic (static) variables:	$n_z = N_{vol} + N_{vol} - 1$	$= 9$

Mass M_i ($i=1,2,...,N_{vol}$) and pressure p are the differential variables, while the mass flows $\dot{m}_{i+1/2}$ ($i=1,2,...,N_{vol}-1$) and the temperatures T_i ($i=1,2,...,N_{vol}$) are the algebraic variables.

Notice that $n_f + n_g = n_y + n_z$ is satisfied for both formulations.

5.5 Concluding remarks

Different methods for obtaining the stationary periodic solution

The essential problem is to find a numerical method for obtaining the stationary periodic solution. The method should be fast, stable and accurate and independent of the specific problem. In general, it is not possible for a method to have all the properties mentioned above, so some kind of compromise will have to be made.

In the next chapters, different solution approaches and numerical methods for the Simple Five -Volume Stirling Model will be analyzed and discussed.

References

[1] Urieli, I. and Berchowitz, D.M.
Stirling Cycle Engine Analysis.
Adam Hilger Ltd, Bristol (1984).

6.0 NUMERICAL METHODS

SOLVING THE MATHEMATICAL MODEL

6.1 Introduction

This chapter deals with the numerical solution of the Simple Five-Volume Stirling Model (SFVSM) problem derived in the previous chapters.

The first part is devoted to putting the mathematical model of the SFVSM-problem in a more accessible form. The whole system of equations is made dimensionless (scaled) and written in a general form that makes it easier to keep a short and consistent formulation. The full system is classified and several additional problems are identified and discussed.

In the second part of the analysis, different numerical methods for solving Initial Value problems (IVPs) and Boundary Value problems (BVPs) are considered. Important features will be discussed with special regard to the application for solving the SFVSM-problem.

The main emphasis is put on numerical methods and approaches that have promising features for obtaining the full cyclic solution (i.e., the periodic steady state solution) in a fast and conceivable way.

The following approaches have been considered:

- Integration-to-Convergence.
- Shooting method.
- Finite-Difference method.
- Optimization.
- Extrapolation.

Only the first three of these will be discussed in detail.

The actual implementation for the SFVSM-problem is carried out in section 6.6-6.8. It should be possible to skip the basic theory in section 6.4-6.5 and go directly to the applications in 6.6-6.8, where the implementations for each of these three approaches are discussed in detail.

A simulation program in form of computer code has been developed for the SFVSM-problem using each of these three selected methods. Results will be discussed in the next chapter, where comparisons concerning the numerical properties such as stability, accuracy and speed also will be made.

Finally, additional numerical problems related to the presence of discontinuities in the equations are identified and discussed.

6.2 General formulation of the SFVSM-problem

6.2.1 Scaling

Consider the system of equations derived for the SFVSM-problem using the formulations from the previous chapter. Because of the different magnitudes of some of the variables (e.g., pressure and mass), it is necessary to scale the problem and make the equations and variables dimensionless in order to obtain a stable and accurate numerical solution.

The following parameters have been chosen as references for the scaling:

Time	: Time period of a cycle.
Pressure	: Required mean pressure of the cycle.
Temperature	: Temperature in the hot heat exchanger.
Mass	: Total mass.

Expressed using the defined variables from chapter 5:

$$t_{ref} = t_p \qquad p_{ref} = p_{mean} \qquad T_{ref} = T_{s,4} \qquad M_{ref} = M_{tot} \tag{6.1}$$

A reference volume can then be defined from the equation of state (ideal gas)

$$V_{ref} \equiv \frac{M_{ref} \cdot R \cdot T_{ref}}{p_{ref}} \tag{6.2}$$

A reference energy as

$$E_{ref} = M_{ref} \cdot c_v \cdot T_{ref} \tag{6.3}$$

and reference mass flow

$$\dot{m}_{ref} = \frac{M_{ref}}{t_{ref}} \tag{6.4}$$

The scaled, dimensionless masses are then given as

$$\tilde{M}_i = \frac{M_i}{M_{ref}} \qquad i = 1,2,...,5 \tag{6.5}$$

and correspondingly for all the other dimensionless variables:

Time:

$$\tilde{t} = \frac{t}{t_p} \tag{6.6}$$

Energy:

$$\tilde{E}_i = \frac{E_i}{E_{ref}} = \frac{E_i}{M_{ref} \cdot c_v \cdot T_{ref}} \qquad i = 1,2,...,5 \tag{6.7}$$

Pressure:

$$\tilde{p} = \frac{p}{p_{ref}} \tag{6.8}$$

Gas temperature:

$$\tilde{T}_i = \frac{T_i}{T_{ref}} \qquad i = 1,2,...,5 \tag{6.9}$$

Solid temperature:

$$\tilde{T}_{s,i} = \frac{T_{s,i}}{T_{ref}} \qquad i = 1,2,...,5 \tag{6.10}$$

Matrix temperature gradient (temperature difference across the regenerator):

$$\tilde{\alpha} = \frac{\alpha \cdot L}{T_{ref}} \tag{6.11}$$

Mass flow:

$$\tilde{m}_{i-1/2} = \frac{\dot{m}_{i-1/2}}{\dot{m}_{ref}} = \frac{\dot{m}_{i-1/2}}{\left(\frac{M_{ref}}{t_{ref}}\right)} \qquad i = 1,2,...,6 \tag{6.12}$$

Apart from making the numerical solution more stable, scaling of the variables and equations also implies that all of the variables are of the same order of magnitude. This makes it easier to find suitable iteration criteria for the iterations required for the solution of the problem.

6.2.2 Basic formulation

Scaled equations

In dimensionless form, the governing equations for the general *i*th volume will, when the basic formulation of the system of equations (see section 5.3.3) is used, typically look like the following:

$$\begin{aligned}
\frac{dM_i}{dt} &= \dot{m}_{i-1/2} - \dot{m}_{i+1/2} \\
\frac{dE_i}{dt} &= \gamma \cdot \left(\dot{m} \cdot \frac{E}{M}\right)_{i-1/2} - \gamma \cdot \left(\dot{m} \cdot \frac{E}{M}\right)_{i+1/2} + \\
&\quad \frac{1}{2} \cdot \left(|\dot{m}_{i-1/2}| + |\dot{m}_{i+1/2}|\right) \cdot \gamma \cdot NTU_i \cdot \left(T_{s,i} - \frac{E_i}{M_i}\right) - (\gamma - 1) \cdot p \cdot \frac{dV_i}{dt} \\
p \cdot V_i - E_i &= 0
\end{aligned} \tag{6.13}$$

where the superscript has been dropped for the scaled variables.

New variables

To systemize the treatment of the equations (especially with regard to the derivation of the analytical expression of the Jacobian of the nonlinear system) and to make the translation into computer code more apparent, new variables will be introduced. The system of equations can then be put in a short, general form and the classification of the problem will be simple.

Now define a vector $\underline{y}$, which consists of the unknown differential (dynamic) variables as a function of time t in the following way:

$$\begin{aligned}
y_i &= M_i \qquad i = 1,2,...,5 \\
y_{5+i} &= E_i \qquad i = 1,2,...,5
\end{aligned} \tag{6.14}$$

and another vector $\underline{z}$, which holds all algebraic (static) variables

$$\begin{aligned}
z_i &= \dot{m}_{i-1/2} \qquad i = 1,2,...,6 \\
z_7 &= p
\end{aligned} \tag{6.15}$$

The number of volumes is identical to the number of components and equal to 5 for the SFVSM-problem.

Notice that the boundary conditions $\dot{m}_{1/2} = \dot{m}_{11/2} = 0$ are included, such that the number of equations effectively could be reduced by two by inserting these directly into the equations. This is carried out in the developed computer code and will also be implemented in the equations here.

It is also convenient to define new (scaled) variables for the parameters used for the determination of the cyclic integral conditions.

Total mass	:	$\lambda_1 = M_{tot}$
Regenerator solid temperature	:	$\lambda_2 = T_{s,3}$
Regenerator temperature gradient (difference)	:	$\lambda_3 = \alpha \cdot L_3$
Cold variable volume solid temperature	:	$\lambda_4 = T_{s,1}$
Hot variable volume solid temperature	:	$\lambda_5 = T_{s,5}$

Notice that with the given scaling $T_{s,4} = 1$ since all temperatures have been made dimensionless with the fixed temperature in hot heat exchanger.

The dimensionless gas temperature in the middle of the regenerator is furthermore defined as an additional variable, i.e.

$$z_8 = T_{s,3} \tag{6.16}$$

Equations and boundary conditions

Consider the system of equations derived for the SFVSM-problem using the basic formulation (see the derivation in section 5.3.3) and scaling.

Introducing the new variables gives the following full system of equations:

Mass:

$$\begin{aligned} \frac{dy_1}{dt} &= -z_2 \\ \frac{dy_2}{dt} &= z_2 - z_3 \\ \frac{dy_3}{dt} &= z_3 - z_4 \\ \frac{dy_4}{dt} &= z_4 - z_5 \\ \frac{dy_5}{dt} &= z_5 \end{aligned} \tag{6.17}$$

Energy:

$$\frac{dy_6}{dt} = -\gamma\cdot\max(z_2,0)\cdot\frac{y_6}{y_1} - \gamma\cdot\min(z_2,0)\cdot\frac{y_7}{y_2} + \frac{1}{2}\cdot|z_2|\cdot\gamma\cdot NTU_1\cdot\left(\lambda_4 - \frac{y_6}{y_1}\right) - (\gamma-1)\cdot z_7\cdot V_1'(t)$$

$$\frac{dy_7}{dt} = \gamma\cdot\max(z_2,0)\cdot\frac{y_6}{y_1} + \gamma\cdot\min(z_2,0)\cdot\frac{y_7}{y_2} - \gamma\cdot\max(z_3,0)\cdot\frac{y_7}{y_2} - \gamma\cdot\min(z_3,0)\cdot\left(z_8 - \frac{\lambda_3}{2}\right) + \frac{1}{2}\cdot(|z_2|+|z_3|)\cdot\gamma\cdot NTU_2\cdot\left(T_{s,2} - \frac{y_7}{y_2}\right)$$

$$\frac{dy_8}{dt} = \gamma\cdot\max(z_3,0)\cdot\frac{y_7}{y_2} + \gamma\cdot\min(z_3,0)\cdot\left(z_8 - \frac{\lambda_3}{2}\right) - \gamma\cdot\max(z_4,0)\cdot\left(z_8 + \frac{\lambda_3}{2}\right) - \gamma\cdot\min(z_4,0)\cdot\frac{y_9}{y_4} + \frac{1}{2}\cdot(|z_3|+|z_4|)\cdot\gamma\cdot NTU_3\cdot(\lambda_2 - z_8) \qquad (6.18)$$

$$\frac{dy_9}{dt} = \gamma\cdot\max(z_4,0)\cdot\left(z_8 + \frac{\lambda_3}{2}\right) + \gamma\cdot\min(z_4,0)\cdot\frac{y_9}{y_4} - \gamma\cdot\max(z_5,0)\cdot\frac{y_9}{y_4} - \gamma\cdot\min(z_5,0)\cdot\frac{y_{10}}{y_5} + \frac{1}{2}\cdot(|z_4|+|z_5|)\cdot\gamma\cdot NTU_4\cdot\left(T_{s,4} - \frac{y_9}{y_4}\right)$$

$$\frac{dy_{10}}{dt} = \gamma\cdot\max(z_5,0)\cdot\frac{y_9}{y_4} + \gamma\cdot\min(z_5,0)\cdot\frac{y_{10}}{y_5} + \frac{1}{2}\cdot|z_5|\cdot\gamma\cdot NTU_5\cdot\left(\lambda_5 - \frac{y_{10}}{y_5}\right) - (\gamma-1)\cdot z_7\cdot V_5'(t)$$

Equation of state:

$$\begin{aligned} z_7\cdot V_1(t) - y_6 &= 0 \\ z_7\cdot V_2 - y_7 &= 0 \\ z_7\cdot V_3 - y_8 &= 0 \\ z_7\cdot V_4 - y_9 &= 0 \\ z_7\cdot V_5(t) - y_{10} &= 0 \end{aligned} \qquad (6.19)$$

The equation for the gas temperature in the middle of regenerator can be found from (5.39) and this gives the following algebraic equation:

$$z_8 - \frac{\lambda_3}{2} \cdot \frac{\exp\left(\lambda_3 \cdot \frac{y_3}{y_8}\right) + 1}{\exp\left(\lambda_3 \cdot \frac{y_3}{y_8}\right) - 1} = 0 \qquad (6.20)$$

and the assumption of no flow through the ends of the variable volumes gives the following (spatial boundary) conditions:

$$\begin{aligned} z_1 &= 0 \\ z_6 &= 0 \end{aligned} \qquad (6.21)$$

which have been inserted in the equations just given.

The SFVSM-problem can in compact form now be stated as

$$\begin{aligned} \underline{y}'(t) &= \underline{f}(t,\underline{y},\underline{z}) \\ 0 &= \underline{g}(t,\underline{y},\underline{z}) \end{aligned} \qquad (6.22)$$

The elements of the vector $\underline{y}$ are mass and internal energy for each volume, while the elements of $\underline{z}$ are mass flows, pressure and regenerator gas temperature.

t is time, $\underline{y}$ and $\underline{z}$ are vectors of dimension n_y and n_z respectively, $\underline{f}$ and $\underline{g}$ are vector functions of dimension n_f and n_g. For the SFVSM-problem $n_y=n_f= 10$ and $n_z=n_g= 8$, so totally the dimension is $n_y+ n_z = 18$.

The boundary conditions in time are periodic, i.e.,

$$\underline{y}(0) = \underline{y}(t_p) \quad , \quad \underline{z}(0) = \underline{z}(t_p) \qquad (6.23)$$

since it is assumed that the solution is periodic with the time period t_p given from the volume variation. Notice that with the given scaling, the dimensionless time t_p is equal to 1, since the real time t has been scaled with the period of the cycle.

Discretization

The exact solution $\underline{y}(t)$ and $\underline{z}(t)$ will be approximated at a finite number of discrete points t_j, j=0,1,...,N by a numerical method. Let $\underline{y}_n$ and $\underline{z}_n$ denote the solution obtained by the numerical method at time level t_n, i.e.,

$$\begin{aligned} \underline{y}_n &\approx \underline{y}(t_n) \\ \underline{z}_n &\approx \underline{z}(t_n) \end{aligned} \tag{6.24}$$

where $\underline{y}_n$ and $\underline{z}_n$ are given as

$$\underline{y}_n = \begin{bmatrix} y_{1,n} \\ y_{2,n} \\ y_{3,n} \\ y_{4,n} \\ y_{5,n} \\ y_{6,n} \\ y_{7,n} \\ y_{8,n} \\ y_{9,n} \\ y_{10,n} \end{bmatrix} = \begin{bmatrix} M_{1,n} \\ M_{1,n} \\ M_{3,n} \\ M_{4,n} \\ M_{5,n} \\ E_{1,n} \\ E_{2,n} \\ E_{3,n} \\ E_{4,n} \\ E_{5,n} \end{bmatrix} , \qquad \underline{z}_n = \begin{bmatrix} z_{1,n} \\ z_{2,n} \\ z_{3,n} \\ z_{4,n} \\ z_{5,n} \\ z_{6,n} \\ z_{7,n} \\ z_{8,n} \end{bmatrix} = \begin{bmatrix} \dot{m}_{1/2,n} \\ \dot{m}_{3/2,n} \\ \dot{m}_{5/2,n} \\ \dot{m}_{7/2,n} \\ \dot{m}_{9/2,n} \\ \dot{m}_{11/2,n} \\ p_n \\ T_{3,n} \end{bmatrix} \tag{6.25}$$

The numerical solution should satisfy the condition of stationary cyclic state variables. Discretizing one cycle into N+1 points with t_j , j = 0,1,2,...,N where t_0= 0 and t_N= 1 implies

$$\underline{y}_0 = \underline{y}_N \qquad , \qquad \underline{z}_0 = \underline{z}_N \tag{6.26}$$

6.2.3 Alternative formulation

Now consider the alternative formulation of the SFVSM-problem where the energy equation has been rewritten such that it is the derivative w.r.t. pressure instead of internal energy (see section 5.3.4). The variables are made dimensionless with the same reference parameters as for the basic formulation.

New variables

The vector $\underline{y}$, which consist of all the differential variables is now given as

$$\begin{aligned} y_i &= M_i \qquad i = 1,2,...,5 \\ y_6 &= p \end{aligned} \tag{6.27}$$

and the vector $\underline{z}$ with the algebraic variables as

$$\begin{aligned} z_i &= \dot{m}_{i-1/2} \qquad i = 1,2,...,6 \\ z_{5+i} &= T_i \qquad i = 1,2,...,5 \end{aligned} \tag{6.28}$$

The parameters λ_i (i=1,2,...5) are defined as for the basic formulation.

The conservation equations of mass are as before, i.e.,

Mass:

$$\begin{aligned} \frac{dy_1}{dt} &= -z_2 \\ \frac{dy_2}{dt} &= z_2 - z_3 \\ \frac{dy_3}{dt} &= z_3 - z_4 \\ \frac{dy_4}{dt} &= z_4 - z_5 \\ \frac{dy_5}{dt} &= z_5 \end{aligned} \tag{6.29}$$

while the conservation equations for energy and the equations of state are different

Energy:

$$\frac{V_1(t)}{\gamma-1}\cdot\frac{dy_6}{dt} = -\frac{\gamma}{\gamma-1}\cdot\max(z_2,0)\cdot z_7 - \frac{\gamma}{\gamma-1}\cdot\min(z_2,0)\cdot z_8 + \frac{1}{2}\cdot|z_2|\cdot\frac{\gamma}{\gamma-1}\cdot NTU_1\cdot(\lambda_4 - z_7) - \frac{\gamma}{\gamma-1}\cdot y_6\cdot V_1'(t)$$

$$\frac{V_2}{\gamma-1}\cdot\frac{dy_6}{dt} = \frac{\gamma}{\gamma-1}\cdot\max(z_2,0)\cdot z_7 + \frac{\gamma}{\gamma-1}\cdot\min(z_2,0)\cdot z_8 - \frac{\gamma}{\gamma-1}\cdot\max(z_3,0)\cdot z_8 - \frac{\gamma}{\gamma-1}\cdot\min(z_3,0)\cdot\left(z_9 - \frac{\lambda_3}{2}\right) + \frac{1}{2}\cdot(|z_2| + |z_3|)\cdot\frac{\gamma}{\gamma-1}\cdot NTU_2\cdot(T_{s,2} - z_8)$$

$$\frac{V_3}{\gamma-1}\cdot\frac{dy_6}{dt} = \frac{\gamma}{\gamma-1}\cdot\max(z_3,0)\cdot z_8 + \frac{\gamma}{\gamma-1}\cdot\min(z_3,0)\cdot\left(z_9 - \frac{\lambda_3}{2}\right) - \frac{\gamma}{\gamma-1}\cdot\max(z_4,0)\cdot\left(z_9 + \frac{\lambda_3}{2}\right) - \frac{\gamma}{\gamma-1}\cdot\min(z_4,0)\cdot z_{10} + \frac{1}{2}\cdot(|z_3| + |z_4|)\cdot\frac{\gamma}{\gamma-1}\cdot NTU_3\cdot(\lambda_2 - z_9) \quad (6.30)$$

$$\frac{V_4}{\gamma-1}\cdot\frac{dy_6}{dt} = \frac{\gamma}{\gamma-1}\cdot\max(z_4,0)\cdot\left(z_9 + \frac{\lambda_3}{2}\right) + \frac{\gamma}{\gamma-1}\cdot\min(z_4,0)\cdot z_{10} - \frac{\gamma}{\gamma-1}\cdot\max(z_5,0)\cdot z_{10} - \frac{\gamma}{\gamma-1}\cdot\min(z_5,0)\cdot z_{11} + \frac{1}{2}\cdot(|z_4| + |z_5|)\cdot\frac{\gamma}{\gamma-1}\cdot NTU_4\cdot(T_{s,4} - z_{10})$$

$$\frac{V_5(t)}{\gamma-1}\cdot\frac{dy_6}{dt} = \frac{\gamma}{\gamma-1}\cdot\max(z_5,0)\cdot z_{10} + \frac{\gamma}{\gamma-1}\cdot\min(z_5,0)\cdot z_{11} + \frac{1}{2}\cdot|z_5|\cdot\frac{\gamma}{\gamma-1}\cdot NTU_5\cdot(\lambda_5 - z_{11}) - \frac{\gamma}{\gamma-1}\cdot y_6\cdot V_5'(t)$$

Equations of state:

$$
\begin{aligned}
& y_6 \cdot V_1(t) - y_1 \cdot z_7 = 0 \\
& y_6 \cdot V_2 - y_2 \cdot z_8 = 0 \\
& y_6 \cdot V_3 - y_3 \cdot \frac{\lambda_3}{\ln\left(\dfrac{z_9 + \dfrac{\lambda_3}{2}}{z_9 - \dfrac{\lambda_3}{2}}\right)} = 0 \\
& y_6 \cdot V_4 - y_4 \cdot z_{10} = 0 \\
& y_6 \cdot V_5(t) - y_5 \cdot z_{11} = 0
\end{aligned}
\tag{6.31}
$$

Boundary conditions at the ends of the variable volumes:

$$
\begin{aligned}
z_1 &= 0 \\
z_6 &= 0
\end{aligned}
\tag{6.32}
$$

For the alternative formulation of the SFVSM-problem, the system of equations is given in the form

$$
\begin{aligned}
\underline{\underline{A}} \cdot \underline{y}'(t) &= \underline{f}(t, \underline{y}, \underline{z}) \\
0 &= \underline{g}(t, \underline{y}, \underline{z})
\end{aligned}
\tag{6.33}
$$

where $\underline{y}$ and $\underline{z}$ are vectors of dimension n_y and n_z respectively and $\underline{\underline{A}}$ is a matrix of dimension n_f x n_y. The elements of the vector $\underline{y}$ are the masses and the pressure, while the elements of $\underline{z}$ are mass flows and temperatures. For the Simple Five-Volume Stirling Model problem and the alternative formulation: n_y=6, n_f=10, n_z=11 and n_g=7 and totally the dimension is n_y+n_z=17. Notice that $n_y+n_z = n_f+n_g$ is satisfied although $n_y \neq n_f$.

Periodic boundary conditions in time are the same as for the basic formulation, i.e.,

$$
\underline{y}(0) = \underline{y}(t_p) \quad , \quad \underline{z}(0) = \underline{z}(t_p) \tag{6.34}
$$

The different formulations of the problem are important. Usually explicit numerical methods for the time integration cannot be applied to a general system of differential-algebraic equations (this will be explained in more details later).

Explicit Runge-Kutta methods can (as it will be shown later in this chapter) only be implemented for the alternative formulation of the system of equations, while implicit Runge-Kutta methods, which will be of main interest in this thesis, can be applied to both formulations.

6.2.4 Integral constraints

In addition to the differential-algebraic equations and the boundary conditions, the solution has to satisfy integral constraints originating from the cyclic conditions. In dimensionless form and with the new variables, these integral equations are (using the expression derived in section 5.3.3 and 5.3.4) given as:

Basic formulation

Mean pressure:

$$\int_{t=0}^{t_p} (z_7 - 1) \cdot dt = 0 \tag{6.35}$$

This integral should be equal to zero because the pressure has been scaled with the required mean pressure.

Enthalpy fluxes through the regenerator:

$$\begin{aligned} \int_{t=0}^{t_p} \left(\gamma \cdot \max(z_3,0) \cdot \frac{y_7}{y_2} + \gamma \cdot \min(z_3,0) \cdot \left(z_8 - \frac{\lambda_3}{2} \right) - \frac{\gamma}{2} \cdot (z_3 + z_4) \cdot z_8 \right) \cdot dt &= 0 \\ \int_{t=0}^{t_p} \left(\gamma \cdot \max(z_4,0) \cdot \left(z_8 + \frac{\lambda_3}{2} \right) + \gamma \cdot \min(z_4,0) \cdot \frac{y_9}{y_4} - \frac{\gamma}{2} \cdot (z_3 + z_4) \cdot z_8 \right) \cdot dt &= 0 \end{aligned} \tag{6.36}$$

Cyclic heat transfer in variable volumes:

$$\begin{aligned} \int_{t=0}^{t_p} \frac{1}{2} \cdot |z_2| \cdot \gamma \cdot NTU_1 \cdot \left(\lambda_4 - \frac{y_6}{y_1} \right) \cdot dt &= 0 \\ \int_{t=0}^{t_p} \frac{1}{2} \cdot |z_5| \cdot \gamma \cdot NTU_5 \cdot \left(\lambda_5 - \frac{y_{10}}{y_5} \right) \cdot dt &= 0 \end{aligned} \tag{6.37}$$

Alternative formulation

The expressions for the integral conditions for the alternative formulation are more or less identical, just with the changed variables. For the sake of completeness the expressions will be given here too.

Mean pressure:

$$\int_{t=0}^{t_p} (y_6 - 1) \cdot dt = 0 \tag{6.38}$$

Enthalpy fluxes through the regenerator:

$$\begin{aligned}
&\int_{t=0}^{t_p} \left(\gamma \cdot \max(z_3,0) \cdot z_8 + \gamma \cdot \min(z_3,0) \cdot \left(z_9 - \frac{\lambda_3}{2} \right) - \frac{\gamma}{2} \cdot (z_3 + z_4) \cdot z_9 \right) \cdot dt = 0 \\
&\int_{t=0}^{t_p} \left(\gamma \cdot \max(z_4,0) \cdot \left(z_9 + \frac{\lambda_3}{2} \right) + \gamma \cdot \min(z_4,0) \cdot z_{10} - \frac{\gamma}{2} \cdot (z_3 + z_4) \cdot z_9 \right) \cdot dt = 0
\end{aligned} \tag{6.39}$$

Cyclic heat transfer in variable volumes:

$$\begin{aligned}
&\int_{t=0}^{t_p} \frac{1}{2} \cdot |z_2| \cdot \gamma \cdot NTU_1 \cdot (\lambda_4 - z_7) \cdot dt = 0 \\
&\int_{t=0}^{t_p} \frac{1}{2} \cdot |z_5| \cdot \gamma \cdot NTU_5 \cdot (\lambda_5 - z_{11}) \cdot dt = 0
\end{aligned} \tag{6.40}$$

The integral conditions can be written in the general form

$$\underline{H}(\underline{\lambda}) = \int_{t=0}^{t_p} \underline{h}(t, \underline{\lambda}, \underline{y}(t;\underline{\lambda}), \underline{z}(t;\underline{\lambda})) \cdot dt = \underline{0} \tag{6.41}$$

where $\underline{H}$ is a vector function and $\underline{\lambda}$ is a vector, both of dimension n_λ where n_λ is the number of cyclic integral conditions. The elements of $\underline{\lambda}$ are the parameters (total mass, solid matrix temperature e.t.c.), whose values should be adjusted, such that the conditions above are satisfied.

For a given value of $\underline{\lambda}$, the system of equations previously defined (using the basic or alternative formulation) with periodic boundary conditions can be solved for the state variables, but in general the integral conditions will not be satisfied. This means that the actual mean pressure of the cycle will be different from the required mean pressure, the net enthalpy flux through regenerator boundaries will not be identical and the net heat transfer in the variable volumes will not be zero (i.e., not cyclic heat transfer). The vector $\underline{\lambda}$ will then have to be modified, but this can only be done iteratively, since the solutions $\underline{y}(t)$ and $\underline{z}(t)$ depend implicitly on $\underline{\lambda}$.

For the Simple Five-Volume Stirling Model problem n_λ=3 without the condition of "cyclic heat transfer" in the variable volumes (parameters are: regenerator matrix temperature, matrix temperature gradient and fixed total mass) and n_λ=5 with the condition of "cyclic heat transfer" (additional parameters are the solid temperature in each of the variable volumes).

6.2.5 Solution invariants

The total mass of the system is assumed to be constant (no leak flow) and this condition has to be satisfied at any time, i.e.,

$$M_{tot} = \sum_{i=1}^{5} M_i(t) = constant \tag{6.42}$$

or using the new variables

$$\lambda_1 = \sum_{i=1}^{5} y_i(t) = constant \tag{6.43}$$

The solution invariant is satisfied automatically by the equations, since

$$\sum_{i=1}^{5} \frac{dM_i}{dt} = \sum_{i=1}^{5} (\dot{m}_{i-1/2} - \dot{m}_{i+1/2}) = 0 \tag{6.44}$$

This is not necessarily true for the numerical solution and different ways to numerically satisfy this solution invariant can be considered (see [1]).

One way to do it is to impose the condition directly and let the algebraic equation

$$\lambda_1 - y_1 - y_2 - y_3 - y_4 - y_5 = 0 \tag{6.45}$$

replace one of the differential equations for conservation of mass within a volume.

This is not always a good idea, since basically it corresponds to replacing the original differential equation with a new one, which has an infinite eigenvalue (time constant). Problems (in form of stiffness) could be expected but the approach has been successfully applied for some of the implementations discussed in following.

A uniform pressure distribution (no spatial change in pressure) through the system can also be classified as an invariant, but it will be very easy to satisfy this condition numerically for the SFVSM-problem by just specifying one variable for the pressure.

6.2.6 General remarks

Discontinuous partial derivatives

It should be noted that the right-hand side of the differential equations has discontinuous partial derivatives with respect to some of the algebraic variables (mass flows) for both formulations. This fact makes it difficult to establish theoretical results, which often require smooth functions and derivatives, and leaves only (in a mathematical sense) a less satisfactory trial-and-error approach. The presence of discontinuities is discussed in further details in section 6.10. Here it is only noted that $\underline{y}$ does not have continuous partial derivatives of second order, i.e.,

$$\underline{y} \notin C^2 \tag{6.46}$$

since $\underline{f}$ does not have first order continuous partial derivatives with respect to $\underline{z}$

$$\frac{\partial \underline{f}}{\partial \underline{z}} \notin C^0 \tag{6.47}$$

and

$$\underline{y}'' = \frac{d\underline{y}'}{dt} = \frac{d\underline{f}}{dt} = \frac{\partial \underline{f}}{\partial \underline{y}} \cdot \frac{d\underline{y}}{dt} + \frac{\partial \underline{f}}{\partial \underline{z}} \cdot \frac{d\underline{z}}{dt} + \frac{\partial \underline{f}}{\partial t} \tag{6.48}$$

General formulation

It is possible to formulate the system of equations as well as the periodic boundary conditions in a more general way. The problem can be stated as

$$\underline{F}(t,\underline{y},\underline{y}',\underline{z}) = \underline{0} \tag{6.49}$$

with

$$\underline{y}(t) = \underline{y}(t + t_p) \qquad \underline{z}(t) = \underline{z}(t + t_p) \tag{6.50}$$

One of the solution approaches considered (the Finite Difference method) will take advantage of the last form of periodic boundary conditions.

Solution strategy

For most of the approaches considered here, the idea is to find a vector $\underline{y}_0=\underline{y}(0)$ such that after using a given numerical method for the time integration of one period the following condition is satisfied: $\underline{y}(t_p) = \underline{y}(0)$.

These approaches differ in the way they determine or update the new value (iterate) of $\underline{y}_0^{[k+1]}$ from the previous iterates. For the Finite Difference method the idea is to determine all variables at all time levels simultaneously.

6.3 Classification

The problem can be classified as a *boundary value problem* (BVP) for a system of *differential-algebraic equations* (DAEs) with *periodic boundary conditions* (periodic in the time domain). Periodic boundary conditions are a special case of non-separated linear boundary conditions.

The system is *non-autonomous* because of the forcing term introduced through the movement of the pistons resulting in a variation of the total volume. The period t_p is assumed to be known and constant (equal to the period of the volume variation).

Furthermore, the periodic solution has to satisfy *integral constraints* originating from the requirement of cyclic conditions in the engine.

Solution *invariants* should be satisfied, e.g., the total mass of the system is constant at any time and the pressure distribution is uniform in space.

The right-hand side of the differential equations has *discontinuous partial derivatives* with respect to some of the algebraic variables. This is an important feature and complicates the numerical solution.

A system of DAEs can be classified further. An important property is the *index*, which can be defined the following way for a general system of nonlinear DAEs given in the form $\underline{F}(t,\underline{y},\underline{y}') = \underline{0}$:

> The index ϑ of a general DAE is defined as the smallest number ϑ of times $\underline{F}(t,\underline{y},\underline{y}')$ must be differentiated with respect to time in order to determine $\underline{y}'$ as continuous function of t and $\underline{y}$.

In general, the higher the index of a DAE, the more difficult it will be to obtain an accurate numerical solution.

Basic formulation

For the basic formulation of the SFVSM-problem the system of equations can be written in the form

$$\begin{aligned} \underline{y}'(t) &= \underline{f}(t,\underline{y},\underline{z}) \\ 0 &= \underline{g}(t,\underline{y},\underline{z}) \end{aligned} \tag{6.51}$$

This is a *semi-explicit system* of differential-algebraic equations.

For this system of DAEs the index is two or higher, because

$$\frac{\partial \underline{g}}{\partial \underline{z}} \tag{6.52}$$

is singular (see [4] pp. 32-34).

This is easy to see that the matrix is singular for the actual system, since several algebraic variables (all the mass flows) are not present in the algebraic equations (equations of state).

Alternative formulation

$$\begin{aligned} \underline{\underline{A}} \cdot \underline{y}'(t) &= \underline{f}(t,\underline{y},\underline{z}) \\ 0 &= \underline{g}(t,\underline{y},\underline{z}) \end{aligned} \tag{6.53}$$

This is a non-trivial system of DAEs and notice that $\underline{\underline{A}}$ is not a square matrix.

6.4 Numerical methods for solving IVPs

6.4.1. Introductory remarks

The Simple Five-Volume Stirling Model problem can be solved as an Initial-Value problem (IVP). The most simple of all approaches considered is the Integration-to-Convergence, where the system of equations just is integrated forward in time until the periodic steady state solution for the state variables is reached.

Solving the problem as a BVP using the Shooting method also involves numerical methods for IVPs. The advantage of dealing with the defined problem as an IVP is obvious. There exists a well developed theoretical understanding and practical implementation of numerical methods for IVPs of ordinary differential equations. In some extent this is also true for systems of differential-algebraic equations (DAEs), though additional considerations have to be made.

In the following, numerical methods for IVPs will be introduced and discussed. The main emphasis will be put on the class of Runge-Kutta methods, which have been used in the developed codes.

The most important classes of numerical methods for solving IVPs for systems of ordinary differential equations are:

- Linear Multistep methods (LMMs).
- Runge-Kutta methods (One Step methods).
- Extrapolation methods.

For stiff systems and general systems of DAEs the most widely used methods are BDF-methods (implicit LMMs) and IRK-methods (implicit Runge-Kutta methods).

In this text the main emphasis will be put on implicit Runge-Kutta methods, but explicit Runge-Kutta methods will also be considered. This choice is not of any decisive importance for obtaining a solution to the problem, but it has been made mainly because of the following facts:

- One-step methods, such as Runge-Kutta methods, do not need a special startup procedure for generating initial values for higher order methods.

- Change of step length during the time integration, for a variable step length algorithm or because of the presence of discontinuities in the equations, can easily be performed using a one-step method.

- Implicit Runge-Kutta methods have much better stability properties than LMMs (including the implicit BDF-methods).

- Explicit methods will be considered for the alternative formulation and high order explicit Runge-Kutta methods have larger areas of absolute stability, than explicit LMMs of the same order.

- The classic fourth order explicit Runge-Kutta method has been used in the Stirling simulation program developed by Carlsen [2] and it can serve as comparison for the other methods considered.

- Extrapolation methods rely on the smoothness of the function, which is unfortunate, since the right-hand side of the differential equation for the SFVSM-problem does not have continuous derivatives with respect to all of the algebraic variables. This rules out the use of extrapolation methods.

6.4.2 Runge-Kutta methods

A general one-step method is given in the form

$$\underline{y}_{n+1} = \underline{y}_n + \Delta t \cdot \Phi(t_n, \underline{y}_n; \Delta t) \tag{6.54}$$

Runge-Kutta methods belong to a class of one-step methods, which can be written as

$$\underline{y}_{n+1} = \underline{y}_n + \Delta t \cdot \sum_{i=1}^{s} b_i \cdot \underline{k}_i \tag{6.55}$$

where

$$\underline{k}_i = \underline{f}\left(t_n + c_i \cdot \Delta t, \underline{y}_n + \Delta t \cdot \sum_{j=1}^{s} a_{ij} \cdot \underline{k}_j\right) \qquad i = 1,2,\ldots,s \tag{6.56}$$

This defines a s-stage Runge-Kutta method. The method is explicit if $a_{ij}=0$ for $j \geq i$ and semi-implicit if $a_{ij}= 0$ for $j>0$ and $a_{ij} \neq 0$ for some $i=j$.

An alternative form is

$$\underline{y}_{n+1} = \underline{y}_n + \Delta t \cdot \sum_{i=1}^{s} b_i \cdot \underline{f}(t_n + c_i \cdot \Delta t, \underline{Y}_i) \tag{6.57}$$

where $\underline{Y}_i$ is defined as

$$\underline{Y}_i = \underline{y}_n + \Delta t \cdot \sum_{j=1}^{s} a_{ij} \cdot \underline{f}(t_n + c_j \cdot \Delta t, \underline{Y}_j) \qquad i = 1,2,\ldots,s \tag{6.58}$$

The elements of $\underline{Y}_i$ are intermediate values (stage variables) and the notation can be extended further by defining the stage derivatives $\underline{Y}_i'$

$$\underline{Y}_i' = \underline{f}(t_n + c_i \cdot \Delta t, \underline{Y}_i) \qquad i = 1,2,\ldots,s \tag{6.59}$$

This last form will be more convenient when dealing with implicit Runge-Kutta methods.

The coefficients of a s-stage Runge-Kutta method are often given in form of a Butcher array

$$\begin{array}{c|cccccc} c_1 & a_{11} & a_{12} & . & . & . & a_{1s} \\ c_2 & a_{21} & a_{22} & . & . & . & a_{2s} \\ . & . & . & . & . & . & . \\ . & . & . & . & . & . & . \\ . & . & . & . & . & . & . \\ c_s & a_{s1} & a_{s2} & . & . & . & a_{ss} \\ \hline & b_1 & b_2 & . & . & . & b_s \end{array} \tag{6.60}$$

or in short vector-matrix notation

$$\begin{array}{c|c} \underline{c} & \underline{\underline{A}} \\ \hline & \underline{b}^T \end{array} \tag{6.61}$$

The difference between explicit, semi-implicit and general (fully) implicit methods when it comes to implementation will be explained in more detail later in this section.

Next important properties, such as accuracy and stability, will be introduced and discussed.

Accuracy

The accuracy of a numerical method for ODEs is expressed in terms of order, which relate the behavior of the error as the step length decreases to zero. The local truncation error T_{n+1} can be defined as

$$T_{n+1} = y(t_{n+1}) - y(t_n) - \Delta t \cdot \Phi\left(t_n, y(t_n); \Delta t\right) \tag{6.62}$$

where y(t) is the exact analytical solution.

A Runge-Kutta method of order p has a local truncation error given (see [3] pp.157-170 concerning Butcher theory)

$$T_{n+1} = \frac{\Delta t^{p+1}}{(p+1)!} \cdot \sum_{r(\tau)=p+1} \alpha(\tau) \cdot \left(1 - \gamma(\tau) \cdot \psi(\tau)\right) \cdot F(\tau) + O(\Delta t^{p+2}) \tag{6.63}$$

where τ, r, α, γ, ψ and F have been introduced.

The total derivative of $\underline{y}$ can be expressed as a linear combination of the elementary differentials. Because of a one-to-one correspondence of rooted trees (from graph theory) and elementary differentials, this simple form for expression for the local truncation error can be derived.

τ is a tree, $r(\tau)$ is the order of the tree, $\gamma(\tau)$ is the density, $\alpha(\tau)$ is the number of essential different ways of labelling the nodes in the rooted tree, $\psi(\tau)$ is given from the elements in the Butcher array and $F(\tau)$ is the corresponding elementary differential (evaluated at t_n). Tables for the values of τ, r, α, γ and ψ can be found in [3], where a full description also is given.

For the applications here it will be enough just to consider the following form for the local truncation error

$$T_{n+1} = O(\Delta t^{p+1}) \tag{6.64}$$

The global truncation error E_{n+1} is defined as

$$E_{n+1} = y(t_{n+1}) - y_{n+1} \tag{6.65}$$

and usually of order p (one lower than the local truncation error) due to accumulation of errors. This is valid under the assumption of no influence from round off errors, stability requirements satisfied and only in the limit $\Delta t \rightarrow 0$.

Explicit methods

For a s-stage explicit Runge-Kutta method, methods of order p=s can be found for s=1,2,3,4. A fifth order method requires at least six stages and higher order methods also have p<s.

Semi-implicit methods

DIRKs are a special class of semi-implicit methods, which have equal values on the main diagonal in $\underline{\underline{A}}$ the Butcher array (i.e., all the a_{ii}'s are equal), which implies that $\underline{\underline{A}}$ has one single eigenvalue of multiplicity s. DIRK methods of order p=3 with s=2 stages and p=4 and s=3 can be found.

Fully implicit methods

The class of Gauss methods consists of methods with order p=2s. Gauss methods have the highest attainable order for an implicit Runge-Kutta method for a given number of stages. Other classical methods (low order methods) include RADAU IA and IIA, and Lobatto III methods. A special class of fully implicit methods is the SIRK methods, which (like the DIRK methods) have s identical eigenvalues of $\underline{\underline{A}}$ from the Butcher array.

For DAEs one cannot expect to obtain the same order of accuracy as for a Runge-Kutta method solving an ODE, i.e., a method, which has order p solving an ODE will in general have order < p when solving a DAE (see [4] pp. 86-106).

In general, different order of accuracy can be found for the differential variables and for the algebraic variable. The higher the index of the DAE, the more difficult it is to obtain high order for all variables. See reference [4] for detailed analysis and discussion of Runge-Kutta methods for solving DAEs.

Stability

All practical numerical methods for ODEs have to be zero-stable (i.e., stable in the limit $\Delta t \to 0$) in order to be convergent. Any real numerical solution has to be computed with a finite step length $\Delta t > 0$ and a requirement for obtaining an accurate solution is that the method is stable for the given step length.

The stability properties of a numerical method for ODEs are especially important for *stiff problems*, where it can be stability concerns that control the step length rather than accuracy. For an analysis and discussion of the context of stiffness see reference [3] pp. 213-224. Here it will only be noted that stiffness, which is a property of the system and not the numerical method, often occurs in problems where time constants of different order of magnitude are present.

Many different stability definitions and concepts can be made (again see [3]), but only some of the classical and most relevant definitions will be introduced in this section.

Linear stability theory is concerned with the trivial test equation

$$\underline{y}' = \underline{\underline{\Lambda}} \cdot \underline{y} \tag{6.66}$$

where $\underline{\underline{\Lambda}}$ is a n x n matrix with n distinct eigenvalues λ_i and all of the eigenvalues have Re $\lambda_i < 0$ for all i=1,2,...n.

The analytical solution of this problem satisfies $\underline{y}(t) \to \underline{0}$ as $t \to \infty$ and if the numerical method does the same for a given step length Δt, the method is said to be stable for that step length. Usually the area of linear (or absolute) stability is plotted in the complex $\lambda \cdot \Delta t$ plane. Any point in this plane for which the numerical solution tends to zero belongs to the area of linear stability and ideally it should include the whole of the negative half plane (and nothing more!), but this is a very severe requirement especially for explicit methods.

A numerical method that has an area of linear stability, which includes the whole of the negative half plane, is said to be *A-stable*, i.e., an A-stable method

$$y_{n+1} \to 0 \qquad as \qquad n \to \infty \tag{6.67}$$

for all Re $\lambda < 0$.

If the following also is satisfied

$$\left| \frac{y_{n+1}}{y_n} \right| \to 0 \qquad as \qquad Re(\Delta t \cdot \lambda) \to -\infty \tag{6.68}$$

then the method is said to be *L-stable*.

Non-linear stability theory is concerned with the genuine nonlinear problem

$$\underline{y}' = \underline{f}(t,\underline{y}) \tag{6.69}$$

If the solution $\underline{y}(t)$ is contractive (see [3] pp.265-266 for a definition and discussion of this property) some powerful results concerning non-linear stability are available.

Let the matrices $\underline{\underline{B}}$ and $\underline{\underline{M}}$ be defined as

$$\underline{\underline{B}} \equiv diag(\underline{b}) \quad , \quad \underline{\underline{M}} \equiv \underline{\underline{B}}\cdot\underline{\underline{A}} + \underline{\underline{A}}^T\cdot\underline{\underline{B}} - \underline{b}\cdot\underline{b}^T \tag{6.70}$$

If $\underline{\underline{B}}$ and $\underline{\underline{M}}$ are non-negative definite then the Runge-Kutta method is said to be *algebraically stable*. Algebraic stability ensures that the method will be stable even for genuine non-linear problems and not only for the trivial linear test equation. The matrix $\underline{\underline{A}}$ and vector $\underline{b}$, in the expression just above, are the coefficients a_{ij} and b_i for the method given from the Butcher array.

The stability properties discussed here are related as follows

Algebraic stability $\Rightarrow$ L-stability $\Rightarrow$ A-stability

Explicit methods

No explicit Runge-Kutta method can be A-stable (or even A_0 or $A(\alpha)$-stable). Regions of absolute stability can only include some part of negative half plane (see [3] for examples). One interesting feature is that the region of absolute stability increases with the order of the method (this is the opposite case of explicit LMMs). All explicit Runge-Kutta methods still have relatively poor stability properties and will be more or less useless for stiff problems.

Semi-implicit methods

There are no DIRK methods of order greater than p=4, which are algebraically stable (see [5] for a proof).

Fully implicit methods

Implicit methods have much better properties with regard to stability. It is possible to have algebraically stable methods or arbitrary high order, e.g., Gauss-methods.

Error estimates

Error estimates are used for monitoring the error and for adjusting the step length accordingly. This has two major advantages, first it gives some idea of the accuracy of the obtained numerical solution and secondly it makes it possible to use large steps in regions where the solution is smooth and thereby reducing the computational cost.

For one-step methods it is very easy to change the step length during the calculation (opposite the LLMs, no interpolation is needed), but to obtain an estimate for the local truncation error is computationally expensive compared to the predictor-corrector methods of the LMMs.

In the implementation of the numerical solution for the SFVSM-problem, both fixed step length algorithms and variable step length algorithms based on error estimates will be considered.

For Runge-Kutta methods the commonly used techniques for obtaining an estimate for the local truncation error are:

- Richardson extrapolation.
- Embedding.

Richardson extrapolation (or deferred approach to the limit) is the standard way to obtain an error estimate for both explicit and implicit methods. Typically, a calculation with time step Δt and $r \cdot \Delta t$ is performed (using the same Runge-Kutta method) and Richardson extrapolation is used to give an estimate for the principal local truncation error.

Consider any method of order p and let $\underline{y}_{n+1}$ denote the actual solution (from t_n with time step Δt) and $\tilde{y}_{n+1}$ the solution obtained from t_{n-1} with a time step $r \cdot \Delta t$, where

$$r = \frac{t_{n+1} - t_{n-1}}{t_{n+1} - t_n} \tag{6.71}$$

The estimate for the principal local truncation error is then

$$EST = \frac{\underline{y}_{n+1} - \tilde{y}_{n+1}}{r^{p+1} - 1} \tag{6.72}$$

The main drawback of this approach, is that s-1 additional function evaluations are needed for an explicit s-stage Runge-Kutta method to obtain the error estimate, which makes it computationally expensive.

Extrapolation is a general idea for obtaining an error estimate, it is widely used and often works very well. Using extrapolation for the actual problem could be somehow questionable, since the partial derivatives of the right side function are not continuous and the extrapolation techniques depend heavily on this property.

Embedding is another widely applied technique for Runge-Kutta methods. The computation of the new value is performed by two different methods of order p and p+1 respectively sharing the same coefficients a_{ij} and c_i in the Butcher array. The difference is an estimate of the local truncation error for the low order method.

Given the following Butcher array

$$\begin{array}{c|c} \underline{c} & \underline{\underline{A}} \\ \hline & \underline{b}^T \\ & \underline{\tilde{b}}^T \\ \hline & \underline{e}^T \end{array} \qquad (6.73)$$

where $\underline{b}^T$ is the vector with the coefficients for the method of order p, $\underline{\tilde{b}}^T$ is the vector of the method with order p+1 and $\underline{e}^T$ is the difference, i.e., $\underline{e}^T = \underline{b}^T - \underline{\tilde{b}}^T$.

The estimate for the local truncation error is given as

$$EST = \Delta t \cdot \sum_{i=1}^{s} \underline{e}_i \cdot \underline{Y}_i \qquad (6.74)$$

Global error bounds can be obtained, but these are very crude and often largely overestimate the actual error. Consequently, global error bounds are useless in a practical computational context and step length control for a variable step length algorithm is always based on error estimates of the local truncation error. If the local truncation error is sufficiently small it is often reasonable to assume that the global error will be small too (at least when no stability problems are encountered).

Fixed step length implementations have mainly been considered for the implicit Runge-Kutta methods, where stability is no problem and the accuracy of the solution is determined by the step length. The most obvious way to "estimate" the (global) accuracy of such a solution is to decrease the step length and observe how much the solution changes. When the solution does not change significantly for a further refinement, it is possible to assume that a sufficient accurate solution is found.

Variable step length has been considered for both explicit and implicit Runge-Kutta methods. Next two simple examples of step length control based on estimates for the local truncation error are given. Both have been implemented in the developed computer code.

Variable step length control

Several more or less sophisticated strategies can be chosen for step length control in a variable step length algorithm. Here only two simple strategies will be considered. Given a method with order p, initial values $\underline{\eta} = \underline{y}_0$, an initial step length Δt_0 and a tolerance TOL (usually provided by the user).

Step length control #1: Step halving/doubling

1) Calculate the new value $\underline{y}_{n+1}$ at time t_{n+1} from $\underline{y}_n$ at t_n using the method and a time step Δt.

2) Calculate the estimate EST for the local truncation error.

3) If EST > TOL then
   set $\Delta t_{new} = \Delta t/2$
   else if $TOL/(2^{p+1}+1) < EST < TOL$ then
   set $\Delta t_{new} = \Delta t$ for the next time step
   n=n+1
   else if $EST < TOL/(2^{p+1}+1)$ then
   use $\Delta t_{new} = 2 \cdot \Delta t$ for the next time step
   n=n+1

4) Set $\Delta t = \Delta t_{new}$ and goto 1)

The local truncation error for a method of order p is $O(\Delta t^{p+1})$, which mean that halving the step length will reduce the error by factor $1/(2^{p+1}+1)$.

Step length control #2: Optimal step length

1) Calculate the new value $\underline{y}_{n+1}$ at time t_{n+1} from $\underline{y}_n$ at t_n using the method and a time step Δt.

2) Calculate the estimate EST for the local truncation error.

3) Calculate the factor for the optimal change in step length

$$\alpha = \sqrt[p+1]{\frac{TOL}{EST}} \qquad (6.75)$$

4) If $\alpha < \alpha_{min}$ then
   set $\alpha = \alpha_{min}$
   else if $\alpha_{min} \le \alpha \le 1$
   continue
   else if $1 \le \alpha \le \alpha_{max}$ then
   n=n+1
   else if $\alpha > \alpha_{max}$ then
   set $\alpha = \alpha_{max}$
   n=n+1

5) Set $\Delta t_{new} = \alpha \cdot \Delta t$

6) Set $\Delta t = \beta \cdot \Delta t_{new}$ and goto 1)

Typical values are: $\alpha_{min} = 0.5$, $\alpha_{max} = 2.0$ and $\beta = 0.90$.

Numerical simulations are performed using the Runge-Kutta methods listed below.

The Butcher arrays for all these methods are given in Appendix D.

Explicit Runge-Kutta methods

Heun's method.

Third order method with three stages (p=3, s=3). The abbreviation RK3 is used for this method in the text.

Classical Runge-Kutta method.

The widely used classical explicit Runge-Kutta method of order four and four stages (p=4, s=4). The abbreviation RK4 is used for this method.

The following explicit methods use embedding to obtain error estimates and they have been considered for variable step length implementations.

England's method.

England's method has six stages and is of order four (p=4, s=6). The method is denoted (4,5) meaning that the method uses the fifth order part for the estimation of the local truncation error, but otherwise runs like a fourth order method.

Fehlberg's method RKF45.

RKF45 has six stages and order four (p=4, s=6). The method is error-tuned, meaning that the coefficients for the estimate of the local truncation error are made small. It is sometimes used with local extrapolation meaning that it runs as a (5,4) method or in other words: RKF54 uses the fifth order method for the integration step and a step length control based on the error estimates for the fourth order method.

Local extrapolation is often used for embedded Runge-Kutta methods to increase the accuracy of the solution by raising the order of the method by one, while the error estimate for the low order method still is used for monitoring of the step length. Higher order methods do not necessarily give smaller error than lower order methods for a finite step length. Therefore one can only assume that the step taken by the high order method and the given step length will be better than without local extrapolation. Nevertheless, many standard codes employ local extrapolation.

Verner's method RKV56

RKV56 has eight stages and order five (p=5, s=8). This method, developed by Verner and used in his DVERK code, is usually also implemented using local extrapolation.

Implicit Runge-Kutta methods

Radau IA and Radau IIA

Both methods have one stage and order one (s=1, p=1). Radau IA and IIA are both algebraically stable (L-stable).

1-stage Gauss method.

All Gauss methods are fully implicit methods, but since this method has only one stage, it can be treated the same way as semi-implicit methods for the implementation. The 1-stage Gauss method has order two (p=2, s=1) and it is algebraically stable (L-stable).

Semi-implicit 2-stage Lobatto IIIB.

Method of order two and with two stages (p=2, s=2). It is only A-stable and not algebraically stable.

These last four implicit Runge-Kutta methods of low order have all been used for preliminary tests of the developed computer code. Having only a few stages, it implies that the computational cost will be small compared to the following higher order implicit methods. This could be advantageous for certain implementations, but this will be discussed in further detail later.

2-stage DIRK method of order 3

An algebraically stable DIRK (Diagonally-Implicit Runge-Kutta) method, which has order three and two stages (p=3, s=2), can be found. The abbreviation DIRK3 will be used for this method.

3-stage DIRK method of order 4

An algebraically stable DIRK method, which has order four and three stages (p=4, s=3), can be found. The abbreviation DIRK4 will be used for this method.

The following embedded semi-implicit Runge-Kutta methods have been used for variable step length implementation:

NT I

The NT I method of Nørsett and Thomsen [6] has three stages and order three (p=3, s=3). NT I is algebraically stable. The embedded method, used for the local error estimates, is of order two.

NT II

The NT II method is taken from the same reference as NT I. The method has four stages and order three (p=3, s=4). NT II is only A-stable and uses a fourth order embedded method for the local error estimates.

6.4.3 Linear Multistep Methods

Linear Multistep methods (LMMs) can be written in the form

$$\sum_{j=0}^{k} \alpha_j \cdot \underline{y}_{n+j} = \Delta t \cdot \sum_{j=0}^{k} \beta_j \cdot \underline{f}_{n+j} \tag{6.76}$$

where $\underline{f}_{n+j} = \underline{f}(t_{n+j}, \underline{y}_{n+j})$ and k denotes the number of steps.

α_j and β_j (j=0,1,2,...,k) are the coefficients of the method. α_0 and β_0 are not both equal to 0 and usually $\alpha_k = 1$.

Explicit methods have $\beta_k = 0$ and $\underline{y}_{n+k}$ may be found directly from

$$\underline{y}_{n+k} = \Delta t \cdot \sum_{j=0}^{k-1} \beta_j \cdot \underline{f}_{n+j} - \sum_{j=0}^{k-1} \alpha_j \cdot \underline{y}_{n+j} \tag{6.77}$$

while implicit methods require the solution of a system of equations in each time step

$$\underline{y}_{n+k} - \Delta t \cdot \beta_k \cdot \underline{f}_{n+k} = \Delta t \cdot \sum_{j=0}^{k-1} \beta_j \cdot \underline{f}_{n+j} - \sum_{j=0}^{k-1} \alpha_j \cdot \underline{y}_{n+j} \tag{6.78}$$

or

$$\underline{y}_{n+k} - \Delta t \cdot \beta_k \cdot \underline{f}(t_{n+k}, \underline{y}_{n+k}) = g \tag{6.79}$$

where g is function $\underline{y}_{n+j}$ and $\underline{f}_{n+j}$ (j=0,1,...,k-1), whose values are already known.

A k-step method requires k-2 additional start up values and function evaluations.

LMMs are often used as predictor-corrector pair, where an explicit method (the predictor) is used to provide an initial guess on the new value for the implicit method (the corrector). Cheap estimates of the local truncation error can be obtained using special predictor-corrector pairs.

Many commercial codes based on LMMs use VSVO-algorithms (Variable Step - Variable Order) to provide greater flexibility.

Adams methods

The class of Adams methods consists of explicit (Adams-Bashforth) and implicit (Adams-Moulton) methods. Adams methods can be written in the form

$$\underline{y}_{n+k} - \underline{y}_{n+k-1} = \Delta t \cdot \sum_{j=0}^{k} \beta_j \cdot \underline{f}_{n+j} \tag{6.80}$$

Adams methods are widely applied in standard solvers for systems of ODEs usually in a predictor-corrector implementation (ABM-methods). The methods can be used for non-stiff problems (no severe stability requirements).

BDF-methods

The class of BDF-methods can be written in the form

$$\sum_{j=0}^{k} \alpha_j \cdot \underline{y}_{n+j} = \Delta t \cdot \beta_k \cdot \underline{f}_{n+k} \tag{6.81}$$

These methods are implicit LMMs, which have good stability properties and are widely used in standard solvers for stiff systems of ODEs and for DAEs.

BDF-methods up to order p=6 are shown in the table just below.

k	α_6	α_5	α_4	α_3	α_2	α_1	α_0	β_k	p
1						1	-1	1	1
2					1	$-\frac{4}{3}$	$\frac{1}{3}$	$\frac{2}{3}$	2
3				1	$-\frac{18}{11}$	$\frac{9}{11}$	$-\frac{2}{11}$	$\frac{6}{11}$	3
4			1	$-\frac{48}{25}$	$\frac{36}{25}$	$-\frac{16}{25}$	$\frac{3}{25}$	$\frac{2}{25}$	4
5		1	$-\frac{300}{137}$	$\frac{300}{137}$	$-\frac{200}{137}$	$\frac{75}{137}$	$-\frac{12}{137}$	$\frac{60}{137}$	5
6	1	$-\frac{360}{147}$	$\frac{450}{147}$	$-\frac{400}{147}$	$\frac{225}{147}$	$-\frac{72}{147}$	$\frac{10}{147}$	$\frac{60}{147}$	6

Table BDF-methods

No BDF-method of order higher than six can be zero-stable.

6.4.4 Extrapolation methods

Extrapolation methods are not used in any of the developed codes and are only mentioned here for the sake of completeness. For an analysis of extrapolation methods, see reference [7].

6.5 Numerical methods for solving BVPs

6.5.1 Introductory remarks

The SFVSM-problem has previously in this chapter been classified as a boundary value problem (BVP), so it is very natural to consider numerical methods specially developed for this type of problem.

The most important classes of numerical methods for solving BVPs for systems of ordinary differential equations are the following (see reference [8] for a general analysis of numerical methods for BVPs):

- Shooting methods.
- Finite Difference methods.

A general BVP for ODEs with non-separated linear boundary conditions can be written as

$$\underline{y}' = \underline{f}(t,\underline{y}) \qquad \underline{\underline{B}}_a \cdot \underline{y}(a) + \underline{\underline{B}}_b \cdot \underline{y}(b) = \underline{\beta} \tag{6.82}$$

where $\underline{y} = \underline{y}(t)$, $a \le t \le b$, $\underline{y} \in \mathbb{R}^n$ and $\underline{f}$: $\mathbb{R} \times \mathbb{R}^n \rightarrow \mathbb{R}^n$.

Only periodic boundary conditions

$$\underline{y}(0) - \underline{y}(t_p) = 0 \tag{6.83}$$

which is a special simple case, will be considered here.

6.5.2 Shooting methods

Shooting methods or Initial-Value methods take advantage of the close theoretical relationship between BVPs and IVPs. The basic idea is to solve the IVP corresponding to the BVP using the advanced numerical methods and analysis available for IVPs.

Single Shooting

The single Shooting method is the most simple of these methods and it can be stated in the following way.

Define an initial guess $\underline{s}$

$$\underline{y}(0;\underline{s}) = \underline{s} \tag{6.84}$$

where $\underline{y}(t;\underline{s})$ denotes the solution at time t given an initial guess $\underline{s}$.

The periodic solution $\underline{y}(t;\underline{s}^*)$ should satisfy

$$\underline{s}^* - \underline{y}(t_p;\underline{s}^*) = \underline{0} \tag{6.85}$$

The vector $\underline{s}^*$ can be found when solving the system of nonlinear equations given as

$$\underline{G}(\underline{s}) = \underline{0} \tag{6.86}$$

where $\underline{G}$ is defined as

$$\underline{G}(\underline{s}) = \underline{s} - \underline{y}(t_p;\underline{s}) \tag{6.87}$$

This is a system of (implicitly given) nonlinear equations and it has to be solved using an iteration method. The most widely used method for solving such problems is Newton's method, which also will be applied here.

Newton's method:

Solve the linearized system

$$\begin{aligned} \underline{G}'(\underline{s}^{[k]})\cdot\Delta\underline{s}^{[k]} &= -\underline{G}(\underline{s}^{[k]}) \\ \underline{s}^{[k+1]} &= \Delta\underline{s}^{[k]} + \underline{s}^{[k]} \end{aligned} \tag{6.88}$$

where the Jacobian of the system is given as

$$\underline{G}'(\underline{s}) = \frac{\partial \underline{G}}{\partial \underline{s}} = \underline{\underline{I}} - \frac{\partial \underline{y}(t_p;\underline{s})}{\partial \underline{s}} \tag{6.89}$$

An analytical expression for the Jacobian can now be found following the procedure outlined in [9].

Define $\underline{\underline{Y}}(t)$ as

$$\underline{\underline{Y}}(t) = \frac{\partial \underline{y}(t;\underline{s})}{\partial \underline{s}} \tag{6.90}$$

then the Jacobian can be written as

$$\underline{G}'(\underline{s}) = \underline{\underline{I}} - \underline{\underline{Y}}(t_p) \tag{6.91}$$

$\underline{\underline{Y}}(t_p)$ can be found from solving the variational system

$$\frac{d}{d\underline{s}}\left(\frac{d\underline{y}}{dt}\right) = \frac{d}{d\underline{s}}\left(\underline{f}(t,\underline{y})\right) \quad \Rightarrow$$

$$\frac{d}{dt}\left(\frac{d\underline{y}}{d\underline{s}}\right) = \frac{d\underline{f}}{d\underline{y}} \cdot \frac{d\underline{y}}{d\underline{s}} \tag{6.92}$$

or

$$\underline{\underline{Y}}' = \underline{\underline{A}} \cdot \underline{\underline{Y}} \tag{6.93}$$

where the following notation has been introduced

$$\underline{\underline{A}} = \frac{d\underline{f}}{d\underline{y}} \tag{6.94}$$

The initial conditions for the variational system can be found from

$$\underline{\underline{Y}}(0) = \frac{\partial \underline{y}(0;\underline{s})}{\partial \underline{s}} = \underline{\underline{I}} \tag{6.95}$$

This gives an analytical expression for $\underline{\underline{Y}}(t_p)$ and implies that the Jacobian can be found numerically by integrating an additional system (6.93) of n x n ODEs.

Remarks:

i) All elements in the matrices $\underline{\underline{A}}$ are functions of t and $\underline{y}$.

ii) The matrix system can be solved columnwise.

iii) If $\underline{s}$ and $\underline{y}$ have n elements then $\underline{\underline{Y}}$ has n^2 elements and solving the variational system means solving 1+n IVPs (the original equation (6.82) + n columns of $\underline{\underline{Y}}$).

iv) The variational system can be solved during the calculation of the original system, so it is not necessary to store the matrix $\underline{\underline{A}}$.

The SFVSM problem (using the basic formulation) has been classified as a boundary value problem of differential-algebraic equations, so it is quite natural to consider this type of system too.

Consider a general BVP for a system of semi-explicit DAEs

$$\begin{aligned} \underline{y}' &= \underline{f}(t,\underline{y},\underline{z}) \\ 0 &= \underline{g}(t,\underline{y},\underline{z}) \end{aligned} \tag{6.96}$$

with periodic boundary conditions

$$\begin{aligned} \underline{y}(0) - \underline{y}(t_p) &= 0 \\ \underline{z}(0) - \underline{z}(t_p) &= 0 \end{aligned} \tag{6.97}$$

where $\underline{y} = \underline{y}(t)$ and $\underline{z} = \underline{z}(t)$.

The approach is similar to the one above. Again define

$$\underline{\underline{Y}}(t) = \frac{\partial \underline{y}(t;\underline{s})}{\partial \underline{s}} \tag{6.98}$$

and then

$$\underline{G}'(\underline{s}) = \underline{\underline{I}} - \underline{\underline{Y}}(t_p) \tag{6.99}$$

$\underline{\underline{Y}}(t_p)$ can now be found from solving the new variational system

$$\begin{aligned} \frac{d}{d\underline{s}}\left(\frac{d\underline{y}}{dt}\right) &= \frac{d}{d\underline{s}}\left(\underline{f}(t,\underline{y},\underline{z})\right) \qquad \Rightarrow \\ \frac{d}{dt}\left(\frac{d\underline{y}}{d\underline{s}}\right) &= \frac{d\underline{f}}{d\underline{y}}\cdot\frac{d\underline{y}}{d\underline{s}} + \frac{d\underline{f}}{d\underline{z}}\cdot\frac{d\underline{z}}{d\underline{s}} \end{aligned} \tag{6.100}$$

or

$$\underline{\underline{Y}}' = \underline{\underline{A}}_{f,y}\cdot\underline{\underline{Y}} + \underline{\underline{A}}_{f,z}\cdot\underline{\underline{Z}} \tag{6.101}$$

where the following notation has been introduced

$$\underline{\underline{Z}}(t) = \frac{d\underline{z}}{d\underline{s}} \quad , \quad \underline{\underline{A}}_{f,y} = \frac{d\underline{f}}{d\underline{y}} \quad , \quad \underline{\underline{A}}_{f,z} = \frac{d\underline{f}}{d\underline{z}} \tag{6.102}$$

Differentiation of $\underline{g}$ with respect to $\underline{s}$ gives

$$0 = \frac{d\underline{g}}{d\underline{y}} \cdot \frac{d\underline{y}}{d\underline{s}} + \frac{d\underline{g}}{d\underline{z}} \cdot \frac{d\underline{z}}{d\underline{s}} \tag{6.103}$$

or

$$\underline{\underline{0}} = \underline{\underline{A}}_{g,y} \cdot \underline{\underline{Y}} + \underline{\underline{A}}_{g,z} \cdot \underline{\underline{Z}} \tag{6.104}$$

where

$$\underline{\underline{A}}_{g,y} = \frac{d\underline{g}}{d\underline{y}} \quad , \quad \underline{\underline{A}}_{g,z} = \frac{d\underline{g}}{d\underline{z}} \tag{6.105}$$

The initial conditions for the variational system can be found from

$$\underline{\underline{Y}}(0) = \frac{\partial \underline{y}(0;\underline{s})}{\partial \underline{s}} = \underline{\underline{I}} \tag{6.106}$$

and solving

$$\underline{\underline{A}}_{g,z} \cdot \underline{\underline{Z}}(0) = -\underline{\underline{A}}_{g,y} \cdot \underline{\underline{Y}}(0) \tag{6.107}$$

for $\underline{\underline{Z}}(0)$.

Remarks:

i) All elements in the matrices $\underline{\underline{A}}$ are functions of t, $\underline{y}$ and $\underline{z}$.

ii) The matrix systems can still be solved columnwise, but the algebraic equations have to be solved simultaneously.

iii) If $\underline{s}$ and $\underline{y}$ each have n_y elements then $\underline{\underline{Y}}$ has n_y^2 elements and solving the variational system means solving $1+n_y$ IVPs (the original equation (6.96) + n_y columns of $\underline{\underline{Y}}$) of dimension n_f.

iv) If $\underline{z}$ has n_z elements then $\underline{\underline{Z}}$ has $n_z \cdot n_y$ elements.

v) If $\underline{\underline{A}}_{g,z}$ is non singular for all t, $\underline{\underline{Z}}$ can be found in terms of $\underline{\underline{Y}}$ and the system can be solved as for the ODE case.

The calculation of $\underline{\underline{A}}$ can often be very tedious and, because of the additional algebraic equation, it is required to solve an extra system of linear equations.

An alternative approach is to calculate the Jacobian $\underline{G}'(\underline{s})$ using a finite-difference approximation in a modified Newton method and this is described further in the section dealing with the actual implementation of the shooting method.

The single Shooting method has two major drawbacks. One drawback is concerned with stability of the numerical method for the time integration. Stability for IVP methods has been discussed for these methods separately in a previous section. The other drawback is concerned with the fact that for nonlinear problems there is no guarantee that for a wrong initial guess $\underline{s}^{[k]}$ the solution $\underline{y}(t;\underline{s}^{[k]})$ exists for all $0 \le t \le t_p$.

The single Shooting method has been tested on the actual SFVSM-problem. A code has been developed using an arbitrary Runge-Kutta method for the time integration and no problems have been encountered. More complex Shooting methods have therefore not been considered for an actual implementation into computer code.

For the sake of completeness, the multiple Shooting method will be briefly described here and it should be mentioned that the idea from multiple Shooting could be advantageous when dealing with the problem of discontinuities (see section 6.10).

Standard multiple shooting

The standard multiple Shooting method overcomes the drawbacks of single Shooting method by dividing the time interval into smaller sub intervals and then performing the time integration for each of these sub intervals.

Consider a mesh $0 = t_0 < t_1 \ldots < t_{N-1} < t_N = t_p$ and an IVP method used for the problem

$$\underline{y}' = \underline{f}(t,\underline{y}) \qquad t_i < t < t_{i+1} \tag{6.108}$$

where $\underline{y} = \underline{y}(t)$, $\underline{y} \in \mathbb{R}^n$ and $\underline{f}$: $\mathbb{R} \times \mathbb{R}^n \rightarrow \mathbb{R}^n$

and initial guesses

$$\underline{y}(t_i) = \underline{s}_i \tag{6.109}$$

$i = 0,1,\ldots,N-1$.

Let $\underline{y}_i(t;\underline{s}_i)$ denote the solution to the problem defined just above. The unknowns are the N vectors $\underline{s}_i$ of dimension n, which can be put into a vector $\underline{s}$ defined as

$$\underline{s} = \begin{bmatrix} \underline{s}_0 \\ \underline{s}_1 \\ \cdot \\ \cdot \\ \cdot \\ \underline{s}_{N-1} \end{bmatrix} \tag{6.110}$$

This gives a system of N·n nonlinear equations

$$\underline{G}(\underline{s}) = \underline{0} \tag{6.111}$$

where $\underline{G}$ is defined as

$$\underline{G}(\underline{s}) \equiv \begin{bmatrix} \underline{s}_1 - \underline{y}_0(t_1;\underline{s}_0) \\ \underline{s}_2 - \underline{y}_1(t_2;\underline{s}_1) \\ \cdot \\ \cdot \\ \cdot \\ \underline{s}_{N-1} - \underline{y}_{N-2}(t_{N-1};\underline{s}_{N-2}) \\ \underline{s}_0 - \underline{y}_{N-1}(t_N;\underline{s}_{N-1}) \end{bmatrix} \tag{6.112}$$

Again this system can be solved using Newton's method. The Jacobian $\underline{G}'(\underline{s})$ will be sparse and have a banded block structure that will be partly destroyed by the periodic boundary conditions.

6.5.3 Finite-Difference methods

For the Finite Difference method, the solution of the BVP is found on a given mesh by approximating the derivatives of the differential equations by finite differences at each mesh point and solving the full system of nonlinear algebraic equations. The periodic boundary conditions can, in a simple way, be included directly into equations implying that the periodic solution is found "at once", i.e., when the algebraic equations are solved.

Only finite difference approximations based on divided differences and Linear Multistep methods are described, since uniform meshes have been considered exclusively. Finite difference approximations based on one-step methods have some advantages for non-uniform meshes and also near boundaries, but for uniform meshes and periodic problems (where periodicity of the variables can apply the necessary boundary values), divided difference and LMM approximations are much simpler to implement in a computer code.

Now consider a discretization using a uniform mesh with N+1 points and mesh size Δt

$$0 = t_0 < t_1 < \ldots < t_N = t_p \quad , \qquad t_n = n \cdot \Delta t \quad , \quad n = 0,1,\ldots,N \tag{6.113}$$

and a general nonlinear BVP with periodic boundary conditions

$$\underline{y}' = \underline{f}(t,\underline{y}) \qquad\qquad \underline{y}(t) = \underline{y}(t+t_p) \tag{6.114}$$

The derivative for the ith variable at time $t=t_n$ can directly be approximated with a divided difference as

$$y_i'(t_n) \approx \frac{\sum_{j=-k}^{k} \alpha_j \cdot y_{i,n+j}}{\beta_0 \cdot \Delta t} \tag{6.115}$$

and inserted in the differential equation, or the whole differential equation can be approximated using a Linear Multistep method as

$$\sum_{j=-k}^{k} \alpha_j \cdot y_{i,n+j} - \Delta t \cdot \sum_{j=-k}^{k} \beta_j \cdot f_{i,n+j} = 0 \tag{6.116}$$

The former of these two approximations can also be included in the last general formulation.

Boundary conditions

The assumption of the existence of a periodic solution with a fixed time period t_p, makes it possible to use the same discretization for all points, since

$$\underline{y}_n = \underline{y}_{n+N} \qquad for \quad all \quad n = 0,1,...,N-1 \tag{6.117}$$

can be used for the mesh points at and near the boundaries in the time domain.

Divided difference approximations

The following divided difference approximations has been considered in the developed codes.

2.order:

$$y'_{i,n} = \frac{y_{i,n+1} - y_{i,n-1}}{2 \cdot \Delta t} \tag{6.118}$$

4.order:

$$y'_{i,n} = \frac{-y_{i,n+2} + 8 \cdot y_{i,n+1} - 8 \cdot y_{i,n-1} - y_{i,n-2}}{12 \cdot \Delta t} \tag{6.119}$$

6.order:

$$y'_{i,n} = \frac{y_{i,n+3} - 9 \cdot y_{i,n+2} + 45 \cdot y_{i,n+1} - 45 \cdot y_{i,n-1} + 9 \cdot y_{i,n-2} - y_{i,n-3}}{60 \cdot \Delta t} \tag{6.120}$$

Higher order methods can be constructed using an increasing number of mesh points.

Linear Multistep methods

Any explicit or implicit LMM, such as an Adams method or a BDF-method, may be used. There is no advantage of using an explicit method since full system of equations still has to be solved. BDF-methods have been used in the codes and the coefficients for these methods (up to order six) are given in section 6.4.3.

6.6 Implementation of the Integration-to-Convergence method

6.6.1 Introductory remarks

The Integration-to-Convergence approach, which also could be named "Fixed-point iteration", "Contraction-mapping method" or "Brute-force integration", is the most simple of all the approaches considered in this thesis and it is probably also the most commonly used for periodic thermodynamic problems such as the Stirling engine. The approach will be used for comparisons with the other approaches and serve as a reference. It should be noted that convergence in this meaning has no relationship to convergence of a numerical method, but only to reaching (i.e., converging to) the cyclic solution.

The basic idea of the Integration-to-Convergence approach is the following:

From a guess on the initial conditions at time t=0, integrate the system of DAEs forward in time using an appropriate IVP code until the stationary periodic conditions are reached or in other words: until the initial values of the state variables at the beginning of one cycle are approximately equal to the values at the end of the cycle.

The advantages of this approach can be summarized as:

- Very simple to implement.
- It is cheap to compute one cycle (at least for explicit IVP methods and non-stiff problems).
- It requires only a guess for the initial values at t=0.

The major disadvantages can be summarized as:

- The solution may not converge towards cyclic conditions unless the initial guess is good, i.e., sufficiently close to the true solution of the cyclic problem.
- The solution may converge very slowly, which implies that integration of many time cycles are required to obtain the cyclic solution. This will be the case when short and long transients are present in the solution (much like a stiff system of equations). It will specifically be a major problem when the heat capacity of the solid regenerator matrix is assumed to be finite in a more sophisticated model.
- If the convergence is very slow, it can be difficult to give a good convergence criterion for the determination of the periodic solution.

- Stability problems will be encountered for explicit methods if the problem is stiff and many time steps will be required for the numerical calculation of one cycle.

- Parameters for the cyclic integral conditions (i.e., regenerator matrix temperature and gradient, solid surface temperatures in the variable volumes and total mass) have to be adjusted after the calculation of the periodic solution for the state variables, which means that outer loops are necessary in the computation.

Standard numerical packages for the integration of IVPs might seem to be a reasonable approach, but the presence of algebraic equations restricts this to packages specially for DAEs. DASSL [4] and LSODI [10] are two well-known public domain codes for solving general systems of DAEs. Both two codes are based on BDF-methods, but are not designed for index two or higher problems. DASSL and LSODI are therefore not directly applicable to the actual problem without significant modifications. Furthermore, it will be difficult to take advantage of the special features of the defined problem.

These facts have made it necessary to develop computer code. A FORTRAN subroutine has been written, which (from a set of initial values) calculates one whole cycle using a specified explicit or implicit Runge-Kutta method. This subroutine is used as a part of the complete code (simulation program), which uses the Integration-to-Convergence approach to find the periodic solution for the SFVSM-problem.

6.6.2 Explicit Runge-Kutta methods

Using an explicit Runge-Kutta method is a standard approach for solving IVPs. No start up procedure is needed, arbitrarily high order can be achieved and the implementation is relatively simple.

Low computational cost is usually the major advantage of using an explicit method. It is not necessary to solve a system of nonlinear equations, and for non-stiff problems, this a very cheap way of obtaining the solution, but if the problem is stiff then the advantage disappears. It will be necessary to use excessively many time steps even when the solution is smooth and for very stiff systems it is not even practically possible to use an explicit method.

Furthermore, additional problems are encountered because of the existence of discontinuous partial derivatives of the right-hand side in the differential equations. This will be discussed further in section 6.10.

For the actual problem, explicit Runge-Kutta methods cannot be used for the basic formulation of the system of equations, but only for the alternative formulation.

Basic formulation

For the basic formulation of the equations (energy equation with time derivative with respect to internal energy as derived in section 6.2.2), it is not possible to use an explicit Runge-Kutta method. This is due to the special properties of the semi-explicit DAE (6.21), which is of a higher index than one as discussed in section 6.3.

For an explicit method $\underline{Y}_1 = \underline{y}_n$ and $\underline{Z}_1 = \underline{z}_n$ since $c_1 = 0$ (the first internal step of an explicit Runge-Kutta is always an Euler step) and $\underline{k}_1$ is then given as

$$\underline{k}_1 = \underline{f}(t_n, \underline{Y}_1, \underline{Z}_1) \tag{6.121}$$

$\underline{Y}_2$ can be calculated as

$$\underline{Y}_2 = \underline{y}_n + \Delta t \cdot a_{12} \cdot \underline{k}_1 \tag{6.122}$$

while $\underline{Z}_2$ has to be found solving

$$\underline{0} = \underline{g}(t_n + c_2 \cdot \Delta t, \underline{Y}_2, \underline{Z}_2) \tag{6.123}$$

For the actual problem, the matrix

$$\frac{\partial \underline{g}}{\partial \underline{z}} \tag{6.124}$$

is singular (i.e., the index of the DAE is two or higher) and this implies that the equation above cannot be solved for $\underline{Z}_2$.

Alternative formulation

Only for the alternative formulation of the SFVSM problem (energy equations with derivatives with respect to pressure) is it possible to solve the problem using an explicit Runge-Kutta method.

The nonlinear system of equations may, in this formulation and under certain assumptions concerning the algebraic variables, be replaced by a smaller and linear sub system. Solving a linear system of equations instead of the full non-linear system is a very essential feature of the alternative formulation. The algebraic variables can now be found at each internal stage opposite the basic formulation.

Furthermore, the explicit method will still be inexpensive regarding the computational cost compared to an implicit method. If it had been necessary to solve a non-linear system, the explicit method would have become just as expensive as an implicit method without having the good stability properties or order of accuracy.

Implementation of an explicit Runge-Kutta method for the alternative formulation

The special structure of the system of differential-algebraic equations for the alternative formulation can be used to simplify the calculation when using an explicit Runge-Kutta method.

Redefining the vector $\underline{y}$ with the differential variables and $\underline{z}$ with the algebraic variables as

$$\underline{y} = \begin{bmatrix} \underline{y}_p \\ \underline{y}_M \end{bmatrix} \quad , \quad \underline{z} = \begin{bmatrix} \underline{z}_{\dot{m}} \\ \underline{z}_T \end{bmatrix} \tag{6.125}$$

where the subscript p, M, $\dot{m}$ and T denote pressure, mass, mass flow and temperature respectively.

Let $\underline{y}_{p,n}$ and $\underline{y}_{M,n}$ denote the numerical solution for pressure and masses at time level $t=t_n$ (given from the previous integration step). For an explicit method the internal stage variables at the first stage (k=1) are given as $Y_{p,1} = y_{p,n}$ and $\underline{Y}_{M,1} = \underline{y}_{M,n}$.

The stage value for the temperatures $\underline{Z}_{T,1}$ can now be found explicitly from the algebraic equations (the equations of state) given in the form $\underline{g}(t, \underline{Z}_{T,1}, Y_{p,1}, \underline{Y}_{M,1}) = 0$.

Assuming (i.e., guessing) the sign of the mass flows $\underline{z}_{\dot{m}}$ makes it possible to solve the following linear system for $Y'_{p,1}$ and $\underline{Z}_{\dot{m},1}$ $(= z_{\dot{m},n})$

$$\underline{\underline{Q}}_1 \cdot \begin{bmatrix} Y'_{p,1} \\ \underline{Z}_{\dot{m},1} \end{bmatrix} = \underline{q}_1 \tag{6.126}$$

where $\underline{\underline{Q}}_1$ and $\underline{q}_1$ are functions of t, $\underline{Z}_{T,1}$ and $Y_{p,1}$ exclusively, when the directions of the mass flows are given.

Finally, $\underline{Y}'_M$ can be found from a simple vector-matrix multiplication

$$\underline{Y}'_{M,1} = \underline{\underline{P}} \cdot \underline{Z}_{\dot{m},1} \tag{6.127}$$

where $\underline{\underline{P}}$ is a constant matrix.

In this way $\underline{Y}'_{p,1}$ and $\underline{Y}'_{M,1}$ are given and now let $\underline{Y}_i$ denote the vector

$$\underline{Y}_i = \begin{bmatrix} Y_{p,i} \\ \underline{Y}_{M,i} \end{bmatrix} \tag{6.128}$$

The explicit Runge-Kutta method is then used for the determination of $\underline{Y}_{p,2}$ and $\underline{Y}_{M,2}$ for the second stage (k=2) after the formula

$$\underline{Y}_i = \underline{y}_n + \Delta t \cdot \sum_{j=1}^{i-1} a_{ij} \cdot \underline{Y}'_j \qquad (6.129)$$

and so on for the remaining stages k=3,4...,s.

The new values at time level t_{n+1} are then given as

$$\underline{y}_{n+1} = \underline{y}_n + \Delta t \cdot \sum_{i=1}^{s} b_i \cdot \underline{Y}'_i \qquad (6.130)$$

Notice that $\underline{z}_{\dot{m},n}$ and $\underline{z}_{T,n}$ (at time level t_n) can be found as $\underline{z}_{\dot{m},n} = \underline{Z}_{\dot{m},1}$ and $\underline{z}_{T,n} = \underline{Z}_{T,1}$ and that $\underline{Q}_k$ and $\underline{q}_k$ must be calculated at all stages k=1,2,...,s.

This can be summarized in the following algorithm.

Algorithm for a s-stage explicit Runge-Kutta method

Let $y_{p,0}$ and $\underline{y}_{M,0}$ be given from an initial guess for the initial state at t=0 and let N denote the total number of time steps, n the actual time step and k the actual stage number.

Fixed step length algorithm:

```
FOR n=0 TO N-1
    FOR k=1 TO s
        Calculate t = t_n+c_k·Δt
        Calculate Y_p,k , Y_M,k
        Calculate Z_T,k
        Solve the linear system for Y'_p,k , Z_ṁ,k
        Calculate Y'_M,k
        IF k=1 THEN put z_ṁ,n = Z_ṁ,k and z_T,n = Z_T,k
    END
    Calculate y_p,n+1 and y_M,n+1 using the stage derivatives and the explicit method.
END
```

This is for a fixed step length algorithm, for a variable step length algorithm the local truncation error has to be estimated and the new step length has to be determined in each step and the total number of steps N is not known in advance.

Variable step length algorithm:

n=0
Give initial step length Δt_{new}
WHILE $t < t_p$ DO
  REPEAT
    $\Delta t = \Delta t_{new}$
    FOR k=1 TO s
      Calculate $t = t_n + c_k \cdot \Delta t$
      Calculate $Y_{p,k}$, $\underline{Y}_{M,k}$
      Calculate $\underline{Z}_{T,k}$
      Solve the linear system for $Y'_{p,k}$, $\underline{Z}_{\dot{m},k}$
      Calculate $\underline{Y}'_{M,k}$
      IF k=1 THEN put $\underline{z}_{\dot{m},n} = \underline{Z}_{\dot{m},k}$ and $\underline{z}_{T,n} = \underline{Z}_{T,k}$
    END
    Calculate error estimates EST
    Calculate new step length Δt_{new}
  UNTIL EST < TOL
  n=n+1
  Calculate $\underline{y}_{p,n+1}$ and $\underline{y}_{M,n+1}$ using the stage derivatives and the explicit method.
END DO
N=n

Remarks:

i) The convergence is sensitive to the initial guess for the state variables and parameter values. For the SFVSM-problem, a sufficiently good initial guess can be provided when using an isothermal Schmidt analysis.

ii) Stability problems have been observed for extreme values of certain parameters, especially for large NTU-numbers in the regenerator.

iii) Difficulties are encountered at points where the mass flows change signs. Failing to find a solution for the small "linear" sub system of equations is the cause and the time step must be reduced to be able to obtain a solution in that particular step.

iv) After cyclic conditions for the state variables have been reached, the iteration on the parameters from the cyclic integral conditions must be performed, increasing computational costs of the Integration-to-Convergence approach.

6.6.3 Implicit Runge-Kutta methods

Compared to explicit methods, implicit Runge-Kutta methods (IRKs) have much better properties concerning stability and attainable order for a given stage number. IRKs are, in general (and fully implicit methods in particular), expensive to use when evaluating the computational cost: These methods are applied mostly for solving stiff systems of ODEs or systems of DAEs.

Fully implicit Runge-Kutta methods have a_{ij}'s above the main diagonal in the matrix $\underline{\underline{A}}$ in the Butcher array, which are non-zero. For a system of n ODEs, using a s-stage fully implicit method implies solving a system of n·s non-linear equations in each time step.

Semi-implicit Runge-Kutta methods have zeros above the diagonal in the matrix $\underline{\underline{A}}$ from the Butcher-array. For these methods it is only necessary to solve s systems of n nonlinear equations and this will be a significant save in the computational cost compared to the fully-implicit methods.

DIRK (Diagonally-Implicit Runge-Kutta) and SIRK (Singly-Implicit Runge-Kutta) methods have $\underline{\underline{A}}$ with only one single eigenvalue of multiplicity s. This implies that it is possible to reuse LU-factorizations of the Jacobian in the iteration for the internal stage values, which greatly reduces the computational cost for large systems.

Here only general semi-implicit Runge-Kutta methods will be considered. DIRK methods are included, but their special properties with regard to the implementation have not been exploited in the developed code.

Semi-implicit Runge-Kutta methods for the solution of the SFVSM-problem

Implicit Runge-Kutta methods can be used for both formulations, and the methods can directly be applied to the system of equations derived in 6.2.2 or 6.2.3, respectively. In principle, the implementations for the two formulations are identical, so only the implementation for the basic formulation is described in detail.

Implementation of a semi-implicit Runge-Kutta method for the basic formulation

In order to compare with explicit Runge-Kutta methods and at the same time try to limit the computational cost, semi-implicit methods will be considered only. The system of nonlinear equations that have to be solved in each stage will be of dimension $n=n_f+n_g$, where n_f and n_g are the number of differential equations and algebraic equations.

It is possible to make implementations that take advantage of the structure of a semi-explicit system of DAEs. From the traditional ODE application of IRKs to the singular perturbation problem

$$\begin{aligned} \underline{y}' &= \underline{f}(t,\underline{y},\underline{z}) \\ \varepsilon\cdot\underline{z}' &= \underline{g}(t,\underline{y},\underline{z}) \end{aligned} \tag{6.131}$$

and in the limiting case $\varepsilon=0$, the following difference equations are derived for a general s-stage implicit Runge-Kutta method

$$\begin{aligned} \underline{Y}_i' &= \underline{f}\left(t_n + c_i\cdot\Delta t, \underline{y}_n + \Delta t\cdot\sum_{j=1}^{s} a_{ij}\cdot\underline{Y}_i', \underline{z}_n + \Delta t\cdot\sum_{j=1}^{s} a_{ij}\cdot\underline{Z}_i'\right) \\ \underline{0} &= \underline{g}\left(t_n + c_i\cdot\Delta t, \underline{y}_n + \Delta t\cdot\sum_{j=1}^{s} a_{ij}\cdot\underline{Y}_i', \underline{z}_n + \Delta t\cdot\sum_{j=1}^{s} a_{ij}\cdot\underline{Z}_i'\right) \end{aligned} \tag{6.132}$$

where $\underline{Y}_i'$ and $\underline{Z}_i'$ are the stage derivatives.

Stage variables $\underline{Y}_i$ and $\underline{Z}_i$ are defined as

$$\begin{aligned} \underline{Y}_i &= \underline{y}_n + \Delta t\cdot\sum_{j=1}^{s} a_{ij}\cdot\underline{Y}_j' \\ \underline{Z}_i &= \underline{z}_n + \Delta t\cdot\sum_{j=1}^{s} a_{ij}\cdot\underline{Z}_j' \end{aligned} \tag{6.133}$$

For a semi-implicit method $a_{ij} = 0$ for $j>i$ so the equations above can be written as

$$\begin{aligned} \underline{Y}_i' &= \underline{f}\left(t_n + c_i\cdot\Delta t, \underline{Y}_i, \underline{Z}_i\right) \\ \underline{0} &= \underline{g}\left(t_n + c_i\cdot\Delta t, \underline{Y}_i, \underline{Z}_i\right) \end{aligned} \tag{6.134}$$

and

$$\begin{aligned} \underline{Y}_i &= \underline{y}_n + \Delta t \cdot \sum_{j=1}^{i} a_{ij} \cdot \underline{Y}'_j \\ \underline{Z}_i &= \underline{z}_n + \Delta t \cdot \sum_{j=1}^{i} a_{ij} \cdot \underline{Z}'_j \end{aligned} \tag{6.135}$$

or

$$\begin{aligned} \underline{Y}'_i &= \frac{\underline{Y}_i - \underline{y}_n - \Delta t \cdot \sum_{j=1}^{i-1} a_{ij} \cdot \underline{Y}'_j}{\Delta t \cdot a_{ii}} \\ \underline{Z}'_i &= \frac{\underline{Z}_i - \underline{z}_n - \Delta t \cdot \sum_{j=1}^{i-1} a_{ij} \cdot \underline{Z}'_j}{\Delta t \cdot a_{ii}} \end{aligned} \tag{6.136}$$

So the system can be solved for the stage variables in the following way

$$\begin{aligned} \underline{Y}_i - \underline{y}_n - \Delta t \cdot \sum_{j=1}^{i-1} a_{ij} \cdot \underline{Y}'_j - \Delta t \cdot a_{ii} \cdot \underline{f}\left(t_n + c_i \cdot \Delta t, \underline{Y}_i, \underline{Z}_i\right) &= \underline{0} \\ \underline{g}\left(t_n + c_i \cdot \Delta t, \underline{Y}_i, \underline{Z}_i\right) &= \underline{0} \end{aligned} \tag{6.137}$$

where the stage derivatives are found from the expression given just above.

The new values at time level n+1 are then finally calculated as

$$\begin{aligned} \underline{y}_{n+1} &= \underline{y}_n + \Delta t \cdot \sum_{i=1}^{s} b_i \cdot \underline{Y}'_i \\ \underline{z}_{n+1} &= \underline{z}_n + \Delta t \cdot \sum_{i=1}^{s} b_i \cdot \underline{Z}'_i \end{aligned} \tag{6.138}$$

An implicit Runge-Kutta method can in a similar way be applied also for the alternative formulation of the system of equations for the SFVSM-problem.

Algorithm for a s-stage semi-implicit Runge-Kutta method

Let $\underline{y}_0$ be given, let n be the actual time step and k the actual stage number.

Fixed step length algorithm:

```
FOR n=0 TO N-1
    FOR k=1 TO s
        t = t_n + c_k·Δt
        m=0
        Give initial guess for Y_k^[0] and Z_k^[0]
        REPEAT
            Calculate the residuals r_f(t, Y_k^[m], Z_k^[m]) and r_g(t, Y_k^[m], Z_k^[m]) from (6.137)
            Check convergence (if convergence OK skip next 3 steps)
            Calculate the Jacobian J
            Solve the linearized system for ΔY_k^[m] and ΔZ_k^[m]
            Calculate new values for Y_k^[m+1] = Y_k^[m] +ΔY_k^[m] and Z_k^[m+1] = Z_k^[m] +ΔZ_k^[m]
            m=m+1
        UNTIL Convergence
        Calculate the stage derivatives Y'_k and Z'_k
    END
    Calculate y_n+1 and z_n+1
END
```

Remarks:

i) Clearly, at stage k, all the previous stage values $\underline{Y}_1,\underline{Y}_2,\ldots,\underline{Y}_{k-1}$ are given and $\underline{Y}_k$ only has to be determined when using a semi-implicit Runge-Kutta method. This will require the solution of a system of n_y+n_z equations in each integration step and in the algorithm Newton's method has been used.

ii) A variable step length implementation can also be considered analogous to the algorithm for the explicit methods.

iii) As it will be shown in the next chapter, a fixed step length code, using an algebraic allystable IRK method, can be used to resolve a cycle using only a few steps without stability problems for the SFVSM-problem, but a code with variable step length based on error estimates, uses significantly more steps to obtain an accurate solution.

iv) Again the parameters for cyclic integral conditions still have to be determined, such that the cyclic conditions are satisfied. This will be discussed in the next section.

6.6.4 Obtaining the periodic steady-state solution

After determining the cyclic solution for the differential and algebraic variables (mass, internal energy, pressure, temperature and mass flow), it remains to satisfy the cyclic integral conditions.

These integral constraints or conditions given in section 6.2.4 express cyclic operation in the regenerator (two equations), cyclic heat transfer in the variable volumes (two equations) and correct required mean pressure of the cycle (one equation), a total of $n_\lambda = 5$ integral equations for the SFVSM-problem.

The unknown parameters (denoted λ_i ,i=1,2,...,n_λ) whose values must be adjusted to satisfy these integral equations are the regenerator matrix temperature and gradient, the solid wall temperatures in the variable volumes and the total mass. For the Integration-to-Convergence method,the adjustment of λ_i's can only be performed by iteration and succeeding the calculation of the cyclic state variables. This implies that another calculation of the cyclic state variables has to be performed with the new parameter values and so on until both the integral constraints and the cyclic state variables are satisfied.

The new iterates of the parameter values λ_i can be calculated using Newton's method. Preliminary tests using a simple secant type method turned out unfavorably compared to a simplified Newton iteration based on finite difference approximation of the Jacobian.

Let the integral conditions be expressed in the form

$$\underline{H} = \int_{t=0}^{t_p} \underline{h}(t,\underline{y},\underline{z},\underline{\lambda})\cdot dt = \underline{0} \tag{6.139}$$

A finite difference approximation of the Jacobian

$$\underline{\underline{J}}_H = \frac{\partial \underline{H}}{\partial \underline{\lambda}} \tag{6.140}$$

can then be calculated using a one-sided difference approximation for the elements

$$\frac{\partial H_i}{\partial \lambda_j} \approx \frac{H_i(\underline{\lambda} + \delta\underline{\lambda}_j) - H_i(\underline{\lambda})}{\delta\lambda_j} \tag{6.141}$$

where

$$\delta\underline{\lambda}_j = \begin{bmatrix} 0 \\ . \\ . \\ 0 \\ \delta\lambda_j \\ 0 \\ . \\ 0 \end{bmatrix} \qquad (6.142)$$

with $i,j = 1,2,...,n_\lambda$.

The problem of finding appropriate values of the $\delta\lambda_j$'s is addressed later in this chapter.

Remarks:

i) The finite difference approximation of the Jacobian requires $n_\lambda = 5$ additional Integration-to-Convergence calculations for the Simple Five-Volume Stirling Model problem.

ii) A modified Newton iteration where the Jacobian only is calculated once (no updates) seems to be sufficient for the SFVSM problem, at least as long as the initial guess for $\underline{\lambda}$ is close to the real solution.

iii) For a more sophisticated model, which includes NTU-numbers as function of mass flows or pressure losses due to friction, it could be suspected that the additional nonlinearities introduced into the equations would cause trouble for the modified Newton iteration on the integral conditions.

6.7 Implementation of the Shooting Method

6.7.1 Introductory remarks

The basic theory for Shooting method for Boundary Value problems (BVPs) has been described in section 6.5. In this section, the actual implementation for the solution of the mathematical model of the Simple Five-Volume Stirling Model problem will be discussed.

The method can be applied to both formulations, i.e., the basic formulation (using an implicit method for the time integration) and for the alternative formulation (using either an explicit method or an implicit method).

Since there is no principal difference between the two formulations only the implementation of the single Shooting method for the basic formulation of the system of equations (see section 6.2.2) is discussed in detail.

Consider the system of semi-explicit DAEs

$$\begin{aligned} \underline{y}' &= \underline{f}(t,\underline{y},\underline{z}) \\ \underline{0} &= \underline{g}(t,\underline{y},\underline{z}) \end{aligned} \tag{6.143}$$

and periodic boundary conditions

$$\underline{y}(0) = \underline{y}(t_p) \qquad \underline{z}(0) = \underline{z}(t_p) \tag{6.144}$$

where, $\underline{y} = \underline{y}(t)$, $\underline{z} = \underline{z}(t)$ and $0 \le t \le t_p$.

6.7.2 Single Shooting method

The single shooting method for this problem can be stated in the following way:

Given a guess $\underline{s}$ for the initial state

$$\underline{s} = \underline{y}(0) \tag{6.145}$$

The system of nonlinear equations

$$\underline{G}(\underline{s}) = \underline{s} - \underline{y}(t_p;\underline{s}) = \underline{0} \tag{6.146}$$

or explicitly

$$\underline{G}(\underline{s}) = \begin{bmatrix} y_1(0) - y_1(t_p) \\ y_2(0) - y_2(t_p) \\ \vdots \\ y_{10}(0) - y_{10}(t_p) \end{bmatrix} = \underline{0} \tag{6.147}$$

has to be solved using an iteration method, such as Newton's method for the solution of nonlinear equations.

The value of $\underline{G}(\underline{s})$ (i.e., the residual) is found using a numerical method for the time integration of one cycle given the initial guess $\underline{s}=\underline{y}_0$, i.e.,

$$\underline{G}(\underline{y}_0) = \underline{y}_0 - \underline{y}_N$$

where $\underline{y}_N \approx \underline{y}(t_p;\underline{s})$ is the numerical solution obtained after one cycle.

Implementation of Newton's method:

The new iterate $\underline{s}^{[k+1]}$ is determined from solving the linearized system

$$\begin{aligned} \underline{G}'(\underline{s}^{[m]})\cdot\Delta\underline{s}^{[m]} &= -\underline{G}(\underline{s}^{[m]}) \\ \underline{s}^{[m+1]} &= \Delta\underline{s}^{[m]} + \underline{s}^{[m]} \end{aligned} \tag{6.149}$$

where the Jacobian of the system is

$$\underline{G}'(\underline{s}) = \frac{\partial \underline{G}}{\partial \underline{s}} = \underline{\underline{I}} - \frac{\partial \underline{y}(t_p;\underline{s})}{\partial \underline{s}} \tag{6.150}$$

An analytical expression (in form of a system of ODEs) for the Jacobian can be found as shown in section 6.5.2, but only a simple finite difference approximation of the Jacobian will be considered here.

A one-sided finite difference approximation for the elements in the Jacobian can be given as

$$\frac{\partial G_i}{\partial s_j} \approx \frac{G_i(\underline{s}+\delta\underline{s}_j) - G_i(\underline{s})}{\delta s_j} \tag{6.151}$$

where

$$\delta \underline{s}_j = \begin{bmatrix} 0 \\ . \\ . \\ . \\ 0 \\ \delta s_j \\ 0 \\ . \\ . \\ 0 \end{bmatrix} \tag{6.152}$$

with $i=1,2,...,n_f$ and $j=1,2,...,n_y$.

The δs_j's have to be chosen so small that the finite difference approximations give a sufficiently good estimate of the elements in the Jacobian. On the other hand, a too small value can contaminate the approximation due to numerical errors introduced. In this case, the numerical errors are <u>not</u> round off errors (whose size usually can be related to the machine precision), but the much larger truncation errors related to the application of the numerical method for the integration of a cycle.

It is difficult to make general recommendations for an optimal choice of the δs_j's, because of the dependency on accuracy of the numerical solution. The order of accuracy of the method and error tolerance (or number of time steps for fixed step length algorithm) will determine how small the δs_j's can be chosen. Furthermore, if a modified Newton iteration (where the Jacobian is not updated in each iteration step) is applied then conditions become even more complex and a trial-and error approach seems to be the only way to do it.

The same relative change Δs_{rel} can be used for each component of the vector, i.e.,

$$\delta s_j = \Delta s_{rel} \cdot s_j \tag{6.153}$$

In the developed codes $\Delta s_{rel} = 0.001\text{-}0.0001$ proved to be working in most cases.

Application of a finite difference approximation of the Jacobian requires the numerical integration of n_y cycles in addition to the time integration of the original system (6.143). Again, just like solving the variational system for the analytical expression for the Jacobian, these are n_y+1 systems of initial value problems, which have to be solved using an appropriate numerical method for IVPs.

The modified Newton method, where the Jacobian is updated only when the residuals $\underline{r}^{[k]} = \underline{G}(\underline{s}^{[k]})$ are not decaying in an adequately fast rate seem to be sufficient for the SFVSM-problem. This will give significant savings in the computational costs (see the discussion in chapter 7).

6.7.3 Obtaining the periodic steady-state solution

The iteration on the cyclic integral conditions can very easily be included in the Shooting method and (as it will be shown in the next chapter) this really gives the method a decisive advantage against the Integration-to-Convergence approach.

Only a small modification is required, the vector $\underline{\lambda}$ with the parameters for the cyclic integral conditions (λ_i, i=1,2,...,n_λ= 5 for the SFVSM-problem) is included in $\underline{s}$, such that

$$\underline{s} = \begin{bmatrix} \underline{y}(0) \\ \underline{\lambda} \end{bmatrix} \tag{6.154}$$

The system of equations is now given as

$$\underline{G}(\underline{s}) = \begin{bmatrix} \underline{y}(0) - \underline{y}(t_p) \\ \underline{H}(t_p) \end{bmatrix} \tag{6.155}$$

where cyclic the integral conditions are written as $\underline{H}(t)$ and

$$H_i = \int_{t=0}^{t_p} h_i(t,\underline{y},\underline{z},\underline{\lambda}) \cdot dt = 0 \tag{6.156}$$

for i=1,2,...,n_λ=5

Remarks:

i) Now, the iteration gives the cyclic state variables and the cyclic integral conditions simultaneously.

ii) The remarks concerning the finite difference approximation of the Jacobian are still valid when the iteration on $\underline{\lambda}$ is included in the Shooting method.

6.8 Implementation of the Finite-Difference method

6.8.1 Introductory remarks

Application of the Finite Difference method for the SFVSM-problem is described in this section. Implementation of the method is possible for both formulations, but since the structures are identical, only the implementation for the basic formulation of the system of equations is shown here.

The differential equations are discretized at all time levels using finite difference approximations and a fixed time step. In combination with the algebraic equations (at the same time levels), the full periodic solution is obtained once and for all after solving the large system of nonlinear equations that arises from the discretization.

6.8.2 Implementation of the method

The following discretizations of the differential equations have been considered:

- Linear Multistep methods (BDF-methods).
- Divided difference approximation.

In this context, the discretized equations can conveniently be written in the form

$$\sum_{j=-k}^{k} \alpha_j \underline{y}_{n+j} = \Delta t \cdot \sum_{j=-k}^{k} \beta_j \underline{f}_{n+j} \qquad (6.157)$$

for time level t_n.

This is slightly different from the usual notation, but it will give a better structure of the Jacobian. For the actual system of DAEs the right hand sides of the differential equations are functions of the algebraic variables too, i.e., $\underline{f}_{n+j} = \underline{f}\,(t_{n+j}, \underline{y}_{n+j}, \underline{z}_{n+j})$.

The algebraic equations can still be written in the form

$$g(t_n, \underline{y}_n, \underline{z}_n) = \underline{0} \qquad (6.158)$$

Time discretization

The time interval is discretized into N+1 equally spaced points, giving N time steps of length (mesh size) Δt

$$\Delta t = \frac{t_p}{N} \qquad t_n = n \cdot \Delta t \qquad n = 0,1,2,\ldots,N \qquad (6.159)$$

Let the unknown variables at time level t_n be given as a vector $\underline{x}_n$

$$\underline{x}_n = \begin{bmatrix} y_{1,n} \\ y_{2,n} \\ \cdot \\ \cdot \\ \cdot \\ y_{10,n} \\ z_{1,n} \\ z_{2,n} \\ \cdot \\ \cdot \\ \cdot \\ z_{8,n} \end{bmatrix} \tag{6.160}$$

The vector has $n_y + n_z = 18$ elements, but the two (boundary) conditions for mass flows (i.e., $z_{1,n} = 0$ and $z_{6,n} = 0$) can be omitted and directly inserted into the system of equations.

The periodicity of the solution gives the following condition

$$\underline{x}_n = \underline{x}_{n+N} \tag{6.161}$$

When this condition is fulfilled, the vector $\underline{x}$ given by

$$\underline{x} = \begin{bmatrix} \underline{x}_0 \\ \underline{x}_1 \\ \underline{x}_2 \\ \cdot \\ \cdot \\ \cdot \\ \underline{x}_{N-1} \end{bmatrix} \tag{6.162}$$

contains the full numerical solution of the problem.

Equations and boundary conditions

The full discretized system of nonlinear equations can now be written as

$$\underline{F}(\underline{x}) = \underline{0} \tag{6.163}$$

For a method with a given number k, the discretized equations at time level n are

$$\underline{F}_n(t_{n-k}, t_{n-k+1}, \ldots, t_{n+k}, \underline{x}_{n-k}, \underline{x}_{n-k+1}, \ldots, \underline{x}_{n+k}) = \underline{0} \tag{6.164}$$

or explicitly for the SFVSM-problem

Mass:

$$\begin{aligned}
F_{1,n} &= \sum_{j=-k}^{k} \alpha_j \cdot y_{1,n+j} - \Delta t \cdot \sum_{j=-k}^{k} \beta_j \cdot (z_{1,n+j} - z_{2,n+j}) = 0 \\
F_{2,n} &= \sum_{j=-k}^{k} \alpha_j \cdot y_{2,n+j} - \Delta t \cdot \sum_{j=-k}^{k} \beta_j \cdot (z_{2,n+j} - z_{3,n+j}) = 0 \\
F_{3,n} &= \sum_{j=-k}^{k} \alpha_j \cdot y_{3,n+j} - \Delta t \cdot \sum_{j=-k}^{k} \beta_j \cdot (z_{3,n+j} - z_{4,n+j}) = 0 \\
F_{4,n} &= \sum_{j=-k}^{k} \alpha_j \cdot y_{4,n+j} - \Delta t \cdot \sum_{j=-k}^{k} \beta_j \cdot (z_{4,n+j} - z_{5,n+j}) = 0 \\
F_{5,n} &= \sum_{j=-k}^{k} \alpha_j \cdot y_{5,n+j} - \Delta t \cdot \sum_{j=-k}^{k} \beta_j \cdot (z_{5,n+j} - z_{6,n+j}) = 0
\end{aligned} \tag{6.165}$$

Energy:

$$\begin{aligned}
F_{6,n} = \sum_{j=-k}^{k} \alpha_j \cdot y_{6,n+j} - \Delta t \cdot \sum_{j=-k}^{k} \beta_j \cdot \Bigg[& -\gamma \cdot \max(z_{2,n+j}, 0) \cdot \frac{y_{6,n+j}}{y_{1,n+j}} - \gamma \cdot \min(z_{2,n+j}, 0) \cdot \frac{y_{7,n+j}}{y_{2,n+j}} \\
& + \frac{1}{2} \cdot |z_{2,n+j}| \cdot \gamma \cdot NTU_1 \cdot \left(\lambda_4 - \frac{y_{6,n+j}}{y_{1,n+j}} \right) - (\gamma - 1) \cdot z_{7,n+j} \cdot V_1'(t_{n+j}) \Bigg] = 0
\end{aligned} \tag{6.166}$$

$$F_{7,n} = \sum_{j=-k}^{k} \alpha_j \cdot y_{7,n+j} - \Delta t \cdot \sum_{j=-k}^{k} \beta_j \cdot \left[\gamma \cdot \max(z_{2,n+j},0) \cdot \frac{y_{6,n+j}}{y_{1,n+j}} + \gamma \cdot \min(z_{2,n+j},0) \cdot \frac{y_{7,n+j}}{y_{2,n+j}} \right.$$
$$- \gamma \cdot \max(z_{3,n+j},0) \cdot \frac{y_{7,n+j}}{y_{2,n+j}} - \gamma \cdot \min(z_{3,n+j},0) \cdot \left(z_{8,n+j} - \frac{\lambda_3}{2} \right)$$
$$\left. + \frac{1}{2} \cdot \left(|z_{2,n+j}| + |z_{3,n+j}| \right) \cdot \gamma \cdot NTU_2 \cdot \left(T_{s,2} - \frac{y_{7,n+j}}{y_{2,n+j}} \right) \right] = 0 \qquad (6.167)$$

$$F_{8,n} = \sum_{j=-k}^{k} \alpha_j \cdot y_{8,n+j} - \Delta t \cdot \sum_{j=-k}^{k} \beta_j \cdot \left[\gamma \cdot \max(z_{3,n+j},0) \cdot \frac{y_{7,n+j}}{y_{2,n+j}} + \gamma \cdot \min(z_{3,n+j},0) \cdot \left(z_{8,n+j} - \frac{\lambda_3}{2} \right) \right.$$
$$- \gamma \cdot \max(z_{4,n+j},0) \cdot \left(z_{8,n+j} + \frac{\lambda_3}{2} \right) - \gamma \cdot \min(z_{4,n+j},0) \cdot \frac{y_{9,n+j}}{y_{4,n+j}}$$
$$\left. + \frac{1}{2} \cdot \left(|z_{3,n+j}| + |z_{4,n+j}| \right) \cdot \gamma \cdot NTU_3 \cdot (\lambda_2 - z_{8,n+j}) \right] = 0 \qquad (6.168)$$

$$F_{9,n} = \sum_{j=-k}^{k} \alpha_j \cdot y_{9,n+j} - \Delta t \cdot \sum_{j=-k}^{k} \beta_j \cdot \left[\gamma \cdot \max(z_{4,n+j},0) \cdot \left(z_{8,n+j} + \frac{\lambda_3}{2} \right) + \gamma \cdot \min(z_{4,n+j},0) \cdot \frac{y_{9,n+j}}{y_{4,n+j}} \right.$$
$$- \gamma \cdot \max(z_{5,n+j},0) \cdot \frac{y_{9,n+j}}{y_{4,n+j}} - \gamma \cdot \min(z_{5,n+j},0) \cdot \frac{y_{10,n+j}}{y_{5,n+j}}$$
$$\left. + \frac{1}{2} \cdot \left(|z_{4,n+j}| + |z_{5,n+j}| \right) \cdot \gamma \cdot NTU_4 \cdot \left(T_{s,4} - \frac{y_{9,n+j}}{y_{4,n+j}} \right) \right] = 0 \qquad (6.169)$$

$$F_{10,n} = \sum_{j=-k}^{k} \alpha_j \cdot y_{10,n+j} - \Delta t \cdot \sum_{j=-k}^{k} \beta_j \cdot \left[\gamma \cdot \max(z_{5,n+j},0) \cdot \frac{y_{9,n+j}}{y_{4,n+j}} + \gamma \cdot \min(z_{5,n+j},0) \cdot \frac{y_{10,n+j}}{y_{5,n+j}} \right. \qquad (6.170)$$
$$\left. + \frac{1}{2} \cdot |z_{5,n+j}| \cdot \gamma \cdot NTU_5 \cdot \left(\lambda_5 - \frac{y_{10,n+j}}{y_{5,n+j}} \right) - (\gamma - 1) \cdot z_{7,n+j} \cdot V_5'(t_{n+j}) \right] = 0$$

Algebraic equations:

$$\begin{aligned} F_{11,n} &= z_{7,n} \cdot V_1(t_n) - y_{6,n} = 0 \\ F_{12,n} &= z_{7,n} \cdot V_2 - y_{7,n} = 0 \\ F_{13,n} &= z_{7,n} \cdot V_3 - y_{8,n} = 0 \\ F_{14,n} &= z_{7,n} \cdot V_4 - y_{9,n} = 0 \\ F_{15,n} &= z_{7,n} \cdot V_5(t_n) - y_{10,n} = 0 \end{aligned} \tag{6.171}$$

$$F_{16,n} = z_{8,n} - \frac{\lambda_3}{2} \cdot \frac{\exp\left(\lambda_3 \cdot \frac{y_{3,n}}{y_{8,n}}\right) + 1}{\exp\left(\lambda_3 \cdot \frac{y_{3,n}}{y_{8,n}}\right) - 1} = 0 \tag{6.172}$$

$$\begin{aligned} F_{17,n} &= z_{1,n} = 0 \\ F_{18,n} &= z_{6,n} = 0 \end{aligned} \tag{6.173}$$

A total n_{eq}=18 equations for each time level.

The full discretized system of nonlinear equations (all time levels) may now be written as

$$\underline{F} = \begin{bmatrix} \underline{F}_0 \\ \underline{F}_1 \\ \cdot \\ \cdot \\ \cdot \\ \underline{F}_{N-1} \end{bmatrix} = \begin{bmatrix} \underline{0} \\ \underline{0} \\ \cdot \\ \cdot \\ \cdot \\ \underline{0} \end{bmatrix} \tag{6.174}$$

or

$$\underline{F}(\underline{x}) = \underline{0} \tag{6.175}$$

This is a system of $n_{eq} \cdot N$ nonlinear equations, which must be solved using an iterative method.

Newton's method is the most widely used method for solving systems of nonlinear equations and it will also apply here.

Calculation of the Jacobian

Using Newton's method involves evaluation of the Jacobian, but it can be calculated analytically from the expressions derived above (tedious work is required, but this has been carried out in the developed codes!).

As an example, the Jacobian for a LMM with k=2 and N=10 time steps will have the following structure

$$\underline{\underline{J}} = \begin{bmatrix}
\underline{\underline{A}}_{0,0} & \underline{\underline{A}}_{0,1} & \underline{\underline{A}}_{0,2} & \underline{\underline{0}} & \underline{\underline{0}} & \underline{\underline{0}} & \underline{\underline{0}} & \underline{\underline{0}} & \underline{\underline{A}}_{0,-2} & \underline{\underline{A}}_{0,-1} \\
\underline{\underline{A}}_{1,-1} & \underline{\underline{A}}_{1,0} & \underline{\underline{A}}_{1,1} & \underline{\underline{A}}_{1,2} & \underline{\underline{0}} & \underline{\underline{0}} & \underline{\underline{0}} & \underline{\underline{0}} & \underline{\underline{0}} & \underline{\underline{A}}_{1,-2} \\
\underline{\underline{A}}_{2,-2} & \underline{\underline{A}}_{2,-1} & \underline{\underline{A}}_{2,0} & \underline{\underline{A}}_{2,1} & \underline{\underline{A}}_{2,2} & \underline{\underline{0}} & \underline{\underline{0}} & \underline{\underline{0}} & \underline{\underline{0}} & \underline{\underline{0}} \\
\underline{\underline{0}} & \underline{\underline{A}}_{3,-2} & \underline{\underline{A}}_{3,-1} & \underline{\underline{A}}_{3,0} & \underline{\underline{A}}_{3,1} & \underline{\underline{A}}_{3,2} & \underline{\underline{0}} & \underline{\underline{0}} & \underline{\underline{0}} & \underline{\underline{0}} \\
. & . & . & . & . & . & . & . & . & . \\
\underline{\underline{0}} & \underline{\underline{0}} & \underline{\underline{0}} & \underline{\underline{A}}_{n,-2} & \underline{\underline{A}}_{n,-1} & \underline{\underline{A}}_{n,0} & \underline{\underline{A}}_{n,1} & \underline{\underline{A}}_{n,2} & \underline{\underline{0}} & \underline{\underline{0}} \\
. & . & . & . & . & . & . & . & . & . \\
\underline{\underline{0}} & \underline{\underline{0}} & \underline{\underline{0}} & \underline{\underline{0}} & \underline{\underline{0}} & \underline{\underline{A}}_{N-3,-2} & \underline{\underline{A}}_{N-3,-1} & \underline{\underline{A}}_{N-3,0} & \underline{\underline{A}}_{N-3,1} & \underline{\underline{A}}_{N-3,2} \\
\underline{\underline{A}}_{N-2,2} & \underline{\underline{0}} & \underline{\underline{0}} & \underline{\underline{0}} & \underline{\underline{0}} & \underline{\underline{0}} & \underline{\underline{A}}_{N-2,-2} & \underline{\underline{A}}_{N-2,-1} & \underline{\underline{A}}_{N-2,0} & \underline{\underline{A}}_{N-2,1} \\
\underline{\underline{A}}_{N-1,1} & \underline{\underline{A}}_{N-1,2} & \underline{\underline{0}} & \underline{\underline{0}} & \underline{\underline{0}} & \underline{\underline{0}} & \underline{\underline{0}} & \underline{\underline{A}}_{N-1,-2} & \underline{\underline{A}}_{N-1,-1} & \underline{\underline{A}}_{N-1,0}
\end{bmatrix} \qquad (6.176)$$

where the block matrices contain all the possible non-zero elements.

The block matrix $\underline{\underline{A}}_{n,j}$ is defined as

$$\underline{\underline{A}}_{n,j} = \frac{\partial \underline{F}_n}{\partial \underline{x}_{n+j}} \qquad (6.177)$$

where n = 0,1,...,N-1 (n is time step) and j = -k, -k+1,..., k (j is step number).

Each $\underline{\underline{A}}_{n,j}$ contains $n_{eq} \cdot n_{eq}$ elements, whose values are non-zero for only approximately 20-25%.

It should be noted that the Jacobian has a band structure and that the matrix is sparse (more pronounced as the number of time steps is increased). This should be exploited in the solution of the linearized system to compensate for the increased number of equations.

The sparse Jacobian also makes other numerical methods than Newton's method less attractive since these methods (e.g., quasi-Newton methods based on rank one and two updates) typically implies fill-ins and destruction of the sparse structure.

6.8.3 Obtaining the periodic steady-state solution

The iteration on the periodic steady-state solution (i.e., periodic state variables and satisfying the cyclic integral conditions) can be implemented in a very simple way, since the integral conditions directly can be included in the system of equations.

A numerical method for the integration of the integral equations gives an approximation

$$H_i = \int_{t=0}^{t_p} h_i(t,\underline{y},\underline{z},\underline{\lambda})\cdot dt \approx \Delta t\cdot\sum_{n=0}^{N} w_n\cdot h_{i,n} \qquad (6.178)$$

where i=1,2,...,n_λ=5 and w_n are the (weight) coefficients of the numerical integration method (e.g., Trapezoidal rule or Simpson's rule, see Appendix E).

This gives only n_λ=5 additional equations for the SFVSM-problem and the full system of equations is now given as

$$\begin{bmatrix} \underline{F} \\ \underline{H} \end{bmatrix} = \underline{0} \qquad (6.179)$$

The calculation procedure can then be the following:

Algorithm for the iteration on a Finite Difference solution of the SFVSM-problem

1) Calculate the residuals $\underline{r}_{F,n}^{[m]} = \underline{F}_n\,(t\,,\,\underline{x}_{n+k}^{[m]}\,,\,\underline{x}_{n+k-1}^{[m]}\,,\ldots,\,\underline{x}_{n-k}^{[m]}\,,\underline{\lambda}^{[m]})$ n= 0,1,...N-1 and $\underline{R}_H^{[m]} = \underline{H}\,(t\,,\,\underline{x}_0^{[m]}\,,\,\underline{x}_1^{[m]}\,,\ldots,\,\underline{x}_{N-1}^{[m]}\,,\underline{\lambda}^{[m]})$.

2) Check for convergence (stationary cyclic conditions), i.e., evaluate $||\underline{r}_{F,n}^{[m]}||$ and $||\underline{r}_H^{[m]}||$.

3) Calculate the Jacobian $\underline{\underline{J}}^{[m]}$ (including the equations $\underline{H}$ and derivatives with respect to $\underline{\lambda}$).

4) Solve the linearized system of equations, i.e., calculate the displacement vectors $\Delta\underline{x}_n^{[m]}$ and $\Delta\underline{\lambda}^{[m]}$ from

$$\underline{\underline{J}}^{[m]}\cdot\begin{bmatrix} \Delta\underline{x}^{[m]} \\ \underline{\lambda}^{[m]} \end{bmatrix} = -\begin{bmatrix} \underline{R}_F \\ \underline{R}_H \end{bmatrix} \qquad (6.180)$$

5) Calculate the new values: $\underline{x}_n^{[m+1]} = \underline{x}_n^{[m]} + \Delta\underline{x}_n^{[m]}$ and $\underline{\lambda}^{[m+1]} = \underline{\lambda}^{[m]} + \Delta\underline{\lambda}^{[m]}$.

6) Put m=m+1 and goto 1).

Superscript [m] denotes the *m*th iteration step.

Vectors $\underline{R}_F$ and $\Delta\underline{x}$ are defined as

$$\underline{R}_F^{[m]} = \begin{bmatrix} \underline{r}_{F,0}^{[m]} \\ \underline{r}_{F,1}^{[m]} \\ \cdot \\ \cdot \\ \cdot \\ \underline{r}_{F,N-1}^{[m]} \end{bmatrix}, \qquad \Delta\underline{x}^{[m]} = \begin{bmatrix} \Delta\underline{x}_0^{[m]} \\ \Delta\underline{x}_1^{[m]} \\ \cdot \\ \cdot \\ \cdot \\ \Delta\underline{x}_{N-1}^{[m]} \end{bmatrix} \tag{6.181}$$

Initial guess

It is important to notice that the Finite Difference method requires an initial guess for all variables at all times. The easiest way to cope with this problem for the SFVSM is to perform an isothermal Schmidt analysis (see Appendix B) to obtain an exact analytical solution to the isothermal problem and use this solution as an initial guess $\underline{x}^{[0]}$ for the SFVSM-problem.

Another possibility is to use an IVP method in order to integrate one cycle forward in time (the IVP method could be of low order, since accuracy is not important for obtaining the initial guess). This only requires a guess for the initial state at t=0 to obtain the values of the variables at the other time levels and the approach will probably be advantageous for more complex problems, where there is no access to a simplified analytical solution to a related problem.

Remarks:

i) The additional equations for the cyclic conditions destroy the banded structure of the Jacobian, since it implies that n_λ=5 rows will be full (have non-zero entries for all time levels).

ii) The Jacobian will still be sparse, since

$$\max\ \%\ non-zero\ elements = \frac{\zeta\cdot(2\cdot k+1)\cdot N\cdot n_{eq}^2 + 2\cdot N\cdot n_{eq}\cdot n_\lambda - n_\lambda^2}{(N\cdot n_{eq}+n_\lambda)^2}\cdot 100\ \% \tag{6.182}$$

where ζ denotes the approximate percentage of non-zero elements in the $\underline{\underline{A}}_{n,j}$ matrices and in the last 5 rows and columns.

For n_{eq}=18 equations in each time step, N=80 time steps (total of 18·80+5=1485 equations), n_λ=5 cyclic integral conditions, $\zeta\approx$0.25 and a method with step number k=2, the non-zero's are less than 2%.

6.9 Other acceleration techniques

6.9.1 Introductory remarks

The Shooting method accelerates the convergence towards cyclic conditions compared to the standard Integration-to-Convergence approach. Other techniques, that use the same kind of idea, include optimization methods and extrapolation methods.

In the next section, only the basic theory for the optimization method will be given just to illustrate an alternative idea.

6.9.2 Optimization

Using an optimization algorithm to find the periodic solution originates from a paper of Nakhla and Branin [11] and an outline of the basic idea will be given below.

It will be convenient to reformulate the problem for the optimization method.

First only a system of ODEs in the form

$$\underline{y}' = \underline{f}(t,\underline{y}) \qquad \underline{y}(0) = \underline{y}_0 \tag{6.183}$$

with periodic boundary conditions

$$\underline{y}(0) - \underline{y}(t_p) = 0$$

will be considered.

Define a function $\underline{F}(\underline{y}_0)$ which is given as

$$\underline{F}(\underline{y}_0) = \underline{y}_0 + \int_{t=0}^{t_p} \underline{f}(t,\underline{y}) \cdot dt \tag{6.185}$$

Clearly this function satisfies

$$\underline{F}(\underline{y}_0) = \underline{y}(t_p;\underline{y}_0) \tag{6.186}$$

Define a new function $\underline{G}(\underline{y}_0)$ as

$$\underline{G}(\underline{y}_0) = \underline{F}(\underline{y}_0) - \underline{y}_0 \tag{6.187}$$

then the problem of determining the stationary cyclic conditions can be expressed as solving the system of implicitly given and non-linear equations:

$$\underline{G}(\underline{y}_0) = \underline{0} \tag{6.188}$$

Define another (scalar) objective function $P(\underline{y}_0)$ as

$$P(\underline{y}_0) = \underline{G}(\underline{y}_0)^T \cdot \underline{G}(\underline{y}_0) \tag{6.189}$$

Hence finding the minimum (the value of $\underline{y}_0$ for which $P(\underline{y}_0)=0$) of this scalar function is equivalent to determining the stationary cyclic conditions.

The optimization problem is non-linear and in some sense constrained (the values of pressure, mass and temperatures should be positive) but is reasonable to assume that the constraints are insignificant close to the minimum and it will be possible to use optimization method for the unconstrained problem providing that the initial guess is sufficiently close to the minimum.

A variety of methods are available for solving general unconstrained optimization problems. Optimization methods are usually classified in terms of order, where zero order methods use only function evaluations, first order methods use function and gradient evaluations, while second order method (Newton's method) uses the Hessian as well.

Function evaluations can be very expensive for the actual problem since it requires numerical time integration of a full cycle. On the other hand, no expressions for the gradient or Hessian are directly available, but as it will be shown next, it is possible to derive an expression for the gradient that is not too expensive.

Proceeding with the procedure outlined in [11]:

The gradient of $P(\underline{y}_0)$, denoted $P'(\underline{y}_0)$, is

$$P'(\underline{y}_0) = 2 \cdot \left(\underline{F}'(\underline{y}_0) - \underline{\underline{I}}\right)^T \cdot \left(\underline{F}(\underline{y}_0) - \underline{y}_0\right) \tag{6.190}$$

The problem is to find a computationally cheap way to compute $\underline{F}'(\underline{y}_0)$

$$\underline{F}'(\underline{y}_0) = \frac{\partial \underline{y}(t_p;\underline{y}_0)}{\partial \underline{y}_0} \tag{6.191}$$

The variational equation for the system of ODEs is given by

$$\underline{\underline{Y}}' = \underline{\underline{A}} \cdot \underline{\underline{Y}} \quad , \quad \underline{\underline{A}} = \frac{\partial \underline{f}}{\partial \underline{y}} \quad , \quad \underline{\underline{Y}} = \frac{\partial \underline{y}(t;\underline{y}_0)}{\partial \underline{y}_0} \tag{6.192}$$

Formally, this equation can be obtained by differentiating the system with respect to $\underline{y}_0$.

The adjoint variational system is given by

$$\underline{x}' = -\underline{\underline{A}}^T \cdot \underline{x} \tag{6.193}$$

Vector $\underline{x}$ satisfies the following equation

$$\left(\underline{\underline{Y}}^T \cdot \underline{x}\right)' = \underline{\underline{Y}}'^T \cdot \underline{x} + \underline{\underline{Y}}^T \cdot \underline{x}' = \left(\underline{\underline{A}} \cdot \underline{\underline{Y}}\right)^T \cdot \underline{x} - \underline{\underline{Y}}^T \cdot \underline{\underline{A}}^T \cdot \underline{x} = 0 \tag{6.194}$$

which means that $\underline{\underline{Y}}^T \cdot \underline{x}$ is constant for all values of t and therefore

$$\underline{\underline{Y}}^T(t) \cdot \underline{x}(t) = \underline{\underline{Y}}^T(0) \cdot \underline{x}(0) = \underline{\underline{Y}}^T(t_p) \cdot \underline{x}(t_p) \tag{6.195}$$

Inserting $\underline{\underline{Y}}(0)=\underline{\underline{I}}$ gives the following relation

$$\underline{x}(0) = \underline{\underline{Y}}^T(t_p) \cdot \underline{x}(t_p) \tag{6.196}$$

Setting $\underline{x}(t_p) = \underline{F}(\underline{y}_0) - \underline{y}_0$ as the "initial values" and integrating the adjoint variational system backwards in time from $t=t_p$ to $t=0$ to obtain $\underline{x}(0)$.

Now the gradient $P'(\underline{y}_0)$ can be written as

$$P'(\underline{y}_0) = 2 \cdot \left(\underline{x}(0) - \underline{x}(t_p)\right) \tag{6.197}$$

Remarks:

i) Any 1.order optimization method may be applied to solve the minimization problem. Input to the code will be the function evaluation $P(\underline{y}_0)$ and the gradient vector $P'(\underline{y}_0)$.

ii) The approach outlined above may be extended to include systems of semi-explicit DAEs in a similar way (see [11]).

6.9.3 Discussion

There is no documentation, which of the alternative acceleration methods that performs best. Skelboe has discussed these methods in a series of papers (see [12] for references), but since none of the methods seem to have outstanding properties for the SFVSM, an actual implementation into computer codes has not been considered for the approaches based optimization methods and on extrapolation methods.

6.10 Discontinuities

6.10.1 Introductory remarks

Initial value problems (IVPs) or boundary value problems (BVPs), in form of ordinary differential equations (ODEs) or differential-algebraic equations (DAEs), where the right-hand side of the system of equations is discontinuous, can be found in many fields of applied science. The problem of how to obtain a robust, sufficiently accurate and fast numerical solution of such a problem is addressed in this section.

The system of differential-algebraic equations derived for the SFVSM-problem previously in this chapter has the following general structure for the basic formulation:

$$\begin{aligned} \underline{y}'(t) &= \underline{f}(t,\underline{y},\underline{z}) \\ 0 &= \underline{g}(t,\underline{y},\underline{z}) \end{aligned} \tag{6.198}$$

and for the alternative formulation:

$$\begin{aligned} \underline{\underline{A}}\cdot\underline{y}'(t) &= \underline{f}(t,\underline{y},\underline{z}) \\ 0 &= \underline{g}(t,\underline{y},\underline{z}) \end{aligned} \tag{6.199}$$

The special structure of the latter, which makes it possible to use an explicit Runge-Kutta method, has been discussed in detail in section 6.3 and section 6.6.2.

For both formulations, the right-hand side given as $\underline{f}$ has partial derivatives which are discontinuous with respect to some of the algebraic variables (specifically the mass flows), i.e.,

$$\frac{\partial \underline{f}}{\partial \underline{z}} \notin C^0 \tag{6.200}$$

This can have significant influence on the behaviour of the numerical solution as it will be discussed in this section. The well-known results from numerical analysis such as convergence of the numerical method, behaviour of the local truncation error or convergence of Newton's method for systems of nonlinear equations, apply only for sufficiently smooth functions.

Therefore, a study of different ways to cope with this additional complication has been carried out.

The section is divided into three principal parts. First a few important theoretical results concerning existence of solutions, uniqueness, continuation of solutions etc. are stated for ODEs with discontinuities. These results are necessary for the basic understanding of the problem and will at the same time be a convenient way of introducing several new concepts. There are no proofs, but relevant references will be given. Additional difficulties are encountered when the analysis is extended to include systems of DAEs.

The second part of the analysis is devoted to the pure numerical aspects. Obtaining a numerical solution, when discontinuities are present in the right-hand side function, involves further difficulties. The accuracy and stability of the numerical method can be directly affected.

Only Runge-Kutta methods are considered in detail, since these methods have been used in the simulation programs for the SFVSM-problem. There are several different possibilities for dealing with discontinuities and the implementation into program code for some of these strategies are discussed.

Finally, the consequences for the SFVSM-problem are considered for the different approaches (mainly for the Integration-to-Convergence method and the Shooting method). The actual implementation for explicit Runge-Kutta methods (using the alternative formulation) and semi-implicit methods Runge-Kutta methods (using the basic formulation) are discussed.

6.10.2 ODEs with discontinuities - mathematical background

Consider the initial value problem

$$\underline{y}' = \underline{f}(t,\underline{y}) \qquad \underline{y}(0) = \underline{y}_0 \qquad t \in [0;\infty[\tag{6.201}$$

where $\underline{y} \in \mathbb{R}^n$, $\underline{f}$: $\mathbb{R} \times \mathbb{R}^n \rightarrow \mathbb{R}^n$ and

$$\underline{f}(t,\underline{y}) = \begin{cases} \underline{f}^+(t,\underline{y}) & \varphi(t,\underline{y}) \geq 0 \\ \underline{f}^-(t,\underline{y}) & \varphi(t,\underline{y}) < 0 \end{cases} \tag{6.202}$$

Assume that $\underline{f}^{(r)}(t,\underline{y})$ is discontinuous (i.e., $\underline{f}$ has a discontinuity of order r) at a point $t=t^*$ in the interval $]0;\infty[$, where the continuous *switching function* φ has a zero, i.e.,

$$\varphi(t^*,\underline{y}(t^*)) = 0 \tag{6.203}$$

and

$$\underline{f}^{+(r)}(t^*,\underline{y}(t^*)) \neq \underline{f}^{-(r)}(t^*,\underline{y}(t^*)) \tag{6.204}$$

. This is illustrated for the scalar case and r=0 in the following figure, where the solution y(t) also is shown:

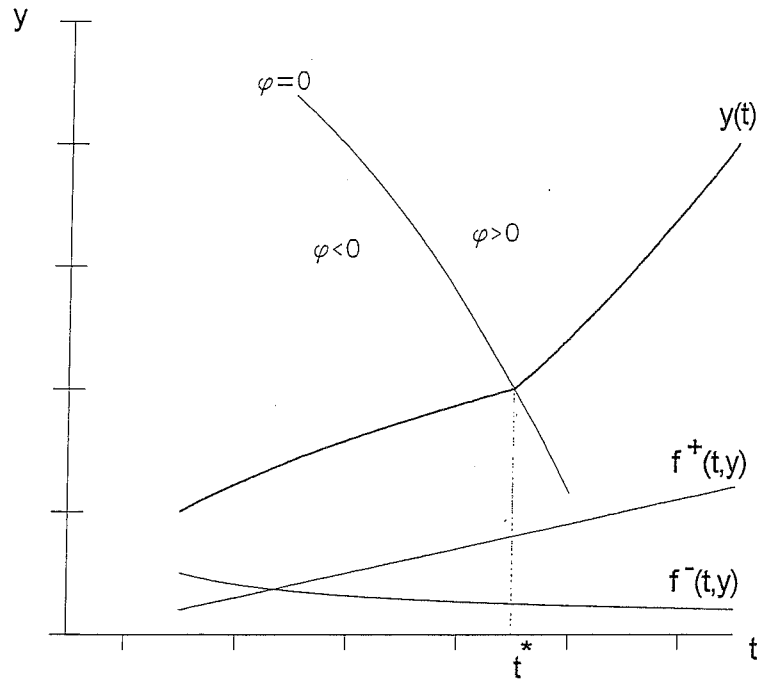

Figure 6.1 Discontinuous right-hand side function.

Assuming that $\underline{f}^+$and $\underline{f}^-$ are continuous and satisfy the usual Lipschitz condition with respect to $\underline{y}$, then only one additional and fairly mild requirement is needed to show existence and uniqueness of the system given by (6.201) and (6.202). This so-called transversality condition (see reference [13]) is required to ensure, that the solution $\underline{y}(t)$ actually crosses the discontinuity and not moves along the curve given by the switching function or ends at the switching point.

In the following, it will be assumed that the solution $\underline{y}(t)$ crosses the discontinuity at an isolated point (i.e., the switching function $\varphi(t,\underline{y}(t))$ changes sign at t^*).

A solution $\underline{y}(t;\underline{y}_0)$ will be continuous and can be composed of two smooth solutions $\underline{y}^+$ and $\underline{y}^-$ that satisfy

$$\begin{aligned} \underline{y}^{+\prime} &= \underline{f}^+(t,\underline{y}) \\ \underline{y}^{-\prime} &= \underline{f}^-(t,\underline{y}) \end{aligned} \tag{6.205}$$

The solution to the defined problem is given as

$$\underline{y}(t) = \begin{cases} \underline{y}^+(t) & 0 \le t \le t^* \\ \underline{y}^-(t) & t < t^* \end{cases} \tag{6.206}$$

where the following conditions are satisfied

$$\underline{y}^{+}(0) = \underline{y}_0$$
$$\underline{y}^{-(j)}(t^*) = \underline{y}^{+(j)}(t^*) \qquad j = 0,1,2,...,r \tag{6.207}$$

Notice that the defined problem in this way can be considered as two separate initial value problems, which can be solved provided the point t^* is known or can be determined.

For more complex problems, where multiple states can be defined or when the switching function can depend on the history of the solution, better definitions for IVPs with discontinuities can be made. Here two alternatives will be mentioned:

Status vector

A status vector sw (switch) can be defined in the following way:

The elements sw_i of the vector sw are switches, whose values uniquely determine which right-hand side to be used in the system of equations. A switch sw_i can only change value (e.g., from -1 to +1) when the corresponding switching function φ_i is zero (changes sign).

A simple example of a status vector could be

$$\underline{sw} = \begin{Bmatrix} sw_1 \\ sw_2 \end{Bmatrix} \tag{6.208}$$

where

$$sw_i = \begin{cases} 1 & if \quad \varphi_i \geq 0 \\ -1 & if \quad \varphi_i < 0 \end{cases} \qquad i = 1,2 \tag{6.209}$$

The right-hand side function f is then given as

$$\underline{f}(t,\underline{y}) = \begin{Bmatrix} f_1(t,\underline{y}) \\ f_2(t,\underline{y}) \end{Bmatrix} \qquad f_1 = \begin{cases} f_1^+ & if \quad sw_1 = 1 \\ f_1^- & if \quad sw_1 = -1 \end{cases} \qquad f_2 = \begin{cases} f_2^+ & if \quad sw_2 = 1 \\ f_2^- & if \quad sw_2 = -1 \end{cases} \tag{6.210}$$

such that it depends on the actual value of sw.

States

One of the most elegant ways of dealing with discontinuities is to define different *states* for which a specific system of equations is valid and then identify the conditions for changing to a new state. This can often be an advantage because it is possible to specify the allowed changes directly.

As a simple example, consider a system with only three different states ("1", "2" and "3") as shown in the figure just below

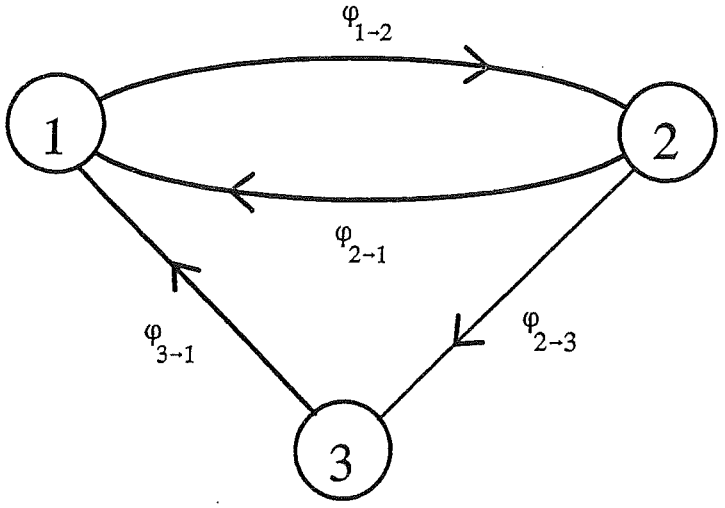

Figure 6.2 States.

A change from state "1" to state "2" is determined by the switching function $\varphi_{1\to 2}$, a change from "2" to "1" by $\varphi_{2\to 1}$ and etc.

Notice that it is not necessary to check all the switching functions since for a given state only certain changes are allowed, e.g., in the example above, it is only necessary to check if $\varphi_{1\to 2}$ is zero (changes sign) when being in state "1".

It is also easy to prevent that a change that is not allowed occurs simply by not specifying a switching function between the states involved. In the example above, only a change to state "1" is allowed when being in state "3". Drawing a path with an arrow from "3" to "1" (and specifying the switching function $\varphi_{3\to 1}$) and no arrow from "3" to "1" automatically takes care of this.

The formulation is also very flexible. The solution always "knows" which state it is in andwhich state it is changing to for a given switching function. In that way, it includes automatically the "history" of the solution.

6.10.3 ODEs with discontinuities - numerical problems

Allowing discontinuities in the right-hand function $\underline{f}(t,\underline{y})$ of the ODEs introduce additional difficulties for the numerical methods. This is a fact regardless of the type of method employed (Linear Multistep method, One step method or Extrapolation method). Crossing a discontinuity of order r in $\underline{f}$ with a step length Δt will, in general, introduce a local error $O(\Delta t^r)$ in the numerical solution.

First consider an ordinary IVP with a smooth right-hand side function.

A general one-step method can be written in the form

$$\underline{y}_{n+1} = \underline{y}_n + \Delta t \cdot \underline{\Phi}(t,\underline{y},\Delta t) \tag{6.211}$$

The local truncation error T_{n+1} can be defined as

$$\underline{T}_{n+1} = \underline{y}(t_{n+1}) - \underline{y}(t_n) - \Delta t \cdot \underline{\Phi}(t_n,\underline{y}(t_n),\Delta t) \tag{6.212}$$

If $T_{n+1} = |\underline{T}_{n+1}| = O(\Delta t^{p+1})$ then the numerical method is said to have order p. For problems without any discontinuities, p is usually equal to the order of the global truncation error, i.e., $E_{n+1} = O(\Delta t^p)$.

A general s-stage Runge-Kutta method can be written in the form

$$\underline{y}_{n+1} = \underline{y}_n + \Delta t \cdot \sum_{i=1}^{s} b_i \cdot \underline{Y}_i' \tag{6.213}$$

where the stage derivatives $\underline{Y}_i'$ are defined as

$$\underline{Y}_i' = \underline{f}(t_n + c_i \cdot \Delta t, \underline{Y}_i) \qquad i = 1,2,\ldots,s \tag{6.214}$$

and stage values

$$\underline{Y}_i = \underline{y}_n + \Delta t \cdot \sum_{j=1}^{s} a_{ij} \cdot \underline{Y}_j' \qquad i = 1,2,\ldots,s \tag{6.215}$$

Now, the problem will be illustrated through a simple example (this is not a proof!). For the sake of simplicity, the only scalar case is considered. The generalization to systems implies the use of Butcher theory (Frechet derivatives, rooted trees etc.).

The smooth solution can be expanded in a Taylor series around t_n

$$y(t_{n+1}) = y(t_n) + \Delta t \cdot y'(t_n) + \frac{1}{2} \cdot \Delta t^2 \cdot y''(t_n) + O(\Delta t^3) \tag{6.216}$$

Since

$$y' = f \qquad and \qquad y'' = \frac{\partial f}{\partial t} + \frac{\partial f}{\partial y}\cdot f = f_t + f_y \cdot f \tag{6.217}$$

the expression can be written as

$$y(t_{n+1}) = y(t_n) + \Delta t \cdot f + \frac{1}{2}\cdot \Delta t^2 \cdot (f_t + f_y \cdot f) + O(\Delta t^3) \tag{6.218}$$

where the function and the derivatives have been evaluated at $(t_n, y(t_n))$, i.e., $f=f(t_n, y(t_n))$ and etc.

The stage derivatives for the Runge-Kutta method may be expressed in terms of f and the derivatives of f.

Consider a general two-stage explicit Runge-Kutta method, then

$$\begin{aligned} Y_1' &= f(t_n, y_n) \\ Y_2' &= f(t_n + c_2 \cdot \Delta t,\ y_n + \Delta t \cdot a_{21} \cdot Y_1') \end{aligned} \tag{6.219}$$

Expanding Y_2' around (t_n, y_n) and using the (row-sum) condition $a_{21} = c_2$

$$Y_2' = f + \Delta t \cdot a_{12} \cdot (f_t + Y_1' \cdot f_y) + O(\Delta t^2) \tag{6.220}$$

Inserting this in (6.213) gives

$$y_{n+1} = y_n + b_1 \cdot \Delta t \cdot f + b_2 \cdot \Delta t \cdot \left(f + \Delta t \cdot c_2 \cdot (f_t + f \cdot f_y)\right) + O(\Delta t^3) \tag{6.221}$$

and the general two-stage method then satisfies

$$y_{n+1} = y_n + \Delta t \cdot (b_1 + b_2) \cdot f + \Delta t^2 \cdot b_2 \cdot c_2 \cdot (f_t + f \cdot f_y) + O(\Delta t^3) \tag{6.222}$$

The idea is to choose the coefficients of the method, such that the terms in the expression above cancel out terms in the Taylor expansion (compare with the expression for the local truncation and the definition of order on the previous page). For a two-stage method of order p=2, this means that the following conditions must be satisfied

$$\begin{aligned} b_1 + b_2 &= 1 \\ b_2 \cdot c_2 &= \frac{1}{2} \end{aligned} \tag{6.223}$$

since then $T_{n+1}=O(\Delta t^3)$ under the assumption $y_n=y(t_n)$.

Now, consider a scalar IVP with a right-hand side f, which is discontinuous of some order r and given in the form (6.201) and (6.202). This is shown for the scalar case and r=0 in the following figure:

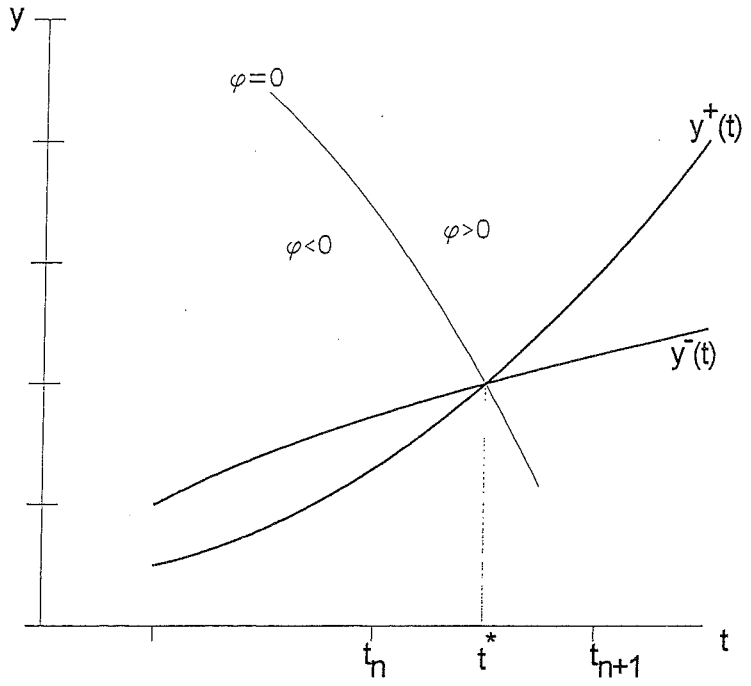

Figure 6.3 Discontinuous right-hand side of order r=0.

A step is taken from t_n to t_{n+1} with a step length Δt and the discontinuity is located at t^*, where $t_n \le t^* \le t_{n+1}$ and θ is defined as

$$\theta = \frac{t^* - t_n}{\Delta t} = \frac{t^* - t_n}{t_{n+1} - t_n} \tag{6.224}$$

Expanding as a Taylor series around $t=t^*$

$$\begin{aligned} \underline{y}(t_n) &= \underline{y}^-(t^*) - \Delta t\cdot\theta\cdot\underline{y}^{-\prime}(t^*) + \frac{1}{2}\cdot\Delta t^2\cdot\theta^2\underline{y}^{-\prime\prime}(t^*) + \ldots \\ \underline{y}(t_{n+1}) &= \underline{y}^+(t^*) + \Delta t\cdot(1-\theta)\cdot\underline{y}^{+\prime}(t^*) + \frac{1}{2}\cdot\Delta t^2\cdot(1-\theta)^2\underline{y}^{+\prime\prime}(t^*) + \ldots \end{aligned} \tag{6.225}$$

Subtraction gives

$$\begin{aligned} y(t_{n+1}) - y(t_n) = {} & \Delta t\cdot\left((1-\theta)\cdot y^{+\prime}(t^*) + \theta\cdot y^{-\prime}(t^*)\right) + \ldots + \\ & \frac{\Delta t^{r+1}}{(r+1)!}\left((1-\theta)^{r+1}\cdot y^{+(r+1)}(t^*) - (-1)^{(r+1)}\cdot\theta^{r+1}\cdot y^{-(r+1)}(t^*)\right) + O(\Delta t^{r+2}) \end{aligned} \tag{6.226}$$

where terms up to order Δt^{r+1} are written out explicitly.

Consider the case where f has discontinuous partial derivatives (i.e., r=1), then $y'^{+} = y'^{-} = y'$ but $y''^{+} \neq y''^{-}$, so

$$y(t_{n+1}) - y(t_n) = \Delta t \cdot y' + \frac{\Delta t^2}{2} \cdot \left((1-\theta)^2 \cdot y^{+\prime\prime}(t^*) - \theta^2 \cdot y^{-\prime\prime}(t^*) \right) + O(\Delta t^3) \qquad (6.227)$$

or

$$y(t_{n+1}) = y(t_n) + \Delta t \cdot f + \frac{\Delta t^2}{2} \cdot \left((1-\theta)^2 \cdot (f_t^+ + f_y^+ \cdot f) - \theta^2 \cdot (f_t^- + f_y^- \cdot f) \right) + O(\Delta t^3) \qquad (6.228)$$

where the evaluations of f and the derivatives are taken at t^*, i.e., $f=f(t^*,y(t^*))$ and etc.

Consider the two-stage method of order two, now expanded around t^* (and not t_n!)

$$y_{n+1} = y_n + \Delta t \cdot (b_1 + b_2) \cdot f + \Delta t^2 \cdot \theta \cdot (b_1 + b_2) \cdot (f_t^- + f \cdot f_y^-) + \Delta t^2 \cdot b_2 \cdot c_2 \cdot (f_t^+ + f \cdot f_y^+) + O(\Delta t^3) \qquad (6.229)$$

The second order term cannot cancel out in the two expressions above for any choice of b_1, b_2 and c_2. This means that $T_{n+1} = O(\Delta t^2)$, i.e, the method will locally be of order one (p=1), which is the same as the order of the discontinuity.

This can be generalized to a s-stage method of order p and a discontinuity in f of order r and further to non-scalar problems.

If $r \geq p$ then the method will not "feel" the discontinuity, and the numerical solution is still of order p.

If $r < p$ then it is not possible to cancel out terms higher than order r, and the solution will be of order r.

All commonly used methods for solving IVPs exhibit this behavior. See [14] for the proof for a general Linear Multistep Method. Runge-Kutta methods have some advantages toward the other numerical methods, when it comes to dealing with discontinuities. The ability of changing step length without any trouble and restarting with high order will be a very convenient feature.

In the following, Runge-Kutta methods will be considered only, since these are used in the simulations programs.

Several different approaches have been proposed in the literature for dealing with discontinuities. In this section, the following will be discussed:

- Primitive approach.
- Standard approach.
- Special Driver approach.

Primitive approach Fixed step length

Using a fixed step length algorithm (no estimate of the local truncation error and without locating the discontinuity) the error introduced will at least be of order r if $\underline{f}^{(r)}$ is discontinuous as just shown. E.g., if $\underline{f}'$ is discontinuous (r=1) then using a fourth order method (p=4) with a fixed step length implies that a local error $O(\Delta t^2)$ will be introduced in the numerical solution with consequences for the overall accuracy of the solution (after the crossing of discontinuity) and for the stability of the method. In the limit $\Delta t \rightarrow 0$, the effect of the discontinuity will usually become small.

Clearly, this strategy is not recommended as a general approach. It is mentioned here only to discuss the consequences, when the presence of a discontinuity in the right-hand side function is completely ignored.

Standard approach Local error control

Most standard codes use some kind of control of the step length based on an estimate of the local truncation error. Crossing a discontinuity will almost always give a significant local error and a good estimate for the local truncation error will detect this and will reject the step until the estimate of the error is sufficiently small.

A tolerance TOL is normally specified and a step is accepted if and only if

$$EST \leq TOL \tag{6.230}$$

The estimate EST is calculated as

$$EST = \|\underline{e}_{n+1}\| \tag{6.231}$$

where $\|\cdot\|$ is some norm and $\underline{e}_{n+1}$ is the vector. which components are the error estimates for the numerical solution $\underline{y}_{n+1}$ at time level t_{n+1}.

The new proposed optimal step length for a method of order p is then given as

$$\Delta t_{new} = \Delta t_{old} \cdot \sqrt[p+1]{\frac{TOL}{EST}} \tag{6.232}$$

Without any restriction on the rate of change in the size of the step length, this approach will most likely not work properly.

Crossing a discontinuity usually leads to large local error and therefore gives a significant reduction in step length. A small step will then be attempted and if the discontinuity is located toward the end of the originally proposed step, the local error will be very small (no discontinuity is felt). This means that the new step is accepted and new large step will be proposed and so on. The final result is that the step length oscillates between a large and a small step close to the discontinuity (see [14] for a more complete discussion).

It is possible to deal with this problem by introducing some restriction on the rate of change of step length, e.g., in the form

$$\Delta t_{new} = \alpha \cdot \Delta t_{old} \tag{6.233}$$

where

$$\tilde{\alpha} = \sqrt[p+1]{\frac{TOL}{EST}} \qquad \alpha = \begin{cases} \tilde{\alpha}_{max} & \tilde{\alpha} > \tilde{\alpha}_{max} \\ \tilde{\alpha} & \tilde{\alpha}_{min} \le \tilde{\alpha} \le \tilde{\alpha}_{max} \\ \tilde{\alpha}_{min} & \tilde{\alpha} < \tilde{\alpha}_{min} \end{cases} \tag{6.234}$$

A typical choice could be $\tilde{\alpha}_{max} = 2$ and $\tilde{\alpha}_{min} = ½$.

With this kind of strategy, the method will cross the discontinuity in a limited number of steps. A proposed step Δt_{new} will be of a reasonable size away from the discontinuity and small only close to the discontinuity.

Remarks:

i) If the estimate of the local truncation error is reliable this approach will be acceptable but not very efficient in most cases.

ii) If the c_i's of the Runge-Kutta method all are less than 1 (no stage values are calculated at t_{n+1} when taking a step from t_n to t_{n+1}) it is not possible to detect a discontinuity located in the interval $[t_n + \max(c_i)\cdot\Delta t \; ; \; t_{n+1}[$ using the approach described above, since the error estimate is then based on values all located before the discontinuity.

Special Driver approach (Polynomial interpolants)

Enright, Jackson, Nørsett and Thomsen [15] have considered a more sophisticated approach, where a polynomial interpolant for the Runge-Kutta method is used to determine the zero of the switching function. The interpolants give a continuous solution between the calculated discrete values obtained from the numerical method. The interpolants can approximate the local solution with any order of accuracy, but some additional function evaluation will be required in most cases.

The right-hand side of the ODE is written as

$$\underline{f}(t,\underline{y}) = \begin{cases} \underline{f}^{-}(t,\underline{y}) & sw = -1 \\ \underline{f}^{+}(t,\underline{y}) & sw = 1 \end{cases} \tag{6.235}$$

and the status switch sw changes value according to the zero of the switching function, i.e., only when

$$\varphi(t,\underline{y}) = 0 \tag{6.236}$$

The key idea is to take a full step across the discontinuity (using only one value of the status switch $sw=sw_n$) and check the status switch after the step is taken. If the switch has changed value ($sw_n \neq sw_{n+1}$), it means that a discontinuity is located between the last two calculated points.

An interpolatory polynomial $\hat{y}(t)$ ($\hat{y}$ is a vector with elements that are polynomials in t) is then formed, based on values of the function and the derivatives in these two points ($\underline{y}_n$, $\underline{f}_n$), and ($\underline{y}_{n+1}$ $\underline{f}_{n+1}$), stage values $\underline{Y}_j$, stage derivatives $\underline{Y}_j'$ and additional points if necessary. Bisection (for the interpolant) is used for determining the location t^* of the discontinuity (the zero of the switching function) and the step from t_n to t^* is taken using the interpolant.

The approach can be summarized in the following implementation strategy:

1) Integration step from t_n to $t_n+\Delta t$ is performed using the current value of the status vector (e.g., sw=-1)

2) If the status vector has not changed during the step (i.e., sw=-1 at $t=t_n+\Delta t$) then check the estimate for the local truncation error. If OK then calculate the new step length and goto step 6). If not OK then reduce the step length and goto step 1)

3) The status vector has changed (i.e., sw=1) and the polynomial interpolant $\hat{y}_n$ is formed based on the internal stage values and additional function evaluations (if needed). The polynomial is used to determine t^* such that $\varphi(t^*, \hat{y}_n(t^*))=0$. The discontinuity point t^* has to be determined numerically within an accuracy consistent with the order and accuracy of the integration method.

4) The new value is of $\underline{y}_{n+1}$ at $t_{n+1}= t^*$ is found using the interpolating polynomial, i.e., $\underline{y}_{n+1}= \hat{y}_n(t^*)$.

5) The status vector is reset (i.e., sw=1) and the step length is reset to Δt.

6) n=n+1 and continue with step 1).

Remarks:

i) In [15] bisection has been used, but more efficient numerical methods for solving nonlinear equations, such as Newton's method, can be applied for solving $\varphi(t^*,\hat{y}_n(t^*))=0$.

ii) If the zero of the switching function is determined accurately enough then the numerical method will be of order p everywhere. This approach is equivalent of solving two IVPs. One starting at t=0 and the other one starting at $t=t^*$. The error, introduced because of the inaccuracy in the determination of the zero of the switching function, can be identified as an error in the initial value.

iii) Detecting the discontinuity (especially higher order $r\geq 1$) or with relaxed tolerance can be numerically difficult.

iv) Differentiation of the polynomial interpolant $\hat{y}$ is straightforward so the derivative of the interpolant $\hat{y}'$ is available. If φ is a simple function of y, this can be used for an effective determination of t^*.

Construction of interpolants

Interpolants for the differential variables can be constructed following the approach outlined in [16]. The polynomial interpolants can for scalar problems (the generalization is straightforward) be written in the form

$$\hat{y}(t) = y_n + \sum_{j=1}^{R} d_j(\theta)\cdot f(t_j,y_j) \tag{6.237}$$

where θ is defined as

$$\theta = \frac{t - t_n}{t_{n+1} - t_n} \tag{6.238}$$

A simple example is given for the fourth order, "classic" Runge-Kutta method just to illustrate the form.

$$\begin{aligned} d_1(\theta) &= \frac{\theta}{3}\cdot(2\cdot\theta^2 - 3\cdot\theta + 2) \\ d_2(\theta) &= \frac{\theta^2}{3}\cdot(-2\cdot\theta + 3) \\ d_3(\theta) &= \frac{\theta^2}{3}\cdot(-2\cdot\theta + 3) \\ d_4(\theta) &= \frac{\theta^2}{6}\cdot(4\cdot\theta - 3) \end{aligned} \tag{6.239}$$

No additional function evaluations are needed (R=s=4). This polynomial interpolates the numerical solution in the interval $[t_n;t_{n+1}]$ to order three. A fourth order interpolant requires additional points.

6.10.4 DAEs with discontinuities

The corresponding initial value problem for a semi-explicit system of differential-algebraic equations can be written as

$$\begin{aligned} \underline{y}' &= \underline{f}(t,\underline{y},\underline{z}) \\ \underline{0} &= \underline{g}(t,\underline{y},\underline{z}) \end{aligned} \tag{6.240}$$

where $\underline{y} \in \mathbb{R}^n$ and $\underline{z} \in \mathbb{R}^m$ are the vectors with the differential variables and the algebraic variables respectively.

A switching function can now be defined as

$$\varphi(t,\underline{y},\underline{y}',\underline{z}) = 0 \tag{6.241}$$

For a general discussion of systems of DAEs, see reference [4]. It should be noticed that it can be difficult to obtain a numerical solution to systems of DAEs even without the presence of discontinuities as discussed previously in this chapter. Theoretical results are difficult to obtain and not much can be found in the literature.

Here, a few numerical strategies will be discussed only.

Primitive approach

In a primitive approach, where the presence of the discontinuity is ignored, there are no additional numerical complications in the implementation compared to a corresponding ODE. However, it is more difficult to solve a DAE and the consequences for the numerical properties, such as stability and accuracy, are not clear. It will depend on the actual problem.

Standard approach

The estimates of the local truncation error can only be applied to the dynamic variables. No error estimates are available for the algebraic variables.

How a discontinuity in the partial derivative with respect to some of the algebraic variables affects the error estimates for the differential variables is not clear. Among other things, it will depend on

- Order of the discontinuity.
- Index of the DAE.
- Order of the numerical method.
- Type of error estimates.
- Accuracy of the algebraic variables.

Again, it is not possible to make many general remarks.

Special Driver approach

Additional difficulties occur when the switching function also depends upon the algebraic variable. An interpolant is required for the determination of the zero of the switching function and there are no interpolants available for the algebraic variable in the same way as for the differential variables.

There are no values directly available for the stage derivatives for the algebraic variable (at least for all explicit methods) and these are needed for the construction of an interpolant of sufficiently high order.

Some different approaches to obtain an interpolant will be discussed next.

Interpolants using differentiation

For semi-explicit DAEs of index one, where $\frac{\partial g}{\partial z}$ is non singular the following idea can be used:
The derivative $\underline{z}'$ can be found explicitly after differentiation of the algebraic part of the system, i.e., all the stage derivatives necessary for the construction of the interpolant can be found.

Remarks:

i) Differentiation of the algebraic part could be difficult.

ii) Finding $\underline{z}'$ means solving a new system of equations which may be nonlinear.

iii) For semi-explicit DAEs of index two or higher this approach cannot be used since $\frac{\partial g}{\partial z}$ is singular and the system of equations cannot be solved for $\underline{z}'$.

iv) If i) is false, it will probably be easier to solve the new system, which is a system of ODEs only.

Interpolants using stage derivatives

Using a semi-implicit Runge-Kutta method makes it possible to obtain stage derivatives even for the algebraic variables. The system of semi-explicit DAEs can be written as

$$\begin{aligned} \underline{Y}_i' &= \underline{f}\left(t_n + c_i \cdot \Delta t,\ \underline{y}_n + \Delta t \cdot \sum_{j=1}^{s} a_{ij} \cdot \underline{Y}_i',\ \underline{z}_n + \Delta t \cdot \sum_{j=1}^{s} a_{ij} \cdot \underline{Z}_i'\right) \\ \underline{0} &= \underline{g}\left(t_n + c_i \cdot \Delta t,\ \underline{y}_n + \Delta t \cdot \sum_{j=1}^{s} a_{ij} \cdot \underline{Y}_i',\ \underline{z}_n + \Delta t \cdot \sum_{j=1}^{s} a_{ij} \cdot \underline{Z}_i'\right) \end{aligned} \qquad (6.242)$$

where $\underline{Y}_i'$ and $\underline{Z}_i'$ are the stage derivatives.

For a semi-implicit method $a_{ij}=0$ for j>i so the equations can be written as (see section 6.4.2)

$$\begin{aligned} \underline{\dot{Y}}_i &= \underline{f}\left(t_n + c_i \cdot \Delta t, \underline{Y}_i, \underline{Z}_i\right) \\ \underline{0} &= \underline{g}\left(t_n + c_i \cdot \Delta t, \underline{Y}_i, \underline{Z}_i\right) \end{aligned} \tag{6.243}$$

where

$$\begin{aligned} \underline{\dot{Y}}_i &= \frac{\underline{Y}_i - \underline{y}_n - \Delta t \cdot \sum_{j=1}^{i-1} a_{ij} \cdot \underline{\dot{Y}}_j}{\Delta t \cdot a_{ii}} \\ \underline{\dot{Z}}_i &= \frac{\underline{Z}_i - \underline{z}_n - \Delta t \cdot \sum_{j=1}^{i-1} a_{ij} \cdot \underline{\dot{Z}}_j}{\Delta t \cdot a_{ii}} \end{aligned} \tag{6.244}$$

This system can be solved for the stage variables in the following way

$$\begin{aligned} \underline{Y}_i - \underline{y}_n - \Delta t \cdot \sum_{j=1}^{i-1} a_{ij} \cdot \underline{\dot{Y}}_j - \Delta t \cdot a_{ii} \cdot \underline{f}\left(t_n + c_i \cdot \Delta t, \underline{Y}_i, \underline{Z}_i\right) &= \underline{0} \\ \underline{g}\left(t_n + c_i \cdot \Delta t, \underline{Y}_i, \underline{Z}_i\right) &= \underline{0} \end{aligned} \tag{6.245}$$

and the stage derivatives can be found from the expressions above.

The stage derivative $\underline{Z}_i'$, i=1,2,...s for the algebraic variable can then be used for the construction of an interpolant in the same way as outlined for the differential variable.

Remarks:

i) The order of accuracy for the algebraic variable can be different from the order of the differential variable. This implies that it can be difficult to determine the zero of the switching within an accuracy, which is consistent with the order of the numerical method.

ii) This approach could probably be used for DAEs of higher index as well.

Interpolants using algebraic manipulations

If the algebraic variables $\underline{z}$ can be expressed in terms of some of the differential variables $\underline{y}$ or/and the derivatives $\underline{y}'$, then it is simple to obtain interpolants for the algebraic variables.

The following strategy could be used:

Interpolants for the differential variables $\hat{y}$ are formed and the interpolants are differentiated if the derivatives of $\underline{y}$ are needed. The interpolants for the algebraic variables are then constructed as $\hat{z} = \hat{z}(\hat{y}, \hat{y}')$.

6.10.5 Discussion of the application for the SFVSM-problem

The equations for the SFVSM-problem are described in detail previously in this chapter and only the special problems due to the presence of the discontinuities will be addressed in detail here. The main emphasis will be laid on the implementation of IVP codes, which is relevant for the Integration-to-Convergence method and the Shooting method.

The problems for the implementation arise, when the numerical solution "crosses" the discontinuity.

- What strategy should be used?
- Which right-hand side function should be used in the time step taken?
- What are the consequences from using the "wrong" function in part of the interval?
- What are the effects concerning stability and accuracy?

It is the right-hand sides of the energy equations that have discontinuous partial derivatives with respect to the mass flows (i.e., some the algebraic variables). Two terms can be identified as sources:

- Upwind convective flux term.
- Convective heat transfer term.

Notice that the discontinuity occurs when the mass flow becomes zero in the energy equation, i.e., the significance of these terms is negligible at least for sufficiently small time steps in the numerical solution.

The switching functions sw_i can be identified as the mass flows such that $\varphi_i=m_{i+½}$ for i=1,2,...,4. The switches sw_i give the sign of the mass flow (i.e., sw_i= -1 for $\varphi_i<0$ and $sw_i=1$ for $\varphi_i\geq 0$).

IVP-integration using an explicit Runge-Kutta method

As discussed previously, explicit Runge-Kutta methods can be used only when the problem is given in form of the alternative formulation. This is due to the special struture of (6.199) (in particular the matrix $\underline{\underline{A}}$). For the alternative formulation of the system of equations, differential variables are pressure and mass ($\underline{y}$) and algebraic variables are mass flow and temperature ($\underline{z}$). Given the calculation procedure outlined in section 6.6.2, the following remarks can be made:

The value of $\underline{y}_n$ is given from the previous integration step. Solving the linear sub system of equations for the mass flows and the derivatives of the pressure, in the form (6.126), requires a guess for the sign of the mass flows (i.e., the switching functions φ_i) at each of the internal stages for the Runge-Kutta method. It is possible to check the assumed value of the status vector, when the linear sub system has been solved.

The status vector can be:

- checked at all stages (i.e., at k=1,2,...,s)

- checked at the first stage only (i.e., at k=1).

Check of the status vector sw at all stages.

If sw is checked at all stages (i.e., for k=1,2,...,s) then the following strategy could be used for a step taken from t_n to $t_n + \Delta t$:

k>1: If $sw_{assumed} = sw_{calculated}$ then accept the stage value else try to calculate the stage again using $sw_{calculated}$. If this fails again then reduce the step length (e.g., halving) and restart the method at k=1 ($t=t_n$).

k=1: If $sw_{assumed} = sw_{calculated}$ then accept the stage values else try to calculate the stage again using $sw_{calculated}$. If this fails again then reduce the step length (e.g., halving) and restart the method at the previous step ($t=t_{n-1}$ and k=1).

The strategy is illustrated in the following figure:

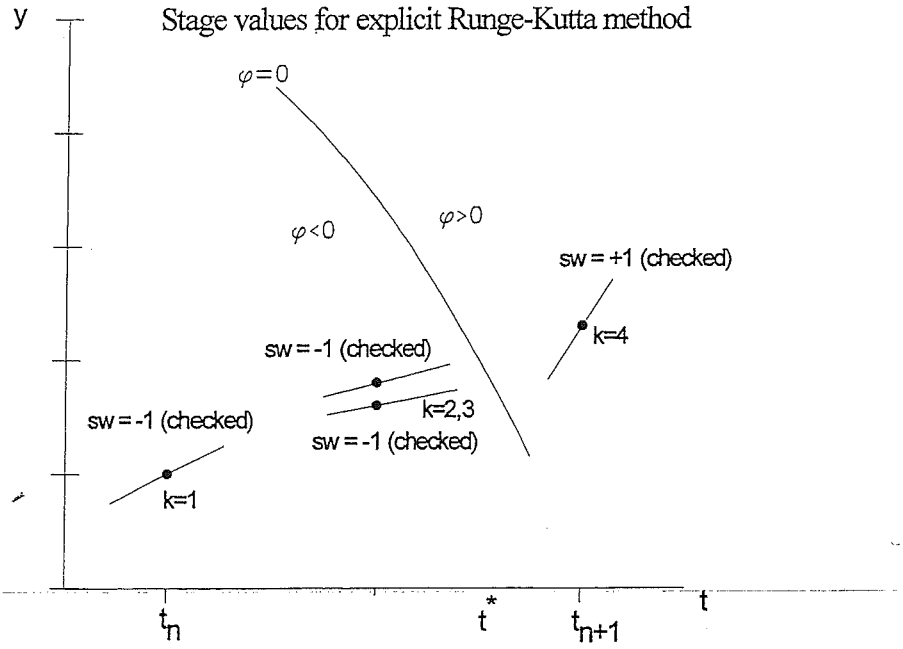

Figure 6.4 Check of switching function at all stages.

Remarks:

i) The method fails if there is no solution to the linear subsystem of equations. Therefore, the whole time step must be made shorter to cope with this additional problem. The problem has been observed for the numerical tests discussed in the next chapter (especially for large time steps).

ii) For a fixed step length implementation, the checking at all stages works very well as long as stability requirements are fulfilled.

iii) For a variable step length implementation, the estimate for the local truncation error will not be valid in a step, where a discontinuity is located because of the use of different functions. This implies that the strategy for finding a nearly optimal step length will be affected. Nevertheless, the approach works very well in practice.

iv) The interpolant cannot be constructed (values from two different solutions y^- and y^+) for the "Special Driver approach".

Check of the status vector sw only at k=1

If sw is checked only at the first stage then the following strategy could be used for a step taken from t_n to $t_n + \Delta t$:

> If $sw_{assumed} = sw_{calculated}$ then the rest of the stage variables Y_i and derivatives Y_i' (k=2,3,...,s) are determined using this value of sw at k=1, else try to calculate the stage at k=1 again using $sw_{calculated}$. If this fails again then reduce the step length (e.g., halving) and restart the method at the previous step ($t=t_{n-1}$ and k=1).

This means that some stages will be calculated using the "wrong" set of equations when a discontinuity is located between t_n and t_{n+1}. The strategy is illustrated in the following figure:

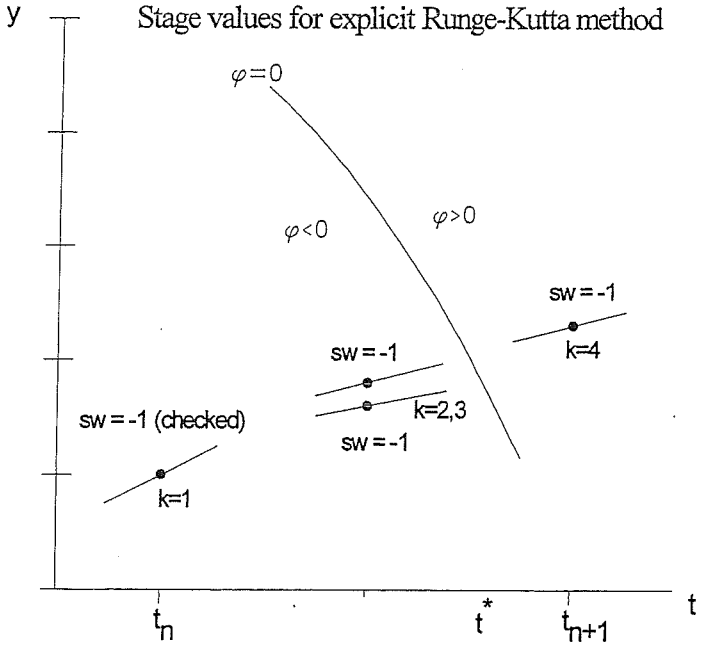

Figure 6.5 Check of switching function at the first stage only.

Remarks:

i) The new value of y_{n+1} is calculated and if $sw_{n+1} = sw_n$ in the next step, then the step from t_n to t_{n+1} is accepted. If $sw_{n+1} \neq sw_n$, it means that one of the switching functions has changed during the step taken.

ii) The more correct "Special Driver approach" can be used. For the actual problem it turns out that an interpolant $\hat{z}$ for the algebraic variables of interest (the mass flows) can be determined using $\hat{y}$ and $\hat{y}'$, since z can be expressed as a simple function of y'. The zero t^* for the switching function is determined using the interpolants for the algebraic variable and a step from t_{n-1} to t^* is taken using the interpolants $\hat{y}$ and $\hat{z}$.

iii) The preliminary numerical tests turned out to be quite negative. It has been difficult to find a cyclic solution and nonphysical values of some of the algebraic variables (mass flows) have been encountered even when using embedded error estimates for the differential variables. The tests have showed that instabilities occur after crossing the discontinuity, when using a wrong value of sw at an internal stage. This also destroys the implementation with the polynomial interpolants.

IVP-integration using a semi-implicit Runge-Kutta method

Implicit and semi-implicit Runge-Kutta methods can be used for both the basic and the alternative formulation.

All the internal stages, the system of nonlinear equations (for the stage values of the differential and algebraic variables) is solved using the correct value of the status switch. This is equivalent of checking k at all stages for the explicit method.

No severe numerical problems (in form of failing the iteration for the stage variables) have been encountered in the numerical tests. This indicates that the problems observed for the explicit methods could be concerned with the poorer stability properties of these methods. Convergence problems could be expected, if the number of volumes is increased in a more sophisticated model, since more than one switching function is likely to change in a time step.

Finite-Difference methods

The Finite-Difference method has only been implemented on a mesh using equally spaced points. The presence of discontinuities has been ignored in the approximation for the derivatives of the differential variables. This means that an error in the finite difference approximation of the derivatives has been made, whenever points on both sides of the discontinuity have been included.

A correct approach, where the discontinuity is located and only points on one side of the discontinuity are used, implies the following problems:

- The finite-difference approximation must be based on non-equally spaced points.
- It is necessary to find the location of the discontinuity using iteration.
- One-sided difference (from both sides) must be used for points close to a discontinuity.

Due to these additional complications other alternatives have not been considered for the Finite-Difference method.

6.10.6 Concluding remarks

The numerical tests showed that the problems regarding accuracy and stability are relatively insignificant for the different approaches, especially for the implicit Runge-Kutta methods and the Finite-Difference method. This fact has made it less interesting to developed computer program with special features to handle discontinuities in the right-hand side function.

References

[1] Gear, C.W.
Maintaining Solution Invariants in the Numerical Solution of ODEs.
SIAM Journal of Scientific and Statistical Computation, vol.7 no.3 (1986).

[2] Carlsen, H.
10 KW Hermetic Stirling Engine for Stationary Applications.
ISEC 6th International Stirling Engine Conference (1993).

[3] Lambert, J.D.
Numerical Methods for Ordinary Differential Systems.
Wiley (1991).

[4] Brenan, K.E.,Campbell S.L. and Petzold, L.R.
Numerical Solution of Initial-Value Problems in Differential-Algebraic Equations.
North-Holland (1989).

[5] Hairer, E.
Highest Possible Order of Algebraically Stable Diagonally Implicit Runge-Kutta Methods.
BIT 20, pp.254-256 (1980).

[6] Nørsett, S.P. and Thomsen, P.G.
Local Error Control in SDIRK-methods.
BIT 26 pp. 100-113 (1986).

[7] Lambert, J.D.
Computational Methods in Ordinary Differential Equations.
Wiley, London (1973).

[8] Arscher, U.M., Mattheij, R.M.M. and Russell, R.D.
Numerical Solution of Boundary Value Problems for Ordinary Differential Equations.
Prentice Hall, Englewood Cliffs, New Jersey (1988).

[9] Aprille, JR., and Trick, T.N.
Steady-State Analysis of Nonlinear Circuits with Periodic Inputs.
Proceedings of the IEEE, vol. 60, no.1 (1972).

[10] Hindmarsh, A.C.
LSODE and LSODI, Two new Initial Value Ordinary Differential Equation Solvers.
ACM-SIGNUM Newsletters, 15 pp.10-11 (1980).

[11] Nakhla, M.S. and Branin, E.H.
Determining the Periodic Response of Nonlinear Systems by a Gradient Method.
Circuit Theory and Applications, vol. 5, pp. 255-273 (1977).

[12] Skelboe, S.
Time-Domain Steady-State Analysis of Nonlinear Electrical Systems.
Doctoral thesis from the Technical University of Denmark (1982).

[13] Mannshardt, R,.
One-Step Methods of Any Order for Ordinary Differential Equations with Discontinuous Right-Hand Sides.
Numerische Mathematik vol. 31, pp. 131-152 (1978).

[14] Thomsen, Per Grove.
Løsning af sædvanlige differentialligninger med diskontinuerte højresider. (Numerical Solution of Ordinary Differential Equations with Discontinuous Right-Hand Sides).
Institute for Mathematical Modelling, Technical University of Denmark.

[15] Enright, W.H., Jackson, K.R., Nørsett, S.P. and Thomsen, P.G.
Effective Solutions of Discontinuous IVPs Using a Runge-Kutta Formula Pair with Interpolants.
Mathematics and Computation, vol 27, pp. 313-335 (1988).

[16] Enright. W.H., Jackson, K.R., Nørsett, S.P. and Thomsen, P.G.
Interpolants for Runge-Kutta Formulas.
ACM Transactions on Mathematical Software, vol 12, No. 3, Sept.1986.

7.0 NUMERICAL TESTS FOR THE SFVSM

7.1 Introduction

In the thesis, several approaches and numerical methods have been considered for the solution of the periodic thermodynamic problem, which has been given in form of a physical and mathematical model of a Stirling engine.

In this chapter, the Simple Five-Volume Stirling Model problem will be used to test and evaluate the different solution approaches and methods analyzed in the previous chapter. Recall that the word "approach" is used for the basic idea of obtaining a solution (e.g., the Shooting method), while "method" means the actual numerical method (e.g., 3.order DIRK method). A simulation program in form of computer code, which solves the mathematical model of the SFVSM-problem using the different approaches, has been written and the developed program is tested on examples using real Stirling engine input data.

The main purposes of this section are primarily to test the implementation and to compare the different approaches and methods and with special concern to extensions to more advanced models. These extensions will include variable heat transfer, pressure losses, variable matrix temperature and spatial discretization and will be discussed further in the next chapter.

Convergence, stability, accuracy, speed and storage will be discussed. These are some of the most important properties of a numerical method used for the solution of a mathematical model obtained from a simulation on a computer.

Convergence ensures that the correct solution to the mathematical model of the problem is obtained in the limit $\Delta t \rightarrow 0$. As the mesh is refined (i.e., the number of steps increased) the numerical solution should converge to the correct solution to the mathematical model. Convergence is a requirement for any reliable numerical method.

Stability is concerned with the propagation of error. The numerical solution will blow up if the applied method is unstable for the given problem, even when the problem is well defined (well posed). A small error, introduced because of the truncation error, will be amplified and the solution will be destroyed in a few steps for a finite time step Δt. Stability is mainly of concern when the defined problem is *stiff*.

The *accuracy* of a numerical method is often given in terms of *order*. The order of a numerical method describes the behaviour of the truncation error in the limit $\Delta t \rightarrow 0$, where a higher order method gives a better solution. For a finite step length, the accuracy of the method is also dependent of the solution and of the error constant of the method. These observations are valid only for sufficiently smooth solutions. When discontinuities are present the conditions may be different as discussed previously in section 6.10.

Speed (CPU-time) is also a very important feature for an implementation of a numerical method, although many large and complex problems which used to require vast amounts of expensive computer time now can be solved on a small 486-based Personal Computer (PC) or a workstation because of the fast development in the area of computer hardware. Still the size and requirement for computing the solutions seems to grow at least as fast as the new technology.

For the simulation of an internal combustion engine, the number of time steps could easily exceed 100000 for just one cycle. A spatial discretization in two or three dimensions requires many mesh points to resolve boundary layers, turbulence and combustion and this takes time even for the powerful computers of today.

This project's ambitions are not at this level. Here, at most, a one-dimensional model of a Stirling engine is considered. Required computing power is not a major problem when only one cycle is to be calculated, but if the convergence towards cyclic conditions is very slow and many different engine designs should be calculated, speed must also be taken into consideration. For design optimizations many parameters (typically 50-100 for a simple model of a real engine) may be varied and this will usually require the calculation of thousands of different engine designs.

The need for *storage* can also be an important factor, but even here the same argument as above is valid. Faster and better computers have reduced the restriction in the size of storage. On a PC, executable program codes are no longer restricted to 640 KB.

7.2 Simulation program for the SFVSM-problem

7.2.1 Introductory remarks

A package for simulation of a five-volume model of a Stirling engine has been developed for educational use at the Laboratory for Energetics. This package has been described in further details in [1] and only the use for the SFVSM-problem will be considered here.

It is possible to select one of the following three approaches for the solution of the mathematical model of the SFVSM (given by the basic formulation of the system of equations):

- Integration-to-Convergence method.
- Shooting method.
- Finite Difference method.

All the approaches share the same subroutines except from those parts, that handle the actual calculation. This makes it possible to directly compare the different approaches with regard to computing speed. The code has been developed with the intention to include additional features, so that some input and output data could have been omitted for the discussion of the SFVSM in this chapter.

7.2.2 Program routines

The general structure of the simulation program and the included subroutines will briefly be described in this section.

Program structure

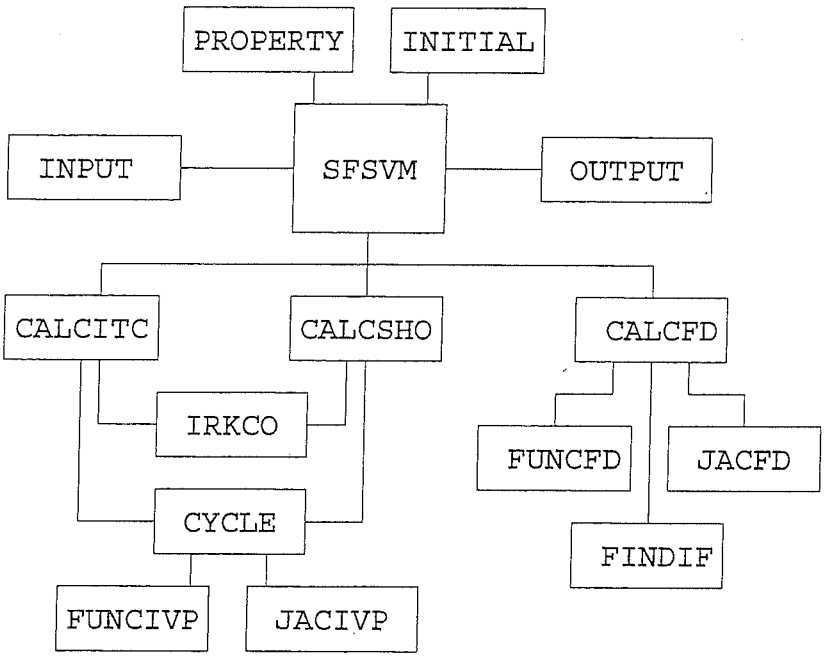

Main files

SFVSM.FOR

This is the main program unit. It controls the different tasks performed by the simulation program.

INPUT.FOR

Subroutine which reads input data from a file specified by the user.

PROPERTY.FOR

Subroutine which holds property data for the specified working gas.

INITIAL.FOR

Subroutine which generates initial guesses for all differential and algebraic variables. For the SFVSM-problem, an isothermal Schmidt-analysis is used and initial guesses can be obtained for all time levels, even though the Integration-to-Convergence method and the Shooting method only require a guess for the values at the initial time.

CALCSHO.FOR

Subroutine which handles the calculation for the Shooting method.

CALCITC.FOR

Subroutine which handles the calculation for the Integration-to-Convergence method.

CYCLE.FOR

This subroutine is common for the Integration-to-Convergence method and the Shooting method. It calculates one full cycle for a given "guess" on the initial state (t=0) and using a numerical method for IVPs specified by the user.

FUNCIVP.FOR

Subroutine used by CYCLE. It returns the function evaluation, i.e., it calculates the right-hand side of the system of equations used for the calculation of the residuals.

JACIVP.FOR

Subroutine used by CYCLE. It returns the analytical Jacobian for the system of equations, i.e., it calculates the partial derivatives of the right-hand side used for the stage iteration.

CALCFD.FOR

Subroutine which handles the actual calculation for the Finite difference method.

FUNCFD.FOR

Subroutine used by CALCFD. It returns the function evaluations for the Finite Difference method.

JACFD.FOR

Subroutine used by CALCFD. It returns the full Jacobian for the Finite Difference method based on the derived analytical expression.

OUTPUT.FOR

Subroutine which writes the output to files, in form of state variables, cyclic parameters and energy balances (including heat transfer, work and efficiency).

IRKCO.FOR

Subroutine which holds the coefficients for the semi-implicit Runge-Kutta methods.

FINDIF.FOR

Subroutine which holds the coefficients for the different discretizations for the Finite Difference method.

<u>Other routines</u>

VECNORM.FOR

Calculates a specified norm of a given vector.

QUAD.FOR

Calculates an integral numerically based on a specified quadrature formula.

LUBKSB.FOR and LUDCMP.FOR

Subroutines which solve a linear system of equations using Gauss elimination and backward substitution (taken from [2]).

SESYS.FOR

Solves a sparse system of linear equations using a direct method (see [3]).

VOL.FOR and DVOL.FOR

User defined subroutine which returns the value of the volumes and the derivatives of volume w.r.t. to time as a function of time for each component (volume).

ERRORS.FOR

Writes error messages to the specified output.

ITCIRK.DAT

Holds the numerical parameters (tolerance, maximal number of iterations etc.) for the Integration-to-Convergence approach.

SHOIRK.DAT

Holds the numerical parameters (tolerance, maximal number of iterations etc.) for the Shooting method.

FD.DAT

Holds the numerical parameters (maximal number of iterations etc.) for the Finite Difference method.

7.2.3 Required input for the SFVSM

Component data

Component number	:	COMPNR
Component type	:	COMPTYPE
Maximal swept volume	:	VSW
Clearance volume	:	VCL
Initial phase angle	:	PHI
NTU-number	:	NTU
Solid temperature	:	TS
Cyclic heat transfer	:	CHTFLAG

General data

Revolutions pr. minute	:	RPM
Required mean pressure	:	PMEAN
Working gas	:	WGASSTR
Gas constant	:	RGAS
Specific heat capacity	:	CP

Numerical data

Numerical method	:	APPROACH
Time integration method	:	METHOD
Fixed / Variable step length	:	VSLFLAG
Number of steps pr. cycle	:	NSTEP
Tolerance	:	TOL
Displacement	:	DELTA

7.2.4 Output

General output data are written to a file specified by the user and the state variables for each component are written to files which contain all the relevant data for the specific components. An example of an output file containing the general data is shown below. The input data is taken from the test example described in the next section.

Example of an output file

```
Test example------------ FVSM17 ----------------- 3.1.1994-------

Working gas: HE      RPM =  1550.0

================================================================================
# Type   Swept Volume   Clearance Volume   Phase Angle   NTU   Solid temperature
-  ---      [m**3]           [m**3]            [°]      -----        [K]
--------------------------------------------------------------------------------
1  VVC   0.00049370      0.00013700          0.00      0.01       336.190 *
2  HEX   0.00000000      0.00021000          0.00      2.00       328.000
3  REG   0.00000000      0.00036800          0.00    150.00       621.974 *
4  HEX   0.00000000      0.00051500          0.00      2.00       973.000
5  VVC   0.00044160      0.00004300        127.20      0.01       931.033 *

* = Solid temperature calculated in simulation

Temperature gradient in REG dT/dx = 545.076 K   Total mass Mtot = 12.2493 g

Mean pressure    Work     Heat in     Heat out     Error     Efficiency    Carnot
    [MPa]         [W]       [W]         [W]        [W]         ----        ----
    8.000     18586.39   36699.44    18113.06     0.00       0.5064      0.6629

================================================================================
Volume  Work      Heat     Enthalpy w Enthalpy e Conduction Dissipation Error
  -      [W]       [W]        [W]        [W]         [W]        [W]       [W]
--------------------------------------------------------------------------------
  1  15654.89      0.00       0.00   15654.89       0.00       0.00      0.00
  2      0.00 -18113.06   15654.89   -2458.17       0.00       0.00      0.00
  3      0.00      0.01   -2458.17   -2458.16       0.00       0.00      0.00
  4      0.00  36699.44   -2458.16   34241.28       0.00       0.00      0.00
  5 -34241.28      0.00   34241.28       0.00       0.00       0.00      0.00

 SHOOTING METHOD

 Solution method     : Semi-implicit DIRK method p=4,s=3
                       No error estimates
 Integration method  : Runge-Kutta method

 Number of time steps      N = 1280
 Total number of iterations =   20
```

7.3 Test data for the SFVSM-problem

7.3.1 Introductory remarks

This Stirling engine has been built by Carlsen [4] and tested at the Laboratory for Energetics, Technical University of Denmark. In a "lumped" parameter formulation, the model of the engine consists of the five classical Stirling components, two variable cylinder volumes, two heat exchangers and one regenerator.

7.3.2 Input data

The following data are input to the simulation program FVSM.

Component no.	1	2	3	4	5
Component type	VVC	HEX	REG	HEX	VVC
Max. swept volume[m^3]	$493.7 \cdot 10^{-6}$				$441.6 \cdot 10^{-6}$
Clearance volume [m^3]	$137 \cdot 10^{-6}$	$210 \cdot 10^{-6}$	$368 \cdot 10^{-6}$	$515 \cdot 10^{-6}$	$43 \cdot 10^{-6}$
Initial phase angle [°]	127.197				0
NTU-number	0.01	2.0	150.0	2.0	0.01
Solid temperature [K]		328		973	
Cyclic heat transfer	Yes	No	Yes	No	Yes

Table Input data for the Simple Five-Volume Stirling Model.

Speed: 1550 RPM
Required mean pressure: p_{mean} = 8 MPa
Working gas: Helium
Gas constant: R = 2079.5 J/kg·K
Specific heat: c_p = 5093 J/kg·K

The following abbreviations have been used for the component types:

VVC: Variable volume (with "cyclic heat transfer").
HEX: Heat exchanger.
REG: Regenerator.

Remarks:

i) The NTU-numbers are taken to be constant for the SFVSM. The actual values are taken as representative values from simulations, where heat transfer is calculated directly as a function of mass flow and geometry (see the discussion of the Extended Five-Volume Stirling Model in chapter 8).

ii) The engine is of Beta-configuration and the equivalent phase angle (phase difference) for an Alpha-configuration is calculated from the expressions derived in Appendix C.

7.4 General results from simulations of the SFVSM-problem

7.4.1 Introductory remarks

It is the intention only to present a few general results from the simulations to give an idea of how the solution to the mathematical model looks like for the differential and algebraic variables for both formulations. All of the different numerical solution approaches, which have been considered here for an actual implementation of computer code (Integration-to-Convergence method, the Shooting method and the Finite Difference method), converge to the same solution, when the number of time steps pr. cycle is increased.

7.4.2 Results using the basic formulation

Mass and internal energy are the differential variables and mass flows and pressure the algebraic variables. In the following figures mass and temperature (derived from mass and internal energy) are shown as a function of time for full cyclic operation (i.e., cyclic state variables and fulfilling the cyclic integral conditions). The results are based on the input data given in the previous table, using the Shooting method with a 4.order DIRK method and fixed step length with 1280 points pr. cycle. A smaller fixed step length or a method using a variable step length based on error estimates (in form of the NT I method, see section 6.4.2) do not provide results different from these.

Masses

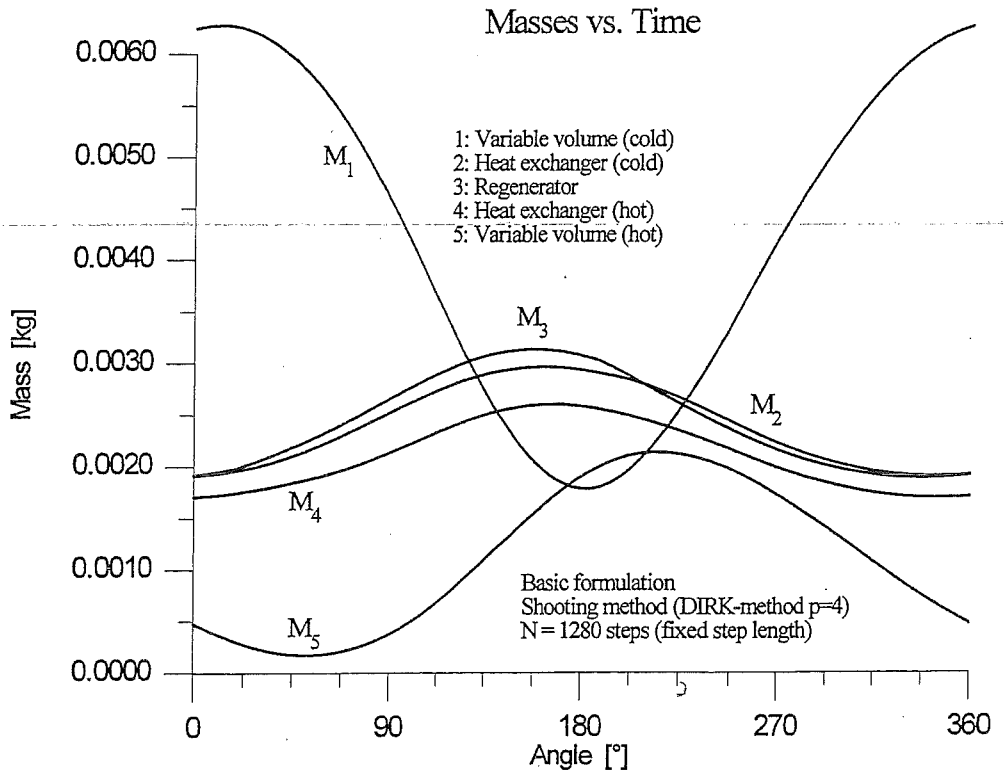

Figure 7.1 Masses contained in each of the five components.

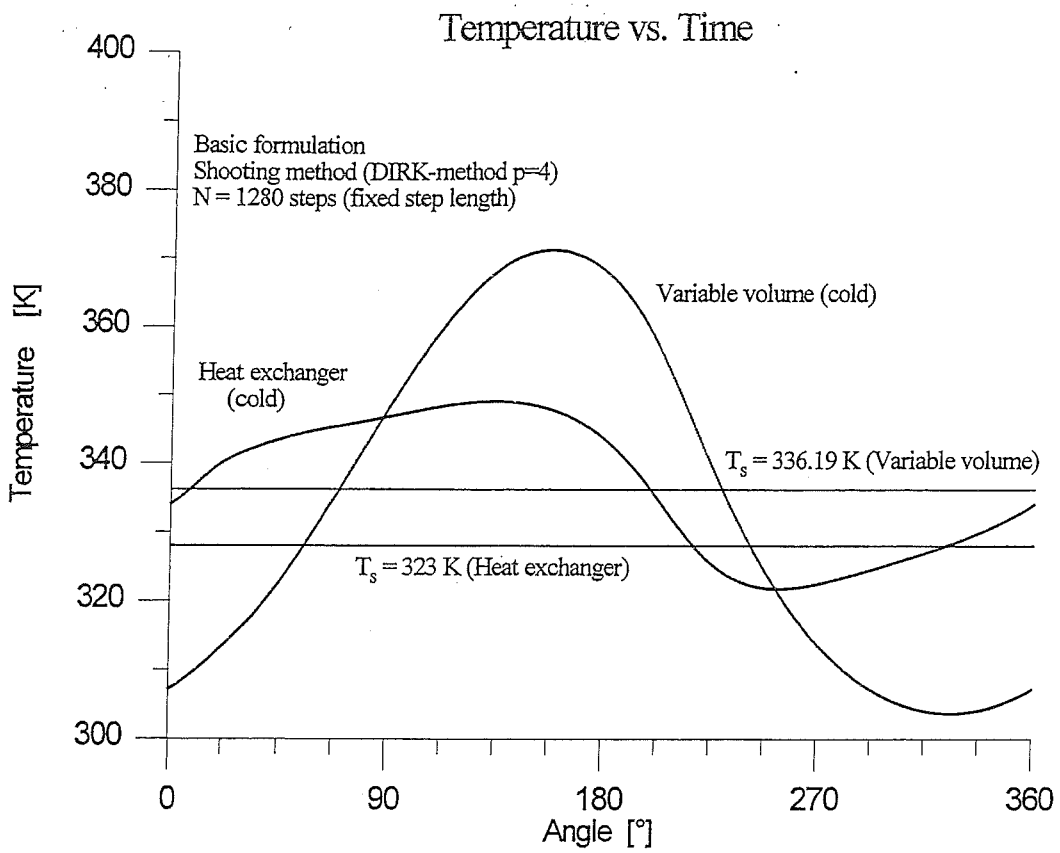

Figure 7.2 Cold end temperatures.

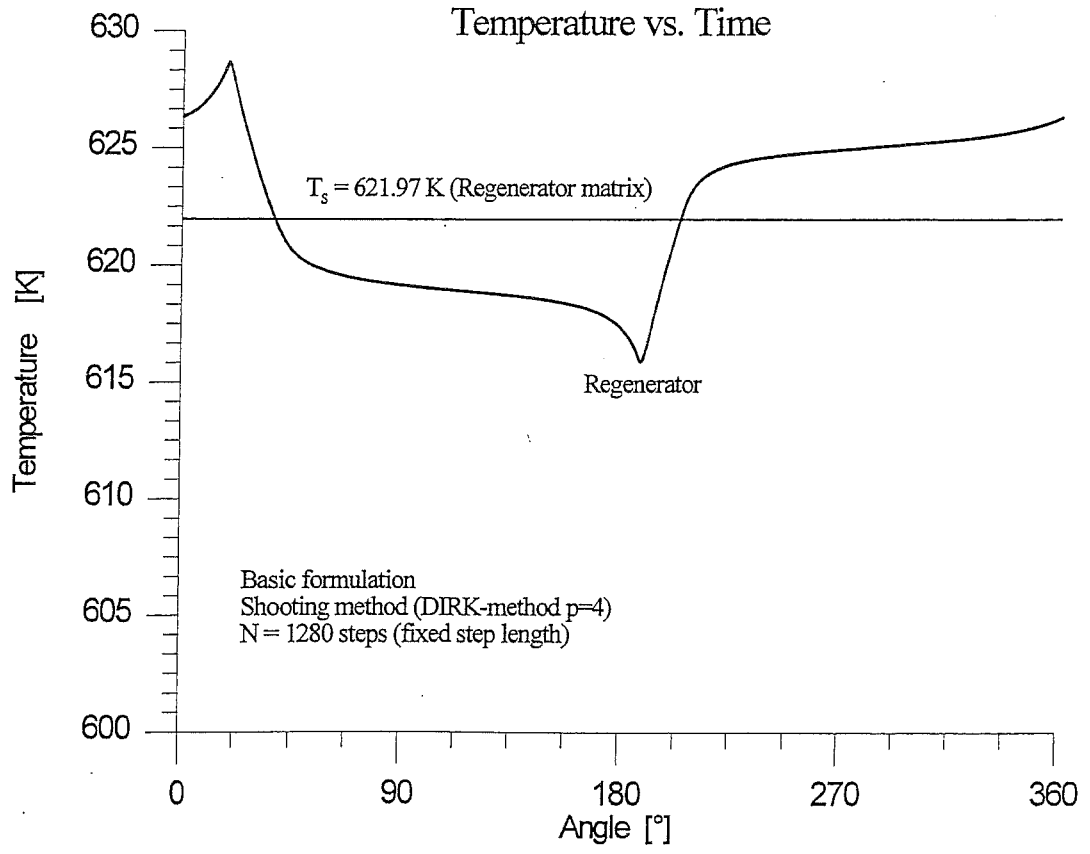

Figure 7.3 Regenerator temperatures.

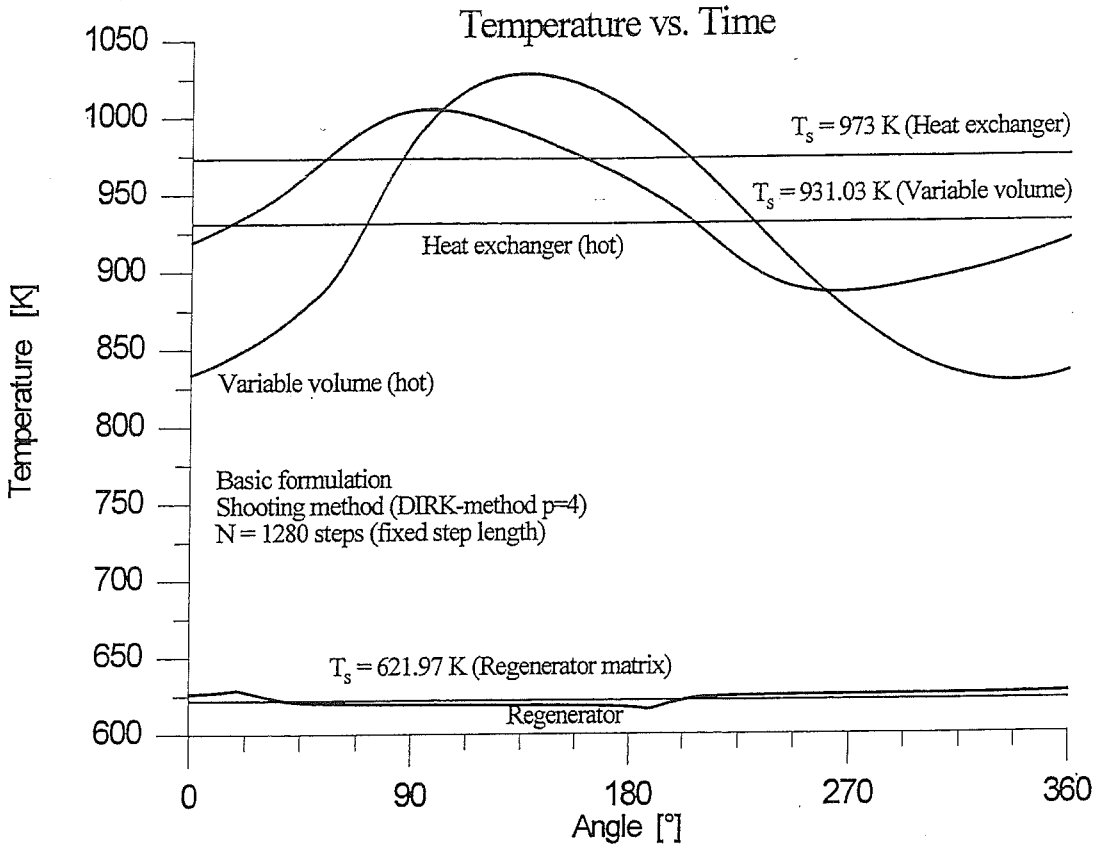

Figure 7.4 Hot end temperatures.

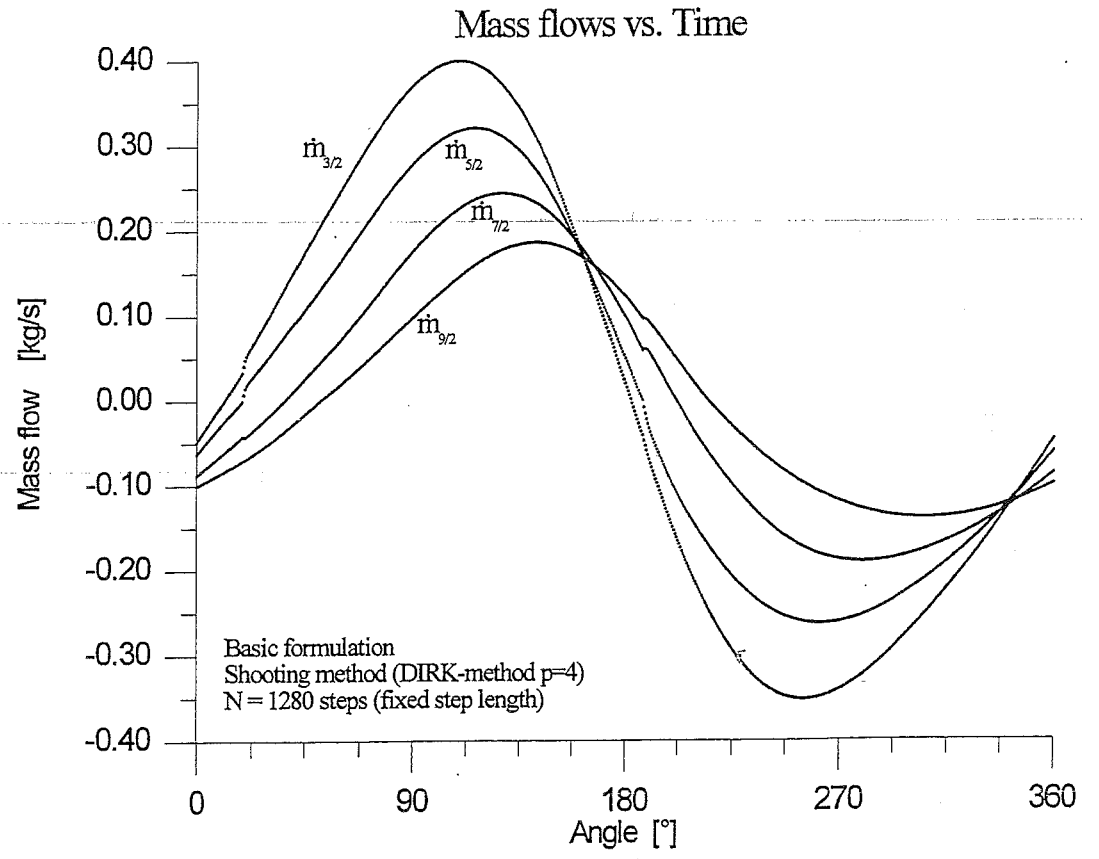

Figure 7.5 Mass flows at the component boundaries.

Pressure

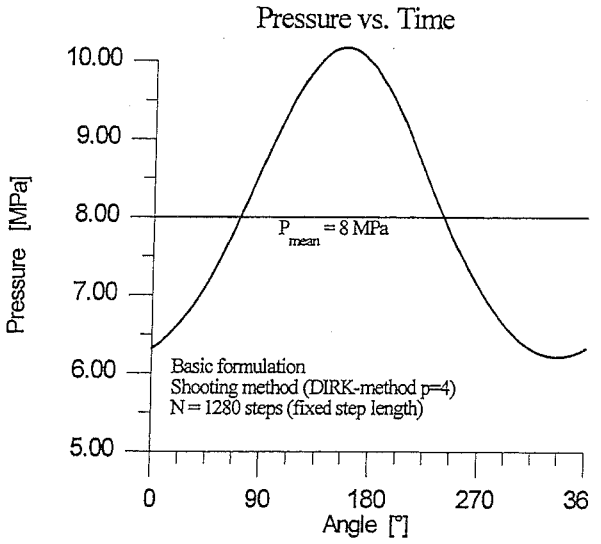

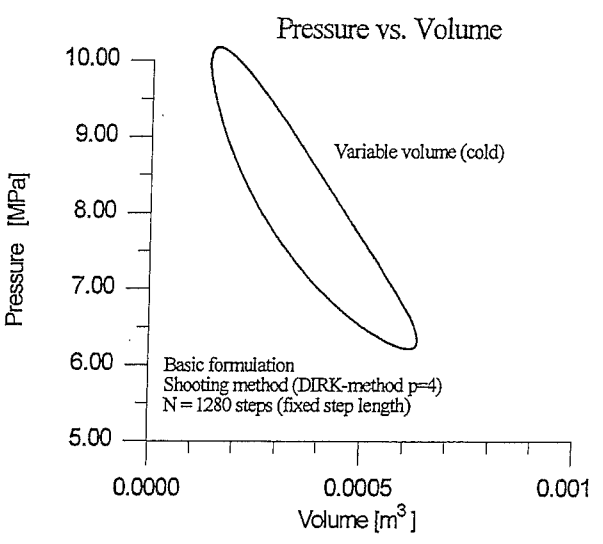

Figure 7.6 Pressure as a function of time. Figure 7.7 Pressure as a function of volume.

7.4.3 Results using the alternative formulation

For the alternative formulation of the SFVSM-problem, mass and pressure are the differential variables, and mass flows and temperatures are the algebraic variables.

The numerical solution of the mathematical model of this formulation (see section 6.2.3) has been found from corresponding simulations. The results are for all variables identical to those obtained from the basic formulation and the results are therefore not shown here. Of course, this is just as expected, since both formulations describe the exact same problem.

Remarks:

i) The simulation program developed for the solution of the SFVSM in the alternative formulation has been used only for comparisons with the other methods because explicit Runge-Kutta methods cannot be applied to the basic formulation.

ii) The explicit Runge-Kutta methods considered in section 6.4.2 (see also Appendix D) have been implemented in an Integration-to-Convergence solution approach only in the program.

iii) A detailed description of the simulation program is omitted.

7.5 Test of stability

7.5.1 Introductory remarks

In this section, the different methods are tested for stability. Explicit Runge-Kutta methods for IVPs can only be used for the alternative formulation as shown in a previous chapter, and special problems are encountered, when the mass flow changes sign at the boundaries of the components and at large values of the mass flows.

For the implicit Runge-Kutta methods for IVPs none of these problems have been observed. Finally, results are given for different finite difference discretizations for the Finite Difference method.

7.5.2 ERK-methods for IVP integration (alternative formulation)

The following explicit Runge-Kutta methods have been tested using a fixed step length

- Heun's 3.order method (RK3).
- Classical 4.order method (RK4).
- Fehlberg's method RKF45.
- Verner's method RKV56.

Butcher arrays for these methods can be found in Appendix D.

The results can be summarized in the following table:

Method	Order	Time steps	Solution characterization
RK3	3	320 (320)	Stable
RK3	3	160 (160)	Oscillatory mass flows
RK4	4	320 (320)	Stable
RK4	4	160 (175)	Oscillatory mass flows
RK4	4	120 (-)	No convergence (unstable)
RKF45	4	160 (-)	No convergence (unstable)
RKF54	5	160 (160)	Stable
RKV56	5	160 (162)	Stable
RKV65	6	160 (161)	Stable
RKV65	6	120 (124)	Stable (signs of small oscillations)
RKV65	6	80 (109)	Oscillatory mass flows

Table Stability of ERK-methods for the SFVSM-problem.

Remarks:

i) The number in the parenthesis is the actual number of time steps for the simulation. If there is no solution to the linear sub system of equations described in section 6.6.2, then an additional point is automatically added (corresponding to halving that particular step), and the procedure is repeated until a solution can be found. This is the reason why the actual number of steps is larger than the required number.

ii) Instabilities at large mass flows are primarily reason why these additional points are necessary. However, some of the difficulties encountered for the explicit methods also occurred when the mass flow changed direction (corresponding to a discontinuity in the right-hand side of a differential equation). This is discussed further in section 6.10.

iii) The numerical solution becomes only gradually nonphysical, meaning that the mass flows slowly start to oscillate for large mass flows and large time steps. The system is forced, and that is probably the reason why the solution does not "explode" after the time when instability occurs and instead the oscillations disappear. In the figure just below two different numerical solutions are shown. One method (RK4) becomes unstable for large mass flows, while the other (RKV56) looks all right all the way through the period.

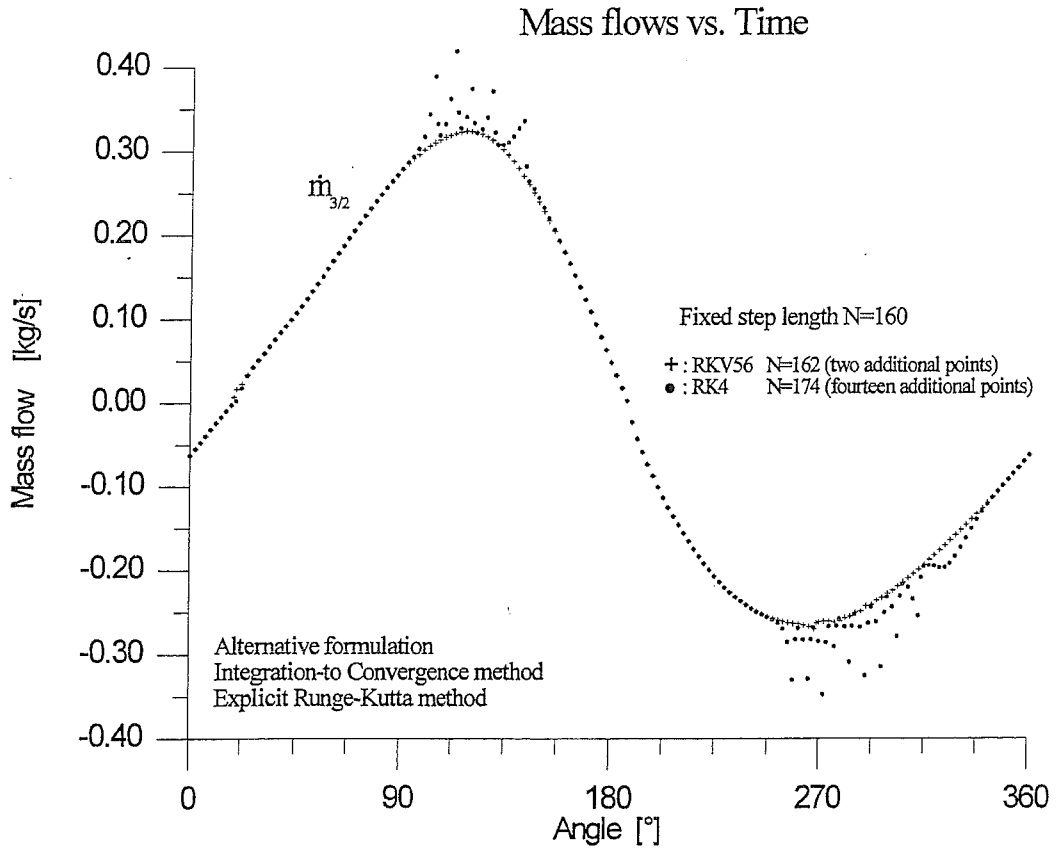

Figure 7.8 Stable and "unstable" mass flows.

Note: It is the periodic steady-state solution which is shown!

iv) These instabilities cannot be found for the differential variables, as it can be seen from the figure below, where mass in the heat exchanger (volume #2) is shown as a function of time for the same two methods.

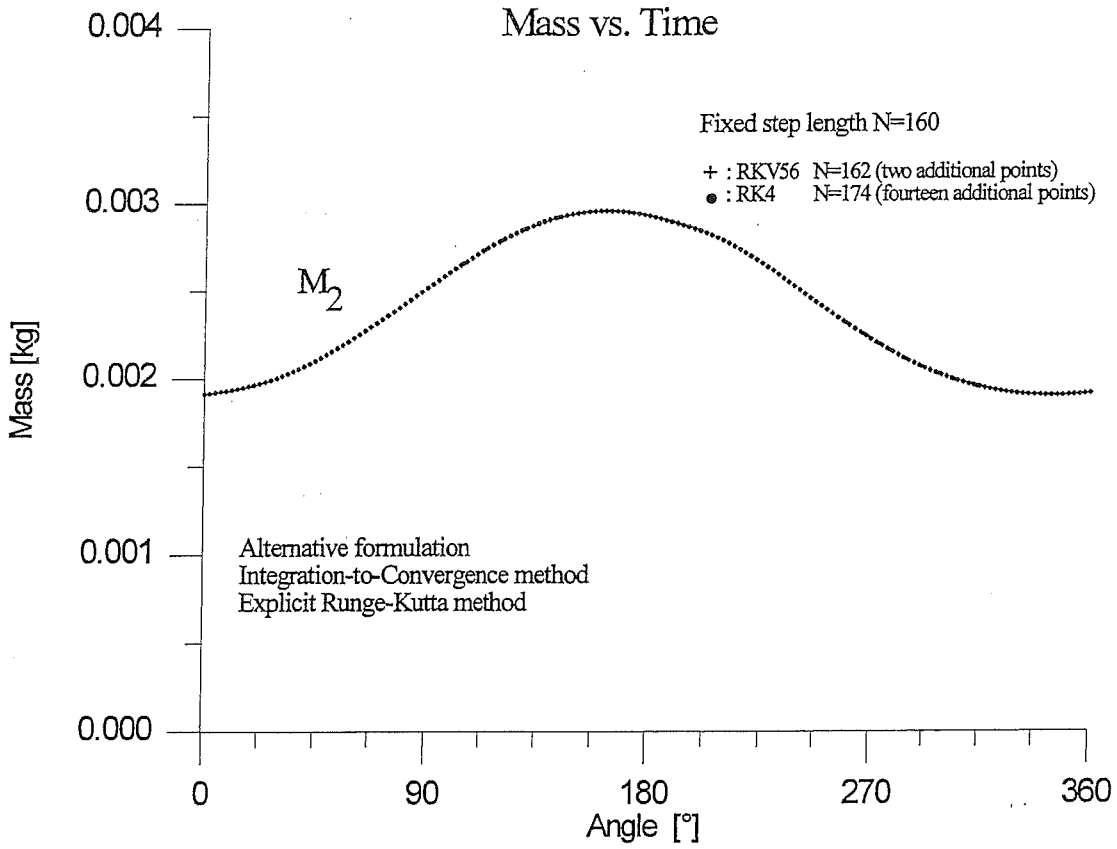

Figure 7.9 Mass in volume #2 for the two different numerical solutions.

v) The "No convergence" in the table means that the iteration on cyclic state variables or cyclic integral conditions failed due to instabilities.

vi) It can be seen that the higher the order of the explicit method, the better the behaviour with regard to stability (in accordance with the stability theory for explicit Runge-Kutta methods).

vii) It might be mentioned that the problems with unstable mass flows do not disappear when using a method with a variable step length based on error estimates for the differential variables.

7.5.3 IRK-methods for IVP integration (basic formulation)

The implicit Runge-Kutta methods have been tested using a fixed number of steps per cycle (fixed step length). Two different step numbers have been applied (N=10 and N=160 steps) and all results are valid for both.

The results are summarized in the following table

METHOD	STAGES	ORDER	ABSOLUTE STABILITY (LINEAR STABILITY)	ALGEBRAIC STABILITY (NON-LINEAR STABILITY)	STABILITY PROPERTIES FOR THE ACTUAL PROBLEM
Radau IA	1	1	L-stable	Algebraically stable	Stable
Radau IIA	1	1	L-stable	Algebraically stable	Stable
Gauss [1)]	1	2	L-stable	Algebraically stable	Oscillations
Lobatto IIIB	2	2	A-stable		Not stable
NT I	3	3	L-stable	Algebraically stable	Stable
NT II	3	4	A-stable		Stable
DIRK s=2	2	3	L-stable	Algebraically stable	Stable
DIRK s=3	3	4	L-stable	Algebraically stable	Stable

[1)] 1-stage Gauss method.

Table Test of stability for IRK-methods used for the SFVSM-problem.

Remarks:

i) Algebraic stability seems to be a very reasonable requirement for the IRK-methods used for the IVP integration of the SFVSM-problem.

ii) For the 1-stage Gauss method, the solution does not blow up, but oscillations in the algebraic variables (mass flows) are observed, and the convergence towards cyclic state variables and cyclic conditions is destroyed.

iii) For the Lobatto IIIB, the iteration on the stage values fails already in the first step. A possible reason could be inconsistent initial guesses for the algebraic variables.

7.5.4 Finite-Difference methods

The stability for these methods has been tested on meshes with N=10 and N=80 points on one full cycle. Only meshes with constant time step length are considered. The results are summarized in the following table:

Method	Order	Number of steps	Solution characterization
Divided Difference	2	10	Stable
Divided Difference	4	10	Stable
Divided Difference	6	10	Stable
BDF-method	1	10	Stable
BDF-method	2	10	Stable
BDF-method	3	10	Stable
BDF-method	4	10	Stable
BDF-method	5	10	Not stable
BDF-method	5	80	Not stable
Trapezoidal method	2	10	Not stable
Trapezoidal method	2	11	Stable
Trapezoidal method	2	12	Not stable
Trapezoidal method	2	80	Not stable
Simpson's method	4	10	Stable

Table Test of stability for the SFVSM-problem using a Finite Difference method.

Remarks:

i) In general, the methods based on divided differences seem to behave very well concerning stability. The same can be said of the BDF-methods up to order four. Fifth and sixth order BDF-methods are unstable, even when using much more than 80 time steps.

ii) The numerical solution blows up using the Trapezoidal method with an even number of steps per cycle. A possible explanation is that some of the eigenmodes of the periodic problem cannot be represented for an even step number.

iii) There are no obvious reasons to use a BDF-method instead of any other Linear Multistep method for the discretization.

iv) The initial guess is generated from an isothermal Schmidt analysis and is relatively close to the true solution. Stability has not been tested for any other initial guesses, and it could be important (especially for problems where one does not have access to a solution to a closely related problem).

7.6 Test of accuracy

7.6.1 Introductory remarks

The accuracy of the different methods is tested in this section. Accuracy means how well the numerical method solves the mathematical model of the problem, and not how the results compare to real engine data. Since there are no analytical results available, the results are checked for convergence as the computational grid is refined. When the results do not change with a further refinement, they are taken to be the solution to the mathematical model.

Some characteristic output variables have been chosen to illustrate the accuracy of the numerical solution. In the way that the results obtained from a given numerical method are compared with the "true" converged solution. In the limit $\Delta t \rightarrow 0$, the following values have been obtained for all methods:

Efficiency:	0.5064
Work input:	15654.89 W
Work output	34241.28 W
Heat input:	36699.43 W
Net enthalpy flux through the regenerator:	- 2458.14 W
Temperature gradient in the matrix:	621.974 K

7.6.2 ERK based IVP code (alternative formulation)

For the solution of the SFVSM-problem, using the alternative formulation and an explicit Runge-Kutta method, the following results are obtained from the simulations:

Fixed step length

Method	p	N	Efficiency	Work in [W]	Heat in [W]	Enthalpy flow (Reg) [W]	Wall temp (Reg) [K]
RK4	4	174	0.5066	15650.15	36698.40	-2458.05	622.203
RK4	4	320	0.5064	15654.89	36699.42	-2458.16	621.974
RKF45	4	320	0.5064	15654.91	36699.44	-2458.21	621.974
RKF54	5	160	0.5064	15654.93	36699.41	-2458.28	621.975
RKF54	5	320	0.5064	15654.91	36699.43	-2458.20	621.974
RKV56	6	162	0.5065	15653.52	36699.72	-2458.18	622.058
RKV65	6	109	0.5065	15653.65	36699.56	-2458.50	622.026
RKV65	6	124	0.5065	15654.52	36699.56	-2458.11	621.985
RKV65	6	161	0.5065	15654.87	36699.43	-2458.13	621.975
RKV65	6	320	0.5064	15654.89	36699.42	-2458.15	621.974

Table Accuracy of explicit Runge-Kutta methods for the SFVSM-problem (fixed step length).

Remarks:

i) Stability seems to be the limiting factor with regard to reducing the step number for these explicit methods, since all of the results are relatively close to the "true" solution. Numerical solutions could not be found using fewer steps due to instabilities (no convergence towards cyclic state variables or cyclic conditions).

ii) For RKV65 (109 time steps) and RK4 (174 time steps) oscillating mass flows are observed (see remarks concerning stability for ERK-methods in section 7.5.2), but the results are still surprisingly close to the "stable" solutions.

Variable step length

Method	p	TOL	N	Efficiency	Work in [W]	Heat in [W]	Enthalpy flow (Reg) [W]	Wall temp (Reg) [K]
RKF45	4	$1{\cdot}10^{-6}$	150	0.5064	15654.95	36699.41	-2458.11	621.974
RKF45	4	$1{\cdot}10^{-8}$	250	0.5064	15654.90	36699.41	-2458.13	621.974
RKF54	5	$1{\cdot}10^{-6}$	135	0.5065	15654.86	36699.01	-2457.63	621.974
RKV56	5	$1{\cdot}10^{-6}$	147	0.5065	15654.94	36699.33	-2458.16	621.974
RKV65	6	$1{\cdot}10^{-4}$	101	0.5065	15655.14	36697.59	-2456.49	621.985
RKV65	6	$1{\cdot}10^{-6}$	126	0.5064	15654.88	36699.38	-2458.10	621.974
RKV65	6	$1{\cdot}10^{-8}$	231	0.5064	15654.89	36699.46	-2458.17	621.974

Table Accuracy of explicit Runge-Kutta methods for the SFVSM-problem (variable step length).

Remarks:

i) The tolerance TOL is absolute, and is used for the differential variables only. It is unnecessary to use relative tolerance because of the introduced scaling of all variables.

ii) Convergence cannot be achieved with much less strict tolerance than the smallest of those shown in the table.

iii) Internal stage values of mass flows have been checked at each stage, implying that the error estimates used for the step length algorithm are incorrect when a discontinuity (i.e., change of sign of mass flow) is located inside the full time step. The alternative of checking the mass flows only at the beginning of each step does not work well (see the discussion of these two strategies in section 6.10).

iv) The iteration criterion for the iteration on cyclic state variables and cyclic integral conditions must be adjusted accordingly to the accuracy of the numerical method (which is given in form of the tolerance).

7.6.3 IRK based IVP code (basic formulation)

For the solution of the SFVSM-problem, using the basic formulation and an implicit Runge-Kutta method, the following results have been obtained from the simulations:

Fixed step length:

Method	p	N	Efficiency	Work in [W]	Heat in [W]	Enthalpy flow (Reg)	Wall temp (Reg) [K]
Radau IA	1	10	0.4063	19537.48	36847.41	-2339.28	625.858
Radau IA	1	40	0.4806	16685.02	36833.26	-2444.77	622.956
Radau IA	1	160	0.5000	15916.24	36738.45	-2454.59	622.214
Radau IA	1	640	0.5048	15720.48	36709.55	-2457.32	622.035
NT I	3	10	0.4991	16018.44	36860.18	-2446.03	622.433
NT I	3	40	0.5063	15655.04	36710.32	-2458.21	621.978
NT I	3	160	0.5064	15655.44	36700.11	-2458.16	621.974
DIRK	3	10	0.4992	15948.66	36730.67	-2445.52	622.432
DIRK	3	160	0.5064	15655.10	36699.97	-2458.20	621.974
DIRK	4	10	0.5047	15782.02	36812.33	-2450.92	622.292
DIRK	4	40	0.5065	15655.50	36701.85	-2458.35	621.985
DIRK	4	160	0.5064	15655.01	36699.49	-2458.13	621.973
DIRK	4	640	0.5064	15654.89	36699.44	-2458.14	621.974
DIRK	4	1280	0.5064	15654.89	36699.43	-2458.14	621.974

Table Accuracy of semi-implicit Runge-Kutta methods for the SFVSM-problem (fixed step length).

Remarks:

i) It is seen that all of the methods shown here converge nicely as the number of time steps is increased. Notice the slow convergence of the 1.order Radau method.

ii) Stability is no problem for the algebraically stable, semi-implicit Runge-Kutta methods (opposite the explicit Runge-Kutta methods), but many time steps are required to obtain a very accurate solution. This is due to the relatively low order of these methods. Recall that the ERKs used for the simulations have high order, while there are no algebraically stable DIRK methods of order higher than four.

iii) The criteria for convergence of the cyclic state variables and cyclic conditions have been chosen so strictly that the error on conservation of energy in each component based on the numerical calculated values for heat, work and enthalpy flow is less than 0.02W and overall less than 0.04 W.

iv) The equations are solved at each stage using the "correct" sign of mass flow, again implying that an error is committed every time the mass flows changes sign during a time step (i.e., crossing a discontinuity in the partial derivative of the right-hand side). In the limit $\Delta t \rightarrow 0$ the influence should become insignificant.

v) Radau IA and Radau IIA (the latter not shown in the table) give identical results.

vi) The fourth order DIRK-method with 1280 time steps is used for reference values.

Variable step length

Method	p	TOL	N	Efficiency	Work in [W]	Heat in [W]	Enthalpy flow (Reg)	Wall temp (Reg) [K]
NT I	3	0.00400	28	0.5059	15678.92	36708.39	-2457.94	622.035
NT I	3	0.00200	53	0.5064	15658.94	36703.86	-2459.55	621.993
NT I	3	0.00100	103	0.5064	15655.77	36700.48	-2458.38	621.975
NT I	3	0.00050	206	0.5064	15654.99	36699.62	-2458.25	621.975
NT I	3	0.00020	514	0.5064	15654.90	36699.45	-2458.16	621.974

Table Accuracy of semi-implicit Runge-Kutta methods for the SFVSM-problem (variable step length).

Remarks:

i) It is seen that even with a few as N=53 steps (for TOL=0.002) the results are within 5 W of the "true" converged solution (compare with the results in section 7.6.1). This is equivalent of a relative "error" less than 0.05%.

ii) The tolerance TOL is absolute and given for the differential variables only. Since all the variables have been scaled, the use of a tolerance based on the relative size of the variables have not been found necessary.

iii) The results of NT I with TOL=0.0005 (N=206) are within 0.2 W of the results obtained from the fixed step length fourth order DIRK method using 1280 time steps.

iv) It has not been possible to obtain a solution by using the NT II method (which is only A-stable) with embedded error estimates in a variable step length algorithm. The time step is reduced repeatedly until it becomes so small that the integration algorithm is aborted. Recall that the method works well for a fixed step length algorithm.

v) The NT I is only a third order method and requires many time steps (compared to the high order explicit Runge-Kutta methods) to obtain an accurate solution. Higher order semi-implicit Runge-Kutta methods with error estimates are preferable. The fourth order DIRK could be applied using Richardson extrapolation for the error estimates, but this has not been tried out here.

7.6.4 Finite Difference method

For the solution of the SFVSM-problem using the basic formulation and the Finite-Difference method the following results have been obtained from the simulations for the different discretizations:

Method	p	N	Efficiency	Work in [W]	Heat in [W]	Enthalpy flow (Reg)	Wall temp (Reg) [K]
Div. Differences	2	10	0.5042	16187.76	37499.18	-2405.12	619.760
Div. Differences	2	40	0.5062	15691.86	36746.14	-2452.74	621.875
Div. Differences	2	160	0.5064	15656.99	36702.29	-2458.00	621.971
Div. Differences	4	10	0.5071	15623.52	36774.57	-2501.34	621.140
Div. Differences	4	40	0.5064	15656.91	36698.67	-2458.17	621.970
Div. Differences	4	160	0.5064	15654.75	36699.45	-2458.27	621.976
Div. Differences	6	10	0.5072	15583.97	36714.82	-2508.63	621.333
Div. Differences	6	40	0.5064	15656.81	36698.33	-2458.03	621.967
Div. Differences	6	80	0.5064	15655.31	36699.58	-2458.39	621.970
Div. Differences	6	160	0.5064	15654.74	36699.37	-2458.26	621.976
BDF	4	10	0.5139	15381.74	36729.90	-2474.43	621.113
BDF	4	40	0.5065	15655.30	36700.94	-2458.35	622.000
Trapez	2	11	0.5082	15442.83	36373.64	-2444.68	622.280
Simpson	4	10	0.5071	15592.44	36718.35	-2507.72	621.363
Simpson	4	40	0.5064	15656.80	36698.48	-2458.11	621.969

Table Accuracy of the Finite-Difference method for the SFVSM-problem.

Remarks:

i) The integrals originating from the determination of the cyclic conditions are calculated using the Trapezoidal rule (which is of order 4 for periodic problems, see the Appendix E). This might be significant for the accuracy of the sixth order divided difference approximation, which only seems to be marginally better than the fourth order approximation.

ii) The Trapezoidal method gives quite good results for N=11 time steps although the iteration failed for both 10 and 12 steps (see the remarks concerning stability of the Finite Difference method in section 7.5.4).

7.7 Test of speed

7.7.1 Introductory remarks

For an approach, which solves the problem using an IVP method, the number of calculated cycles is the determining factor for the required computing time given the same IVP method and the same number of steps or tolerance. The Shooting method can be considered as a convenient way to accelerate the convergence towards cyclic operation and the idea works well for the SFVSM-problem as the results show in the table below.

Both the Integration-to-Convergence method and the Shooting method require only a guess for the initial state (time t=0), while the Finite Difference method solves the full system of equations (at all time points) requiring a guess at all discrete times. The number of cycles for this last approach means number of iterations for the large nonlinear system of difference equations.

7.7.2 Cyclic Convergence

Approach	Method	p	N	Number of cycles
Integration-to-Convergence	Radau IA	1	10	60
Integration-to-Convergence	Radau IA	1	160	58
Integration-to-Convergence	NT I	3	10	56
Integration-to-Convergence	NT I	3	160	58
Integration-to-Convergence	DIRK	4	10	56
Integration-to-Convergence	DIRK	4	160	58
Shooting method	Radau IA	1	10	21
Shooting method	Radau IA	1	160	19
Shooting method	NT I	3	10	19
Shooting method	NT I	3	160	19
Shooting method	DIRK	4	10	19
Shooting method	DIRK	4	160	19
Finite-Difference method	Divided	6	10	4
Finite-Difference method	Divided	6	40	4
Finite-Difference method	BDF	4	40	4
Finite-Difference method	Trapezoidal	2	11	4

Table Number of cycles (iterations) required for the different approaches for the SFVSM.

Remarks:

i) The required number of cycles is apparently independent, of both method and step number for all of the solution approaches.

ii) For the Integration-to-Convergence approach, typically 21-25 cycles are required for the calculation of the finite difference approximation of the Jacobian for the iteration on cyclic integral conditions (no update of the Jacobian).

iii) 15 cycles are required (10 differential variables and 5 cyclic conditions) for the calculation of the finite difference approximation of the Jacobian for the Shooting method. This means that the numerical solution to the periodic steady-state solution of the problem converged in only 4 iterations (no update of the Jacobian).

iv) The Jacobian for the calculation of the cyclic condition for the Integration-to-Convergence method and the Jacobian for the Shooting method have both been determined numerically using one-sided finite-differences, and it has been noticed that the convergence towards cyclic conditions is affected by the size of the displacement δ. A value too small of δ gives a Jacobian, which is polluted by the global error of the numerical solution (no convergence in most cases) and a value too large value of δ the convergence is significantly slower. For accurate methods (meaning many time steps and high order), it has been possible to use a very small δ.

v) The Trapez-method is unstable for N even, but behaves just like the other finite difference approximations for N uneven with regard to convergence to the periodic steady-state solution.

vi) The Integration-to-Convergence method is penalized further, when the assumption of infinite heat capacity of the solid regenerator matrix is omitted. This will be shown for the Extended Five-Volume Stirling Model discussed in chapter 8.

7.7.3 CPU-time

A comparison of some of the most promising methods has been made with regard to actual CPU-time. The codes have not been fully optimized, and the results should only be taken as guidelines. Tolerance and criteria for the convergence of the iterations are adjusted so that the absolute numerical error in the energy balance for each volume is less than 0.01 W.

For the Integration-to-Convergence method and the Shooting method the required computer time is roughly proportional to the number of cycles required to obtain full cyclic operation.

For the Finite-Difference method, due to the heavy computation of the Jacobian and the solution of the linearized system, a sparse solver is necessary even when only relatively few time steps are used. The application of a sparse solver (in form of the subroutine SESYS, see reference [3]) reduces the computing time by a factor 10 compared to a direct full matrix solution, even at moderately low step numbers.

The following relative computing times are obtained:

Approach	Method	s	p	N	Work in [W]	Work out [W]	Relative CPU-time
Integration-to-Convergence	RK4	4	4	320	15654.89	34241.28	0.12
Integration-to-Convergence	RKV56	8	6	202	15654.89	34241.28	0.18
Integration-to-Convergence	DIRK	3	4	80	15654.56	34240.84	0.32
Integration-to-Convergence	DIRK4	3	4	160	15655.01	34241.35	0.58
Shooting method	DIRK3	2	3	160	15655.10	34241.37	0.10
Shooting method	DIRK4	3	4	80	15654.56	34240.84	0.08
Shooting method	DIRK4	3	4	160	15655.01	34241.35	0.15
Shooting method	DIRK4	3	4	1280	15654.89	34241.28	1.00
Shooting method	NT I	3	3	105	15655.53	34242.16	0.10
Shooting method	NT I	3	3	514	15654.90	34241.32	0.43
Finite-Difference method	Divided		4	160	15654.75	34241.09	0.22
Finite-Difference method	Divided		6	40	15656.81	34240.31	0.06
Finite-Difference method	Divided		6	160	15654.74	34241.11	0.57

Table Relative computing times for selected combinations of approach and methods.

Remarks:

i) The DIRK-method of order 4 using 1280 time steps has been used as reference. On the 33/66 MHz 486 DX2-based PC, 100% or 1.00 is equal to 815 seconds.

ii) The iteration criteria are set strict (less strict criteria would, of course, imply less computing time) and so that each of the different solution approaches have approximately equal requirements for accuracy.

7.8 Discussion

When solving the SFVSM-problem as an initial value problem, it is relatively simple to make the implementation into computer code. A standard numerical method for IVPs can be used for the time integration, and only a guess for the initial state is needed. The coupled algebraic equations are important, in a way that it is possible for the alternative formulation only to use an explicit Runge-Kutta method.

Using the basic formulation and an IRK-method for the IVP integration gives a stable and accurate solution using only a limited number of time steps, while explicit Runge-Kutta methods used for the alternative formulation, require more time steps due to stability concerns. If a very accurate solution is required, explicit methods may still be attractive, since high order methods are available, and because many time steps are needed for the computationally expensive implicit methods.

IRK-methods may be used for the alternative formulation, but then the advantage for this formulation disappears since a nonlinear system of equations has to be solved at each stage. Recall that for an explicit method only a small linear system has to be solved due to the special structure of the differential-algebraic system.

Extension of the Simple Five-Volume Stirling Model to include heat transfer given in form of a variable NTU-number can only be done with some trouble using the explicit Runge-Kutta methods and the alternative formulation. This is because of the additional nonlinearities (introduced through the dependence of mass flows on the NTU-number). For the basic formulation and the implicit methods there are no significant problems with such an extension.

For the classical Integration-to-Convergence approach the convergence towards cyclic condition is slow even for the SFVSM, and more serious problems can be expected when extensions (such as a variable regenerator matrix temperature) are included in the model. The major advantage of this method is the simple and straightforward implementation.

The Shooting method seems to be reliable and a much faster alternative. Acceleration towards cyclic operation is significant, and the cyclic state variables are found and the cyclic integral conditions are fulfilled simultaneously. The implementation is almost as simple as for the Integration-to-Convergence approach, and the two approaches give identical results when using the same IVP method and the same step number.

Stability for both these approaches is dependent of the stability for the given IVP-method used for the time integration. As mention just above, an explicit Runge-Kutta method requires many time steps, while a semi-implicit Runge-Kutta method, which is algebraically stable, behaves nicely even with as few time steps as 10.

The Finite Difference method has some very interesting features for the actual problem. The convergence towards the periodic steady-state solution is very fast and the approach looks very stable for various finite difference approximations.

Drawbacks for the Finite Difference method are:

- Requirements for a guess for all of the variables at all times (this is actually not a problem when a Schmidt-analysis can be used as here for the SFVSM-problem).
- Rate of growth in required computing time and storage for an increased number of time steps.
- Tedious work required for setting up all the equations for the function evaluations and (especially) for the derivation and calculation of the analytical Jacobian.

Some interesting and promising combinations of the different approaches and methods might also be considered:

- The Integration-to-Convergence method with a low order IRK-method could be used for generating initial guesses for high order IVP-methods or the Finite-Difference method.
- A few cycles could be calculated using the Integration-to-Convergence method to give a better guess for the initial values before switching to the Shooting method.
- The periodic steady-state solution could be found using a low order IRK method with a few time steps only before switching to a high order method in order to get an accurate solution.
- The periodic steady-state solution could be found using a Finite Difference method with a few time steps only before switching to high order IVP-methods in order to get an accurate solution.

References

[1] Commisso, M. B.
FVSM - Users Manual version 1.1
Laboratory for Energetics, Technical University of Denmark (1994).

[2] Press, W.H, Teukolski, S.A., Vetterling W.T. and Flannery, B.P.
Numerical Recipies in FORTRAN 2nd edition.
Cambridge University Press (1992).

[3] Houbak, N.
SESYS A Sparse matrix Linear Equation Solver - Users Guide.
Risø-M-2527 (1985).

[4] Carlsen, H.
10 KW Stirling Engine for Stationary Applications.
ISEC 6th International Stirling Engine Conference (1993).

8.0 ADVANCED STIRLING MODELS

8.1 Introduction

Two different and more sophisticated Stirling models are analyzed in this chapter. One model will include additional physical losses, while the other model will include a spatial discretization.

The first part of this chapter is devoted to the analysis and discussion of a Stirling model which is based on a direct extension of the Simple Five-Volume Stirling Model (SFVSM) described in chapter 6. This new Extended Five-Volume Stirling Model (EFVSM) also uses the "lumped" formulation with five volumes, where each volume equals one specific component, but the following additional features are included:

- Variable NTU-number.
  Instead of a constant NTU-number, the heat transfer is now given as a function of geometry and mass flow in all components. This introduces new nonlinearities in the energy equation for both formulations.

- Variable matrix temperature in the regenerator.
  The heat capacity of regenerator matrix is no longer assumed to be infinite. This means that a differential equation for the internal energy (temperature) of the regenerator matrix has to be added to the system of equations. The assumption of finite heat capacity in the solid matrix greatly affects the performance of the numerical methods, as will be shown later in this chapter.

- Pressure losses due to friction.
  The effect of friction is partly included into the system of equations. A static pressure loss given as a function of geometry and mass flow is considered here only. The effect of dissipation will also be included in the energy equation.

- Heat conduction through gas and matrix in the regenerator.
  Since the assumption of a linear temperature distribution in the gas and in the solid matrix is kept, it is very easy to include the effect of heat conduction through the regenerator into the system of equations.

The necessary expressions are derived in this section, but the implementation is not discussed in the same detail as for the SFVSM-problem. These extensions make the code as general as any existing model based on and within the limitations of the five components - five volumes "lumped" formulation.

The effect of friction is included directly and not as a correction to the calculated values of work and heat transfer, which makes this simulation program more thermodynamic realistic than the code developed by Carlsen [1]. However, it should be noted that Carlsen's program includes a number of parasitic losses, which gives simulation results that are quite good compared to real engine performance.

In the second part of this chapter another and different extension of the SFVSM is considered. While the EFVSM still is based on a "lumped" formulation, the Multi-Volume Stirling Model (MVSM) now includes a one-dimensional spatial discretization.

The MVSM has the following features:

- Arbitrary number of components.
  Any number and combination of components can be included in the model.

- New component type: Manifold volumes.
  Manifold volumes between the classical Stirling components can be defined as separate components.

- Spatial discretization in one dimension.
  Each component can be divided into an arbitrary number of sub volumes implying that the spatial variation of each of the variables inside a component may be found. The temperature profile in the regenerator is no longer restricted to a linear temperature gradient in gas and matrix.

- Variable heat transfer in form of a variable NTU-number.
  The NTU-number is calculated as a function of geometry and mass flow for each component as for the EFVSM.

- Variable solid temperature.
  It is possible to specify constant solid temperature (in form of fixed temperature, "cyclic" heat transfer or adiabatic walls), otherwise an additional differential equation is solved for the conservation of energy of the solid.

- Uniform pressure distribution in space.
  Pressure losses have not been included in this model.

The MVSM is closer to the state-of-the-art models in Stirling analysis, although the momentum equation has been used in a very simplified form.

8.2 Extended Five-Volume Stirling Model (EFVSM)

8.2.1 Introductory remarks

The additional features of the Extended Simple Five-Volume Model (EFVSM) are discussed in this section.

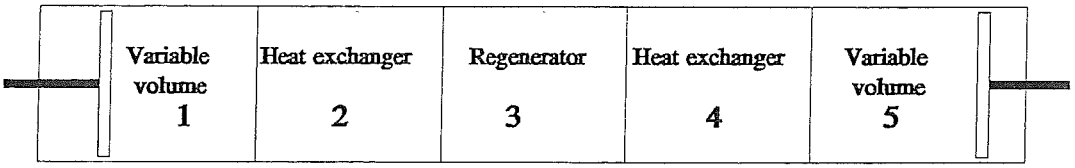

Figure 8.1 Five component Stirling engine.

First the incorporation of variable convective heat transfer will be considered. The expressions for NTU-number as a function of mass flow, geometry and the properties of matter will be put in a general form, which is convenient for a mathematical treatment and for the implementation in a computer code. The NTU-number will be written as an explicit function of the mass flow, and it is this dependence of mass flow that makes the whole system of equations more nonlinear and excludes the direct use of an explicit Runge-Kutta method for time integration (outlined for the alternative formulation of the SFVSM in section 6.6.2).

Heat conduction will briefly be discussed. Usually heat conduction in the flow direction is ignored, since it is insignificant for most Stirling engine designs. However, there is a temperature difference of typically 500-600 K across the regenerator, and in some extreme cases heat conduction might have importance for the heat transport through the regenerator. The assumption of constant gradient of gas and matrix in the regenerator makes it trivial to include this phenomenon in the system of equations.

Then the assumption of variable regenerator matrix temperature is discussed. The assumption of linear and identical temperature gradients in gas and matrix is retained, but now the solid matrix temperature is allowed to vary. This means that the heat capacity of the matrix now is finite, and an additional differential equation for conservation of energy in the solid matrix has to be solved.

Finally pressure losses due to friction will be considered. A "static" pressure difference can be calculated from a simplified form of the equation of conservation of momentum. In a one-dimensional formulation, the friction terms can be replaced by an equivalent friction force. All other terms than friction are neglected, and the resulting expression will be an algebraic equation, which gives the pressure difference across a volume as a function of mass flow (geometry and properties of matter given). The dissipation (work done by the friction forces) must also be included in the equation for conservation of energy.

8.2.2 Convection heat transfer

The convection heat transfer $\dot{Q}_{conv}$ is written in the form

$$\dot{Q}_{conv} = |\dot{m}|\cdot c_p \cdot NTU \cdot (T_s - T)$$

where $\dot{m}$ is mass flow, c_p specific heat capacity (constant pressure) and T_s and T are the temperatures of solid and gas respectively.

As mentioned in chapter 3, steady-flow correlations for heat transfer (and friction) are usually applied in Stirling analysis in the lack of better expressions. The "quasi-steady approximation" will also be used here, where some of the most popular of these steady flow correlations will be used as examples.

Convection heat transfer in the regenerator

Many different experimental studies have been carried out for the heat transfer in Stirling regenerators. The following expression, which is widely applied in Stirling analysis, will be used as an example:

Miyabe e.a. [2] gives the heat transfer in form of a Nusselt number Nu:

$$Nu = 0.42 \cdot Re^{0.56} \tag{8.2}$$

The thread diameter d_w is used as characteristic length and the Nusselt number is defined as

$$Nu = \frac{d_w \cdot h}{k} \tag{8.3}$$

h is the mean heat transfer coefficient and k is the thermal heat conductivity.

The Reynolds number is also based on the thread diameter d_w, i.e.,

$$Re = \frac{d_w \cdot u}{\nu} = \frac{d_w \cdot \dot{m}}{A_c \cdot \mu} \tag{8.4}$$

which implies that the mean heat transfer coefficient is given as

$$\begin{aligned} h &= 0.42 \cdot k \cdot d_w^{-0.44} \cdot (A_c \cdot \mu)^{-0.56} \cdot |\dot{m}|^{0.56} \\ &= \frac{0.42 \cdot c_p}{A_c \cdot Pr} \cdot \left(\frac{d_w}{A_c \cdot \mu} \right)^{-0.44} \cdot |\dot{m}|^{0.56} \end{aligned} \tag{8.5}$$

In terms of a NTU-number, this can be written as

$$NTU = \frac{h \cdot A}{|\dot{m}| \cdot c_p} = \frac{0.42}{Pr} \cdot \frac{A}{A_c} \cdot \left(\frac{d_w}{A_c \cdot \mu} \right)^{-0.44} \cdot |\dot{m}|^{-0.44} \tag{8.6}$$

The geometry (see the definitions in chapter 4), in form of heat transfer area A, free flow area A_c and thread diameter d_w, is given for a specific regenerator, and under the assumption of constant properties the NTU-number is seen to be a nonlinear function of the mass flow alone.

Convection heat transfer in the heat exchangers

Many different designs for heat exchangers can be found, but for Stirling engines the most common type is a tube heat exchanger. In Kays and London [3], $St \cdot Pr^{2/3}$ is shown as a function of the Reynolds number for experimental data for tube heat exchangers. Based on the figures, Carlsen and Andersen [4] have found the following expressions:

Laminar flow: $Re < 2465$

$$St \cdot Pr^{2/3} = \left(\frac{Re}{1000}\right)^{-0.7418} \cdot 10^{\left(10 \cdot \frac{A_c}{A} - 2.2823\right)} \tag{8.7}$$

Transition: $2465 \leq Re \leq 10000$

$$St \cdot Pr^{2/3} = \left(\frac{Re}{1000}\right)^{0.1177} \cdot 10^{\left(10 \cdot \frac{A_c}{A} - 2.6191\right)} \tag{8.8}$$

Turbulent flow: $10000 < Re$

$$St \cdot Pr^{2/3} = \left(\frac{Re}{1000}\right)^{-0.1984} \cdot 10^{\left(10 \cdot \frac{A_c}{A} - 2.3027\right)} \tag{8.9}$$

The expression for the transition region is an approximation which gives $St \cdot Pr^{2/3}$ as a continuous function of Re.

The NTU number can be written as a function of $St \cdot Pr^{2/3}$ (see section 4.4.4)

$$NTU = \frac{A}{A_c} \cdot Pr^{-2/3} \cdot St \cdot Pr^{2/3} \tag{8.10}$$

or

$$NTU = \frac{A}{A_c} \cdot Pr^{-2/3} \cdot 10^{\left(10 \cdot \frac{A_c}{A} - C_2\right)} \cdot \left(\frac{D_h}{1000 \cdot \mu \cdot A_c}\right)^{C_1} \cdot |\dot{m}|^{C_1} \tag{8.11}$$

The constants C_1 and C_2 are taken from one of the three expressions above depending on the Reynolds number Re

$$Re = \frac{D_h \cdot u}{\nu} = \frac{D_h \cdot \dot{m}}{A_c \cdot \mu} \tag{8.12}$$

which is based on the hydraulic diameter D_h

$$\frac{D_h}{4 \cdot L} = \frac{A_c}{A} \tag{8.13}$$

In terms of the mean heat transfer coefficient h, the equation can be written as

$$h = \frac{c_p}{A_c} \cdot Pr^{-2/3} \cdot 10^{\left(10 \cdot \frac{A_c}{A} - C_2\right)} \cdot \left(\frac{D_h}{1000 \cdot \mu \cdot A_c}\right)^{C_1} \cdot |\dot{m}|^{C_1 + 1} \tag{8.14}$$

Convection heat transfer in the variable volumes

Complex flow and heat transfer conditions are present in the variable volumes. The length and diameter are often of the same size and the real flow is two- or three-dimensional and turbulent. Another complication is that the heat transfer area (solid wall to gas) is variable in time, since it is a function of the actual position of the piston.

In the simple models, it is assumed that cylinder walls are adiabatic, but as it has been discussed in chapter 5, this is not a very good approximation and important information will be lost. A simple model must at least include a fixed effective heat transfer area A_{eff} and a constant wall temperature T_s, which could be determined by setting the condition of cyclic heat transfer.

In reference [4], Carlsen uses a one-dimensional turbulent flow correlation for flow inside a tube to represent heat transfer in the variable cylinder volumes. The Nusselt number is given as

$$Nu = 0.023 \cdot Pr^{0.4} \cdot Re^{0.8} \tag{8.15}$$

where the hydraulic diameter D_h is used as characteristic length.

Using the definitions for Nusselt number, Prandtl number and Reynolds number this implies that the mean heat transfer coefficient h is given as

$$\begin{aligned} h &= 0.023 \cdot k \cdot D_h^{-0.2} \cdot (A_c \cdot \mu)^{-0.8} \cdot |\dot{m}|^{0.8} \\ &= \frac{0.023 \cdot c_p}{A_c} \cdot Pr^{-0.6} \cdot \left(\frac{D_h}{A_c \cdot \mu}\right)^{-0.2} \cdot |\dot{m}|^{0.8} \end{aligned} \tag{8.16}$$

In terms of a NTU-number, this can be written as

$$NTU = \frac{h \cdot A_{eff}}{|\dot{m}| \cdot c_p} = 0.023 \cdot Pr^{-0.6} \cdot \frac{A_{eff}}{A_c} \cdot \left(\frac{D_h}{A_c \cdot \mu}\right)^{-0.2} \cdot |\dot{m}|^{-0.2} \tag{8.17}$$

In all cases the convection heat transfer $\dot{Q}_{conv}$ has the generic form

$$\dot{Q}_{conv} = a \cdot |\dot{m}|^{b} \cdot c_p \cdot (T_s - T) \tag{8.18}$$

and the NTU-number

$$NTU = a \cdot |\dot{m}|^{b-1} \tag{8.19}$$

where the coefficients are specific for the given component.

Regenerator (Miyabe)

$$a = \frac{0.42}{Pr} \cdot \frac{A}{A_c} \cdot \left(\frac{d_w}{A_c \cdot \mu} \right)^{-0.44} \tag{8.20}$$

$$b = 0.56$$

Heat exchanger (Carlsen)

$$a = \frac{A}{A_c} \cdot Pr^{-2/3} \cdot 10^{\left(10 \cdot \frac{A_c}{A} - C_2\right)} \cdot \left(\frac{D_h}{1000 \cdot \mu \cdot A_c} \right)^{C_1} \tag{8.21}$$

$$b = C_1 + 1$$

Variable volumes (Carlsen)

$$a = 0.023 \cdot Pr^{-0.6} \cdot \frac{A_{eff}}{A_c} \cdot \left(\frac{D_h}{A_c \cdot \mu} \right)^{-0.2} \tag{8.22}$$

$$b = 0.8$$

8.2.3 Conduction heat transfer in the regenerator

Heat conduction in the regenerator parallel to the flow direction will occur due to the temperature gradient. In the Simple Five-Volume Model the temperature gradients in matrix and gas are assumed to be constant and equal. Constant temperature gradient (i.e., linear temperature profile) means in particular that the gradients at the boundaries are equal. The heat conducted into and out of the regenerator volume is therefore equal, and no heat from conduction is stored in the regenerator. The net result is that heat is transferred from the hot heat exchanger to the cold heat exchanger. This will contribute to the regenerator "loss" (net heat transfer through the regenerator), which reduces the performance of the engine.

Let k_g and k_M denote the heat conductivity in gas and matrix respectively. The heat transfer by conduction $\dot{Q}_{cond}$ through the regenerator for simple geometries can then be given as

$$\begin{aligned} \dot{Q}_{cond} &= k_g \cdot \varrho \cdot A_{fr} \cdot \frac{dT}{dx} + k_M \cdot (1 - \varrho) \cdot A_{fr} \cdot \frac{dT_M}{dx} \\ &= k_g \cdot A_c \cdot \frac{dT}{dx} + k_M \cdot \frac{1 - \varrho}{\varrho} \cdot A_c \cdot \frac{dT_M}{dx} \end{aligned} \tag{8.23}$$

where A_{fr} is the frontal area and ϱ is the porosity.

This actually represents the worst case since the thermal contact is imperfect. The wires or threads in the regenerator are in reality only in solid contact at certain points, and the effective heat conduction area through the solid material will be smaller than in the expression above.

Using the assumptions of constant and equal temperature gradients, i.e.,

$$\frac{dT_M}{dx} = \frac{dT}{dx} = \alpha \tag{8.24}$$

give the following expression

$$\dot{Q}_{cond} = \left(\frac{\varrho \cdot k_g + (1 - \varrho) \cdot k_M}{\varrho} \right) \cdot A_c \cdot \frac{dT}{dx} \tag{8.25}$$

When an effective heat conductivity k_{eff} is introduced as

$$k_{eff} = \frac{\varrho \cdot k_g + (1 - \varrho) \cdot k_M}{\varrho} \tag{8.26}$$

the formula can be written in the form

$$\dot{Q}_{cond} = k_{eff} \cdot A_c \cdot \alpha \tag{8.27}$$

This expression can be used to evaluate the conduction heat transfer through the regenerator and it is very easily implemented into the computer code.

8.2.4 Heat transfer in the variable volumes

The penetration depth of temperature fluctuations in the solid walls of the variable volumes is small. This is partly because of the high capacity of heat in the solid walls compared to the heat capacity in the gas, and partly because of the speed of temperature fluctuations in these volumes (related to the period of the cycle).

As discussed previously, a reasonable approach for evaluation of the heat transfer in a variable volume is to assume that the condition of "cyclic heat transfer" is satisfied. This means that the surface temperature of the solid wall is constant over a cycle, but attains a value such that the net heat transfer (from gas to wall) is zero over one cycle. Some Stirling people call this for "adiabatic", which is rather unfortunate since instant heat transfer takes place at the solid wall - gas interface and in some cases this heat transfer can be an important factor for the performance of the engine (see [5]). Infinite heat transfer is equivalent to an isothermal volume, and a true adiabatic volume (i.e., no instant heat transfer) represents the other extreme case. The expression for the heat transfer between gas and solid surface in form of a NTU-number or a heat transfer coefficient h have been given previously in this chapter.

In reality, there will likely be a net heat transfer over one time period from the variable volumes to a temperature reservoir in- or outside the engine. In some cases, a better approximation than "cyclic" heat transfer could be attractive. One possibility is to keep the assumption of a fixed temperature on the solid surface inside the variable volume. Instead of determining this temperature from a requirement of zero net heat transfer during one cycle, the net heat transfer from the inside walls to the fixed temperature reservoir could be determined.

Let UA denote the overall heat transfer coefficient from inside the solid surface to the temperature reservoir, such that the instant heat loss is given as

$$\dot{Q}_{heatloss} = UA \cdot (T_s - T_{res}) \tag{8.28}$$

T_{res} is the temperature of the reservoir and the temperature on the inside of the walls T_s is determined from

$$\int_{t=0}^{t_p} |\dot{m}| \cdot c_p \cdot NTU \cdot (T - T_s) \cdot dt + \int_{t=0}^{t_p} UA \cdot (T_{res} - T_s) \cdot dt = 0 \tag{8.29}$$

or

$$\int_{t=0}^{t_p} |\dot{m}| \cdot c_p \cdot NTU \cdot (T - T_s) \cdot dt + UA \cdot (T_{res} - T_s) \cdot t_p = 0 \tag{8.30}$$

This can easily be implemented in the developed simulation programs.

As a remark, real experiments have shown that the actual temperature in the solid walls varies with a phase difference compared to the temperature in the gas. This is not reproduced using the expression from above.

8.2.5 Variable matrix temperature

A major weakness in the SFVSM is the assumption of constant solid matrix temperature in the regenerator. The theoretical extension is simple; a differential equation for the internal energy of the solid matrix can easily be stated and included into the governing system of equations, but this will have significant impact on the behaviour of the solution and for the numerical methods.

Due to the relatively large heat capacity of the solid matrix compared to the working gas, the temperature will only slowly (i.e., after many cycles) converge to the periodic steady-state analogous to the conditions in a real Stirling engine. Another way to express this situation is that a new time constant, which is many times larger than the period of the cycle, is introduced in the system of equations.

The time required for the computation of the numerical solution using the Integration-to-Convergence method will be significantly affected from this, as it will be shown later in this chapter in section 8.2.10.

Next, the additional differential equation for the solid regenerator matrix is given:

Conservation of energy for the solid matrix

$$M_s \cdot c_s \cdot \frac{dT_s}{dt} = |\dot{m}| \cdot c_p \cdot NTU \cdot (T - T_s) \tag{8.31}$$

where M_s is mass and c_s is specific heat capacity for the regenerator matrix.

The assumption of a linear temperature gradient in the matrix (and gas) is kept. This does not change the equation above when the mean temperature (which is identical to the temperature in the middle of the regenerator) is used.

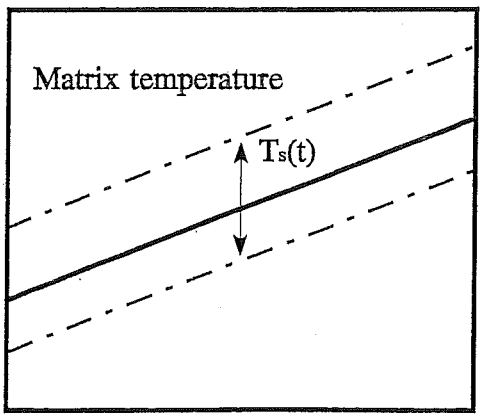

Figure 8.2 Variable solid matrix temperature in a regenerator with linear temperature gradient.

8.2.6 Friction losses

Pressure losses

The pressure is assumed to be uniform in space in the Simple Five-Volume Model. This assumption is somewhat justified by the fact that in a well-designed Stirling engine the pressure fluctuations around the average spatial pressure are small compared to the actual absolute value of the pressure. Uniform pressure greatly simplifies the numerical solution of the problem, since the equation for conservation of momentum is reduced to an assumption of pressure as a function of time only. Pressure losses due to friction, acceleration and acoustics (pressure information travelling as a sound wave) are completely ignored. In this way significant properties are lost, partly with respect to the flow conditions, and partly in form of an idealized calculation of the performed work and heat in- and output.

It is possible to adjust the overall performance from a simulation of an engine, by correcting work and heat transfer. This can be done by using the obtained values for velocity or mass flow from the simulation to calculate a pressure loss due to friction and the corresponding work done by these forces (dissipation). The effect of these corrections will then be a smaller work output from the expansion piston, higher work input on the compression piston, less heat input in the heater and more heat out in the cooler. The underlying assumption is that the pressure losses do not affect the thermodynamic state. It is difficult to justify that this really is the case; nevertheless it is better than just ignoring any pressure losses, especially in a real design, where heat exchangers and regenerator have to be optimized with regard to heat transfer. This kind of correction has been used by Carlsen is his Stirling code [1].

A less idealized approach is obtained by including a "static" pressure loss. If the time dependent term and convective term are ignored in the momentum equation, then the pressure gradient in space is given as a function of the viscous stress. This means that for a one-dimensional model, dp/dx is a function of an equivalent friction force. The equations for the static pressure difference can be included directly into the system of equations as additional algebraic equations.

For one-dimensional compressible flow the equation for conservation of momentum in differential form is given as

$$\frac{\partial}{\partial t}(\rho \cdot u \cdot A_c) + \frac{\partial}{\partial x}(\rho \cdot u^2 \cdot A_c) = -\frac{\partial}{\partial x}(p \cdot A_c) + \tau_w \cdot \frac{A}{L} \qquad (8.32)$$

where τ_w is the equivalent wall friction (see section 4.3 where also the geometric parameters are defined). No volume forces have been included since it is gas flow which is of interest.

Ignoring the two first terms in this equation (see Bauwens [6] for a discussion of this assumption) and assuming a constant free-flow area A_c, it implies

$$\frac{dp}{dx} = \frac{A}{A_c \cdot L} \cdot \tau_w \qquad (8.33)$$

It should be noted that the assumption of constant free-flow area only is a good approximation inside a component. On the interface between two components abrupt changes can and will occur.

A friction factor f (Fanning) can be defined for one-dimensional compressible flow

$$f \equiv \frac{\tau_w}{\frac{1}{2}\cdot\rho\cdot u^2} \tag{8.34}$$

which implies that

$$\frac{dp}{dx} = f\cdot\frac{4}{D_h}\cdot\frac{1}{2}\cdot\rho\cdot u^2 \tag{8.35}$$

since the hydraulic diameter is defined as

$$\frac{D_h}{L} \equiv 4\cdot\frac{A_c}{A} \tag{8.36}$$

Pressure difference Δp over the length L is then given as

$$\Delta p = \frac{dp}{dx}\cdot L = f\cdot\frac{4\cdot L}{D_h}\cdot\frac{1}{2}\cdot\rho\cdot u^2 = f\cdot\frac{4\cdot L}{D_h}\cdot\frac{\dot{m}^2}{2\cdot\rho\cdot A_c^2} = \frac{f\cdot L^2}{2}\cdot\frac{4\cdot L}{D_h}\cdot\frac{\dot{m}^2}{M\cdot V} \tag{8.37}$$

or

$$\Delta p = \frac{f\cdot L^2}{2}\cdot\frac{A}{A_c}\cdot\frac{\dot{m}^2}{M\cdot V} \tag{8.38}$$

Notice that the equation is expressed using the mass M and volume V of the considered volume. This is convenient, since the system of equations is solved for the extensive variables.

The equivalent friction force F_{fr} can be defined as

$$F_{fr} = \tau_w\cdot A = \Delta p\cdot A_c \tag{8.39}$$

The energy dissipation due to friction (work done by friction forces) is then given as

$$\dot{E}_{diss} = \Delta p\cdot A_c\cdot u = A_c\cdot f\cdot\frac{4\cdot L}{D_h}\cdot\frac{1}{2}\cdot\rho\cdot|u|^3 = f\cdot\frac{4\cdot L}{D_h}\cdot\frac{|\dot{m}|^3}{2\cdot\rho^2\cdot A_c^2} = \frac{f\cdot L^2}{2}\cdot\frac{4\cdot L}{D_h}\cdot\frac{|\dot{m}|^3}{M^2} \tag{8.40}$$

or

$$\dot{E}_{diss} = \frac{f\cdot L^2}{2}\cdot\frac{A}{A_c}\cdot\frac{\dot{m}^3}{M^2} \tag{8.41}$$

This term should, for the sake of consistency, be included as a heat source term (always positive) in the equation for conservation of energy.

The friction factor f is usually given as a function of the geometry and a Reynolds number.

Next some typical examples of expressions for friction factors for the classical Stirling components will be given:

Regenerator

Miyabe [2] gives the following expression (all Reynolds numbers)

$$f = \frac{33.6}{Re} + 0.337 \tag{8.42}$$

where the Reynolds number is based on the mesh distance.

Carlsen [7] gives the following expression based on his own experiments

$$f = 40.15 \cdot Re^{-0.932} + 0.301 \tag{8.43}$$

where the hydraulic diameter D_h is the characteristic length for the Reynolds number.

Heat exchanger

An analytical expression exists for laminar flow inside circular tubes of diameter d

$Re_d < 2300$

$$f = \frac{16}{Re_d} \tag{8.44}$$

For turbulent flow empirical correlations must be used. For heat exchangers Martini [8] gives the following expression, which is widely applied in Stirling analysis:

$Re_d > 2300$

$$f = 0.0457 \cdot Re_d^{-0.2} \tag{8.45}$$

Carlsen [4] corrects this expression for in- and outflow losses.

Variable volumes

The flow is at least two-dimensional and irregular due to effects from piston motion, in- and outflow conditions and a relative large length to diameter ratio.

The pressure loss due to friction in these volumes is usually considered insignificant.

General expressions for friction losses and dissipation

To maintain a possibility to include in- and outflow losses, the friction factor will be written in the following general form

$$f = C_1 \cdot Re^{C_2} + C_3 = C_1 \cdot \left(\frac{D}{A_c \cdot \mu} \right)^{C_2} \cdot |\dot{m}|^{C_2} + C_3 \tag{8.46}$$

where D is a characteristic length.

The pressure difference over the component length L can now be written as

$$\Delta p = - \frac{A}{A_c} \cdot \frac{L^2}{2 \cdot M \cdot V} \cdot \left[C_1 \cdot \left(\frac{D}{A_c \cdot \mu} \right)^{C_2} \cdot |\dot{m}|^{C_2} + C_3 \right] \cdot |\dot{m}| \cdot \dot{m} \tag{8.47}$$

and the dissipation

$$\dot{E}_{diss} = \frac{A}{A_c} \cdot \frac{L^2}{2 \cdot M^2} \cdot \left[C_1 \cdot \left(\frac{D}{A_c \cdot \mu} \right)^{C_2} \cdot |\dot{m}|^{C_2} + C_3 \right] \cdot |\dot{m}|^3 \tag{8.48}$$

The results for the friction factor expressions can be summarized as follows:

Regenerator:

Miyabe (characteristic length: mesh distance)

$C_1 = 33.6$ $C_2 = -1$ $C_3 = 0.337$

Carlsen (characteristic length: hydraulic diameter)

$C_1 = 40.15$ $C_2 = -0.932$ $C_3 = 0.301$

Heat exchangers (tubes):

Martini

$C_1 = 16$	$C_2 = -1$	$C_3 = 0$	$Re < 2300$
$C_1 = 0.0457$	$C_2 = -0.2$	$C_3 = 0$	$Re > 2300$

Carlsen

$C_1 = 16$	$C_2 = -1$	$C_3 = C_4 \cdot 4 \cdot \frac{A_c}{A}$	$C_4 = 0.25$ *to* 1.0	$Re < 2300$
$C_1 = 0.0457$	$C_2 = -0.2$	$C_3 = C_4 \cdot 4 \cdot \frac{A_c}{A}$	$C_4 = 0.25$ *to* 1.0	$Re > 2300$

8.2.7 Scaling

Convection heat transfer

The expression for the NTU-number is already dimensionsless, but may be put in a convenient form introducing a reference Reynolds number Re_{ref} using the reference variables defined in section 6.2.1. This will explicitly give the dependence of mass flow. The NTU-number can be written as:

$$NTU = C \cdot Re_{ref}^{1-b} \cdot |\tilde{m}|^{b-1} \tag{8.49}$$

where C is a dimensionless constant and

$$Re_{ref} = \frac{D}{A_c \cdot \mu} \cdot \frac{M_{ref}}{t_{ref}} \qquad \tilde{m} = \frac{\dot{m}}{\left(\frac{M_{ref}}{t_{ref}} \right)}$$

Conduction heat transfer

The expression for the heat conduction can be scaled in the following way

$$\frac{\dot{Q}_{cond}}{\frac{M_{ref} \cdot c_v \cdot T_{ref}}{t_{ref}}} = \frac{\frac{k \cdot A}{L}}{\left(\frac{M_{ref} \cdot c_v}{t_{ref}} \right)} \cdot \frac{\frac{dT}{dx} \cdot L}{T_{ref}} \quad \Rightarrow \tag{8.51}$$

$$\tilde{Q}_{cond} = \tilde{k} \cdot \tilde{\alpha}$$

where

$$\tilde{k} = \frac{\frac{k \cdot A}{L}}{\left(\frac{M_{ref} \cdot c_v}{t_{ref}} \right)} \qquad \tilde{\alpha} = \frac{\frac{dT}{dx} \cdot L}{T_{ref}} \tag{8.52}$$

Pressure loss and dissipation

An additional reference variable has to be introduced for the scaling of these equations. There is no obvious choice for this reference variable which gives a fully satisfactory dimensionless form. The following variables could be used for a reference for either length or speed

- Speed of sound (at the reference temperature).
- Period of the cycle.
- Length of the component.
- Stroke.
- Total length of the machine.

It has been chosen to use the speed of sound at the reference temperature as a reference velocity, i.e.,

$$u_{ref} = \sqrt{\gamma \cdot R \cdot T_{ref}} \tag{8.53}$$

The period of the cycle has already been chosen as the natural reference for the time scale, i.e.,

$$t_{ref} = t_p \tag{8.54}$$

and then a reference length L_{ref} can be defined from the two others (in order not to introduce unnecessarily many reference parameters) as

$$L_{ref} = u_{ref} \cdot t_{ref} \tag{8.55}$$

Typical values for a Stirling engine using Helium as a working gas are

$\gamma = 1.667$
$R = 2079$ J/(kg·K)
RPM = 1550
$T_{Heater} = 1000$ K

which gives following reference parameters

$$\begin{aligned} T_{ref} &= 1000\ K \\ t_{ref} &= \frac{60}{1550} = 38.7 \cdot 10^{-3} s \\ L_{ref} &= 38.7 \cdot 10^{-3} s \cdot \sqrt{1.667 \cdot 2079 J/(kg \cdot K) \cdot 1000\ K} \approx 72\ m \end{aligned} \tag{8.56}$$

Notice that the reference length L_{ref} is much larger than any other length involved. This confirms that the pressure information propagates in a time scale which is a magnitude smaller than the scales related to the mass and energy equations.

The dimensionless pressure loss can then be written as

$$\frac{\Delta p}{p_{ref}} = \frac{f}{2}\cdot\frac{L^2\cdot\gamma}{t_{ref}^2\gamma\cdot R\cdot T_{ref}}\cdot\frac{4\cdot L}{D_h}\cdot\left(\frac{\dot{m}}{\frac{M_{ref}}{t_{ref}}}\right)^2\cdot\frac{M_{ref}\cdot V_{ref}}{M\cdot V} \quad \Rightarrow$$

$$\Delta\tilde{p} = \frac{\gamma\cdot f\cdot\tilde{L}^2}{2}\cdot\frac{4\cdot L}{D_h}\cdot\frac{\tilde{m}^2}{\tilde{M}\cdot\tilde{V}} \qquad (8.57)$$

and the dimensionless dissipation as

$$\frac{\dot{E}_{diss}}{\frac{M_{ref}\cdot c_v\cdot T_{ref}}{t_{ref}}} = \frac{f}{2}\cdot\frac{L^2\cdot\gamma}{t_{ref}^2\gamma\cdot R\cdot T_{ref}}\cdot\frac{R}{c_v}\cdot\frac{4\cdot L}{D_h}\cdot\left(\frac{\dot{m}}{\frac{M_{ref}}{t_{ref}}}\right)^3\cdot\left(\frac{M_{ref}}{M}\right)^2 \quad \Rightarrow$$

$$\tilde{E}_{diss} = \gamma\cdot(\gamma-1)\cdot\frac{f\cdot\tilde{L}^2}{2}\cdot\frac{4\cdot L}{D_h}\cdot\frac{\tilde{m}^3}{\tilde{M}^2} \qquad (8.58)$$

An order-of-magnitude analysis for the expression for the pressure loss shows that the pressure differences in space will be small compared to the absolute value of the pressure.

8.2.8 System of equations

Alternative formulation

Introducing the nonlinearities in form of the variable NTU-numbers and friction losses, makes the direct application of the explicit Runge-Kutta method impossible. The derived sub system of equations (see the derivation in section 6.2.3) is no longer linear if the NTU-number is a function of the mass flow, and a kind of ad hoc linearization is needed for the solution procedure, when an explicit Runge-Kutta method is applied.

Implicit Runge-Kutta methods may be used for both formulations. The alternative formulation could still be attractive, since it has fewer differential variables than the basic formulation when friction losses (which gives a spatial distribution of pressure) are excluded. However, as soon as friction is included, there are no differences and the basic formulation, which has the governing equations in conservation form, is preferred.

For these reasons, only the basic formulation of the system of equations has been considered in the following.

Basic formulation

The system of governing equations for one volume (component) for the general *i*th volume:

$$\frac{dM_i}{dt} = \dot{m}_{i-1/2} - \dot{m}_{i+1/2}$$

$$\frac{dE_i}{dt} = \gamma \cdot \left(\dot{m} \cdot \frac{E}{M}\right)_{i-1/2} - \gamma \cdot \left(\dot{m} \cdot \frac{E}{M}\right)_{i+1/2} + \dot{Q}_{i,conv} + \dot{W}_i + \dot{E}_{i,diss} \qquad (8.59)$$

$$\Delta p_i = p_{i+1/2} - p_{i-1/2} = -\left(\frac{A}{A_c}\right)_i \cdot \frac{\gamma \cdot L_i^2}{2 \cdot M_i \cdot V_i} \cdot \left[C_1 \cdot \left(\frac{D}{A_c \cdot \mu}\right)^{C_2} \cdot |\dot{m}|^{C_2} + C_3\right]_i \cdot |\dot{m}_i| \cdot \dot{m}_i$$

$$p_i \cdot V_i - E_i = 0$$

These equations have been scaled using the reference variables defined in the previous section and in section 6.2.1 (superscripts have been omitted).

For the variable volumes $\Delta p=0$ and $\dot{E}_{diss}=0$ and for all other volumes $\dot{W}=0$.

8.2.9 Test data

The developed simulation codes are tested on the same test example using the same input data as for SFVSM, but the required additional information is provided in the following table:

Component no.	1	2	3	4	5
Component type	VVC	HEX	REG	HEX	VVC
Max. swept volume [m^3]	$493.7 \cdot 10^{-6}$				$441.6 \cdot 10^{-6}$
Clearance volume [m^3]	$137 \cdot 10^{-6}$	$210 \cdot 10^{-6}$	$368 \cdot 10^{-6}$	$515 \cdot 10^{-6}$	$43 \cdot 10^{-6}$
Initial phase angle [°]	127.197				0.000
Free flow area [m^2]	$8.66 \cdot 10^{-3}$	$1.06 \cdot 10^{-3}$	$8.37 \cdot 10^{-3}$	$1.21 \cdot 10^{-3}$	$8.66 \cdot 10^{-3}$
Heat transfer area [m^2]	$26.6 \cdot 10^{-3}$	$305.4 \cdot 10^{-3}$	10.394	$220.2 \cdot 10^{-3}$	$25.5 \cdot 10^{-3}$
Cyclic heat transfer	Yes	No	Yes	No	Yes
Solid temperature [K]		328		973	
Solid wall mass [kg]			0.821		

Table Input data for the Extended Five-Volume Stirling Model.

Speed: 1550 RPM
Required mean pressure: p_{mean} = 8 Mpa
Working gas: Helium
Gas constant: R = 2079.5 J/(kg·K)
Gas specific heat capacity: c_p= 5093 J/(kg·K)
Matrix specific heat capacity: c_M= 570 J/(kg·K)
Matrix porosity: ϱ = 0.78
Matrix thread diameter: $d_w = 0.04 \cdot 10^{-3}$m

The complete set of engine data is given in Appendix F.

VVC, HEX and REG denote variable volume (with cyclic heat transfer), heat exchanger and regenerator respectively.

In the EFVSM it is possible to specify, which new features should be included in the actual simulation. This makes it easy to study the importance of each of these, partly with regard to the simulation of the performance of the engine, and partly with regard to influence on the effectiveness of the numerical approaches and methods.

8.2.10 Results

In this section, the most important results for the EFVSM are discussed.

First some general results introducing and illustrating the new features of this model will be given in form of figures showing the NTU-number, the solid matrix temperature and the pressure difference between the two variable volumes. Then the significance of each of these new features will be addressed and finally, the importance for the applied numerical approaches will be discussed for interesting numerical methods selected among those considered for the SFVSM-problem.

The NTU-number is shown as a function of time for the regenerator, heat exchangers and variable volumes in the following three figures.

Regenerator

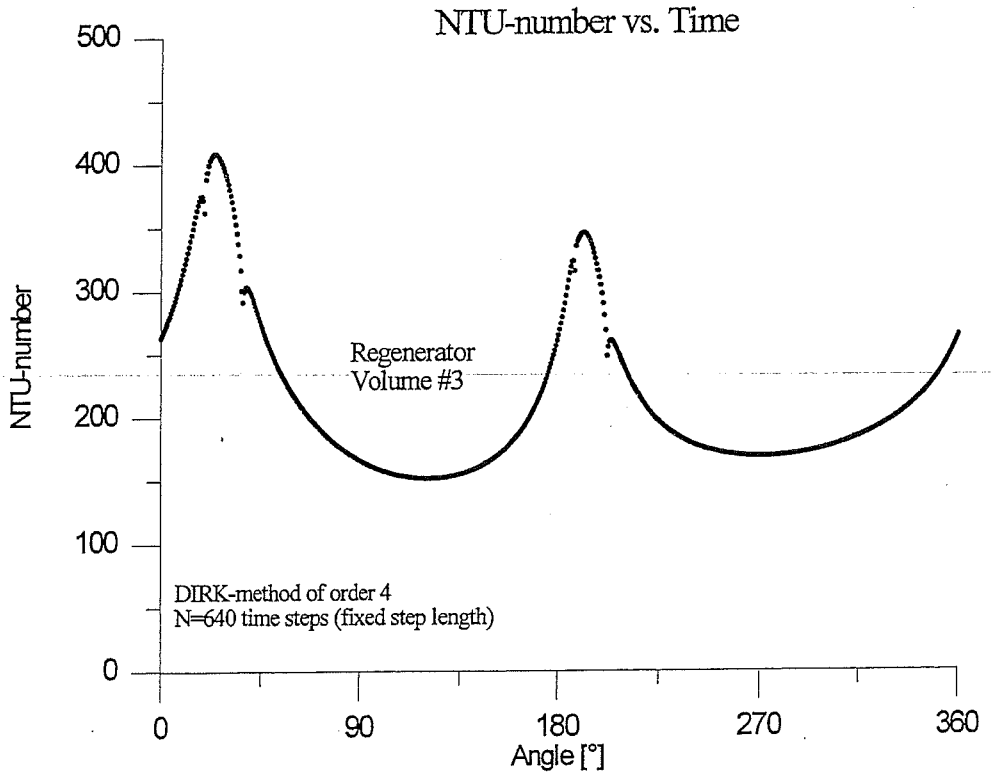

Figure 8.3 NTU-number in the regenerator.

Heat exchangers

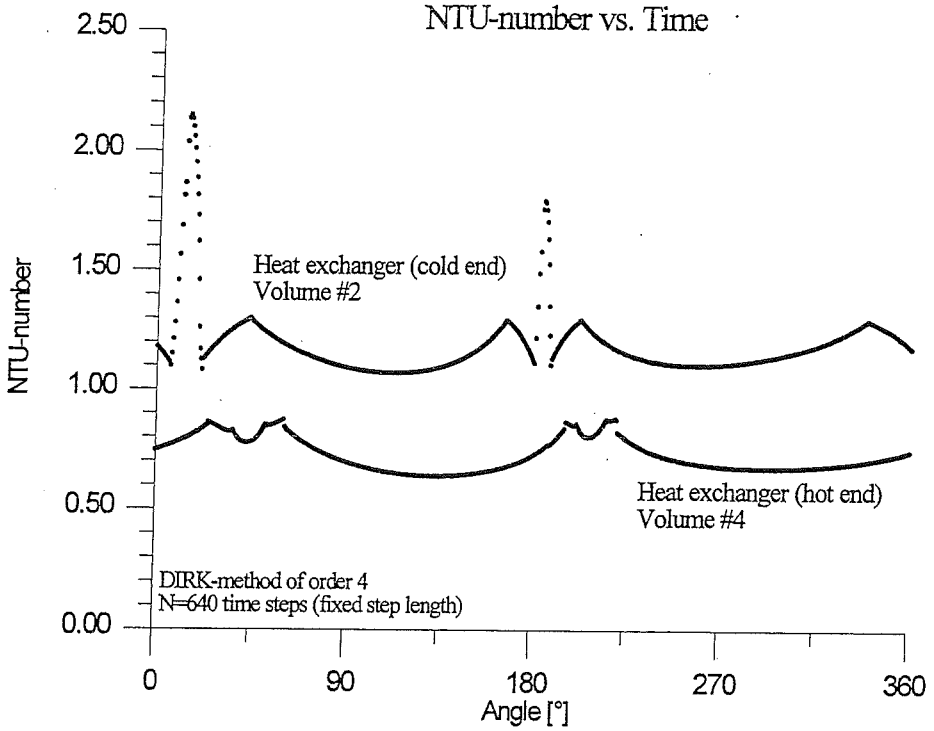

Figure 8.4 NTU-numbers in the heat exchangers.

Variable volumes

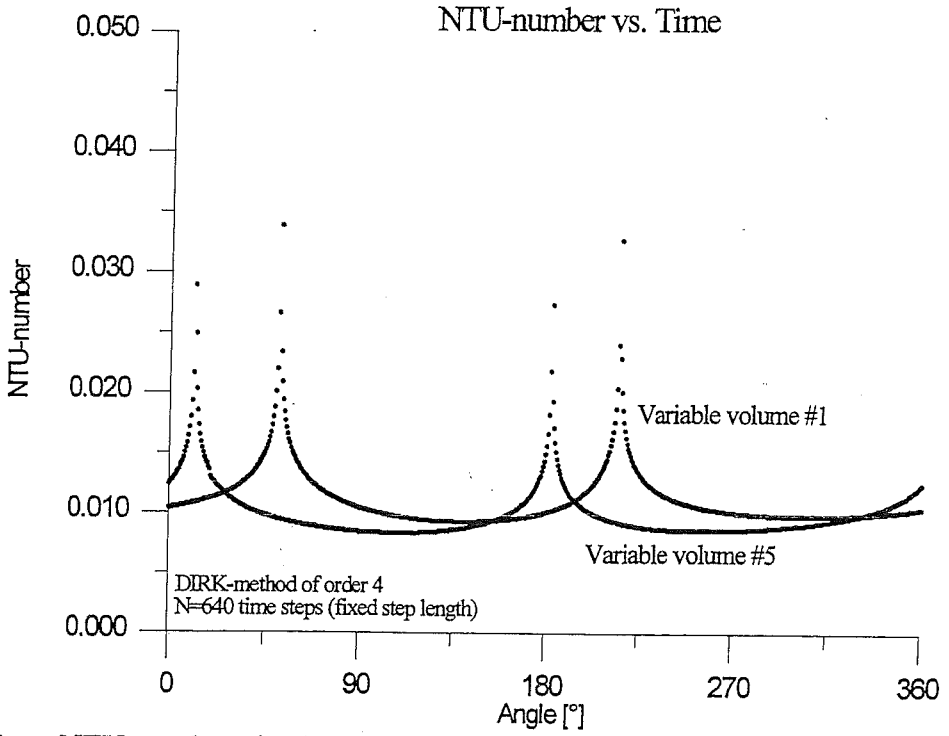

Figure 8.5 NTU-numbers in the variable volumes.

The peaks of the NTU-numbers are due to small values of the mass flows. When the mass flow tends to zero the NTU-number becomes infinite (see the definition for the NTU-number).

Next, the matrix temperature in the middle of the regenerator together with the gas temperature (in the middle of the same volume) is shown as function of time. It should be noted that the convective heat transfer is calculated using this temperature difference.

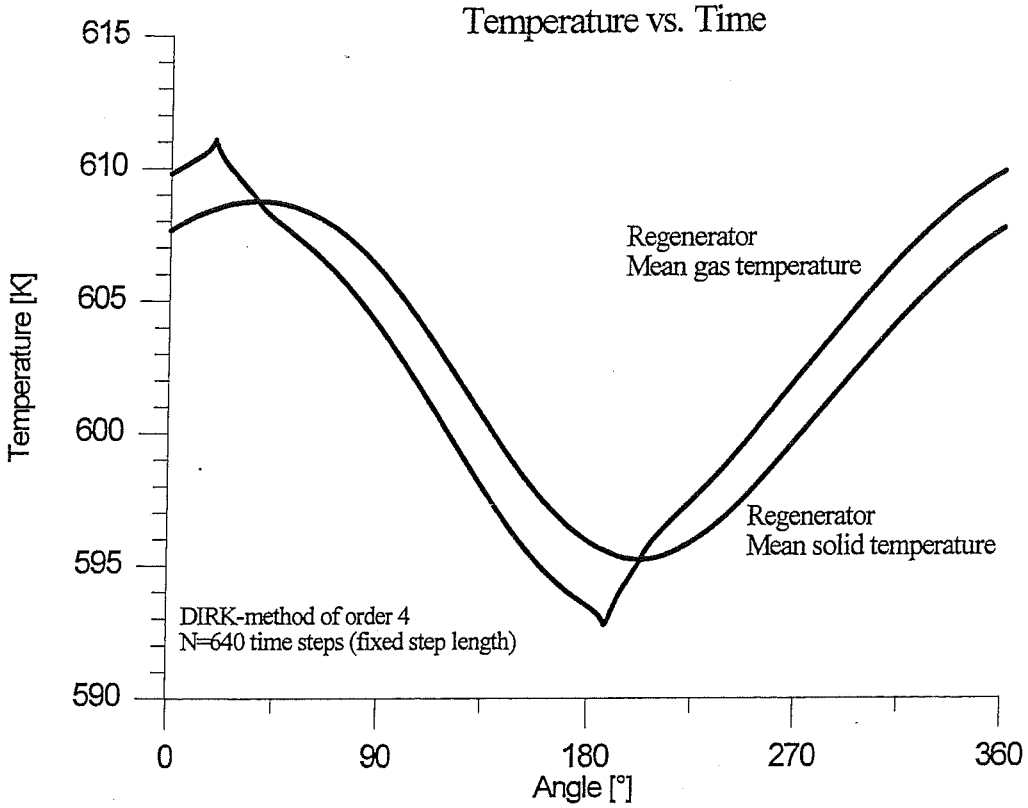

Figure 8.6 Gas and solid matrix temperature in the regenerator.

The pressure difference between the two variable volumes (due to friction) is shown in the following figure.

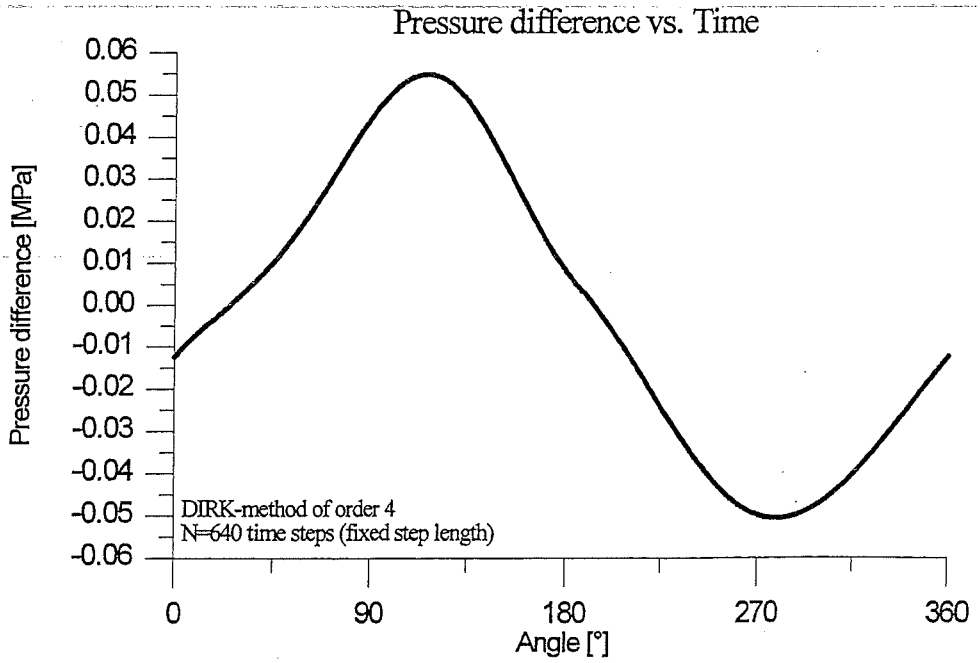

Figure 8.7 Pressure difference between the two ends of the Stirling engine.

Next the importance of each of the new features will be discussed and compared to the results from the SFVSM-problem

	[1] SFVSM	Variable [2] NTU-number	Heat [3] conduction	Variable [4] matrix temperaure	Pressure [5] losses and dissipation	[6] EFVSM
Efficiency	0.5064	0.4999	0.5057	0.5060	0.5012	0.4932
Work in [W]	15655	16298	15656	16027	15988	16989
Work out [W]	34241	34404	34239	34067	33886	33962
Heat in [W]	36699	36218	36750	35656	35713	34418
Heat out [W]	18113	18111	18166	17616	19108	18699
Reg. loss [W]	2458	1814	2458	1589	3001	1542
Heat cond. [W]			53			47
Dissipation [W]					1088	1053
Temp.grad. [K]	545.1	479.2	545.0	547.7	545.9	484.0
Total mass [g]	12.2493	12.3832	12.2490	12.2529	12.2265	12.3477

[1] Results from the SFVSM, no additional features included.
[2] Calculation of heat transfer using variable NTU-number as function of mass flow included.
[3] Calculation of heat conduction through the regenerator included.
[4] Finite heat capacity of regenerator matrix.
[5] Calculation of pressure losses and dissipation included.
[6] Results from the full EFVSM, all additional features included.

Remarks:

i) The numerical results are obtained using the Shooting method and the 4. order DIRK method and a fixed step length with N=640 steps for one cycle. All the results have been checked using the NT I method with a tolerance TOL=0.0002.

ii) It should be mentioned that the fixed NTU-numbers used in the simulation of SFVSM-problem have been based on tests with the EFVSM, implying that the results from SFVSM are better (i.e., closer to the EFVSM) than it could have been expected from pure guesses on the NTU-numbers.

iii) The NTU-number used in the simulation of the SFVSM are in general smaller than the "real" NTU-numbers. This results in the fact that the effect of each feature is not directly comparable in the table above.

iv) The mean pressure is calculated as the pressure on the compression piston (i.e., the pressure in variable volume #1).

v) Only heat conduction seems to be insignificant for the simulation results. All the other features affect the outcome.

vi) One must be careful not to draw too many conclusions from just one test example, but other tests have shown similar tendencies.

vii) Real engine efficiencies are in the order of 0.2-0.3, and even if the external losses (e.g., mechanical losses) are to be included in the simulation models, the results are still significantly better than the reality. Additional parasitic losses must be added to obtain results closer to real engine performance. This subject will not be pursued further in this thesis, since it is the numerical methods which are of primary concern.

Numerical tests

The following table shows the number of cycles required for convergence to the periodic steady-state solution for each of the numerical approaches considered in this thesis.

Method		SFVSM	Variable NTU-number	Heat conduction	Variable matrix temperature	Pressure losses and dissipation	EFVSM
I-to-C	DIRK4 [1]	64	79	64	606	65	907
	DIRK4 [2]	64	79	64	604	65	911
	NT I [3]	64	79	64	600	65	907
Shooting	DIRK4 [1]	19	21	19	20	19	20
	DIRK4 [2]	20	20	20	20	20	21
	NT I [3]	20	20	19	20	19	20
Finite Diff.	DD6 [4]	4	5	4	4	4	4
	DD6 [5]	4	4	4	4	4	4
	Simpson[6]	4	6	4	4	4	4

1) Fixed step length N=640.
2) Fixed step length N=40.
3) Variable step length TOL=0.0002.
4) Divided differences of order six, N=160 steps.
5) Divided differences of order six, N=40 steps.
6) Simpson's method, N=160 steps.

Remarks:

i) For the Finite-Difference method, the "number of cycles" given in the table is identical to the number of iterations for full system of nonlinear equations. The periodic steady-state solution is found at once for this approach.

ii) When the assumption of fixed solid matrix temperature in the regenerator is abandoned, the performance of the Integration-to-Convergence (which already is poor for the SFVSM) really decreases and becomes impossible to use in practice.

iii) Seemingly, there are no problems using the Shooting method. The method behaves just as for SFVSM for each of the new features (variable NTU-number, heat conduction, etc.) introduced, and even the full EFVSM is solved very fast.

iv) The same can be said about the Finite-Difference method. The performance of the method is basically unaffected by these new features.

This concludes the analysis and discussion of the five volume Stirling models. The conclusions and the further discussion of the most important results will be continued in chapter 9.

8.3 Multi-Volume Stirling Model (MVSM)

8.3.1 Introductory remarks

In this section the Multi-Volume Stirling Model (MVSM) is formulated. In this model an arbitrary number of components may be defined, and each of these components (with the exception of the variable volumes) may be divided into a number of smaller sub volumes. This means that a true spatial variation within each component now may be studied in detail, as opposed to the previous "lumped" formulation. The new formulation is equivalent of a Finite-Volume type discretization of the governing system of partial differential equations (PDEs) and, coupled with a numerical method for the time integration of ordinary differential equations (ODEs). This is similar to semi-discretizations methods for systems of PDEs, such as the Methods of Lines.

MVSM is still only one-dimensional in space and the flux terms at the boundaries are evaluated as a first order upwind difference analogous to the SFVSM. Problems regarding numerical diffusion have been observed, and some modifications will be discussed.

The first part of this section is devoted to the actual discretization and modelling. The physical model is shortly described and then translated into a mathematical model. Each of the components is divided into a number of sub volumes (corresponding to a Finite Volume discretization), and the new mathematical model consists of a system of differential-algebraic equations (DAEs) in form of the well-known equations for conservation of mass, momentum and energy and an equation of state for each of these sub volumes.

The last part addresses the numerical methods and the actual implementation in computer code. A test example is given, and simulation results are shown and discussed. The implementations for all three approaches (Integration-to-Convergence, Shooting and Finite Difference) are discussed in this section.

8.3.2 Physical model

An arbitrary number of components can be defined for a model of a given Stirling engine. The following component models have been developed for the simulation of the considered Stirling engine:

- Variable cylinder volume.
- Heat exchanger (tube).
- Regenerator.
- Manifold volume.

Only the last of these components has not been described in detail previously.

Variable volumes

The volume variations in these volumes are still assumed to be given explicitly. Heat transfer conditions may be specified in form of the condition of "cyclic heat transfer", a fixed NTU-number (this case includes adiabatic walls for NTU=0) or a constant wall temperature (non-zero net heat transfer for one cycle).

Heat exchangers

As for the SFVSM and EFVSM, the heat transfer conditions in the heat exchanger components are approximated by assuming a constant solid wall surface temperature.

Regenerator

The assumption of a linear temperature gradient in the regenerator is omitted, since it is now possible to get a "real" spatial variation of temperature inside the regenerator due to the one-dimensional spatial discretization discussed next.

A fixed regenerator matrix temperature, determined from the condition of "cyclic heat transfer" has been used to describe the heat transfer conditions. However, the implementation of variable solid temperature for the solid matrix has also been considered in some detail.

Manifold volumes

Manifold volumes are inactive volumes placed between two of the other components. These are typically fittings or other connection volumes which contribute to the total dead volume inside the engine. Large dead volumes will significantly degrade the performance of the engine, so including manifold volumes in a proper way could be important for obtaining realistic simulation results. Heat transfer conditions may be given in the same form as for the variable volumes.

The assumption of uniform pressure distribution in space in the whole engine is retained from the SFVSM, which means that the equation for conservation of momentum is reduced to the trivial conditions of just one uniform pressure in space. No friction or other pressure losses are included, but the extension to a full system of equations, where the "true" momentum equation is included, will be discussed later in this section.

8.3.3 Discretization

A spatial discretization of the given physical model of a Stirling engine with N_{comp} components (typically in form of two variable volumes, two heat exchangers, a regenerator and one or more manifold volumes located between the other components) is now considered in detail.

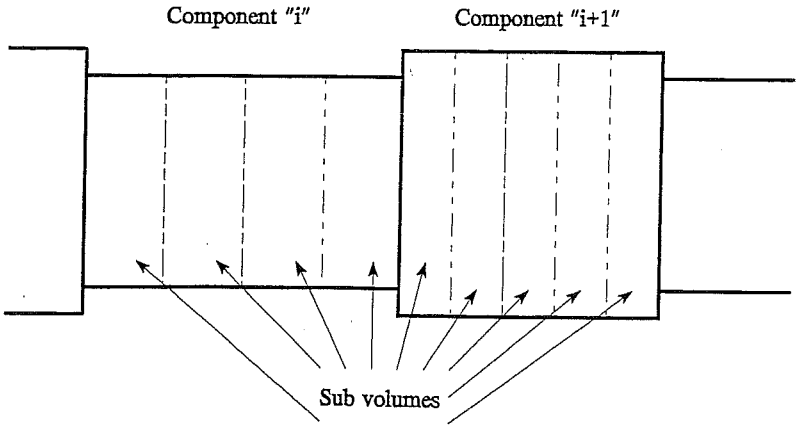

Figure 8.8 Components and sub volumes in the MVSM.

Spatial discretization (Finite Volume)

Consider a general component with a fixed volume (i.e., regenerator, heat exchanger or manifold volume for a Stirling engine).

The *k*th component of length L_k is divided into $N_{sv,k}$ sub volumes (finite volumes) of constant length Δx

$$\Delta x = \frac{L_k}{N_{sv,k}} \tag{8.60}$$

The following figure shows the *i*th volume and the two adjacent volumes (i-1 and i+1) for a given component

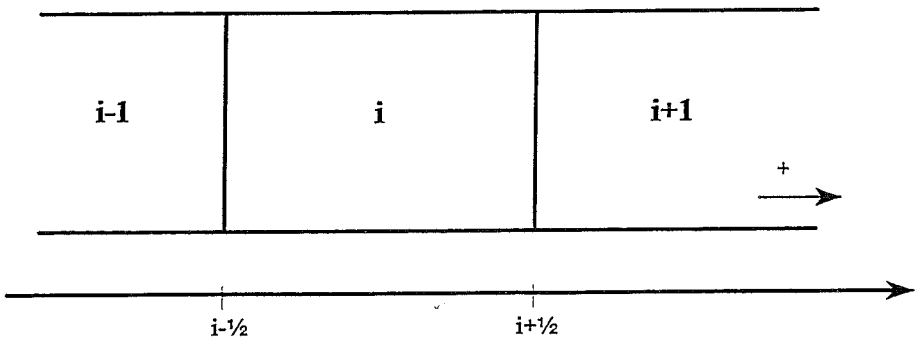

Figure 8.9 Sub volumes in a general component.

The free flow area A_c in a sub volume in the *k*th component is assumed to be constant and then given as

$$A_c = A_{c,k} \tag{8.61}$$

and the heat transfer area A

$$A = \frac{A_k}{N_{sv,k}} \tag{8.62}$$

where $A_{c,k}$ and A_k are the free flow area and heat transfer area respectively for the component.

The total number of sub volumes for the full discretization of the engine is given as

$$N_{tot} = \sum_{k=1}^{Ncomp} N_{sv,k} \tag{8.63}$$

8.3.4 Equations and boundary conditions

Now, consider a general sub volume. A general conservation law can be written in the following form (see chapter 4)

$$\begin{aligned} \int_{\Delta x} \frac{\partial U}{\partial t} \cdot dx &= \int_{\Delta x} \frac{\partial \phi}{\partial x} \cdot dx + \int_{\Delta x} S \cdot dx \quad \Rightarrow \\ \frac{d\overline{U}}{dt} \cdot \Delta x &= \phi(x_{i+1/2}) - \phi(x_{i-1/2}) + \overline{S} \cdot \Delta x \end{aligned} \tag{8.64}$$

where U is a specific variable, ϕ is the flux term, S the source term and the superscripts indicate the averaged value (in space) of the variable.

If the cross-sectional area A_c is assumed to be constant inside the component, then the equations of conservation of mass, momentum and energy in semi-discretized form for the *i*th sub volume can be written as:

Conservation of mass:

$$\frac{d}{dt}\left(\rho \cdot A_c \cdot \Delta x\right)_i = \left(\rho \cdot A_c \cdot u\right)_{i-1/2} - \left(\rho \cdot A_c \cdot u\right)_{i+1/2} \tag{8.65}$$

Conservation of momentum:

$$\frac{d}{dt}\left(\rho \cdot u \cdot A_c \cdot \Delta x\right)_i = \left(\rho \cdot A_c \cdot u^2\right)_{i-1/2} - \left(\rho \cdot A_c \cdot u^2\right)_{i+1/2} - \left((p \cdot A_c)_{i+1/2} - (p \cdot A_c)_{i-1/2}\right) + F_{fric,i} \tag{8.66}$$

Conservation of energy:

$$\frac{d}{dt}\left(\rho \cdot e \cdot A_c \cdot \Delta x\right)_i = \left(\rho \cdot A_c \cdot u \cdot \left(e + \frac{p}{\rho}\right)\right)_{i-1/2} - \left(\rho \cdot A_c \cdot u \cdot \left(e + \frac{p}{\rho}\right)\right)_{i+1/2} + \dot{Q}_{conv,i} + \dot{W}_i + \dot{E}_{diss,i} \tag{8.67}$$

Equation of state:

$$p \cdot V_i = (\gamma - 1) \cdot E_i \tag{8.68}$$

where the total energy is given as

$$E_i = \rho_i \cdot V_i \cdot e_i = M_i \cdot e_i \tag{8.69}$$

Pressure losses are neglected and together with the assumption of a uniform pressure in space this implies that

$$F_{fric} = 0 \qquad \dot{E}_{diss} = 0 \tag{8.70}$$

and

$$p_{i-1/2} = p_{i+1/2} = p_i \tag{8.71}$$

Mass flow at boundary "i+½" is defined as

$$\dot{m}_{i+1/2} = (\rho \cdot A_c \cdot u)_{i+1/2} \tag{8.72}$$

The convection heat transfer for the *i*th volume can be written as

$$\dot{Q}_{conv,i} = |\dot{m}_i| \cdot c_p \cdot NTU_i \cdot (T_{s,i} - T_i) \tag{8.73}$$

where

$$NTU_i = NTU(|\dot{m}_i|) \tag{8.74}$$

Flux evaluation at the boundaries of the sub volumes must also be considered. Mass flows (or velocities) are directly calculated (defined) at the boundaries, but other variables are defined only in the middle of the volumes (as average values). The values of these variables at the boundaries have to be specified in order to evaluate the convective enthalpy flux term in the energy equations

A simple first order upwind flux evaluation is applied in the MVSM (analogous to the SFVSM and EFVSM). Each of the small sub volumes is considered as at one uniform state ("stirred" volume), and the flux out of such a volume and into adjacent volumes are given by that particular state only.

This is illustrated in the following figure:

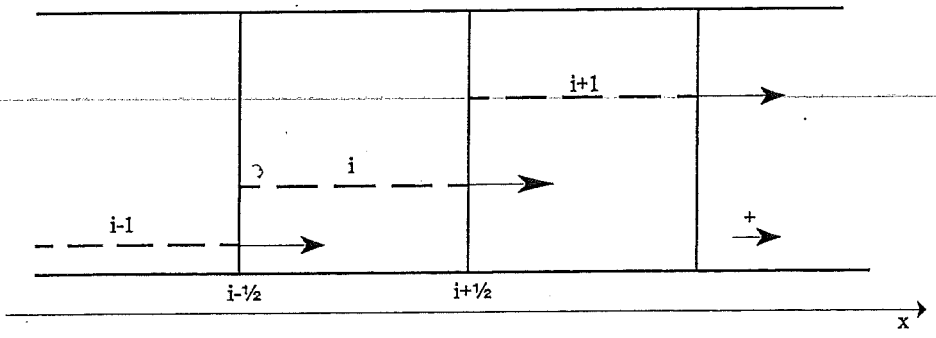

Figure 8.10 Upwind flux evaluation (shown for positive mass flows; $\dot{m}_{i+½} > 0$ and $\dot{m}_{i-½} > 0$).

E.g., the specific energy on boundary "i+½" is evaluated as

$$e_{i+1/2} = \begin{cases} e_i & \dot{m}_{i+1/2} > 0 \\ e_{i+1} & \dot{m}_{i+1/2} < 0 \end{cases} \tag{8.75}$$

and similar on boundary "i-½" and for the other variables which have to be evaluated at the boundaries.

Variable volumes

A component in form of a variable cylinder volume is treated as one large bulk volume. This makes the treatment of time dependent forcing term in form of the specified volume variation much easier. No moving boundaries and additional equation for conservation of volume have to be included into the system of equations. Furthermore the flow inside these volumes is highly irregular so a one-dimensional model will probably not give better results than the "lumped" model.

Because the volume variation is assumed to be given explicitly (e.g., sinusoidal piston motion), the actual volume and the derivative w.r.t. time are known at all times and the work can then be calculated as

$$\dot{W}_i = -p \cdot \frac{dV_i}{dt} \tag{8.76}$$

The convection heat transfer, in form of a variable NTU-number, is calculated using (8.73) and the expressions derived in section 8.2.2 for the variable volumes.

Heat exchanger

Volumes are constant in these components, and there are therefore no work term. The solid wall surface temperature is assumed to be constant (given as input data), and the convection heat transfer is calculated using (8.73) and the expressions derived in section 8.2.2 for the heat exchangers.

The component may be divided into an arbitrary number of sub volumes, such that the spatial variation can be resolved.

Regenerator

The volume is constant (no work term). "Cyclic heat transfer" condition is used for the heat transfer unless variable matrix temperature has been specified. For variable matrix temperature an additional differential equation, for the internal energy of the solid, has to be solved for each of the sub volumes in the component. Again, the convection heat transfer is calculated using (8.73) and the expressions derived for the regenerator in section 8.2.2.

The regenerator can be divided into an arbitrary number of sub volumes, such that the spatial variation can be resolved. As it will be shown later, a very fine resolution will be required for this component, in particular if an accurate numerical solution is to be obtained using an upwind difference for the flux term.

Manifold volumes

Volumes are constant in these components too (no work term). The condition of "cyclic heat transfer" is specified. Convection heat transfer is calculated using the expression derived for the variable volumes (i.e., flow inside a cylinder).

The component can (if necessary) be divided into an arbitrary number of sub volumes.

This gives the following general system of equations for the *i*th sub volume using the defined extensive variables

Conservation of mass

$$\frac{dM_i}{dt} = \dot{m}_{i-1/2} - \dot{m}_{i+1/2} \tag{8.77}$$

Conservation of energy

gas:

$$\frac{dE_i}{dt} = \left(\gamma \cdot \dot{m} \cdot \frac{E}{M}\right)_{i-1/2} - \left(\gamma \cdot \dot{m} \cdot \frac{E}{M}\right)_{i+1/2} + |\dot{m}_i| \cdot c_p \cdot NTU_i \cdot \left(T_{si} - \frac{E_i}{M_i \cdot c_v}\right) - p \cdot \frac{dV_i}{dt} \tag{8.78}$$

solid:

$$M_s \cdot c_s \cdot \frac{dT_{si}}{dt} = |\dot{m}_i| \cdot c_p \cdot NTU_i \cdot \left(\frac{E_i}{M_i \cdot c_v} - T_{si}\right) \tag{8.79}$$

"Conservation of momentum"

Under the assumptions made, the momentum equation is reduced to

$$p_{i-1/2} = p_{i+1/2} = p \tag{8.80}$$

A "correct" treatment of the fluid dynamics, within the limitations of one-dimensional flow and empirical correlations for friction and heat transfer, still requires solving the Euler equations (conservation of mass, momentum and energy and the equation of state for inviscid gas flow, see chapter 4) with additional source terms for friction and heat transfer.

Even though the Mach number usually is very small (no shocks), the flow must still be treated as compressible due to the thermal effects.

For the Euler equations pressure information (in the characteristic variables) propagates with speed u+c and u-c, where u is the velocity of the fluid and c is the local speed of sound. For Helium and temperatures around 900 K, c is equal to 1800 m/s. A typical regenerator length is 0.05m and discretizing the regenerator in space, with for example 200 elements (this will be necessary in order to avoid too much numerical diffusion due to the upwind flux discretization, as discussed later in this section) it gives a cell length $\Delta x = 0.00025$m.

A stability restriction (CFL-type), which is very common for hyperbolic problems, is the following

$$\Delta t < \frac{\Delta x}{\max(u \pm c)} \tag{8.81}$$

or a maximal step length of less than $\Delta t = 0.167 \cdot 10^{-6}$ sec (u is ignored).

A fast Stirling engine runs at 1800 RPM (0.033s pr. cycle), which means that approximately 200000 time steps should be used for the calculation of just one cycle. This is costly in time and money (even on the supercomputers of today) and a very good reason not to include the true momentum equation.

Boundary conditions

Periodic solution in the time domain with period t_p, i.e.,

$$p(t) = p(t + t_p) \qquad M_i(t) = M_i(t + t_p) \qquad E_i(t) = E_i(t + t_p) \tag{8.82}$$

etc.

In particular, this gives periodic boundary conditions in time

$$p(0) = p(t_p) \qquad M_i(0) = M_i(t_p) \qquad E_i(0) = E_i(t_p) \tag{8.83}$$

In space, no flux through the ends of the engine gives the following two conditions:

$$\dot{m}_{1/2} = 0 \qquad \dot{m}_{N_{tot}+1/2} = 0 \tag{8.84}$$

For the Stirling models considered, this will be the end of each of the two variable volumes.

8.3.5 Cyclic integral conditions

The actual mean pressure must still be identical to the required mean pressure p_{mean}, which gives one of the cyclic integral conditions.

$$p_{mean} - \frac{1}{t_p} \cdot \int_{t=0}^{t_p} p \cdot dt = 0 \tag{8.85}$$

It could be mentioned here that the main reason for being strict concerning the exact required mean pressure is that for comparisons between different design (e.g., in an optimization routine) the work output mainly is dependent on the mean pressure of the cycle.

For each of the sub volumes in a component, where the condition of "cyclic heat transfer" has been specified, the following condition must be satisfied.

$$\int_{t=0}^{t_p} |\dot{m}_i| \cdot c_p \cdot NTU_i \cdot \left(T_{si} - \frac{E_i}{M_i \cdot c_v} \right) \cdot dt = 0 \tag{8.86}$$

There is no condition for the enthalpy flow as for the SFVSM and EFVSM, since the assumption of a linear temperature gradient in the regenerator has been omitted.

This concludes the treatment of equations and boundary and integral conditions of the MVSM.

8.3.6 Numerical methods

The three numerical solution approaches

- Integration-to-Convergence method.
- Shooting method.
- Finite Difference method.

which the thesis has been concentrating about, have also been used in the simulation programs developed for the MVSM.

From the results and conclusions for the SFVSM and EFVSM the following promising numerical methods have been selected for the simulations

- 4.order DIRK method with a fixed step length for the Integration-to-Convergence method.
- 4.order DIRK method with a fixed step length for the Shooting method.
- 3.order NT I method variable step length for the Shooting method.
- 6.order divided difference approximation for the Finite Difference method.

The implementation is in principle identical to the description in chapter 6.

Some additional problems are encountered for the numerical solution of the MVSM compared to the simpler models based on the "lumped" formulation.

The requirement for speed and storage makes a PC less suitable for this model and the following simulations had to be run on a workstation (HP 715 Apollo). Convergence, from refinement of the discretization step, to the true solution of the mathematical model of the MVSM could not be achieved due to hardware limitations. Requirements for CPU-time and storage makes it impossible to obtain a sufficiently fine resolution in space.

With the increasing number of volumes, the system of equations also increases in size. Each volume implies at least two (or three if the solid temperature is variable) differential equations and one algebraic equation. An example; two variable volumes (2 sub volumes), three manifolds (3 sub volumes), two heat exchangers (40 sub volumes, 20 in each component) and one regenerator (160 sub volumes), a total of 205 volumes. This will give a system of 410 differential equations, 205 algebraic equation and 166 integral conditions under the assumption of "cyclic heat transfer" in all other components but the heat exchangers.

For approaches based on the IVP integration (i.e., the Integration-to-Convergence method and the Shooting method) this implies that a system of 410+205=615 nonlinear equations must be solved at each stage of the semi-implicit Runge-Kutta integration.

For the Shooting the finite difference calculation of the Jacobian will require 410+126=536 cycles! Only a few iterations are then needed for obtaining the periodic steady-state solution, but the overall cost is still high.

The Finite Difference method is penalized most (regarding the need for storage and speed) of the approaches considered here. Using N=80 time steps on a cycle, the method requires the solution of a system of (410+205)·80+125=49325 equations for each iteration step!

8.3.7 Test data

The same real engine example, as for the SFVSM and EFVSM, is used for the MVSM. Three manifold volumes have been included in order to represent the actual design of the engine better, such that the model now has a total of 8 components.

Component no.	1	2	3	4	5	6	7	8
Component type	VVC	MVC	HEX	MVC	REG	MVC	HEX	VVC
# of sub volumes	1	1	20	1	80	1	20	1
Max. swept	$493.7 \cdot 10^{-6}$							$441.6 \cdot 10$
Dead volume [m^3]	$137 \cdot 10^{-6}$	$42 \cdot 10^{-6}$	$191 \cdot 10^{-6}$	$19 \cdot 10^{-6}$	$368 \cdot 10^{-6}$	$75 \cdot 10^{-6}$	$440 \cdot 10^{-6}$	$43 \cdot 10^{-6}$
Initial phase angle	127.197							0.000
Free flow area [m^2]	$8.66 \cdot 10^{-3}$	$3.85 \cdot 10^{-3}$	$1.06 \cdot 10^{-3}$	$3.85 \cdot 10^{-3}$	$8.37 \cdot 10^{-3}$	$3.85 \cdot 10^{-3}$	$1.21 \cdot 10^{-3}$	$8.66 \cdot 10^{-3}$
Heat transfer area	$26.6 \cdot 10^{-3}$	$2.4 \cdot 10^{-3}$	$305.4 \cdot 10^{-3}$	$1.1 \cdot 10^{-3}$	10.394	$4.3 \cdot 10^{-3}$	$220.2 \cdot 10^{-3}$	$25.5 \cdot 10^{-3}$
Cyclic heat transfer	Yes	Yes	No	Yes	Yes	Yes	No	Yes
Solid temperature			328				973	
Solid wall mass [kg]					0.821			

Speed: 1550 RPM
Required mean pressure: p_{mean} = 8 Mpa
Working gas: Helium
Gas constant: R = 2079.5 J/(kg·K)
Gas specific heat capacity: c_p= 5093 J/(kg·K)
Matrix specific heat capacity: c_M= 570 J/(kg·K)
Matrix porosity: ϱ = 0.78
Matrix thread diameter: $d_w = 0.04 \cdot 10^{-3}$m

The following abbreviations have been used:

VVC: Variable volume with cyclic heat transfer.
MVC: Manifold volume with cyclic heat transfer.
HEX: Heat exchanger.
REG: Regenerator.

The complete set of data is given in Appendix F.

8.3.8 Results

General results from the simulation programs for the MVSM are shown in this section

Comp. # Method	1	2	3	4	5	6	7	8	N	Efficiency	Work in [W]	Heat in [W]	Enthalpy flow [W]
DIRK4	1	1	5	1	10	1	5	1	10	0.3332	14171	48556	-18207
DIRK4	1	1	5	1	10	1	5	1	200	0.3336	14050	48375	-18155
DIRK3	1	1	5	1	10	1	5	1	200	0.3336	14080	48376	-18156
DIRK4	1	1	10	1	80	1	10	1	10	0.4950	13986	36594	-4492
DIRK4	1	1	10	1	80	1	10	1	80	0.4968	13867	36470	-4487
DIRK4	1	1	10	1	80	1	10	1	200	0.4968	13866	36470	-4487
DIRK3	1	1	10	1	80	1	10	1	200	0.4968	13866	36471	-4487

Table Significance of the discretization in time.

Comp. # Method	1	2	3	4	5	6	7	8	N	Efficiency	Work in [W]	Heat in [W]	Enthalpy flow [W]
DIRK3	1	1	10	1	40	1	10	1	200	0.4649	13783	38705	-6925
DIRK3	1	1	10	1	80	1	10	1	200	0.4968	13866	36471	-4487
DIRK3	1	1	10	1	160	1	10	1	200	0.5146	13907	35320	-3236
DIRK3	1	1	10	1	190	1	10	1	200	0.5176	13913	35136	-3037
DIRK3	1	1	40	1	80	1	40	1	200	0.5203	12028	35797	-5144
DIRK3	1	1	20	1	80	1	20	1	200	0.5006	13199	36416	-4987
DIRK3	1	1	10	1	80	1	10	1	200	0.4968	13866	36471	-4487
DIRK3	1	1	5	1	80	1	5	1	200	0.4884	14282	36007	-4137

Table Significance of the discretization in space.

Remarks:

i) As mentioned, convergence of the numerical method for the spatial discretization could not be found. This is due to the hardware limitations of the HP Apollo 715 workstation regarding both speed and storage. Implementation on a more powerful computer has not been carried out.

ii) The number of time steps is less critical for the obtained simulation results than the number of sub volumes. For a given spatial dicretization the results do not change much when the time step is refined. The same cannot be said for a refinement of the spatial step.

iii) The calculated heat input, work input and regenerator loss as a function of the number of sub volumes in regenerator is shown in the following figure:

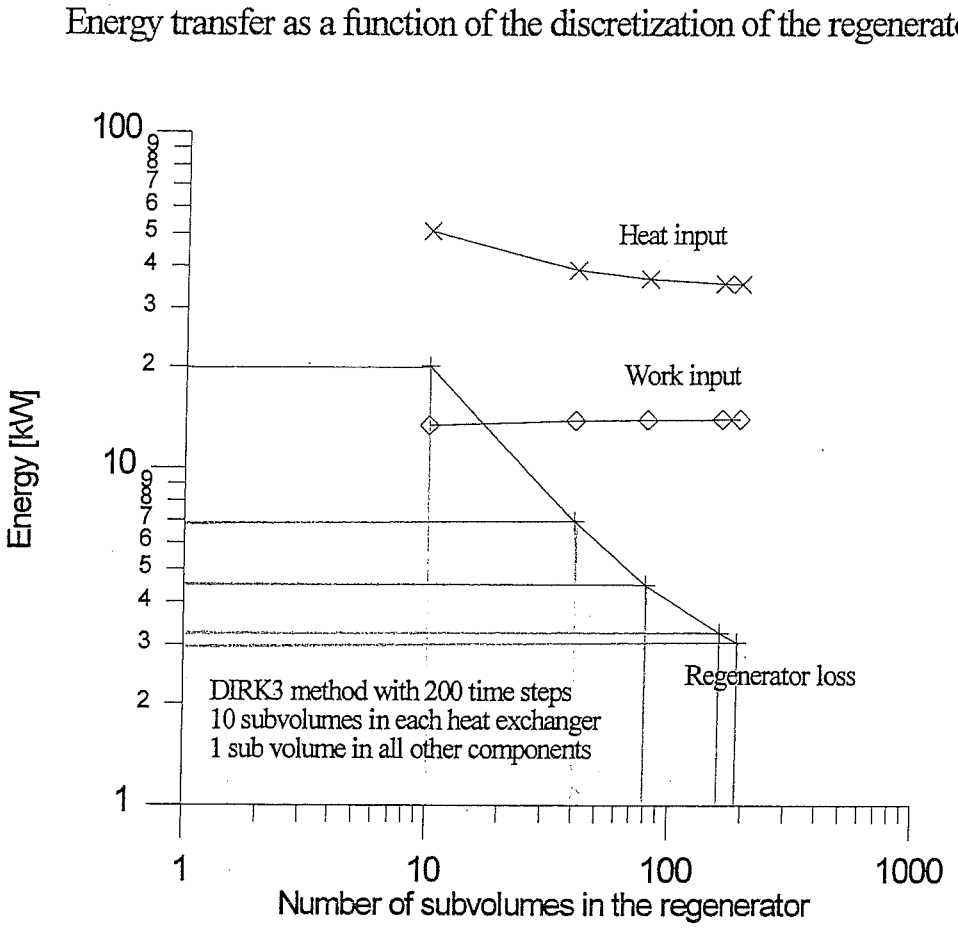

Figure 8.11 Work, heat transfer and enthalpy flux for the MVSM.

iv) The regenerator loss (net enthalpy flux through the regenerator) is seen to be very dependent of the number of sub volumes in the regenerator. Due to the steep temperature gradient in this component, the numerical solution is polluted by errors introduced from the low first order upwind discretization. The numerical error is equivalent to a second order (diffusive) term, and is often called numerical diffusion. Experimental studies indicate that the regenerator loss from an engine like the one used for the test example should be in the order 1-2 kW.

The problem of numerical diffusion will be discussed in more detail later in this section.

v) The temperature profile (fixed solid temperature) is shown in the following figure:

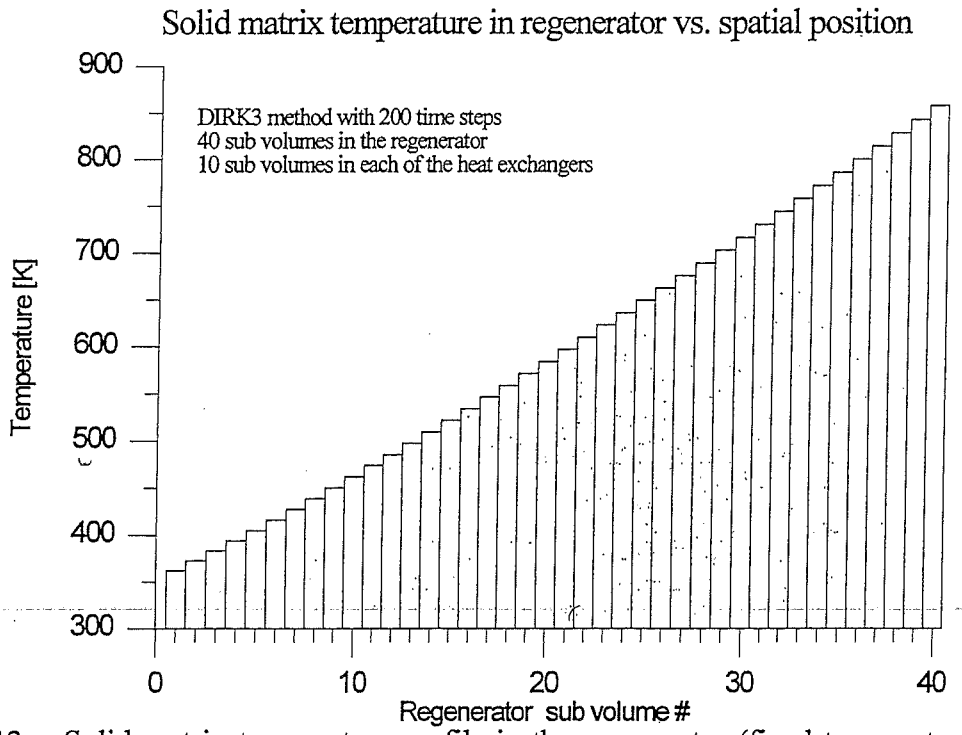

Figure 8.12 Solid matrix temperature profile in the regenerator (fixed temperature).

The assumption of a linear temperature profile, which has been made in the SFVSM and EFVSM, seems to be very reasonable judging by this example.

vi) The net heat transfer for each sub volume in the heat exchangers (cold heat exchanger is component #3 and hot heat exchanger is #7) is shown in the following figures:

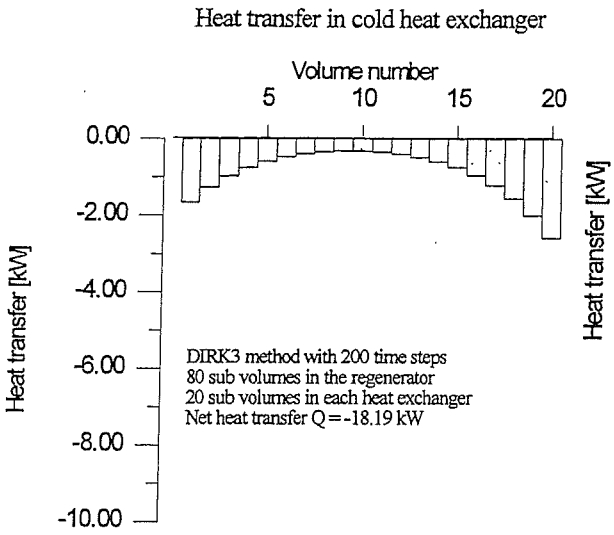

Figure 8.14 Cold heat exchanger.

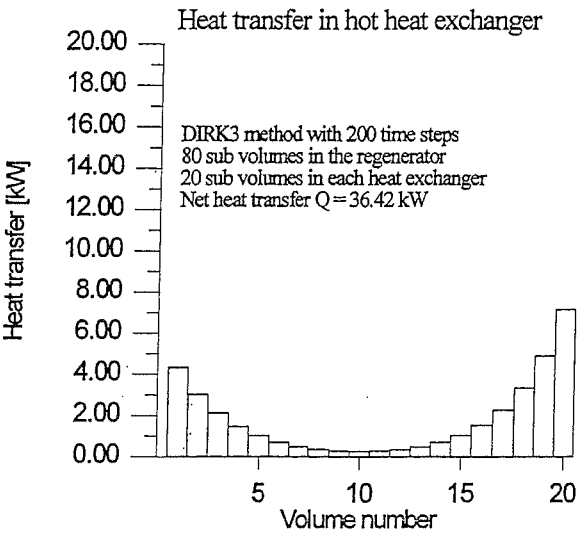

Figure 8.13 Hot heat exchanger.

When the number of sub volumes in a heat exchanger is increased, then the net heat transfer in the sub volumes in the middle of the component becomes very small as it can be seen from the following figures:

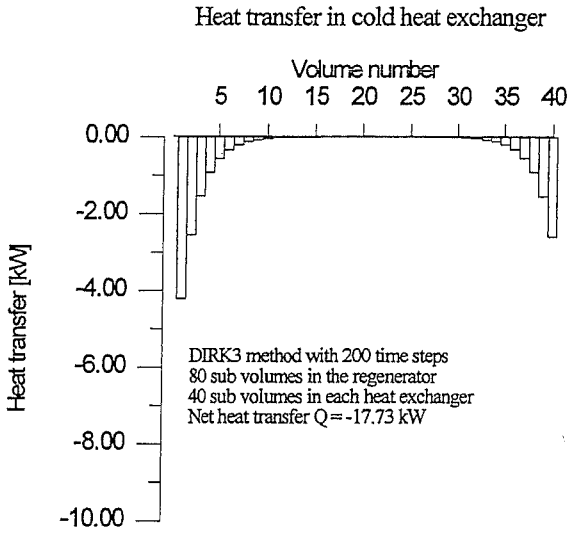

Figure 8.15 Cold heat exhanger.

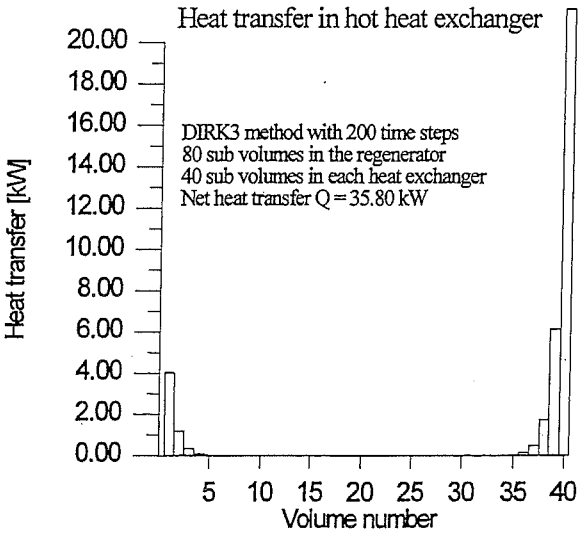

Figure 8.16 Hot heat exchanger.

The sub volumes in the middle of the heat exchangers are almost isothermal through the cycle, but the overall heat transfer for the whole heat exchanger still is depending on the number of sub volumes in the component (see the last table on page 8.36).

vii) The numerical solution should be independent of the discretization. This is a basic requirement for having confidence in the obtained numerical results. Since a further spatial refinement still gives significantly different results, this has not been achieved for the MVSM within the given hardware limitations. More than 500 sub volumes in the regenerator might be necessary, when using a first order spatial discretization.

viii) Convergence for the Shooting method is very fast, as soon as the numerical calculation of the Jacobian has been carried out. Only 3-5 iterations (i.e., additional cycles) are required for obtaining the periodic steady state solution.

ix) The initial guess is generated from a Schmidt analysis, where the manifold volumes have been included in the other components, and a linear variation of the variables within each component has been assumed.

Numerical diffusion

Problems in computational fluid dynamics are encountered, when discontinuities or steep gradients are present in a flow dominated by convection. This is the case especially for hyperbolic problems.

First order upwind representation of the flux terms give rise to *numerical diffusion*. This phenomenon destroys the solution by smearing, i.e., sharp variations in the variables will vanish due to the artificial diffusion introduced by the numerical method. Higher order upwind differences or central difference approximations could be obvious alternatives, but both give rise to oscillations which are not physical (entropy violations).

This has been discussed and analyzed in a general context by many authors (e.g., [9], [10]), also with the implementation for a Stirling engine in mind, see reference [11]. Numerical methods which in some extent solve these problems for the Euler equations and other hyperbolic problems have been developed.

The simplest and classical example is the linear convection problem

$$\frac{\partial u}{\partial t} + a \cdot \frac{\partial u}{\partial x} = 0 \qquad (8.87)$$

For a finite-volume volume discretization and the flux term evaluated in an upwind manner it gives the following semi-discrete form

$$\frac{du}{dt} = \begin{cases} \frac{a}{\Delta x} \cdot (u_i - u_{i-1}) & a>0 \\ \frac{a}{\Delta x} \cdot (u_{i+1} - u_i) & a<0 \end{cases} \qquad (8.88)$$

. The classical explicit first order upwind scheme is then (for the case a>0)

$$u_{i,n+1} = u_{i,n} - \sigma \cdot (u_{i,n} - u_{i-1,n}) \qquad \sigma = \frac{a \cdot \Delta t}{\Delta x} \tag{8.89}$$

where n,n+1 denotes the time levels and σ is a parameter called the Courant number.

This scheme is only stable for

$$0 \leq \sigma = \frac{a \cdot \Delta t}{\Delta x} \leq 1 \tag{8.90}$$

This so-called CFL-condition expresses that the mesh (in form of Δx and Δt) should be chosen such that "the domain of dependence of the differential equation should be contained in the domain of dependence of the discretized equation", see reference [9] pp.288-89. The damping (numerical diffusion) increases when the Courant number decreases.

Implicit schemes have better stability properties, but the problem of numerical diffusion remains.

It is not the intention here to go deeper into a theoretical discussion of the subject of numerical diffusion, but instead to concentrate on the importance for the MVSM-problem.

The semi-discretized form is used for an IVP integration using a semi-implicit Runge-Kutta method (for the Integration-to-Convergence method and the Shooting method). It comes as no surprise that severe problems are encountered regarding numerical diffusion. In the last table on page 8.36, it is easy to see the importance of the number of sub volumes in the regenerator.

The cure is to use excessively many volumes in the regenerator. For a consistent and stable method and in the limit of $\Delta x \rightarrow 0$, the numerical solution should converge to the true solution of the mathematical model. It may be noticed that the regenerator loss is not close to the converged value, even when using as many as 190 sub volumes in this component.

The "realistic" low efficiency, in the simulation of the engine on a coarse grid, is mainly due to the numerical diffusion introduced by the first order upwind discretization.

Furthermore, it should be noted that the refinement in form of the increasing number sub volumes makes the whole system of equations stiff. This has been discussed in reference [12] pp.254-259 in the context of semi-discretization methods for the solution of PDEs.

A simple hybrid method (discretization) might be considered as an alternative. The internal sub volumes in the regenerator could be discretized using a central second order difference for the flux term, while the end sub volumes of the regenerator could be discretized in the usual upwind manner. This idea has not been implemented into computer code, because of the time limitations of this project.

References

[1] Carlsen, H.
10 KW Stirling Engine for Stationary Applications.
ISEC 6th International Stirling Engine Conference (1993).

[2] Miyabe, H., Takahashi, S., and Hamagnchi, K.
An Approach to the Design of a Stirling Engine Regenerator Matrix Using Packs of Wire Gauzes.
17th IECEC proceedings (1982).

[3] Kays, W.M. and London, A.L.
Compact Heat Exchangers.
McGraw Hill (1980).

[4] Carlsen, H. and Andersen, N.E.
Report no. 3, Heat Exchangers.
Laboratory for Energetics, Technical University of Denmark (1985).

[5] Carlsen, H., Commisso,M.B. and Lorentzen, B.
Maximum Obtainable Efficiency for Engines and Refrigerators based on the Stirling Cycle.
25th IECEC proceedings, pp.366-71 (1990).

[6] Bauwens, L.
Consistency, Stability, Convergence of Stirling Engine Models.
25th IECEC vol.5. pp.352-58 (1990).

[7] Carlsen, H. and Andersen, N.E.
Report no. 4.2, Regenerator.
Laboratory for Energetics, Technical University of Denmark (1985).

[8] Martini, W.R.
Stirling Engine Design Manual.
DOE/NASA/3152-87/1 (1978).

[9] Hirsch, C.
Numerical Computation of Internal and External Flows vol. I and II.
John Wiley and sons. Ltd. (1991).

[10] LeVeque, R.J.
Numerical Methods for Conservation Laws.
Birkhäuser Verlag (1992).

[11] Fokker, H. and van Eekelen, J.A.M.
Typical Phenomena of the Stirling Cycle as Encountered in a Numerical Approach.
13th IECEC proceedings, pp.1746-52 (1978).

[12] Lambert, J.D.
Numerical Methods for Ordinary Differential Systems.
Wiley (1991).

9.0 DISCUSSION AND CONCLUSIONS

9.1 Introduction

In this section the general results from the previous chapters will be discussed and analyzed. The main part is devoted to separate discussions of the three Stirling engine models considered in the thesis:

- Simple Five-Volume Stirling Model (SFVSM).
- Extended Five-Volume Stirling Model (EFVSM).
- Multi-Volume Stirling Model (MVSM).

Different approaches for obtaining a numerical solution to the defined mathematical models have been tried out, and the principal results and general conclusions from the simulations are stated.

Finally, the application of the developed methods and ideas to other related thermodynamic problems will be addressed.

9.2 The SFVSM-problem

9.2.1 General remarks

A simple five-volume model (SFVSM) of a Stirling engine has been made for the purpose of studying and comparing different solution approaches including the choice of a specific numerical method.

Each of the traditional five components in a Stirling engine, i.e., two variable cylinder volumes, two heat exchangers and one regenerator, is treated as one single volume. The simple physical model is translated into a complete mathematical model, which includes a "lumped" formulation of the equations for conservation of mass and energy, an equation of state, boundary conditions and some additional integral constraints concerning the required mean pressure of the cycle, "cyclic heat transfer" conditions and net enthalpy flux through the regenerator.

The basic system of governing equations has been classified as a system of differential-algebraic equations (DAEs) with periodic boundary conditions in time, which actually makes the problem a boundary value problem (BVP).

All the equations have been scaled (i.e., made dimensionless) using natural reference parameters. This is significant for the robustness of the numerical methods applied, and has made it easier to specify more uniform parameters for the iterations.

9.2.2 Numerical methods

As just mentioned, the problem has been classified as a BVP, but nevertheless the most common approach is to solve the problem as an initial value problem (IVP) and just integrate forward in time until the periodic conditions are satisfied. In this thesis this approach has been called the Integration-to-Convergence method, but other authors use "Brute-force integration" or "Contraction Mapping method" as well.

In the previous chapters two other approaches which are classical methods for the solution of BVPs have also been considered in detail:

- The Shooting method.
- The Finite Difference method.

The Shooting method is still based on an IVP integration of the defined system of equations for the problem, but it can be considered as a convenient way of accelerating the convergence towards cyclic conditions. In the developed simulation program the Jacobian (in Newton's method for the solution of nonlinear equations) used by the Shooting method has been calculated numerically using a finite difference approximation. The iteration on the parameters for the cyclic integral conditions could directly and very easily be included into the iteration on the cyclic state variables.

For the Finite Difference method, the system of DAEs has been transformed into a system of algebraic equations by replacing derivatives with finite difference approximations. This implies that all equations for all discrete time levels (defined by the discretization in time) are solved simultaneously. The cyclic integral conditions could also very easily be included into this calculation for this approach.

Semi-implicit Runge-Kutta methods have been used for the IVP integration in the thesis mainly for two reasons. Firstly, these methods have much better stability properties than the explicit methods. This implies that fewer time steps are required, which will be advantageous if many cycles are needed to obtain a periodic solution. Secondly, explicit Runge-Kutta methods can only be applied to the alternative formulation due to the DAE structure, and extensions (in form of the additional nonlinearities introduced in the EFVSM) imply that the explicit methods cannot be used without severe modifications. Semi-implicit Runge-Kutta methods are a compromise between the computational cheap explicit methods and the very expensive fully implicit methods. Fixed step length implementation as well as a variable step length based on error estimates have been carried out and worked satisfactorily.

Linear Multistep methods or simple divided differences have been used for the finite difference approximations of the derivatives for the Finite Difference method. Fixed step length implementation only has been considered, since it is difficult to obtain error estimates and to change the step length.

The two approaches based on IVP integration require a guess for the initial values only(i.e., at time t=0), while the Finite Difference method requires a guess on all variables at all discrete time levels.

9.2.3 What method to use?

Integration-to-Convergence method

Even for the simplest of the three considered Stirling models (the SFVSM), the Integration-to-Convergence method is less attractive than the other approaches regarding speed. The convergence towards cyclic state variables is rather slow, although a relative good initial guess is available from an isothermal Schmidt analysis. Furthermore, the parameters for the cyclic integral conditions (i.e., solid temperatures in variable volumes and regenerator, matrix gradient and total mass) still have to be adjusted so that these conditions are satisfied.

In this implementation, the parameters for the cyclic integral conditions are determined from a modified Newton method based on a finite approximation of the Jacobian, and although cheaper ways are possible (secant type methods or quasi-Newton methods) this is still a severe drawback of the method.

Typically around 60 cycles have to be calculated for obtaining the solution. 20 cycles to find the cyclic state variables, 20 to find the Jacobian and 20 for the iteration on the cyclic integral conditions. Usually updating the Jacobian is unnecessary.

The Shooting method

The Shooting method holds great promises. Implementation into computer code is in principle as simple as for the Integration-to-Convergence method, because one cycle is integrated using an IVP method in the same way.

The method is faster than the Integration-to-Convergence, since fewer cycles are required for the determination of cyclic operation conditions, and since the iteration on the parameters for cyclic integral conditions are included directly.

Integration of a full cycle for each of the differential variables and for each parameter of the cyclic integral conditions are required for the numerical approximation of the Jacobian. The number equals 15 for the SFVSM and then only 4-5 iterations are usually enough for the determination of full cyclic operation for the test example. The total of 19-20 cycles should be compared with the required 50-60 cycles for the Integration-to-Convergence method.

IVP-integration methods have been used for the Integration-to-Convergence method and the Shooting method. No stability problems are encountered when using algebraically stable semi-implicit Runge-Kutta methods. 10 time steps are sufficient to obtain a qualitatively correct solution, but the requirement for an accurate solution is stricter. Accepting a relative numerical error (compared to the "true" converged solution) of less than 0.1% for the calculated work and heat transfer, 120-150 time steps are required for the fixed step length implementation of the fourth order DIRK method, while 100 time steps seemed adequate for the third order NT I method with a variable step length based on embedded error estimates of the local truncation error.

The Finite Difference method

The Finite-Difference method also looks very promising for the SFVSM-problem. The method is very robust for many different finite difference approximations, and the convergence towards periodic steady-state solution is very fast. Only 4-5 iterations are required to obtain the full cyclic solution.

Drawbacks for the Finite Difference methods may be found. Requirements for computing power and storage grow very fast with the number of time steps. For the SFVSM the number of differential and algebraic variables is fixed and equal to 21. With an example of 100 time steps for one cycle to obtain an accurate solution and with 5 unknown parameters for the cyclic integral conditions, it will give a total of 2105 unknown variables. The Jacobian will then contain more than four million elements and even though it will be very sparse, it still puts some demand for computational power and storage. A "sparse" solver for the linearized system is a necessary requirement even for the SFVSM, if the approach is to compete with the Shooting method regarding computational speed and accuracy. Furthermore, no error estimate is directly available and it is more difficult to change the step length since the approximations of the derivatives are based on equal step length (fixed time step) and interpolations are required for arbitrary step length.

Generally speaking for all the approaches considered, the influence from the presence of discontinuities seemed rather unclear, but the implemented methods worked very well for the SFVSM-problem. All methods apparently converge to the same solution when the step length is refined.

9.3 The EFVSM-problem

9.3.1 General remarks

The Extended Five-Volume Stirling Model (EFVSM) is still based within the limitations of a five-volume model, which means that the spatial variation with each volume is completely lost. The usefulness of the results widely depends on the accuracy of the component models, but the EFVSM now includes a number of features which bring the physical and mathematical model closer to real conditions. Most important are the following features:

- Heat transfer in form of a variable NTU-number.
- Variable matrix temperature in the regenerator.
- Pressure losses due to friction.

The NTU-number has been expressed as a function of geometry and mass flows for each component in the Stirling engine.

An additional differential equation for the internal energy (temperature) of the regenerator matrix has been included into the governing system of equations.

A static pressure loss (and corresponding dissipation) from a reduced momentum equation has also been incorporated into the system of equations. The pressure difference through a component is then given in form of an additional algebraic equation.

9.3.2 What method to use?

Integration-to-Convergence method
As expected the Integration-to-Convergence method is penalized further when the simple Stirling model is extended to include the features mentioned just above in the EFVSM.

Introducing the variable matrix temperature as a new dynamic variable and the corresponding differential equation meant that the number of cycles required to obtain a cyclic solution is increased from 50-60 to 600-900 for the Stirling engine test example, which has been described in chapter 7 and chapter 8. In practice, this makes the use of the Integration-to-Convergence method unacceptable in a design situation where hundreds of different configurations have to be calculated, e.g., as an input to an optimization routine.

Shooting method
This method is basically unaffected by the extensions made in the EFVSM, only 19-21 cycles are required to obtain the full cyclic solution for the test example.

No stability problems have been encountered when using the algebraically stable semi-implicit Runge-Kutta for the IVP-integration. Just as few time steps as for the SFVSM could be used for the time integration of one cycle. It should be noted that the explicit Runge-Kutta methods cannot be applied for the EFVSM-problem without severe modifications due to the additional nonlinearities introduced. The implementation of the semi-implicit Runge-Kutta methods isunaffected regarding complexity and speed.

Finite Difference method
This method is also unaffected by the new features introduced in the EFVSM, and still 4-5 iterations only are needed to obtain the full cyclic solution.

The mathematical model of the EFVSM-problem could be solved by the Shooting method or the Finite Difference method in less than three minutes on a 33/66 MHz 486-PC within an accuracy of 0.1% compared to the "true" converged solution.

It must be concluded that both the Shooting method and the Finite-Difference methods are superior to the traditional Integration-to-Convergence method for the SFVSM and EFVSM, i.e., for simple Stirling engine models based on the five components - five volume "lumped" formulation.

9.4 The MVSM-problem

9.4.1 General remarks

A model based on a true one dimensional spatial discretization for a Stirling engine has been developed in form of the Multi-Volume Stirling Model (MVSM). The intention has been to study the behavior of the considered approaches and methods for a model which is closer to the actual fluid dynamics and thermodynamic conditions inside a real Stirling engine.

The MVSM is based on the classical equations, i.e., partial differential equations for conservation of mass, momentum and energy in form of the Navier-Stoke's equations and an equation of state for the working gas.

However, important simplifications have been introduced. Foremost in form of the assumption of one-dimensional flow, which means that heat transfer and friction must be modelled empirically. The governing system of equations then becomes identical with the Euler equations for inviscid flows with the exception of some additional source terms. The assumption of uniform pressure in space has been made to reduce the computational cost, but this implies that the momentum equation becomes useless and the model less realistic.

A Finite Volume type discretization has been used, and the convective fluxes at the boundaries are evaluated in an upwind manner. Because of the low first order spatial discretization, it comes as no surprise that problems with numerical diffusion are observed.

Numerical diffusion together with the steep gas temperature gradient in the regenerator give rise to a very large net enthalpy flux through the regenerator, when a grid too coarse is used for the spatial discretization in the regenerator.

The "correct" low efficiency from the simulations when using relatively few sub volumes, is solely due to these numerical errors. According to studies carried out by Carlsen, the regenerator loss is of the size 1-2 kW for a typical Stirling engine regenerator used for the real test example. More than 200 sub volumes in this component could seem to be a requirement for obtaining a sufficiently accurate numerical solution when a first order upwind evaluation of the flux term is used.

Alternatively, the fluxes at the inner sub volume boundaries in the regenerator could have been evaluated using a second central difference, but this has not been implemented into computer code.

9.4.2 What method to use?

Integration-to-Convergence method
The increased number of sub volumes and variables makes the convergence towards cyclic conditions slower and the increased size of the system of equations makes this approach very time consuming. When the solid matrix temperature in the regenerator is assumed to be variable in time, then it is almost impossible to obtain the full cyclic solution. For the MVSM, more than a thousand cycles are required in order to find the cyclic state variables for the test example.

Shooting method
This method seems promising concerning required computing time, but only as long as the total number of sub volumes is relatively small. The spatial accuracy of the solution will then be rather poor and in the case of a first order upwind evaluation of the flux term the numerical solution will be destroyed by the numerical diffusion.

The iteration on the "cyclic heat transfer" temperatures rises problems for the MVSM when the number of sub volumes becomes large for both methods discussed above. It is no problem for the "cyclic heat transfer" in the variable volumes. There is only one volume for each of these components and therefore one solid temperature only. Problems occur for the regenerator. Consider a regenerator with 200 volumes, then additional 200 cycles should be integrated for the numerical calculation of the Jacobians for both the Integration-to-Convergence method (iteration on the cyclic integral conditions) and for the Shooting method (iteration on the full cyclic state).
For a variable matrix temperature in the regenerator component, no additional cycles will have to be integrated for the former of these two approaches, but now the convergence towards cyclic state variables becomes unacceptably slow just as it is discussed above.

Finite Difference method
Heavy computation is required when this method is applied for the MVSM-problem. Increasing number of volumes and many time steps make even computations on workstations suffer, and other more powerful tools must be used if many designs are to be calculated. A number of 150 volumes and 100 time steps give more than 40000 nonlinear equations, and the Jacobian will contain more than $1.6 \cdot 10^9$ elements. Although most of these are zero and a sparse solver should be applied for the solution this will still be a very large system of linear equations.

None of the approaches or numerical methods considered here seem to be very attractive for the MVSM-problem and the "correct" momentum equation and pressure losses have not even been considered for this model. However, no obvious alternatives are available. A compromise between spatial accuracy and required computational power must be made, and the simple first order upwind discretization of the flux term used here does not seem to be a good idea because of the numerical diffusion (at least not for the internal volumes in the regenerator).

These difficulties for one-dimensional codes are probably also the most important reason why simple models (such as the Five-Volume Stirling Models) still are used for basic design considerations.

9.5 Application for real Stirling engine simulations

The simulation results for all models give results too optimistic compared to real engine performance, but this is not unexpected since known losses have not been incorporated into the developed model. Foremost

- Mechanical losses.
- Burner losses.
- Parasitic losses.

The dynamics of the mechanical system for the engine has not been discussed at all in this thesis. The volume variation has just been assumed to be sinusoidal in both cylinder volumes with a given constant speed. Detailed studies of the mechanical losses can be carried out, but in a simple analysis these are often evaluated as a percentage of the work output. Including an overall mechanical loss like this would, of course, have brought the simulation results closer to the real conditions in form of lower efficiency and lower work output, but since it does not change anything for the numerical approaches and methods applied, and since these losses are very specific for each engine, corrections for mechanical losses have been omitted.

It is very difficult to include the parasitic losses into the system of equations in a thermodynamically correct way. Usually these losses are studied separately and the estimates are based on experience or actual measurements. For this reason and because the parasitic losses may be very dependent of the specific engine design, these losses have been omitted from the simulation program to keep the results as general as possible.

All commercial codes apply some kind of calibration, i.e., the different losses are adjusted using factors to make the simulation results in agreement with the specific engine type performance. These kinds of manipulations are required for even the best one-dimensional Stirling codes.

9.6 Other ideas

Other ideas for obtaining a quick periodic solution include:

- Optimization methods.
- Extrapolation methods.
- Spectral methods.

The first two of these three are based on IVP integration and can, in the same way as the Shooting method, be considered as ways to accelerate the convergence towards the cyclic state. The theoretical basis for the implementation of an optimization method has been given here and extrapolation has only been mentioned as an alternative. Any clear advantages for these two methods regarding the actual problem are not found, so the implementation into computer code has not been carried out.

Spectral methods hold some interesting properties. The periodicity of the problem makes it very natural to express each of the variables in Fourier series. A discrete Fourier transform could be used for the discretization and the fast FFT (Fast Fourier Transform) could be used for the numerical solution.

Due to problems in form of the nonlinearities and the discontinuities in the equations this idea has not been pursued further in the thesis, but it remains an open question of the possibilities for this idea. In the HFAST code (see chapter 3) the two first harmonics of a Fourier series for each variable have been used with promising results.

9.7 Application for other thermodynamic cycles

In general, all theoretical cycles can easily be analyzed, the cycles can be drawn in a state diagram (for an engine typically a pressure-volume diagram or a temperature-entropy diagram) and the efficiency and output in form of heat or work can be directly calculated. This is opposite of the real cycle, which is embodied in a thermodynamic device such as an engine, a heat pump or a refrigerator. Usually the real cycle is much more complex (as discussed in chapter 2) and the device has to be modelled carefully. The real embodiments give raise to cycles that are not even close to theoretical cycles.

In this thesis, simple models of reciprocating devices based on *closed,* thermodynamic cycles have been discussed. The Stirling engine has been chosen as the model example, but many of the ideas and conclusions can be used for other related thermodynamic devices.

The following features should be included in these devices:

- Thermodynamic cycles.
- Reciprocating devices.
- Components.
- Periodic solution.

Thermodynamic cycles in real device embodiment in form of reciprocating devices have been considered. It must be possible to divide the device into a number of components or at least models of the different parts of the device should be treated separately. All variables should be periodic in time with a fixed period given from external forces.

Although the main emphasis in this thesis has been put on the Stirling engine, the discussion for solution approaches should in large extent also be valid for related thermodynamic cycles such as devices based on the Vuilleumier cycle or Ericsson cycle. Also for internal combustion engines and other devices based on open cycles, it should be possible to use some of these ideas.

9.8 Concluding remarks

Two models for Stirling engines, based on the five components - five volumes idea, have been described in detail namely the Simple Five-Volume Stirling Model (SFVSM) and the Extended Five-Volume Model (EFVSM). Three different solution approaches have been considered, one traditional in form of the Integration-to-Convergence method and two alternatives in form of the Shooting method and the Finite-Difference method.

The implementations into computer code of these three approaches have been carried out and the superiority of the two new approaches has clearly been demonstrated in the numerical tests presented in chapter 7 and chapter 8. Reduced computational cost and gain in robustness for obtaining the periodic steady-state of the problem have been significant as displayed in these chapters.

Furthermore, using an algebraically stable semi-implicit Runge-Kutta method for the time integration is advantageous for both the Integration-to-Convergence method and the Shooting method. A stable solution for one cycle can be obtained using relatively few time steps. This is important, since the calculation of many cycles can be required to obtain the periodic steady-state solution.

Different possibilities for combining the approaches and methods also seem interesting. Applying a low order, cheap method with good stability properties in order to find the cyclic solution (using only few time steps) and then applying a high order method to get an accurate solution (using many time steps) looks like a promising idea for a quick way to obtain the periodic steady-state solution.

The "lumped" formulation of the SFVSM and EFVSM makes it impossible to study the spatial variation within each component.

Therefore, a more sophisticated model in form of the Multi-Volume Stirling Model (MVSM), which features a one-dimensional spatial discretization of the Stirling engine, has been developed. It is then possible to study the application of the numerical approaches on a model which has better potential for describing the thermodynamics and fluid dynamics of the real Stirling engine. Fluxes at the boundaries are evaluated as first order upwind differences, and problems with numerical diffusion have been encountered due to the low order discretization.

The Shooting method has been used for the actual simulations, but none of the approaches developed for the simple models seem to be completely successful in terms of accuracy and speed for the MVSM.

APPENDIX

A: Mass and internal energy in a volume with a linear temperature gradient

B: Isothermal Schmidt Analysis

C: Stirling engine configurations

D: Runge-Kutta methods

E: Numerical integration

F: Stirling engine test data

Appendix A

Mass and internal energy in a volume with a linear temperature gradient

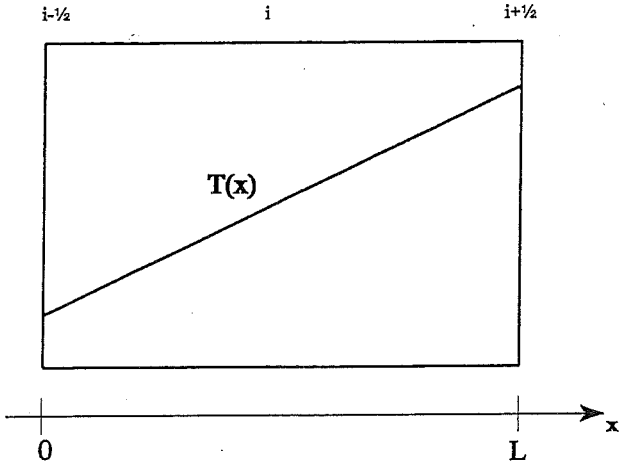

Figure A.1 Volume with linear temperature profile.

Let the constant temperature gradient α be defined as

$$\alpha = \frac{dT}{dx} \tag{A.1}$$

then the temperature in the shown volume is given by the expression

$$T(x) = T_i + (x - \frac{L}{2})\cdot\alpha \tag{A.2}$$

Now the following additional assumptions are made

- Uniform pressure p.
- Constant cross sectional area A_c.
- Ideal gas.

The total mass in the volume is then given as

$$M = \int_V \rho\cdot dV = \int_{x=0}^{L} \frac{p\cdot A_c}{R\cdot T}\cdot dx = \frac{p\cdot A_c}{R}\cdot\int_{x=0}^{L} \frac{1}{T_i + (x-\frac{L}{2})\cdot\alpha}\cdot dx$$

$$= \frac{p\cdot A_c}{R}\cdot\left[\frac{1}{\alpha}\cdot\ln(\alpha\cdot x + T_i - \frac{L}{2}\cdot\alpha)\right]_0^L = \frac{p\cdot V}{R\cdot\alpha\cdot L}\cdot\ln\left(\frac{T_i + \alpha\cdot\frac{L}{2}}{T_i - \alpha\cdot\frac{L}{2}}\right) \tag{A.3}$$

Define the mean logarithmic temperature T_{ln} as

$$T_{ln} = \frac{\alpha \cdot L}{\ln\left(\frac{T_i + \alpha \cdot \frac{L}{2}}{T_i - \alpha \cdot \frac{L}{2}}\right)} = \frac{T_{i+1/2} - T_{i-1/2}}{\ln\left(\frac{T_{i+1/2}}{T_{i-1/2}}\right)} \tag{A.4}$$

and get the expression

$$p \cdot V = M \cdot R \cdot T_{ln} \tag{A.5}$$

The arithmetic mean T_i can also be expressed in terms of T_{ln}

$$T_i = \frac{\alpha \cdot L}{2} \cdot \frac{\exp\left(\frac{\alpha \cdot L}{T_{ln}}\right) + 1}{\exp\left(\frac{\alpha \cdot L}{T_{ln}}\right) - 1} \tag{A.6}$$

The total internal energy in the volume is given as

$$\int_V \rho \cdot e \cdot dV = \int_{x=0}^{L} \frac{p}{R \cdot T} \cdot c_v \cdot T \cdot A_c \cdot dx = p \cdot V \cdot \frac{c_v}{R} = \frac{p \cdot V}{\gamma - 1} \tag{A.7}$$

which is identical to the result for a volume with a uniform temperature distribution.

So for a constant volume with a linear temperature gradient (e.g., the regenerator in five-volume Stirling models)

$$\frac{d}{dt}\int_V \rho \cdot e \cdot dV = \frac{V}{\gamma - 1} \cdot \frac{dp}{dt} = \frac{d}{dt}(M \cdot c_v \cdot T_{ln}) \tag{A.8}$$

Notice that the rate of change is expressed in terms of the logarithmic mean temperature T_{ln}.

Appendix B

Isothermal Schmidt analysis

The analysis is due to Schmidt (1871) and has been used for many years. The results can be found in all standard text books dealing with Stirling machines and here only basic results required for the generation of the initial guesses for the more sophisticated analysis is given.

In the Schmidt analysis, the assumption of isothermal variable volumes is kept, but now internal volumes are present in the heat exchangers and the regenerator. Furthermore, a sinusoidal variation of the variable volumes is assumed. The heat exchangers and the regenerator are still considered ideal in the sense of infinite heat transfer from solid to gas.

Nomenclature (subscript)

- C: compression
- E: expansion
- H: heat exchanger
- R: regenerator
- cl: clearance volume
- sw: swept volume

Volumes

Variable volumes:

$$V_C(t) = V_{clC} + V_{swC}\cdot\frac{1+\cos(\omega\cdot t)}{2}$$
$$V_E(t) = V_{clE} + V_{swE}\cdot\frac{1+\cos(\omega\cdot t+\varphi)}{2} \qquad (B.1)$$

Volumes of the heat exchangers (V_{HC} and V_{HE}) and volume of the regenerator (V_R) are all constant.

Temperatures

Temperature in the variable volume (compression end): T_{HC}
Temperature in the heat exchanger (compression end): T_{HC}
Temperature in the heat exchanger (expansion end): T_{HE}
Temperature in the variable volume (expansion end): T_{HE}

Linear temperature profile in regenerator (between T_{HC} and T_{HE}).

Mean logarithmic temperature $T_{R,ln}$ in the regenerator

$$T_{R,\ln} = \frac{T_{HE} - T_{HC}}{\ln\left(\frac{T_{HE}}{T_{HC}}\right)} \tag{B.2}$$

Pressure

Define

$$c = \frac{1}{2}\cdot\sqrt{\left(\frac{V_{swC}}{T_{HC}}\right)^2 + 2\cdot\cos\varphi\cdot\frac{V_{swC}\cdot V_{swE}}{T_{HC}\cdot T_{HE}} + \left(\frac{V_{swE}}{T_{HE}}\right)^2} \tag{B.3}$$

and

$$s = \frac{V_{swC}}{2\cdot T_{HC}} + \frac{V_{clC}}{T_{HC}} + \frac{V_{HC}}{T_{HC}} + \frac{V_R}{T_{R,\ln}} + \frac{V_{HE}}{T_{HE}} + \frac{V_{swE}}{2\cdot T_{HE}} + \frac{V_{clE}}{T_{HE}} \tag{B.4}$$

$$\beta = \tan^{-1}\left(\frac{V_{swE}\cdot\sin\varphi}{V_{swE}\cdot\cos\varphi + V_{swE}\cdot\frac{T_{HE}}{T_{HC}}}\right) \tag{B.5}$$

The pressure is then given as

$$p(t) = \frac{M_{tot}\cdot R}{s + c\cdot\cos(\omega\cdot t + \beta)} \tag{B.6}$$

Mass

From the equation of state (ideal gas)

$$M_C(t) = \frac{p(t)\cdot V_C(t)}{R\cdot T_{HC}}$$

$$M_{HC}(t) = \frac{p(t)\cdot V_{HC}}{R\cdot T_{HC}}$$

$$M_R(t) = \frac{p(t)\cdot V_R}{R\cdot T_{\ln,R}} \qquad \text{(B.7)}$$

$$M_{HE}(t) = \frac{p(t)\cdot V_{HE}}{R\cdot T_{HE}}$$

$$M_E(t) = \frac{p(t)\cdot V_E(t)}{R\cdot T_{HE}}$$

Mass flows

The derivative of pressure is:

$$\frac{dp}{dt} = p'(t) = \frac{M_{tot}\cdot R\cdot\omega\cdot c\cdot\sin(\omega\cdot t+\beta)}{\left(s + c\cdot\cos(\omega\cdot t+\beta)\right)^2} \qquad \text{(B.8)}$$

The derivatives of volume with respect to time for the variable volumes are:

$$\frac{dV_C}{dt} = V_C'(t) = -\frac{\omega}{2}\cdot V_{swC}\cdot\sin(\omega\cdot t)$$

$$\frac{dV_E}{dt} = V_E'(t) = -\frac{\omega}{2}\cdot V_{swE}\cdot\sin(\omega\cdot t+\varphi) \qquad \text{(B.9)}$$

all other derivatives of volume are identical zero (constant volumes).

The derivatives of mass with respect to time are then given by the expressions

$$\frac{dM_C}{dt} = M_C'(t) = \frac{V_C(t)}{R \cdot T_{HC}} \cdot p'(t) + \frac{p(t)}{R \cdot T_{HC}} \cdot V_C'(t) \tag{B.10}$$

$$\frac{dM_{HC}}{dt} = M_{HC}'(t) = \frac{V_{HC}(t)}{R \cdot T_{HC}} \cdot p'(t) \tag{B.11}$$

$$\frac{dM_R}{dt} = M_R'(t) = \frac{V_R(t)}{R \cdot T_{\ln,R}} \cdot p'(t) \tag{B.12}$$

$$\frac{dM_{HE}}{dt} = M_{HE}'(t) = \frac{V_{HE}(t)}{R \cdot T_{HE}} \cdot p'(t) \tag{B.13}$$

$$\frac{dM_E}{dt} = M_E'(t) = \frac{V_E(t)}{R \cdot T_{HE}} \cdot p'(t) + \frac{p(t)}{R \cdot T_{HE}} \cdot V_E'(t) \tag{B.14}$$

and finally for the mass flow

$$\dot{m}_{C \to HC} = -M_C'(t) \tag{B.15}$$

$$\dot{m}_{HC \to R} = -\left(M_C'(t) + M_{HC}'(t)\right) \tag{B.16}$$

$$\dot{m}_{R \to HE} = -\left(M_C'(t) + M_{HC}'(t) + M_R'(t)\right) \tag{B.17}$$

$$\dot{m}_{HE \to E} = -\left(M_C'(t) + M_{HC}'(t) + M_R'(t) + M_{HE}'(t)\right) = M_E'(t) \tag{B.18}$$

The work output from one cycle is given as

$$W = W_C + W_E \tag{B.19}$$

where

$$W_C = \pi \cdot V_{swC} \cdot p_{mean} \cdot \sin\beta \cdot \frac{\sqrt{1-b^2}-1}{b}$$

$$W_E = \pi \cdot V_{swE} \cdot p_{mean} \cdot \sin(\beta-\varphi) \cdot \frac{\sqrt{1-b^2}-1}{b} \tag{B.20}$$

and the efficiency η for engine operation:

$$\eta = 1 - \frac{T_{HC}}{T_{HE}} \tag{B.21}$$

which is identical to the Carnot efficiency (maximal efficiency for an engine operating between two temperature levels T_{HC} and T_{HE}).

The mean pressure p_{mean} of the cycle is given as

$$p_{mean} = \int_{t=0}^{t_p} p(t) \cdot dt = \frac{M_{tot} \cdot R}{\sqrt{s^2 - c^2}} \tag{B.22}$$

Notice that the mean pressure is proportional to the total mass and to specify a mean pressure is equivalent to specify the total mass.

In this way, the Schmidt analysis can provide initial values for a one-step Runge-Kutta method.

1) Specify the mean pressure and calculate the total mass.

2) Insert time t=0 in the expressions above to get the initial pressure and masses.

But the Schmidt analysis can also provide for initial guesses on all variables at all times using the expressions above for any value of t.

Appendix C

Stirling engine configurations

Alpha-, Beta- and Gamma-engines are the most common mechanical configurations in Stirling engines.

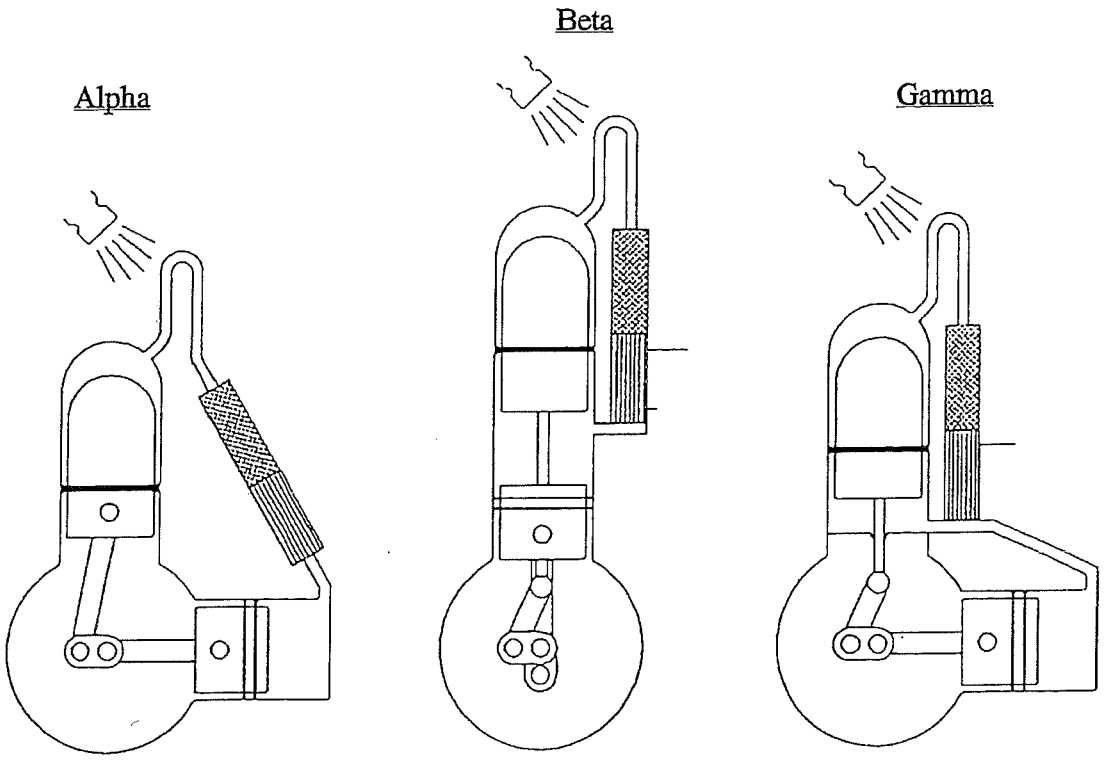

Figure C.1 Stirling engine configurations.

It can be shown that for Beta- and Gamma-engines it is possible to define an equivalent Alpha-engine.

An equivalent swept volume $\tilde{V}_{swC}$ and an equivalent initial phase angle $\tilde{\varphi}_C$ for the compression volume is all that is required for a calculation of the equivalent alpha-engine instead of the original Beta- or Gamma-engine.

Beta-engines

For Beta-engines, the total volumes (including clearance/dead volume and swept/variable volumes) in the two cylinders can be written as

$$V_C(\alpha) = V_{clC} + V_{swC}\cdot\frac{1+\cos(\alpha+\varphi_C)}{2} + V_{swE}\cdot\frac{1-\cos(\alpha+\varphi_E)}{2} - V_{overlap}$$
$$V_E(\alpha) = V_{clE} + V_{swE}\cdot\frac{1+\cos(\alpha+\varphi_E)}{2} \qquad (C.1)$$

when a sinusoidal piston motion is assumed.

The angle is defined as $\alpha=\omega\cdot t$ and the two phase angles and φ_C and φ_E denote the initial angle at time t=0. Usually only one of these two are specified, since it is the difference that is of interest, but here it has been chosen to derive the expressions in this general manner.

The variation of volume in the compression cylinder is dependent of the position of the piston in the compression cylinder and the position of the displacer in the expansion cylinder due to the special construction of a Beta-engine (see the figure on the previous page). The volume $V_{overlap}$ can be removed in the compression cylinder because

$$S_C\cdot\frac{1+\cos(\alpha+\varphi_C)}{2} + S_E\cdot\frac{1-\cos(\alpha+\varphi_E)}{2} \geq 0 \qquad (C.2)$$

where S_C and S_E are the strokes in respectively the compression cylinder and the expansion cylinder.

It is advantageous regarding the performance of the engine to keep the dead volume down, so the best choice of $V_{overlap}$ is

$$V_{overlap} = B_E\cdot Min\left(S_C\cdot\frac{1+\cos(\alpha+\varphi_C)}{2} + S_E\cdot\frac{1-\cos(\alpha+\varphi_E)}{2}\right) \qquad (C.3)$$

where B_E is the bore in the expansion cylinder.

The minimum can be found from differentiation with respect to the crank angle α and setting this derivative equal to zero, i.e.,

$$-\frac{1}{2}\cdot S_C\cdot\sin(\alpha+\varphi_C) + \frac{1}{2}\cdot S_E\cdot\sin(\alpha+\varphi_E) = 0 \qquad (C.4)$$

After some trivial algebraic and trigonometric manipulations

$$\tan\alpha = -\frac{\frac{S_C}{S_E}\cdot\sin\varphi_C - \sin\varphi_E}{\frac{S_C}{S_E}\cdot\cos\varphi_C - \cos\varphi_E} \qquad (C.5)$$

This expression defines two angles in the interval $[0;2\pi[$. Let α_{min} and α_{max} denote the angle where V_C has its minimum and maximum value respectively ($\alpha_{min} = \alpha_{max} \pm \pi$).

$V_{overlap}$ is now given as

$$V_{overlap} = B_E\cdot\left(S_C\cdot\frac{1+\cos(\alpha_{min}+\varphi_C)}{2} + S_E\cdot\frac{1-\cos(\alpha_{min}+\varphi_E)}{2}\right) \qquad (C.6)$$

An equivalent swept volume $\tilde{V}_{swC}$ can be defined as

$$\tilde{V}_{swC} = V_C(\alpha_{max}) - V_{clC} \qquad (C.7)$$

Finally, an equivalent phase difference (the difference in phase angle between when the maximal volume in expansion volume and maximal volume in compression volume) is given as

$$\Delta\varphi = \alpha_{max} - \varphi_E \qquad (C.8)$$

and a new equivalent initial phase angle $\tilde{\varphi}_C$ for the compression volume can be defined as

$$\tilde{\varphi}_C = -\alpha_{max} \qquad (C.9)$$

Now it is possible to use the Alpha-engine analysis for Beta-engines as well.

The only difference is that the total volume in the compression cylinder is given as

$$V_C(t) = V_{clC} + \tilde{V}_{swC}\cdot\frac{1+\cos(\omega\cdot t+\tilde{\varphi}_C)}{2} \qquad (C.10)$$

where $\tilde{V}_{swC}$ and $\tilde{\varphi}_C$ are taken from the expressions derived above.

Gamma-engines

For Gamma-engines, the analysis can be applied as well. Now, the correction

$$V_{overlap} = 0 \qquad (C.11)$$

is given and must be inserted in the expression (C.1).

Appendix D

Runge-Kutta methods

Numerical simulations have been performed using the Runge-Kutta methods listed below. The coefficients of the methods (a_{ij},b_i and c_i where i,j=1,2,...s) are given in form of the Butcher arrays. Stage number is denoted s and order of accuracy is denoted p.

Explicit methods

Heun's method (p=3, s=3)

$$\begin{array}{c|cccc} \underline{c} & \underline{\underline{A}} \\ \hline & \underline{b}^T \end{array} = \begin{array}{c|cccc} 0 & 0 & 0 & 0 \\ \frac{1}{3} & \frac{1}{3} & 0 & 0 \\ \frac{2}{3} & 0 & \frac{2}{3} & 0 \\ \hline & \frac{1}{4} & 0 & \frac{3}{4} \end{array} \qquad \text{(D.1)}$$

Classical explicit Runge-Kutta method (s=4, p=4)

$$\begin{array}{c|cccc} \underline{c} & \underline{\underline{A}} \\ \hline & \underline{b}^T \end{array} = \begin{array}{c|cccc} 0 & 0 & 0 & 0 & 0 \\ \frac{1}{2} & \frac{1}{2} & 0 & 0 & 0 \\ \frac{1}{2} & 0 & \frac{1}{2} & 0 & 0 \\ 1 & 0 & 0 & 1 & 0 \\ \hline & \frac{1}{6} & \frac{1}{3} & \frac{1}{3} & \frac{1}{6} \end{array} \qquad \text{(D.2)}$$

The following explicit Runge-Kutta methods use embedding to obtain estimates for the local truncation error.

England's method (s=6, p=4)

$$
\begin{array}{cc} \underline{c} & \underline{\underline{A}} \\ & \underline{b}^T \\ & \tilde{\underline{b}}^T \\ & \underline{e}^T \end{array} =
\begin{array}{ccccccc}
0 & 0 & 0 & 0 & 0 & 0 & 0 \\
\frac{1}{2} & \frac{1}{2} & 0 & 0 & 0 & 0 & 0 \\
\frac{1}{2} & \frac{1}{4} & \frac{1}{4} & 0 & 0 & 0 & 0 \\
1 & 0 & -1 & 2 & 0 & 0 & 0 \\
\frac{2}{3} & \frac{7}{27} & \frac{10}{27} & 0 & \frac{1}{27} & 0 & 0 \\
\frac{1}{5} & \frac{28}{625} & -\frac{1}{5} & \frac{546}{625} & \frac{54}{625} & -\frac{378}{625} & 0 \\
 & \frac{1}{6} & 0 & \frac{2}{3} & \frac{1}{6} & 0 & 0 \\
 & \frac{1}{24} & 0 & 0 & \frac{5}{48} & \frac{27}{56} & \frac{125}{336} \\
 & -\frac{1}{8} & 0 & -\frac{2}{3} & -\frac{1}{16} & \frac{27}{56} & \frac{125}{336}
\end{array}
\qquad \text{(D.3)}
$$

Fehlberg's method RKF45 (s=6, p=4)

$$
\begin{array}{cc} \underline{c} & \underline{\underline{A}} \\ & \underline{b}^T \\ & \tilde{\underline{b}}^T \\ & \underline{e}^T \end{array} =
\begin{array}{ccccccc}
0 & 0 & 0 & 0 & 0 & 0 & 0 \\
\frac{1}{4} & \frac{1}{4} & 0 & 0 & 0 & 0 & 0 \\
\frac{3}{8} & \frac{3}{32} & \frac{9}{32} & 0 & 0 & 0 & 0 \\
\frac{12}{13} & \frac{1932}{2197} & -\frac{7200}{2197} & \frac{7296}{2197} & 0 & 0 & 0 \\
1 & \frac{439}{216} & -8 & \frac{3680}{513} & -\frac{845}{4104} & 0 & 0 \\
\frac{1}{2} & -\frac{8}{27} & 2 & -\frac{3544}{2565} & \frac{1859}{4104} & -\frac{11}{40} & 0 \\
 & \frac{25}{216} & 0 & \frac{1408}{2565} & \frac{2197}{4104} & -\frac{1}{5} & 0 \\
 & \frac{16}{135} & 0 & \frac{6656}{12825} & \frac{28561}{56430} & -\frac{9}{50} & \frac{2}{55} \\
 & \frac{1}{360} & 0 & -\frac{128}{4275} & -\frac{2197}{75240} & \frac{1}{50} & \frac{2}{55}
\end{array}
\qquad \text{(D.4)}
$$

RKF45 is error-tuned, meaning that the coefficients for the estimate of the local truncation error are made small. The method is often used with local extrapolation meaning that it uses the fifth order method for the integration step and a step length control based on the error estimates for the fourth order method. The method is then denoted RKF54.

. Verner's method RKV56 (s=8, p=5)

$$
\begin{array}{cccc}
\underline{c} & \underline{\underline{A}} & = & \begin{array}{ccccccccc}
0 & 0 & 0 & 0 & 0 & 0 & 0 & 0 & 0 \\
\frac{1}{6} & \frac{1}{6} & 0 & 0 & 0 & 0 & 0 & 0 & 0 \\
\frac{4}{15} & \frac{4}{75} & \frac{16}{75} & 0 & 0 & 0 & 0 & 0 & 0 \\
\frac{2}{3} & \frac{5}{6} & -\frac{8}{3} & \frac{5}{2} & 0 & 0 & 0 & 0 & 0 \\
\frac{5}{6} & -\frac{165}{64} & \frac{55}{6} & -\frac{425}{64} & \frac{85}{96} & 0 & 0 & 0 & 0 \\
1 & \frac{12}{5} & -8 & \frac{4015}{612} & -\frac{11}{36} & \frac{88}{255} & 0 & 0 & 0 \\
\frac{1}{15} & -\frac{8263}{15000} & \frac{124}{75} & -\frac{643}{680} & -\frac{81}{250} & \frac{2484}{10625} & 0 & 0 & 0 \\
1 & \frac{3501}{1720} & -\frac{300}{43} & \frac{297275}{52632} & -\frac{319}{2322} & \frac{24068}{84065} & 0 & \frac{3850}{26703} & 0
\end{array} \\
\underline{b}^T & & & \begin{array}{ccccccccc}
\frac{13}{160} & 0 & \frac{2375}{5984} & \frac{5}{16} & \frac{12}{85} & \frac{3}{44} & 0 & 0 \\
\frac{3}{40} & 0 & \frac{875}{2244} & \frac{23}{72} & \frac{264}{1955} & 0 & \frac{125}{11592} & \frac{43}{616} \\
\frac{1}{160} & 0 & -\frac{75}{17952} & -\frac{1}{144} & \frac{12}{1955} & \frac{3}{44} & -\frac{125}{11592} & -\frac{43}{616}
\end{array} \\
\tilde{\underline{b}}^T & & & \\
\underline{e}^T & & &
\end{array}
\qquad \text{(D.5)}
$$

Usually, the method is implemented using local extrapolation (RKV65).

Semi-implicit methods

1-stage Radau IA and Radau IIA (s=1, p=1)

$$
\begin{array}{ccc}
\underline{c} & \underline{\underline{A}} & = \begin{array}{cc} 0 & 1 \\ & 1 \end{array} \\
& \underline{b}^T &
\end{array}
\quad , \quad
\begin{array}{ccc}
\underline{c} & \underline{\underline{A}} & = \begin{array}{cc} 1 & 1 \\ & 1 \end{array} \\
& \underline{b}^T &
\end{array}
\qquad \text{(D.6)}
$$

Both methods are algebraically stable (L-stable).

1-stage Gauss method (s=1, p=2)

$$
\begin{array}{ccc}
\underline{c} & \underline{\underline{A}} & = \begin{array}{cc} \frac{1}{2} & \frac{1}{2} \\ & 1 \end{array} \\
& \underline{b}^T &
\end{array}
\qquad \text{(D.7)}
$$

This method is a fully implicit method, but since it has only one stage it can be treated the same way as semi-implicit methods for the implementation. The method is algebraically stable (L-stable).

Semi-implicit 2-stage Lobatto IIIB (s=2, p=2)

$$\begin{array}{c|cc} \underline{c} & \underline{\underline{A}} \\ \hline & \underline{b}^T \end{array} = \begin{array}{c|cc} 0 & \frac{1}{2} & 0 \\ 1 & \frac{1}{2} & 0 \\ \hline & \frac{1}{2} & \frac{1}{2} \end{array} \qquad \text{(D.8)}$$

This method is only A-stable and not algebraically stable.

2-stage DIRK (Diagonally-Implicit Runge-Kutta) method (s=2)

$$\begin{array}{c|cc} \underline{c} & \underline{\underline{A}} \\ \hline & \underline{b}^T \end{array} = \begin{array}{c|cc} \frac{3\cdot\nu-1}{6\cdot\nu} & \frac{3\cdot\nu-1}{6\cdot\nu} & 0 \\ \frac{1+\nu}{2} & \nu & \frac{1-\nu}{2} \\ \hline & \frac{3\cdot\nu^2}{3\cdot\nu^2+1} & \frac{1}{3\nu^2+1} \end{array} \qquad \text{(D.9)}$$

The method is of order three (p=3) for all values of $\nu \neq 0$ and a DIRK method for $\nu = \pm 3^{-1/2}$. The method is algebraically stable only for $\nu < 0$.

3-stage DIRK (Diagonally-Implicit Runge-Kutta) method (s=3)

$$\begin{array}{c|ccc} \underline{c} & \underline{\underline{A}} \\ \hline & \underline{b}^T \end{array} = \begin{array}{c|ccc} \frac{1+\nu}{2} & \frac{1+\nu}{2} & 0 & 0 \\ \frac{1}{2} & -\frac{\nu}{2} & \frac{1+\nu}{2} & 0 \\ \frac{1-\nu}{2} & 1+\nu & -1-2\cdot\nu & \frac{1+\nu}{2} \\ \hline & \frac{1}{6\nu^2} & 1-\frac{1}{3\nu^2} & \frac{1}{6\nu^2} \end{array} \qquad \text{(D.10)}$$

This DIRK method is of order four (p=4) for the following values of ν:

$$\nu = \frac{2}{\sqrt{3}}\cdot\cos 10^\circ \quad , \quad \nu = -\frac{2}{\sqrt{3}}\cdot\cos 50^\circ \quad , \quad \nu = -\frac{2}{\sqrt{3}}\cdot\cos 70^\circ \qquad \text{(D.11)}$$

but the method is algebraically stable only for the first of these three.

The following embedded semi-implicit Runge-Kutta methods has been used for variable step length implementation:

NT I (s=3, p=3)

$$\begin{array}{cc|ccc} & & \frac{5}{6} & \frac{5}{6} & 0 & 0 \\ & & \frac{29}{108} & -\frac{61}{108} & \frac{5}{6} & 0 \\ \underline{c} & \underline{A} & & & & \\ & \underline{b}^T & \frac{1}{6} & -\frac{23}{183} & -\frac{33}{61} & \frac{5}{6} \\ & \tilde{\underline{b}}^T & & \frac{25}{61} & \frac{36}{61} & 0 \\ & \underline{e}^T & & \frac{26}{61} & \frac{324}{671} & \frac{1}{11} \\ & & & -\frac{1}{61} & \frac{72}{671} & -\frac{1}{11} \end{array} \qquad \text{(D.12)}$$

The three-stage NT I method (Nørsett and Thomsen) of order three is algebraically stable. The method uses a second order embedded method for the estimate of the local truncation error.

NT II (s=4, p=3)

$$\begin{array}{cc|ccccc} & & \frac{5}{6} & \frac{5}{6} & 0 & 0 & 0 \\ & & \frac{10}{39} & -\frac{15}{26} & \frac{5}{6} & 0 & 0 \\ \underline{c} & \underline{A} & 0 & \frac{215}{54} & -\frac{130}{27} & \frac{5}{6} & 0 \\ & \underline{b}^T & & & & & \\ & \tilde{\underline{b}}^T & \frac{1}{6} & \frac{4007}{6075} & -\frac{31031}{24300} & -\frac{133}{2700} & \frac{5}{6} \\ & \underline{e}^T & & \frac{32}{75} & \frac{169}{300} & \frac{1}{100} & 0 \\ & & & \frac{61}{150} & \frac{2197}{2100} & \frac{19}{100} & -\frac{9}{14} \\ & & & \frac{1}{50} & -\frac{119}{350} & -\frac{9}{50} & \frac{9}{14} \end{array} \qquad \text{(D.13)}$$

The four-stage NT II method (Nørsett and Thomsen) of order three is only A-stable. The method uses a fourth order embedded method for the estimate of the local truncation error.

Appendix E

Numerical Integration

Introductory remarks

Consider the following problem:

Calculate the integral

$$I(f) = \int_{t=a}^{b} f(t) \cdot dt \tag{E.1}$$

where the function f(t) is given as values in N+1equally spaced points

$$t_j = t_0 + j \cdot \Delta t \qquad \Delta t = \frac{t_N - t_0}{N} \qquad j = 0,1,\ldots,N \tag{E.2}$$

where t_0=a and t_N=b.

An interpolatory quadrature formula designed for equally spaced nodes can be used to obtain a numerical approximation I_N to the integral

$$I_N \approx I(f) \tag{E.3}$$

There are two aspects, which must be taken into consideration before selecting a numerical method for the integration for the actual problem, where the function (in form of the variables) is found from a numerical solution of a system of differential-algebraic equation:

- Accuracy of the numerical method that has been used for the solution of the system of ODEs (or DAEs) should in some sense be in accordance the accuracy of numerical integration method. How should the order of accuracy for the two methods be chosen, such that one of the methods do not destroy the accuracy of the overall solution and such that the iteration on the integral conditions can be carried out successfully .

- Under the assumption of a periodic solution (i.e., periodic function), additional information is directly available for the numerical integration methods.

Newton-Cotes interpolation formulas

Two of the most widely used methods for numerical integration are the Trapezoidal rule and Simpson's rule. These two methods will be described, and higher order methods will also be discussed.

Trapezoidal rule

$$I_T = \frac{b-a}{2}\cdot\left(f(a)+f(b)\right) \tag{E.4}$$

The truncation error is given by

$$E_T = -\frac{f''(\xi)}{12}\cdot(b-a)^3 \tag{E.5}$$

To increase the accuracy, all the nodes are used, i.e., the interval is divided into sub intervals and then the method is applied. This composite version of the Trapezoidal rule is given as

$$I_{N,T} = \frac{\Delta t}{2}\cdot\left(f(t_0) + f(t_N) + 2\cdot\sum_{j=1}^{N-1} f(t_j)\right) \tag{E.6}$$

with a truncation error

$$E_{N,T} = -\frac{f''(\xi)}{12}\cdot(b-a)\cdot\Delta t^2 \tag{E.7}$$

A variant of this method is known as the corrected trapezoidal method and is given as

$$I_{CT} = \frac{b-a}{2}\cdot\left(f(a)+f(b)\right) + \frac{(b-a)^2}{12}\cdot\left(f'(a) - f'(b)\right) \tag{E.8}$$

The first term is identical to the Trapezoidal rule. It requires the evaluation of the derivatives at a and b, but the truncation error is now given as

$$E_{CT} = -\frac{f''''(\xi)}{720}\cdot(b-a)^5 \tag{E.9}$$

For the composite version, all the derivatives at the internal points cancel out and only the contributions from t_0 and t_N are left, hence.

$$I_{N,CT} = \frac{\Delta t}{2}\cdot\left(f(t_0) + f(t_N) + 2\cdot\sum_{j=1}^{N-1} f(t_j)\right) + \frac{\Delta t^2}{12}\cdot\left(f'(t_0) - f'(t_N)\right) \tag{E.10}$$

and

$$E_{N,CT} = -\frac{f''''(\xi)}{720}\cdot(b-a)\cdot\Delta t^4 \tag{E.11}$$

For smooth periodic functions with

$$f(t_0) = f(t_N) \qquad f'(t_0) = f'(t_N) \tag{E.12}$$

the method is identical to the Trapezoidal rule and it is seen that the method will be of order 4 with an error constant 1/720.

The Trapezoidal rule can also be used, when the points are not equally spaced. This will be an advantage, when the points are generated with an IVP-code with variable step length for the numerical solution of a system of ODEs.

The method is the simplest of all for numerical integration. Nevertheless, it is very robust and performs well for functions without derivatives of high order.

Simpson's rule

$$I_S = \frac{b-a}{6}\cdot\left(f(a) + 4\cdot f\left(\frac{a+b}{2}\right) + f(b)\right) \tag{E.13}$$

The truncation error is given by

$$E_S = -\frac{f''''(\xi)}{2880}\cdot(b-a)^5 \tag{E.14}$$

The composite Simpson rule is given as

$$I_{N,S} = \frac{\Delta t}{3}\cdot\left(f(t_0) + f(t_N) + 2\cdot\sum_{j=1}^{\frac{N-2}{2}} f(t_{2\cdot j}) + 4\cdot\sum_{j=0}^{\frac{N-2}{2}} f(t_{2\cdot j+1})\right) \tag{E.15}$$

with a truncation error

$$E_{N,S} = -\frac{f''''(\xi)}{180}\cdot(b-a)\cdot\Delta t^4 \tag{E.16}$$

This is the same order as the corrected trapezoidal rule, but with a larger error constant.

Simpson's rule cannot be directly applied to problems where the points are not equally spaced.

Higher order methods

Higher order methods (like Bode's rule) perform better than the Trapezoidal rule and Simpson's rule, but for sufficiently smooth functions only, i.e., the derivatives of high order have to exist otherwise the advantage will disappear.

Extrapolation methods

Extrapolation is a general approach, which can be used when an approximation I(Δt) to an unknown I_0 can be found. The approximation can be computed for every Δt≠0 and the following assumptions are made

$$I(\Delta t) \rightarrow I_0 \qquad as \qquad \Delta t \rightarrow 0 \tag{E.17}$$

and

$$I_0 = I(\Delta t) + \sum_{i=k}^{m} I_i \cdot \Delta t^i + C_m(\Delta t) \cdot \Delta t^{m+1} \tag{E.18}$$

where I_i and C_m are independent of Δt.

This formula can be used to obtain a better approximation to I_0 (small Δt) the following way:

Compute I(Δt) using two different values of Δt (step sizes), i.e., calculate $I(\Delta t_1)$ and $I(\Delta t_2)$ where $\Delta t_1=\Delta t$ and $\Delta t_2=r\cdot\Delta t$ ($0<r\leq 1$). After some trivial algebra, the following expression is obtained

$$I_0 = \frac{I(r\cdot\Delta t) - r^k \cdot I(\Delta t)}{1 - r^k} + \sum_{i=k+1}^{m} I_i \cdot \Delta t^i + C_m(\Delta t) \cdot \Delta t^{m+1} \tag{E.19}$$

which means that

$$\tilde{I} = \frac{I(r\cdot\Delta t) - r^k \cdot I(\Delta t)}{1 - r^k} \tag{E.20}$$

is a better approximation to I_0 (the first term in error expansion is of higher order, which means smaller error for small Δt)

This approach is called Richardson extrapolation.

For the widely used choice of r=½, the formula can be written as

$$\tilde{I} = \frac{2^k \cdot I\left(\frac{\Delta t}{2}\right) - I(\Delta t)}{2^k - 1} \tag{E.21}$$

Romberg Integration

Romberg integration is a widely used method, which uses the combination of the Trapezoidal rule and Richardson extrapolation.

Algorithms for numerical integration of periodic function (equally spaced points)

Calculation of

$$I(f) = \int_{t=0}^{t_p} f(t) \cdot dt \tag{E.22}$$

where

$$f(0) = f(t_p) \tag{E.23}$$

The approximation $I_Q(f)$ given as

$$I(f) \approx I_Q = \sum_{i=0}^{N} w_i \cdot f_i \tag{E.24}$$

where w_i are the weight functions and $f_i = f(t_i)$

Trapezoidal rule

For the Trapezoidal rule the weight coefficients have the following values

$$w_i = 1 \qquad i=1,2,...,N-1 \tag{E.25}$$

and

$$I_Q = \Delta t \cdot \sum_{i=0}^{N-1} w_i \cdot f_i \tag{E.26}$$

It does not matter whether N is even or uneven.

Simpson's rule

For Simpson's rule the weight coefficients have the following values for N even

$$\begin{aligned} w_0 &= \frac{1}{3} \\ w_{2i} &= \frac{2}{3} \qquad i=1,2,...,\frac{N-2}{2} \\ w_{2i+1} &= \frac{4}{3} \qquad i=1,2,...,\frac{N-2}{2} \\ w_N &= \frac{1}{3} \end{aligned} \tag{E.27}$$

and

$$I_Q = \Delta t \cdot \sum_{i=0}^{N} w_i \cdot f_i \tag{E.28}$$

For N uneven, the expression must be slightly modified. Using $f_{N+1}=f_1$ as an additional condition gives the correct number of points.

Algorithms for numerical integration of periodic function (non-equally spaced points)

For non-equally spaced points, the trapezoidal rule can still be applied since it is only based on two adjacent points. This will be the same as using the method on N intervals.

A better approach, which also can be used on equally spaced points, can be designed because of the way the function values are generated.

The function values are calculated from variables that are given from the numerical solution of a system of ordinary differential equations (ODEs). These variables are found using a numerical method such as a Runge-Kutta method. It turns out that the applied numerical method very conveniently can be used for the numerical integration of the function as well.

Requiring a calculation of the integral

$$I = \int_{t=0}^{t_p} f(t,y,z) \cdot dt \tag{E.29}$$

Define the initial-value problem

$$I' = f(t,y,z) \quad , \quad I(0) = 0 \tag{E.30}$$

and solve this problem using the numerical method (e.g., the Runge-Kuta method).

This will give the required result with the accuracy of the numerical method. Notice that this will be cheap since y and z (and all the stage values for the Runge-Kutta method) already are calculated.

This last approach has turned out to work very well for the Integration-to-Convergence method and the Shooting method in the developed simulation programs. The iteration on the cyclic integral conditions is much better (meaning faster, more smooth and more accurate) when the Runge-Kutta method itself is used for the numerical integration.

Appendix F

Stirling engine test data

The Stirling engine developed by Carlsen and is described in his paper "10 KW Stirling Engine for Stationary Applications", ISEC 6th International Stirling Engine Conference (1993) has been used as the test example for the simulations

Data

General data:

Configuration	: Beta-engine
Speed	: RPM = 1550
Phase angle	: $\varphi_\beta = 70°$
Equivalent α-engine angle	: $\varphi_C = 127.197°$
Working gas	: Helium (He)
Required mean pressure	: $p_{mean} = 8$ MPa
Number of components	: 8

Properties of gas (temperature 650 K)

Gas constant	: R = 2079 J/(kg·K)
Specific heat capacity (const. p)	: c_p = 5193 J/(kg·K)
Specific heat capacity ratio	: γ = 1.66
Kinematic viscosity	: μ = 33.2·10^{-6} N·s/m^2
Prandtl number	: Pr = 0.657

Component 1: Variable volume (cold - working piston)

Stroke	: S = 60·10^{-3} m
Bore	: B = 95·10^{-3} m
Diameter of cylinder	: D = 105·10^{-3} m
Diameter of piston rod	: D_{rod} = 12·10^{-3} m
Gap displacer-piston	: l = 1,5·10^{-3} m
Additional dead volume	: V_{DA} = 32·10^{-6} m^3

Swept volume

$$V_{sw} = S \cdot \frac{\pi}{4} \cdot (B^2 - D_{rod}^2) = 418.5 \cdot 10^{-6}\ m^3$$

Dead volume

$$V_D = l \cdot \frac{\pi}{4} \cdot B^2 + S \cdot \frac{\pi}{4} \cdot (D^2 - B^2) + V_{DA} = 136.9 \cdot 10^{-6}\ m^3$$

Equivalent maximal volume

$$V_{max} = 493.7 \cdot 10^{-6}\ m^3$$

Overlap volume

$$V_{overlap} = 183.2 \cdot 10^{-6}\ m^3$$

Effective heat transfer area

$$A = S \cdot \pi \cdot B = 17.9 \cdot 10^{-3}\ m^2$$

Component 2: Manifold volume (variable volume cold)

Diameter	: D = 70·10^{-3} m
Length	: L = 11·10^{-3} m

Volume of gas

$$V = L \cdot \frac{\pi}{4} \cdot D^2 = 42 \cdot 10^{-6}\ m^3$$

Effective heat transfer area

$$A = L \cdot \pi \cdot D = 2.4 \cdot 10^{-3}\ m^2$$

Component 3: Heat exchanger (cold)

Type	: Tubes
Solid wall temperature	: T_s = 328 K
Number of tubes	: N_{tube} = 216
Diameter of tubes	: D_{tube} = 2,5·10^{-3} m
Length	: L = 180·10^{-3}m

Hydraulic diameter

$$D_h = D_{tube} = 2.5 \cdot 10^{-3}\ m$$

Free flow area

$$A_c = N_{tube} \cdot \frac{\pi}{4} \cdot D_{tube}^2 = 1.06 \cdot 10^{-3}\ m^2$$

Volume of gas

$$V = A_c \cdot L = 191 \cdot 10^{-6}\ m^3$$

Heat transfer area

$$A = N_{tube} \cdot L \cdot \pi \cdot D_{tube} = 305.4 \cdot 10^{-3}\ m^2$$

Component 4: Manifold volume (regenerator cold end)

Diameter	: D = 70·10^{-3} m
Length	: L = 5·10^{-3} m

Volume of gas

$$V = L \cdot \frac{\pi}{4} \cdot D^2 = 19 \cdot 10^{-6}\ m^3$$

Effective heat transfer area

$$A = L \cdot \pi \cdot D = 1.1 \cdot 10^{-3}\ m^2$$

Component 5: **Regenerator**

Type	: Packed bed
Regenerator material	: Steel
Specific heat capacity	: $c_M = 0.57 \cdot 10^3$ J/K·kg
Density	: $\rho_M = 7.9 \cdot 10^3$ kg/m³
Porocity	: $\varrho = 0.78$
Thread diameter	: $d_{tr} = 0.04 \cdot 10^{-3}$ m
Inner diameter	: $D_i = 115 \cdot 10^{-3}$ m
Outer diameter	: $D_o = 164 \cdot 10^{-3}$ m
Length	: $L = 44 \cdot 10^{-3}$ m

Frontal area

$$A_{fr} = \frac{\pi}{4} \cdot (D_o^2 - D_i^2) = 10.7 \cdot 10^{-3}\ m^2$$

Free flow area

$$A_c = \varrho \cdot A_{fr} = 8.4 \cdot 10^{-3}\ m^2$$

Volume of gas

$$V = \varrho \cdot A_{fr} \cdot L = 368.5 \cdot 10^{-6}\ m^3$$

Length of matrix thread

$$l_{tr} = \frac{(1 - \varrho) \cdot A_{fr} \cdot L}{\frac{\pi}{4} \cdot d_{tr}} = 82.710 \cdot 10^3\ m$$

Heat transfer area

$$A = \pi \cdot d_{tr} \cdot l_{tr} = 10.394\ m^2$$

Hydraulic diameter

$$D_h = 4 \cdot L \cdot \frac{A_c}{A} = 0.142 \cdot 10^{-3} m$$

Heat transfer area to free flow area ratio

$$\alpha = \frac{A}{A_c} = 1241.0$$

Mass of matrix

$$M_M = (1 - \varrho) \cdot \rho_M \cdot A_{fr} \cdot L = 0.821\ kg$$

Component 6: **Manifold volume (regenerator hot end)**

Diameter	: $D = 70 \cdot 10^{-3}$ m
Length	: $L = 19.5 \cdot 10^{-3}$ m

Volume of gas

$$V = L \cdot \frac{\pi}{4} \cdot D^2 = 75 \cdot 10^{-6}\ m^3$$

Effective heat transfer area

$$A = L \cdot \pi \cdot D = 4.3 \cdot 10^{-3}\ m^2$$

Component 7: **Heat exchanger (hot)**

Type	: Tubes
Solid wall temperature	: $T_s = 973$ K
Number of tubes	: $N_{tube} = 24$
Diameter of tubes	: $D_{tube} = 8 \cdot 10^{-3}$ m
Length	: $L = 365 \cdot 10^{-3}$m
Hydraulic diameter	: $D_h = 8 \cdot 10^{-3}$ m

Heat transfer area

$$A = N_{tube} \cdot L \cdot \pi \cdot D_{tube} = 220.2 \cdot 10^{-3}\ m^2$$

Free flow area	: $A_c = 1.21 \cdot 10^{-3}$ m²
Volume of gas	: $V = 440 \cdot 10^{-3}$ m⁻³

Component 8: **Variable volume (hot - displacer)**

Stroke	: $S = 51 \cdot 10^{-3}$ m
Bore	: $B = 105 \cdot 10^{-3}$ m
Gap displacer - cylinder wall	: $d = 0.75 \cdot 10^{-3}$ m
Gap displacer - cylinder top	: $t = 1.5 \cdot 10^{-3}$ m
Gap length	: $l = 80 \cdot 10^{-3}$ m
Additional dead volume	: $V_{DA} = 10 \cdot 10^{-6}$ m⁻³

Maximal volume

$$V_{max} = S \cdot \frac{\pi}{4} \cdot B^2 = 441.6 \cdot 10^{-6}\ m^3$$

Dead volume

$$V_D = l \cdot \frac{\pi}{4} \cdot (B^2 - (B - 2 \cdot d)^2) + t \cdot \frac{\pi}{4} \cdot B^2 + V_{DA} = 43 \cdot 10^{-6}\ m^3$$

Effective heat transfer area

$$A = S \cdot \pi \cdot B = 16.8 \cdot 10^{-3}\ m^2$$

Component no.	1	2	3	4	5	6	7	8
Component type	Variable volume	Manifold volume	Heat exchanger	Manifold volume	Regenerator	Manifold volume	Heat exchanger	Variable volume
Max. variable volume [m³]	$493.7 \cdot 10^{-6}$							$441.6 \cdot 10^{-6}$
Dead volume [m³]	$137 \cdot 10^{-6}$	$42 \cdot 10^{-6}$	$191 \cdot 10^{-6}$	$19 \cdot 10^{-6}$	$368 \cdot 10^{-6}$	$75 \cdot 10^{-6}$	$440 \cdot 10^{-6}$	$43 \cdot 10^{-6}$
Initial phase angle [°]	127.197							0.000
Heat transfer area [m²]	$17.9 \cdot 10^{-3}$	$2.4 \cdot 10^{-3}$	$305.4 \cdot 10^{-3}$	$1.1 \cdot 10^{-3}$	10.394	$4.3 \cdot 10^{-3}$	$220.2 \cdot 10^{-3}$	$16.8 \cdot 10^{-3}$
Solid temperature [K]			328				973	
Solid mass [kg]					0.821			